

Synthesis of new substituted organosulfur donors for the preparation of conductive and multifunctional materials.

A thesis submitted in partial fulfilment of the requirements of Nottingham Trent

University for the degree of Doctor of Philosophy

By

Matteo Zecchini

March 2015

School of Science and Technology

Nottingham Trent University

Clifton Lane

Nottingham

NG11 8NS

United Kingdom

Declaration.

I hereby certify that the work embodied in this thesis is the result of my own investigations except where reference has been made to published literature.

“This work is the intellectual property of the authors and may also be owned by the Nottingham Trent Univeristy. You may copy up to 5% of this work for private study, or personal, non-commercial research. Any re-use of the information contained within this document should be fully referenced, quoting the author, title, university, degree level and pagination. Queries or request for any other use, or if a more substancial copy is required, should be directed in the owner(s) of the Intellectual Property Rights.”

Abstract.

The work presented in this thesis focused on the preparation of three main type of compounds: i) bridged dimeric BEDT-TTF donors (chapter 2), ii) enantiopure substituted EDT-TTF donors with hydrogen bonding functionalities (chapter 3) and iii) BEDT-TTF substituted ligands and their ability to form multifunctional materials (chapter 4).

In chapter 2 the preparation of novel BEDT-TTF donors containing an alkene in the side such as (I) and (II) is reported. Single crystals of oxidised material have been prepared and conductivities have been measured. A radical cation salt of (I) with I_2/I_3^- was found to be a semiconductor at r.t.

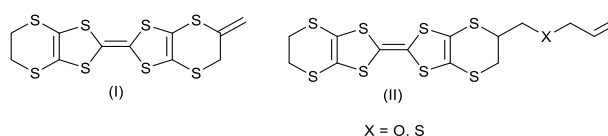


Figure 1. Donors containing an alkene functionality on the side chain.

The preparation of dimeric BEDT-TTFs such as (III) has been investigated using different substrates and strategies but the reactivity towards the second cyclisation was found to be the issue.

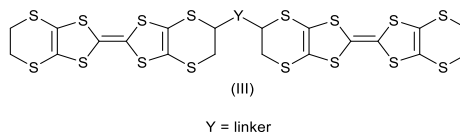


Figure 2. Desired dimer system (III).

The chapter 3 contains the preparation of novel enantiopure EDT-TTF derivatives, whose side chains were designed to guide the packing in the solid state by involving non-covalent interactions such as hydrogen bonding and/or additional π - π stacking interactions as in donors (IV) and (V).

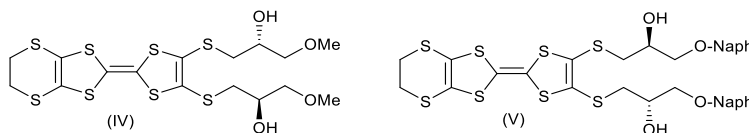


Figure 3. Examples of enantiopure donors prepared in chapter 3.

In chapter 4 the investigation of the coordination chemistry of novel BEDT-TTF substituted ligand (VI) with first row transition metals has started. The magnetism of some of the new complexes formed has been measured.

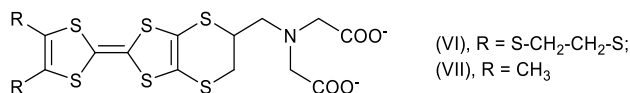


Figure 4. Type of BEDT-TTF ligands designed for metal complexes preparation.

Acknowledgements.

First of all I would like to, or better I really want to thank my supervisor, Prof John Wallis, for all the help and support you constantly gave me from my very first day at Trent...a grey morning dated 24th of January 2011. Thanks (a lot) also for the passion and the constant positivity you were able to transfer to me during my time here and especially in the moments when I messed up with the chemistry and wasted a lot of your (and my) time and why not... money! I am also very grateful for the many many and many more times when you made me laugh with your jokes and *oooooh!!* that contributed to make the CELS Synthetic Chemistry lab that great environment that it is. And of course thank you very much for the opportunity to start and (hopefully) finish this great experience that was my PhD. You have been really important for me and I could not have asked for more or for a different person.

I would like to thank Dr Gareth Cave for your friendship, for the opportunity to carry out some extra work (Biocity) that keep me alive during the last year and indeed to introduced me to the Whisky. Thanks also for bringing me to Scotland...amazing!!! . On the other side I am not so happy about your love for chilly which you tried to transfer me in many ways sometimes without asking first!!!! And of course thanks for the help and support you offered me. Thanks also to Katie, Henry and Bella to make me feel part of a family and for the funny moments.

I would like to thank Dr Chris Garner for the help he gave every time I decided to bother you instead of John. You were always there to help...even if you were always saying: "Sorry I didn't answer your question"... which was not true. And of course I apologise, and I am thankful at the same time, for all the occasions where I came to your office saying that the NMR was down!!! I genuinely wanted to learn more and being helpful but I am also sure you wanted me to piss off and never come back to your office!!!! I honestly think we should make you a monument for that!

Thanks to Dr Lee Martin for taking 10 minutes to talk with me everytime we saw each other even if you were really busy. And of course thanks not to punch me back when I punched you during the footy!!!

A very special thank to Dr Funck, just Muriel when I started, and Daniel "my friend" Guest for being really good friends, supportive and helpful especially during my first year at Trent. I am also very happy I can still share some amazing moments with them even if

we are not anymore in the same office or city!! I have to say you guys kept me company during some of the most horrible moments of my PhD...right “my friend”????...I would also like to thank Adam Close which is without any doubts a very nice guy! I also met some other amazing people such as Victoria Mundell, Roy Hodginson and Kyle Baldwin which I thank for the good time inside and outside the lab.

Also I would like to thank all the guys who shared with me the “second part” of my time here at Trent, Laurence “Bitch” Grey, Daniel “Miserable” Cotton, Tom “Encyclopedia” Pearsons, Jordan “Party boy” Lopez, Karen “Master of grammar/Potato Queen” Davies and Zayd “Incredible” Westcott who have all to listen to my “beautiful” vocal exercises all day long for many many days!!!! Thank you all also for being always present for a chat or a pint when I needed most.....and for being my friends. You have made the lab a very special place to be part of.

I would also like to thank Dr Patrick Huddleston for the unbelievable passion for chemistry which you transferred not only to me but to every student in the lab!!! Also I really enjoy our talks on Inspector Montalbano and on what to see over the weekend wherever I was going to go.

Thanks also to Mr Mark Sladen for all the help during the student lab modules and also for being a really nice guy!!!

Thanks also to all the students, Bsc, MChem, MRes and Erasmus who came across me in the CELS lab.

Thank you, again, to Dr Lee Martin for your help with measurements and given training (electrocrystallisation technique and conductivity of single crystal and X-ray diffractometer) and also to Jordan Lopez for helping me with the preparation of H-cells and electrocrystallisation experiments. Thanks also the the EPSRC National X-ray service at Southampton for the X-ray data, to the EPSRC National Mass Spectrometry service at Swansea for the mass spectrometry data and also to Mr Stephen Boyer at London Metropolitan University for providing the elemental analysis data. Thanks also to Dr Emma Smith at Nottingham Trent University for helping me with the measurements of the cyclovoltammetry of final compounds and also to Dr Melanie Pilkington at Brock University, Canada, for providing magnetic measurements and valuable information on their interpretation.

Thanks also to Mr Suketu Shah to gave me the opportunity to work for Biocity Nottingham Ltd and support me during my time there.

And almost at the end a huge thank to Chiara, my girlfriend, to take me to the UK and to be a very special person with which I spent many experiences in these five years. Thanks also for being really patience with me, for listening to mine complains and to be there (in York) everytime I needed you. I am very glad I am still with you. Thanks, for me you are amazing.

Finally at the end, the last thanks is for my parents, for being really supportive and constantly present not only during my time in UK but in every moment I needed support.... without your help I would not have gone much further than collage.

...and of course they will be happy to know that I finally finished studying...no more degree after this!! I need to find a job!!!! And become a man!!!

Dedication.

To my family, my mum Antonella and my dad Sergio. I would not have gone really far without your help and support.

To Chiara for sharing with me the good and bad moments of these challenging years.

Abbreviations.

2D	Two dimensional
A	Electron acceptor or charge carrier anion
Å	Angstrom (10^{-10} m)
AcOH	Acetic acid
BEDO-TTF (BO)	Bis(ethylenedioxy)-tetrathiafulvalene
BEDT-TTF (ET)	Bis(ethylenedithia)-tetrathiafulvalene
CBP	4,4'-Di(N-carbazolyl)biphenyl
CERN	European Organization for Nuclear Research
CHCl ₃	Chloroform
CHN	Carbon Hydrogen Nitrogen elemental analysis
CT	Charge-transfer
D	Electron donor molecule
DBTOF	Dibenzotetraoxofulvalene
DCM	4-dicyanomethylene-2-methyl-6-(p-dimethylaminostyryl)-4H-pyrene
DCM	Dichloromethane
DMF	N,N-dimethylformamide
DMSO	Dimethylsulfoxide
E _a	Activation Energy
EDOT	3,4-ethylenedioxy-thiophene
EDT-TTF	Ethylenedithia-tetrathiafulvalene
EtOAc	Ethyl acetate
EU	European Union
E _v	Valence electrons energy
HCl	Hydrochloric acid
HRMS	High resolution mass spectra
MAGLEV	Magnetic levitation
MDOT	3,4-methylenedioxy-thiophene
MeOH	Methanol

MS	Mass spectrometry
NaOMe/MeOH	Sodium methoxide in methanol
NMR	Nuclear magnetic resonance
PCBM	[6,6]-phenyl C ₆₁ butyric acid methyl ester (PCBM)
PDOT	3,4-propylenedioxy-thiophene
PEDOT	Poly(3,4-ethylenedioxy-thiophene)
PSS	Poly(4-styrenesulfonic acid)
r.t.	Room temperature
T _c	Superconducting transition temperature
TCNQ	Tetracyanoquinodimethane
THF	Tetrahydrofuran
TLC	Thin layer chromatography
TM-TSF	Tetramethyl-tetrathiafulvalene
T _N	Transition temperature to paramagnetism (from anti/ferri-magnetisms)
TTF	Tetrathiafulvalene
V _{g-s}	Voltage gate-source
V _{s-d}	Voltage gate-drain
XRD	X-ray diffraction
ZnO	Zinc oxide

Table of contents

Declaration.....	2
Abstract.....	3
Acnowledgements.....	4
Dedication.....	7
Abbreviations.....	8
Table of contents.....	10
Table of figures.....	13
Chapter 1.....	20
Introduction.....	20
1.1 Early history of the TTF electron donor molecule.....	21
1.1.2 Overview of the TTF and BEDT-TTF donor's main features. Crystal packing of TTF and BEDT-TTF derivatives.....	23
1.2 Electrical conductivity in solids.....	25
1.2.1 Band theory in metals, semiconductors and insulators. ^{14,15)}	25
1.2.2 Superconductivity.....	29
1.2.3 Applications of semiconductors and superconductors.....	33
1.2.4. OFETs, OLEDs and OPVs.....	34
1.2.5. The SQUID ²⁹⁾	39
1.2.6. Conductivity measurements.....	40
1.2.7. Electrocrystallisation ³⁰⁾	41
1.3 Magnetism.^{14,15)}.....	43
1.4 Organic conductors.....	47
1.4.1. Carbon based molecules.....	47
1.4.2. Polymers.....	48
1.4.3. Overview of TTF substituted donors for conducting materials and some of their applications.....	51
1.4.4 Fullerene-based polymers and oligomers for photovoltaic applications.....	54
1.4.5 TTF as a building block for molecular switches, receptors, molecular machine and its use in organic synthesis.....	55
1.5 Bibliography.....	60

Chapter 2	66
Attempted synthesis of BEDT-TTF dimers and related substituted BEDT-TTF donors obtained.	66
2.1 Introduction.....	67
2.2 Background.....	73
2.3 Result and Discussion	79
2.3.1 Ether and thio-ether bridged BEDT-TTF dimers.	79
2.3.2 Attempted preparation of dimeric BEDT-TTF system by reacting two substituted ET donors together.	85
2.3.3 Attempting the synthesis of dimeric BEDT-TTF systems using optically active linkers.....	95
2.3.4 Progress in the preparation of bis-substituted BEDT-TTF donors.....	102
2.3.5 Progress in the preparation of new substituted donors from allyl-oxo-methyl-BEDT-TTF (60).....	105
2.3.6 Preparation of radical cation and charge transfer salts by electrocrystallisation and diffusion experiments.	108
2.4 Conclusions and Future work.....	119
2.5 Experimental Part.....	120
2.6 Bibliography.	141
Chapter 3	145
Preparation of novel enantiopure TTF derivatives.	145
3.1 Introduction.....	146
3.2 Background.....	151
3.3 Results and discussion.	156
3.3.1 Preparation of novel enantiopure donors capable of hydrogen-bonding interactions at different levels.....	156
3.3.2 Preparation of racemic and enantiopure donors where hydrogen-bonding is coupled with enhanced π - π stacking interactions.....	157
3.3.3 Preparation of donors from racemic and enantiopure 2-methoxymethyl-oxirane.	164
3.3.4 Preparation of an asymmetric chiral hexol donor (70).....	167
3.3.5 Attempted preparation of the new enantiopure tetrol donor (71).....	171

3.3.6 Cyclic voltammetry of the new donors prepared.....	175
3.4 Conclusions and future work.....	177
3.5 Experimental part.....	179
3.6 Bibliography.....	196
Chapter 4	200
Synthesis of new metal binding BEDT-TTF donors and their magnetic properties.....	200
4.1 Introduction.....	201
4.2 Background.....	204
4.3. Results and Discussion.....	207
4.3.1 Synthesis of the new BEDT-TTF donors containing the iminodiacetate ligand.....	207
4.3.2 Preparation, characterisation and investigation of the magnetic properties of metal complexes formed using donor (39).....	216
4.3.4 Cyclic voltammetry of the new donor synthesised.....	235
4.4 Conclusions and future work.....	237
4.5 Experimental part.....	238
4.6 Bibliography	248

Table of figures

Figure 1. Donors containing an alkene functionality on the side chain.	3
Figure 2. Desired dimer system (II).	3
Figure 3. Examples of enantiopure donors prepared in chapter 3.	3
Figure 4. Type of BEDT-TTF ligands designed for metal complexes preparation.	3
Figure 5. Bis-substituted TTF donors prepared by Prinzbach and co-workers.	22
Figure 6. Oxidation of donor (11) to its radical cation and dication species.	22
Figure 7. The bis(ethylenedithio)tetrathiafulvalene donor.	23
Figure 8. Mono and bis –cationic species become aromatic after oxidation of the neutral molecule.	23
Figure 9. Multiple non-covalent interactions available for the stacked BEDT-TTF donors.	24
Figure 10. The tetramethyl-tetraselenafulvalene donor.	24
Figure 11. Energy band diagrams for a metal.	26
Figure 12. Energy band diagrams for an insulator.	26
Figure 13. Log. conductivity 1/temperature plot for metals, semiconductors and insulators.	27
Figure 14. Semiconductor energy bands at r.t.	27
Figure 15. Silicon 2D lattice and boron doped silicon 2D lattice.	28
Figure 16. Dopant species with energy level close to the valence band.	28
Figure 17. Silicon 2D lattice and phosphorus-doped silicon 2D lattice.	29
Figure 18. Dopant species with energy level close to the conduction band.	29
Figure 19. Plot of the resistivity of mercury at few degrees Kelvin.	30
Figure 20. The Meissner effect. The lines of the magnetic flux a) penetrate the sample ($T > T_c$) and b) avoid the sample by passing around it ($T < T_c$). In situation b) the magnetic field inside the sample is zero.	31
Figure 21. Magnetisation behaviour for a) type I and b) type II superconductors in response to an external magnetic field.	33
Figure 22. Schematic representation of a p-n junction.	35
Figure 23. Schematic representation of forward and reverse biased.	36
Figure 24. Schematic OFET device structure.	37
Figure 25. Example of constituent of the active layer in an OLED device.	38
Figure 26 ²⁷⁾ . Schematic structure of an OLED device.	38

Figure 27. Schematic composition of an organic solar cell.	39
Figure 28. PEDOT and PSS polymer and the fullerene derivative PCMB.....	39
Figure 29. Schematic illustration of the SQUID components.....	40
Figure 30. Schematic representation of the four-probe method to measure the resistivity of a sample.	41
Figure 31. Typical electrocrystallisation experiment apparatus.....	42
Figure 32. Orientation of magnetic moments a) in paramagnetic materials at all temperatures, b) in ferromagnetic, c) antiferromagnetic and d) ferrimagnetic materials at low temperatures.	43
Figure 33. $1/\chi$ plotted against Temperature for Curie and Curie-Weiss law.....	45
Figure 34. Plot of χ against T for a) a paramagnetic material, b) a ferromagnetic and c) antiferromagnetic materials at low temperatures.	45
Figure 35. Violanthrene (16) and Isoviolanthrene (17).....	47
Figure 36. Bond connectivity in polyethylene and polyacetylene. Unsaturation in polyacetylene allow electron to flow through the polymer.....	48
Figure 37. Example of known doped conductive polymers.....	49
Figure 38. Monomers of dialkyloxythiophene and the PEDOT and PSS polymers.	50
Figure 39. A few examples of TTF-based polymers.....	50
Figure 40. TTF-based polymers prepared by Shimizu and Yamamoto.	51
Figure 41. Examples of a TTF-based polymer where TTF is in the main chain.	51
Figure 42. TSF (32) and TM-TSF (15) donors.	52
Figure 43. ⁵²). Donor molecules giving superconducting salts with the number of superconductor species and the highest T_c recorded in brackets.	52
Figure 44. Oxygen based donors.....	53
Figure 45. The molecular rectifiers proposed by Aviram and Ratner (35) and prepared by Metzger et al. (36).....	53
Figure 46. Examples of substituted C_{60} fullerene oligomers.	54
Figure 47. Example of molecular dumbbell system.....	55
Figure 48. Example of a TTF-crown-ether receptor with high sensitivity for sodium. .	55
Figure 49. Standard preparation of tetrasubstituted TTF donor (45).....	56
Figure 50. Example of cationic receptor based on a calix[4]arene with amide substituted TTF donor.	57
Figure 51. Examples of TTF substituted receptors with a conjugated core.....	57
Figure 52. Anion receptor based on substituted TTF.....	57

Figure 53. Example of a calix[4]pyrrole reported in the literature.	58
Figure 54. Example of a disubstituted TTF as a receptor for neutral guest.	58
Figure 55. ⁸²⁾ Example of how the two units can assemble and act as a molecular machine.	59
Figure 56. Radical polar crossover reaction mechanisms.	59
Figure 57. Example of various types of TTF dimer depending on the linkage between the two units.	67
Figure 58. Classification of the TTF dimers depending on the spacer in between the two TTF units.	68
Figure 59. Different types of condensed TTF donors.	68
Figure 60. The two different connections for the TTF unit to interact with each other.	68
Figure 61. Redox processes for a TTF dimer and formation of radical cations and multi-cationic species.	69
Figure 62. Examples of the strategies that can be adopted to enhance dimensionality.	69
Figure 63. Emphasis on the difference between TTF and BEDT-TTF.	70
Figure 64. Conjugated TTF dimers based on sulphur and selenium network atoms.	72
Figure 65. Examples of conjugated dimers with an unsaturation in the linker.	72
Figure 66. Different examples of π -extended-TTF systems.	72
Figure 67. Generic desired targeted BEDT-TTF dimer.	73
Figure 68. Proposed mechanism for the single electron reduction reaction between carbon disulphide and metallic sodium in DMF.	76
Figure 69. Mechanism of the exchange sulphur-oxygen reaction on substrate (47) using mercury (II) acetate.	78
Figure 70. Mechanism of the phosphite mediated coupling to furnish the BEDT-TTF building block.	78
Figure 71. Comparisons of the tlc plates developed at different conditions for the attempted deprotection of donor (73) with NaH and CsOH.	87
Figure 72. Comparison between the tlc plates developed for the two different methodology.	88
Figure 73. Proposed mechanism for the displacement of cyano-ethyl group.	89
Figure 74. Hybridisation of carbon next to the sulphur in the system investigated.	89
Figure 75. Identification of the reagents involved on the developed tlc plate.	89
Figure 76. The second electrophile added to the reaction mixture.	90

Figure 77. Identification of the reagents involved onto the tlc plate developed for monitoring of the reaction.	91
Figure 78. Quenching the reaction with AcOH should led to the formation of donor (86).	91
Figure 79. Donor (93) reported in the literature which is an isomer of donor (92).	94
Figure 80. New targeted dimeric BEDT-TTF system.	94
Figure 81. New targeted donor (121) able to undergo further cyclisation reaction.	103
Figure 82. Targeted compound for diffusion and electrocrystallisation experiments. ..	105
Figure 83. Resonance of the negative charge in the thiocyanate anion.	105
Figure 84. Donors analysed by C.V.	109
Figure 85. Conjugation effect which contribute to the slightly different behaviour of the donor (92).	109
Figure 86. Molecular structure of the salt (92).ClO ₄ with anisotropic displacement parameters drawn at the 50% level, and only one orientation of the disordered anion shown.	111
Figure 87. Crystal packing of the salt (92).ClO ₄	111
Figure 88. Inter-dimer S···S contacts in the salt (92).ClO ₄	112
Figure 89. Face to face radical cation pair surrounded by triiodide anions and iodine molecules in the crystal structure of (92)I ₃ ·0.5I ₂ . Anisotropic displacement parameters are drawn at the 50% level.	113
Figure 90. The c rystal structure of (92) I ₃ ·0.5I ₂ showing the lines of triiodide anions lying between donor cation pairs and cross linked with iodine molecules.	113
Figure 91. S···S contacts within a radical cation pair and between adjacent pairs in the crystal structure of (92) I ₃ ·0.5I ₂	114
Figure 92. Resistivity response to the temperature changes of the crystal of (92)I ₃ ·0.5I ₂	115
Figure 93. Resistivity response to the 1/temperature changes of the crystal of (92)I ₃ ·0.5I ₂	115
Figure 94. Packing in the unit cell as a) ball and stick and b) spacefill viewed down to the a axis.	116
Figure 95. Crystal structure of (60)·2ClO ₄ viewed down the <i>a</i> axis.	116
Figure 96. View of the donor cation of (60) showing the two disordered orientations of the side chain and how they overlap.	117
Figure 97. Contacts (Å) between the donor dication and perchlorate anions.	118

Figure 98. Future strategy to realise bridged-BEDT-TTF dimers.	119
Figure 99. Some of the new donors prepared which could be polymerise	119
Figure 100. Chiral anion and TTF derivate donor electrocrystallised together.	149
Figure 101. A few examples of the donors involved in the electrocrystallisation with chiral anion (TRISPHAT).	150
Figure 102. Crystal packing of (35) ₄ Fe(III) ₂ (oxalate) ₅ with oxalate bridges in evidence.	153
Figure 103. Example of bis-pyrrole –TTF’s.	155
Figure 104. Target donors from substituted epoxides as starting materials.	156
Figure 105. Targeted mixed donor (70), tetrol (71) and octol (72).	157
Figure 106. Targeted donors to combine hydrogen bonding and π - π interactions.	158
Figure 107. Examples of chiral donors bearing H bonding groups reported in the literature.	164
Figure 108. Targeted cross- and homo-coupled donors to be prepared.	164
Figure 109. Desired cross-coupled donor (112) and the two homo-coupled donors formed in the coupling reaction.	170
Figure 110. Donors characterised by C.V.	176
Figure 111. Novel enantiopure donors prepared.	177
Figure 112. Examples of TTF derivatives bearing organic radicals by Suguwara <i>et al.</i>	202
Figure 113. TTF donors substituted with organic radicals by Pilkington <i>et al.</i>	202
Figure 114. Proton NMR for alkene (39).	208
Figure 115. Enlargement for the zones where extra peaks are seen and where NH-CH ₂ - in the starting material should fall if present.	208
Figure 116. Proton signals split after cyclisation reaction (red arrows).	210
Figure 117. Crystal structure of <i>a</i>) donor (43) and <i>b</i>) its packing in the unit cell viewed from <i>a</i> axis.	211
Figure 118. Infinite line of donors connected through S---S intermolecular interactions viewed along <i>a</i>) <i>c</i> and <i>b</i>) <i>b</i> axis.	211
Figure 119. Characteristic “Y” shaped formed by donors packing one next to each other.	212
Figure 120. Proposed structure for Fe (II) complex with ligand (39).	217
Figure 121. $\chi(T)$ vs T data for Fe (II) complex of (39).	218
Figure 122. $1/\chi$ vs T data for Fe (II) complex of (39).	218

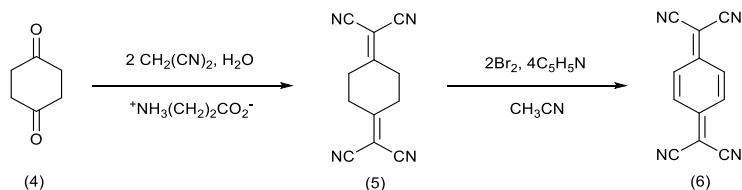
Figure 123. Proposed structure for Ru (III) complex with ligand (39).....	219
Figure 124. $\chi(T)$ vs T data for Ru (III) complex of (39).....	219
Figure 125. $1/\chi$ vs T data for Ru (III) complex of (39).....	220
Figure 126. Proposed structures for Mn (II) complex of (39).....	221
Figure 127. $\chi(T)$ vs T data for Mn (II) chloride complex of (39).....	221
Figure 128. $1/\chi$ vs T data for Mn (II) chloride complex of (39).....	221
Figure 129. Proposed structures for Mn ^(II) (hfac) ₂ complex with ligand (39).....	222
Figure 130. $\chi(T)$ vs T data for Mn ^(II) (hfac) ₂ complex of (39).....	222
Figure 131. $1/\chi$ vs T data for Mn ^(II) (hfac) ₂ complex of (39).....	223
Figure 132. IR spectra of starting material and solid obtained-Mn (II) (hfac) ₂ -complex.	223
Figure 133. Enlargement for the -CF ₃ zone for manganese salt (blue line) and for the complex formed (green line)......	224
Figure 134. Proposed structures for Zn (II) triflate complex with ligand (39).....	225
Figure 135. IR spectra for zinc triflate and the complex of (39) with zinc triflate.	225
Figure 136. IR spectra for the manganese (II) triflate and the complex with ligand (39).	226
Figure 137. Enlargement in the characteristic triflate zone.	226
Figure 138. Proposed structures for Dy (III) complex with ligand (39). Reaction in ACN.	227
Figure 139. $\chi(T)$ vs T data for Dy (III) (triflate) ₃ complex with (39). Reaction in ACN.	227
Figure 140. $1/\chi$ vs T data for Dy (III) (triflate) ₃ complex with (39). Reaction in ACN.	228
Figure 141. Proposed structures for Dy (III) complex with ligand (39). Reaction in MeOH.....	228
Figure 142. $\chi(T)$ vs T data for Dy (III) (triflate) ₃ complex with (39). Reaction in MeOH.	228
Figure 143. $1/\chi$ vs T data for Dy (III) (triflate) ₃ complex with (39). Reaction in MeOH.	229
Figure 144. IR spectra for the Dy(III) (triflate) ₃ and the two complexes formed with ligand (39).....	229
Figure 145. Enlargement of the critical zone for triflate bands.	230
Figure 146. Proposed structures for Pr(III) triflate complex with ligand (39).....	230

Figure 147. IR spectra for praseodimium (III) triflate and its complex with ligand (39)	231
Figure 148. Enlargement for the characteristic triflate zone.....	231
Figure 149. Diol donors in their <i>trans</i> and <i>cis</i> conformation.....	232
Figure 150. Suggested structure for the complex (10)	233
Figure 151. A possible structure for complex (11)	234
Figure 152. An alternative structure for complex (11)	234
Figure 153. Proposed structure for complex (12)	234
Figure 154. An alternative structure for complex (12) following hydrolysis of the metal salt.....	235
Figure 155. Donors characterised by CV measurement.....	235

Chapter 1

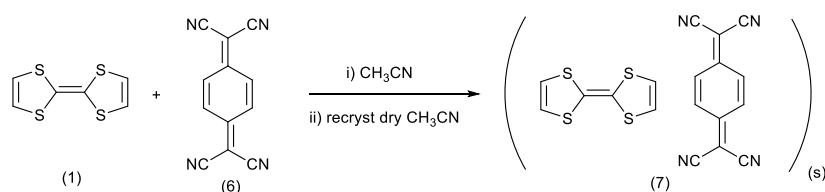
Introduction.

prepared by the chemists of Du Pont. It was the tetracyano-*p*-quinodimethane molecule (**6**), known as TCNQ ⁵).



Scheme 3 Preparation of TCNQ by Du Pont chemists.

Then the real sparkle occurred when the two molecules were mixed together by Cowan, Perlstein *et al.* to generate a 1:1 complex of TTF:TCNQ which when recrystallized gave an electrical conductivity value σ_{\max} of $1.47 \cdot 10^4 \text{ ohm}^{-1} \cdot \text{cm}^{-1}$ at 66 K ⁶).



Scheme 4. Preparation of the 1:1 complex between TTF and TCNQ.

It is worth to say that a series of compounds (**8**) – (**10**) containing the core of TTF (**1**) had been reported shortly before ⁷) charge-transfer complex (**2**) but without any description of their properties.

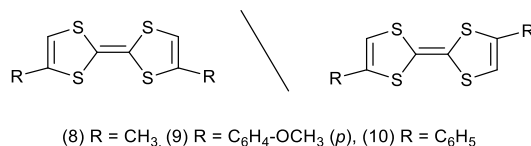


Figure 5. *Bis*-substituted TTF donors prepared by Prinzbach and co-workers.

Another publication by Hunig *et al.* ⁸) reported *via* polarography that the dibenzo derivative (**11**) is reversibly oxidised to the radical cation (**12**) and the dication (**13**).

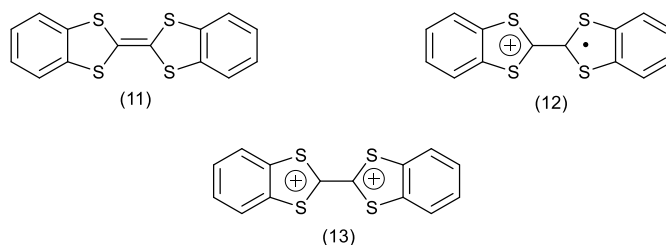


Figure 6. Oxidation of donor (**11**) to its radical cation and dication species.

Another important step in the history of TTF derivatives as organic conductors was the preparation of the donor known as, BEDT-TTF or ET (**14**), which has been a successful building block for the preparation of organic superconductors in the TTF family ⁹).

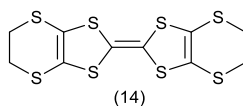


Figure 7. The bis(ethylenedithio)tetrathiafulvalene donor.

These were some of the beginning facts that triggered the explosion of interest in the TTF based molecules and their potential application as active organic conductors in electronic devices. Still nowadays the TTF is the main heterocyclic system studied and used for the preparation of organic metals, semiconductors and superconductors ¹⁰⁾. Many reviews have been dedicated to this topic ¹¹⁾ and according to a recent publication ¹²⁾ there are more than ten thousand published papers on the preparation, property investigation and application of TTF derivatives.

1.1.2 Overview of the TTF and BEDT-TTF donor's main features.

Crystal packing of TTF and BEDT-TTF derivatives.

The possibility for the TTF electron donor of showing electrical conductivity finds its origin in the planarity of its structure and in their face to face π - π stacking ability in order to form long chains of donors where the non-covalent interactions play a major role in “linking” of the molecule to one another. Also the non-covalent S---S interactions between the sulphurs of one donor with the sulphurs of the donor above and below is really important to keep the species at the right distance to each other. The order of this distance is from around 3.3 Å upwards. Indeed the TTF donor once oxidised is able to delocalise the charge onto both rings and also in the cationic species formed the stabilisation is enhanced by the gain aromaticity of the system as outlined in figure 8 ¹²⁾ below.

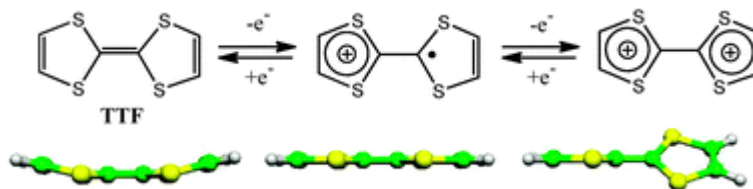


Figure 8. Mono and bis -cationic species become aromatic after oxidation of the neutral molecule.

The comparison of the TTF molecule with BEDT-TTF and its stacking interaction, after oxidation, makes clear why the addition of peripheral dihydro-dithiin rings increases the self-assembling (and to an increase of dimensionality) was and still is one of major trends in TTF chemistry. This expansion increase the non-covalent S---S interaction not only with the donors above and below (S---S between sulphurs in the dithiin rings) but

also with the donors forming the other columns. In this way there will be non-covalent interactions between the pair and among the pairs of donors (Figure 9).

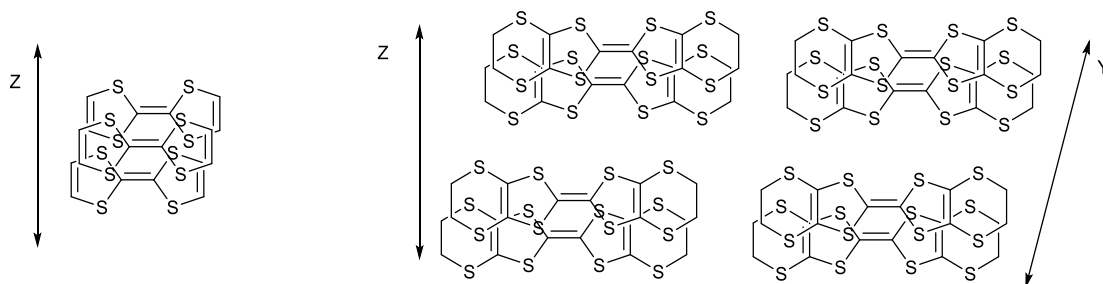


Figure 9. Multiple non-covalent interactions available for the stacked BEDT-TTF donors.

This is also the reason why there are examples of quasi 2D-superconductors based on the BEDT-TTF donor, while the superconductors based on the tetramethyl-tetraselenafulvalene (**15**), TM-TSF, are quasi one-dimensional¹³.

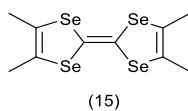


Figure 10. The tetramethyl-tetraselenafulvalene donor.

1.2 Electrical conductivity in solids.

1.2.1 Band theory in metals, semiconductors and insulators.^{14,15)}

The electric conductivity in the solid state is a bulk property of materials which can be described as the measure of how easily the electron can jump from the valence band to the conduction band of the solid involved. An understanding of how the electrons flow is given by the band theory of solids. According to how easily the electrons flow in a solid lattice the materials have been divided into metals, semiconductors and insulators. The differences among them are related to:

- 1) the band structure of the material involved,
- 2) whether the valence bands are full or partially full,
- 3) the magnitude of any energy gap involved for the “jump” of an electron from the full to the empty bands.

In a metal the valence band consists of the electrons which occupy the valence shell of each orbital where the energy levels are so close to one another that the electrons can be seen as delocalised over the entire lattice through a giant orbital. For example in the case of sodium which has an electron configuration of $1s^2 2s^2 2p^6 3s^1$ every atom has an electron in its $3s$ orbital, which for the number of atoms present in a mole of sodium can be seen as a mole of electrons delocalised over the entire lattice of metallic sodium. For the transition metals it is the d the electrons which are delocalised on the entire lattice. This is why all metals are good conductors of electricity. In a metal the band structure has the following configuration: the highest occupied band, the valence band, is only partially full and touches or overlaps the conducting band so for the electrons the jump does not require energy ($E \leq \sim 0.01$ eV) because there is no gap between the valence and the conducting band.

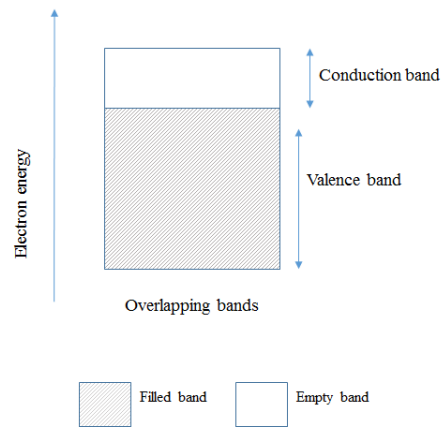


Figure 11. Energy band diagrams for a metal.

In the case of an insulator the valence band is completely full and it is separated by a large gap from the conduction band, the band with the next energy level, which is completely empty. For example diamond is a good insulator and the jump between the two bands requires ~ 6 eV, which means that hardly any electrons can jump and the conductivity is negligible.

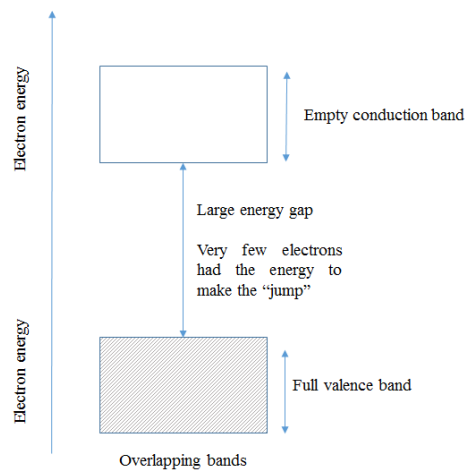


Figure 12. Energy band diagrams for an insulator.

In the case of semiconductors the topic is a bit more extensive and more cases need to be considered. A semiconductor has similar band structure to the insulator, where the valence band is full and the conductive band is empty, but the energy between the two is not as large as for the insulator and it is usually between 0.5-3.0 eV. In this situation a few electrons have the energy required and electrical conductivity is possible.

A general formula to describe the conductivity is given by:

$$\sigma = n \cdot e \cdot \mu;$$

where n is the number of current carrying species, e is their charge and μ is their mobility. In a metal n is large but μ decreases when the temperature rises (electron-photon collisions). This means that for a metal the conductivity gradually decreases as the temperature

goes up. In a semiconductor n is quite small and it may increase by the action of temperature or by doping the semiconductor. In the former case n increases exponentially with temperature and so does σ , even if there is small change in μ (intrinsic semiconductors). In the latter case the addition of dopants creates more mobile carriers, and thus a bigger n , and these are in larger number than the number generated by an increase in temperature. This means that n is independent of the temperature and σ decreases with temperature (extrinsic semiconductors).

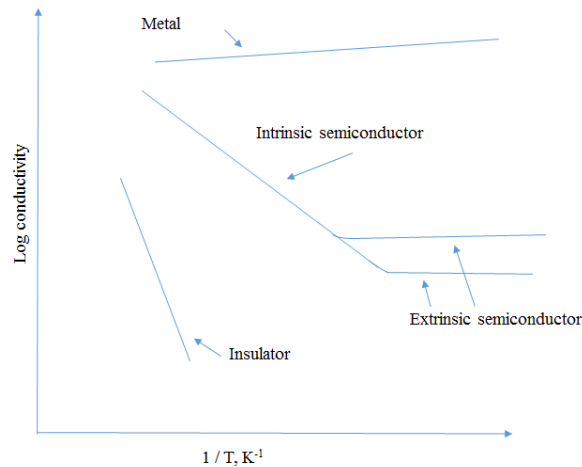


Figure 13. Log. conductivity 1/temperature plot for metals, semiconductors and insulators.

For an intrinsic semiconductor the band theory at r.t. presents a situation like the one outlined in Figure 14. At r.t. few electrons have enough energy to leave the valence band and “jump” into the conduction band. In this way they create holes in the valence band, as many as there are electrons in the conductive band. Now at this stage the valence band is only partially full and it may conduct electricity and this is what the holes do too.

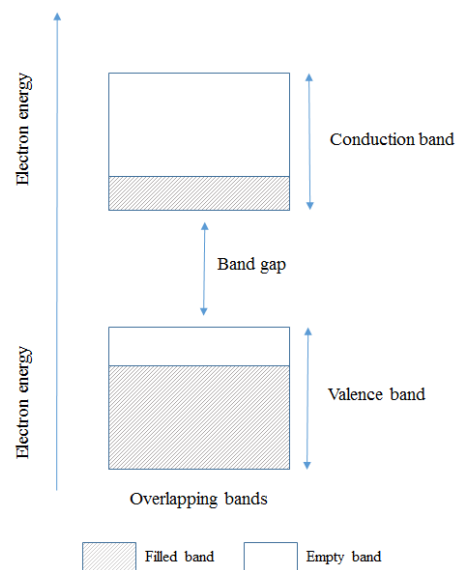


Figure 14. Semiconductor energy bands at r.t.

In extrinsic semiconductors there are dopants, commonly called impurities, which means that some other atoms have been added into an intrinsic semiconductor to modify its conductivity. What kind of atom can be added to modify a semiconductor depends on what atoms form the semiconductor. A simple example is to consider a silicon based semiconductor. Silicon has four valence electrons and it is connected with other four silicon atoms in its 2D bonding arrangements. A possibility is to add an impurity coming from the Group Three such as boron or gallium. With its three valence electrons the boron atom insert in the lattice an electrodeficient bond which is associated with an atomic orbital that sits at the top of the valence band (Figure 15). Because of its electron deficiency this energy level is called acceptor level. The energy gap ($E_a - E_v$) between the valence band and the acceptor level is around 0.1 eV, much smaller than the normal 1.1 eV in the pure silicon semiconductor. The electrons from the valence band have sufficient energy (at r.t.) to jump on to the acceptor level to fill the electron deficiency (or hole). This originates the conductivity in a *p*-type semiconductor such as a boron doped silicon semiconductor. The name *p*-type take its origin from the fact that the electron deficiency (on the acceptor level) is presented as a hole (intended as positively charged in opposition to the charge of the electron) and the conduction mechanisms depends on their presence.

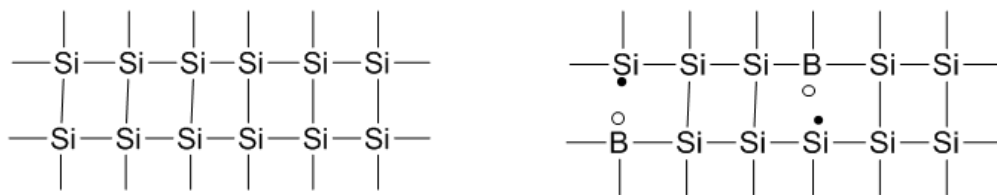


Figure 15. Silicon 2D lattice and boron doped silicon 2D lattice.

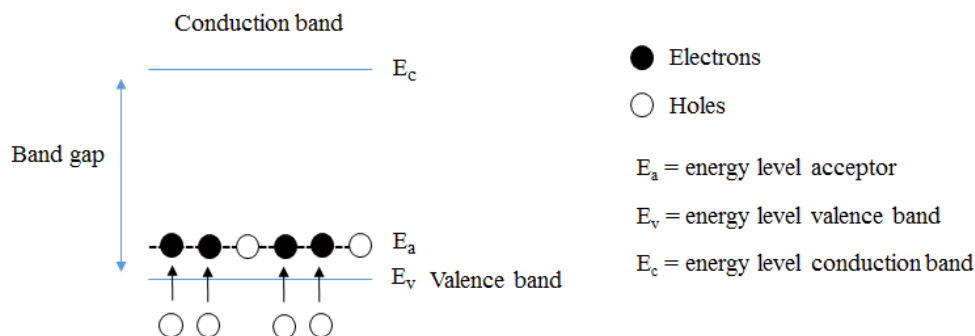


Figure 16. Dopant species with energy level close to the valence band.

The second and opposite way of doping an intrinsic semiconductor is by adding a donor atom, such as phosphorus from Group Five. When a phosphorus atom is introduced into the silicon lattice its five valence electrons can be seen as a donor of one electron which is weakly bound and available for conduction. As presented in the energy level figure, the

impurities have an energy level really close to the conduction band and this means that the “jump” does not need the usual 1.1 eV of a normal silicon semiconductor. The electron that passed from the valence band to the conduction band is available for conduction, and this means that the conduction is by electrons, which is given the name *n*-type semiconductors.



Figure 17. Silicon 2D lattice and phosphorus-doped silicon 2D lattice.

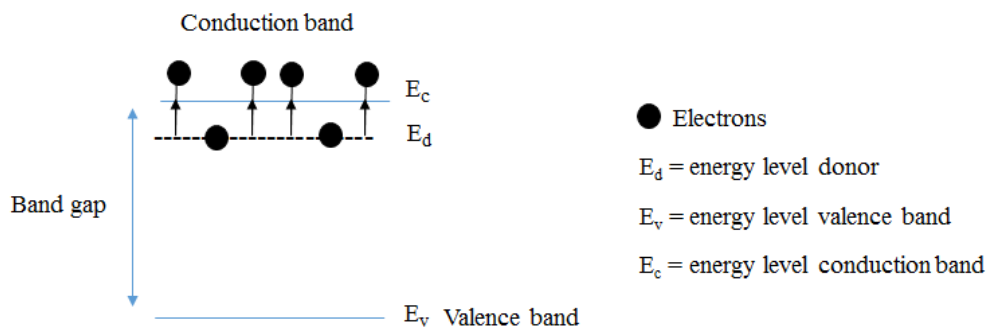


Figure 18. Dopant species with energy level close to the conduction band.

In conclusion, according to the dopant species inserted into the silicon semiconductor it is possible to have two different mechanisms of conduction *a*) by holes, in the case of introduction of acceptor atoms which are electron deficient compared to silicon, or *b*) by electrons, by doping the silicon with atoms which contain more valence electron than silicon. It is important to mention that by having the impurities new allowed energy levels have been introduced in the energy gap between valence and conduction band, which is not possible for the pure material.

1.2.2 Superconductivity.

The phenomenon of superconductivity was observed for the first time by K. Onnes in 1911¹⁶⁾ soon after liquid helium became available in a research lab. During an experiment Onnes was measuring the electrical resistivity of mercury at very low temperature when suddenly at 4.2 K it dropped to zero as shown in Figure 19.¹⁷⁾ This transition to perfect

electrical conductivity is a characteristic of a number of metals and alloys and the temperature at which this phenomenon happens is called T_c . This is a fixed temperature which depends on the material. The electrical resistance of the mercury at this temperature was measured to be $10^{-5} \Omega$ (should really be zero). A few elements are known to become superconductors under pressure.

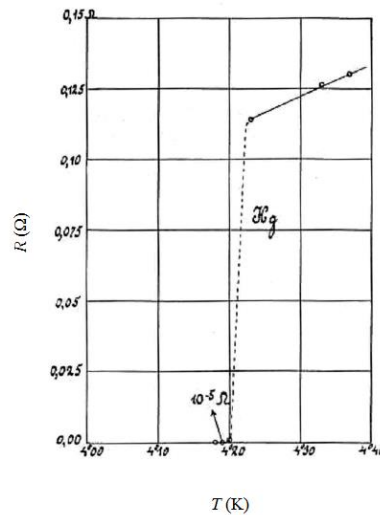


Figure 19. Plot of the resistivity of mercury at few degrees Kelvin.

Superconductivity is a very exciting property and there has been a continuous interest in superconductors with increasingly high T_c and this stimulate physicists, chemists and materials scientists to discover better superconductors. Without going in too much detail there are at least three major milestones in the early history of superconductivity which are worth mentioning, after its experimental observation described above:

1. the observation of the Meissner effect in 1933 ¹⁸⁾,
2. the Bardeen-Cooper-Schrieffer (BSC) theory proposed in 1957 ¹⁹⁾,
3. the Josephson effect discovered in 1962 ²⁰⁾.

Point one is very important and is the result of the discovery by Meissner and Ochsenfeld that a superconductor exhibits perfect diamagnetism as well as perfect electrical conductivity. For a sample exposed to an external magnetic field the lines of the magnetic flux penetrate the sample. When the sample is cooled down to temperatures below its T_c , when its superconductivity emerges, the lines of magnetic flux do not penetrate the sample anymore but just surrounding it as shown in the Figure 20. ^{14 b,c)}

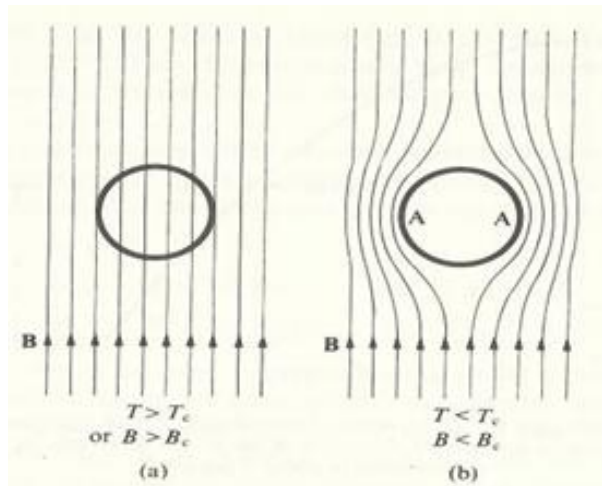


Figure 20. The Meissner effect. The lines of the magnetic flux a) penetrate the sample ($T > T_c$) and b) avoid the sample by passing around it ($T < T_c$). In situation b) the magnetic field inside the sample is zero.

Point two is the theory generally accepted to explain the superconductivity of simple elements such as tin, iridium and mercury and of alloys. It is worth mentioning that for complex systems, like the ceramic superconductors, such as $\text{YBa}_2\text{Cu}_3\text{O}_7$ ²¹⁾ discovered in 1986-87, the understanding is still limited and more theoretical work has to be done. Before the BSC theory an important step was the observation by Maxwell²²⁾ and by Reynolds, Serin, Wright and Nesbitt²³⁾ in the 1950s of the “isotope effect” which gave a relation between the isotopic mass (of mercury) and the T_c temperature. This relation suggests that the interaction responsible for the superconductivity involves deformation of the lattice since the isotopic constitution does not affect the lattice structure of an element or its chemical properties or the static electrical properties such as the Fermi level. This kind of deformation can be related to the attraction between an electron and nearby positive ions of the lattice. This possibility was, independently from the isotopic effect, investigating by Fröhlich²⁴⁾ in the same year (1950). This deformation, together with the local electrical polarisation of the lattice would interact with a second electron to produce an attractive force between the two electrons. This was the basis of Cooper’s work which demonstrated that any source of attraction between a pair of electrons would produce an instability on the Fermi level and generate the formation of “bound pairs” which would lead to further bound pair formation. These pairs of electron are known as “Cooper pairs” and form a ground state above the Fermi surface^{9,25)}

The Josephson effect, also known as the d.c. Josephson effect, was observed by Brian Josephson during his studies on a superconducting ring interrupted by a thin insulating layer. According to Josephson the electron can tunnel through this insulating layer ($< 10 \text{ \AA}$) without the contribution of an external current. This was quite remarkable since in a

normal conductor the current only flows in response to an applied voltage difference and in the presence of a continuous electrical connection. According to this theory an electrical current can flow between two superconductors separated by non-superconducting or insulating layer. This non-conducting layer between the two superconducting units is called a Josephson junction¹⁵⁾. One of the most important application of this discovery is a device named SQUID (Superconducting Quantum Interference Device). This device allows scientists to detect weak magnetic fields.

The BCS theory and the Josephson effect were such important discoveries for the scientific community that all the scientists involved were awarded the Nobel prize for Physics in 1972 for the American physicists John Bardeen, Leon Cooper and John Schrieffler and in the year 1973 for the british scientist Brian D. Josephson.

Superconductors are divided into two major categories named Type I and Type II and their behaviour in response to an applied external magnetic field B is outlined in Figure 21^{14 b,c)}. In the situation *a)* is described the behaviour of type I superconductors. The magnetisation M has a linear relation with the applied external magnetic field up to a critical value called B_c . Above this point the superconductivity appears and the magnetic field does not penetrate into the sample (Meissner effect) so M is zero. Type I superconductors show a perfect diamagnetism, which allow them to be repelled by a magnetic field, and are mostly metals such as mercury, aluminium, and gallium. For the type II superconductors the difference is well described in Figure 21 *b)* where the transition to a superconducting state is not as sharp as for the type I and goes through a region of “mixed state” behaviour. The magnetisation reaches its maximum at a critical B_{c1} value and after that point the superconductivity state is shown but there is still magnetisation through the sample, until a second critical value of magnetic field called B_{c2} . Only at this point is the magnetisation zero. Among the type II superconductors are metals, metal oxides and alloys. To this category belong also the recently discovered superconducting ceramic compounds (cuprates).

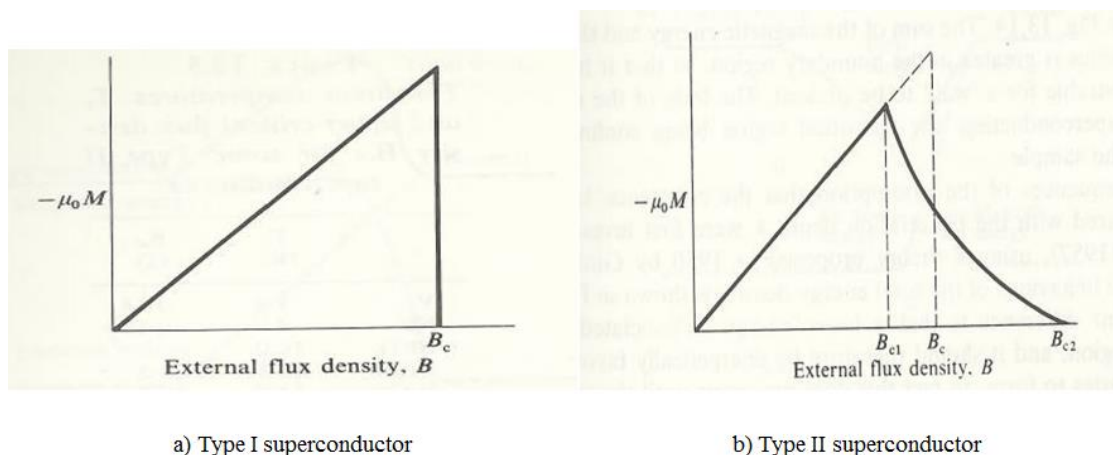


Figure 21. Magnetisation behaviour for a) type I and b) type II superconductors in response to an external magnetic field.

1.2.3 Applications of semiconductors and superconductors.

The aim of semiconductors based on organic materials is to replace the inorganic based semiconductors on a large scale once the performances of the organic based devices is as good as or better than the traditionally used inorganic based devices. A few examples are already commercially available but the technology has not spread out yet on a worldwide scale and into aspects of everyday life. LED (light emitting diode), FET (field-effect transistor) and PhotoVoltaic materials (PV) would be replaced by OLED, OFET (organic-LED/FET) and OPV (organic PV) devices fabricated from organic molecules.

The example of the OLED is probably the most common and the most known due to the presence of this technology in many commercial TV screens and mobile phones ²⁶⁾. Organic photovoltaics (OPVs) or organic solar cells are another interesting application and in this case the organic molecule can replace the silicon based technology or simply cooperate with the inorganic part since the challenge is to have a system which harvests the light, and a component which transport the electrical current. These systems can be organic-organic or organic-inorganic interfaces; the goal is to increase the efficiency of converting the energy captured from sunlight into electrical current ²⁷⁾. Transistors are an important part of the modern electronic devices and the wide application for the organic transistor is for OFETs, organic field-effect transistor where the organic based device would have many advantages compare to the silicon based one ²⁸⁾. Among them is the flexibility which take its origin from the substrate which can be plastic for the OFET but has to be glass in most of the cases for the FET device. This is because the traditionally silicon made FET are made under very extreme conditions such as high vacuum and high

temperature. An OFET can be prepared at r.t. Not less important is the cost at which inorganic and organic semiconductors are made. The inorganic based conductor require a really high purity for the silicon involved which require an expensive purification process while the organic conductors are based on carbon and their high level of purity is reached without expensive treatments.

On the downside most of the organic based devices are still at the prototype scale or their performances are not yet good enough with issues such as low carrier mobility, shorter lifetime than silicon based devices or not stable under the ambient conditions. Superconductivity has found one of its application in magnetic levitation which became known for its example in Birmingham, England, with the world's first MAGLEV train for commercial service. Unfortunately the project have been abandoned in the 1995²⁹⁾. Other examples are present in Japan, China and America. Another important use of superconductors is in the magnets for MRI (Magnetic Resonance Imaging) a non-invasive technique to determine what is going on inside the human body; and as mentioned before in the SQUID (Superconducting Quantum Interference Device) capable of recording very weak magnetic fields. Another application where superconductors played a major role is in the Large Hadron Collider (LHC) at CERN where high energy particles are being accelerated at a speed close to the speed of light to investigate their interaction and to provide explanation to fundamental laws of nature²⁵⁾.

1.2.4. OFETs, OLEDs and OPVs.

Donors based on TTF and its derivatives have many applications, some of them are still relatively new and some others have been a constant presence in the literature such as in the case of OFETs, organic-field effect transistors, OLEDs, organic-light emitting diodes and OPVs, organic photovoltaics. Since these devices are often related with TTF derivatives (and organic conductors in general) a brief overview of their working principles is given. The main constituent of the semiconductor devices mentioned above is the p-n junction which is presented in Figure 22³⁰⁾.

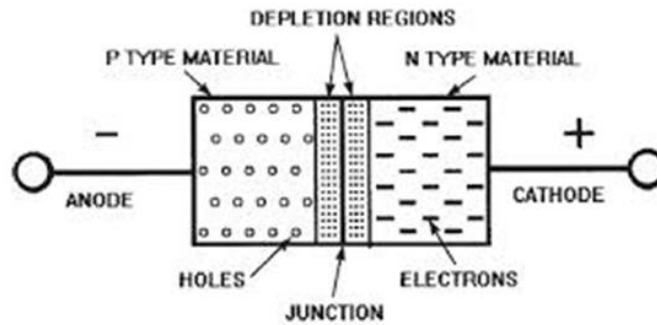


Figure 22. Schematic representation of a p-n junction.

As the name says the two different kind of materials are put together in this device, so on one side is a semiconductor doped with an acceptor which creates holes in the lattice of the semiconductor (silicon doped with boron for example, *p*-type material) and on the other side is a semiconductor doped with a donor which creates free electrons in the lattice of the semiconductor (silicon doped with phosphorus, *n*-type material). The two different species want to diffuse into each other, the electrons want to diffuse into the *p*-type material to “neutralise” the holes and the same for the holes towards the *n*-type region. This diffusion process happens up to a certain point which culminates with the creation of a charge-free zone called the depletion zone. Basically when an electron or a hole tries to diffuse into the other zone, as soon as it enters the depletion zone is repelled back into its region due to the lack of charges in the depletion zone. To have diffusion into the opposite zone a voltage should be applied to furnish some energy to holes and electrons to go through the depletion zone. In this situation there is no current flowing into the p-n junction. To make something happen we should apply a voltage to the electrodes and the choice of connecting cathode or anode to the p-or n-zone makes a big difference and can create a forward or reverse p-n junction. The two cases are outlined schematically in Figure 23 and compared with the zero voltage situation.

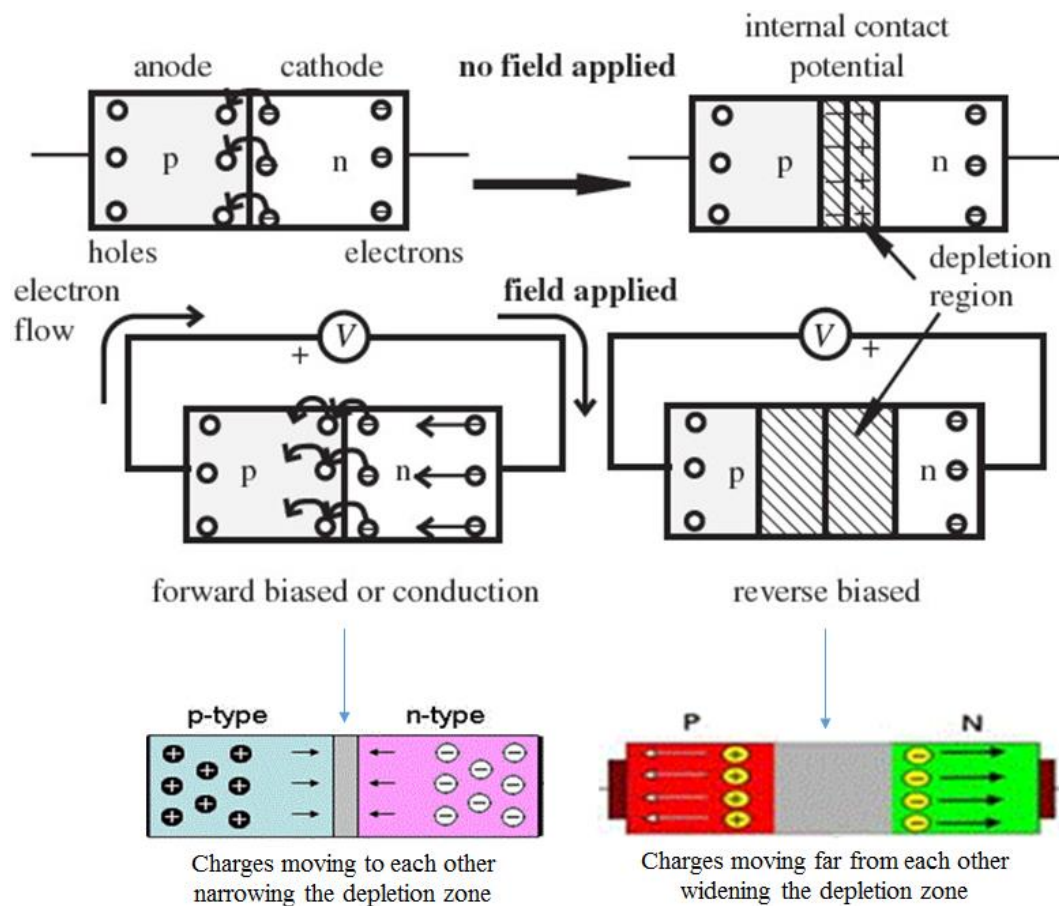


Figure 23. Schematic representation of forward and reverse biased.

When the p -region is connected to the positive electrode (anode) and the n -region with the negative electrode (cathode) the charges are pushed towards each other, the energy furnished to the particles is enough to overcome the energy barrier (depletion zone) and a current flows in the junction. In the opposite situation where the p -region is connected to the negative electrode (cathode) and the n -region with the positive electrode (anode) the charges are pushed away from each other and toward their respective electrodes. In this way the depletion zone is wider and there is no current flowing in the system ¹⁴⁾.

OFET ²⁸⁾.

An OFET device can be found in circuits and /or displays and its schematic structure is presented in Figure 24. There are various geometries for an OFET device according to the position of the gate (top or bottom) and according to the contacts between the metal electrodes and the active layer.

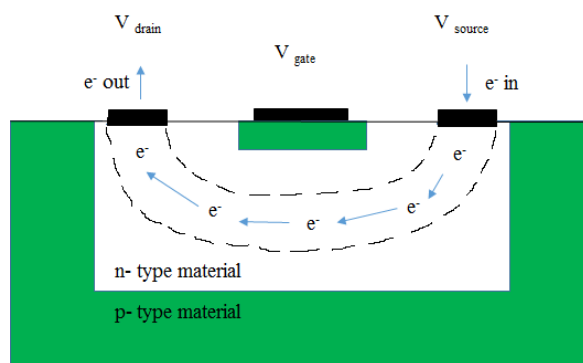


Figure 24. Schematic OFET device structure.

The picture in Figure 24 represents a p-n junction where the active material for electron conduction is an *n*-type polymer or small molecule. The electrons can flow from source to drain in response to a voltage V_{s-d} applied. The metal electrodes are attached to the semiconducting layer. The electrons are flowing into the semiconductor's channel and if only the voltage V_{s-d} is applied the electrons will flow with ease but at the same time they are repelled by the charges present in the *p*-type material so the channel is not as wide as the *n*-type zone. If in this situation a voltage $-V_{g-s}$ is applied ($-V_{g-s}$ is in opposition to the V_{s-d} that is why it is minus) the repulsion between the charges in the *n*-type and *p*-type material is increasing and the channel for the electron conduction in the *n*-type material is narrowing. The extreme situation is when $-V_{g-s}$ is bigger than V_{s-d} and there are no electrons flowing in the *n*-channels. In this case the current is zero, so in principle the transistor can be used to control the current between two electrodes by applying a second voltage at the gate.

OLED ²⁶⁾.

An OLED is a solid-state device where the active layer can be an organic polymer or small organic molecules and whose main constituents are: *a*) the cathode, *b*) two organic layers, one which transports the electrons and the second one to emit light, *c*) the anode and *d*) a substrate. The anode and the substrate are usually stuck together where the former is likely to be made of iridium tin oxide (ITO) due its high transparency. The conductive layer can be made of polymers such as polyaniline or small molecules as in the case of aluminium quinolone (Alq_3) while the emitting layer can be made of CBP (red light) and/or DCM (green light) and/or perylene (blue light). The Aluminium quinolone can also be used a green light emitter (Figure 25).

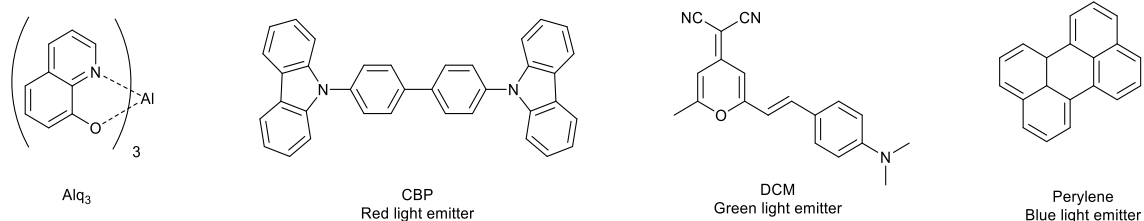


Figure 25. Example of constituent of the active layer in an OLED device.

The OLED device's composition is outlined in the Figure 26.²⁷⁾ Electrons are pushed from the cathode to the emissive layer and at the same the anode removes electrons from the conductive layer creating holes. When at the interface between the two layers the electrons fill the holes the energy released is emitting in the form of photons.

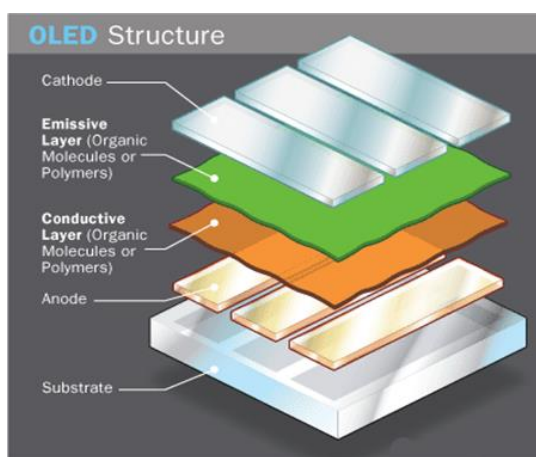


Figure 26³¹⁾. Schematic structure of an OLED device.

OPV³²⁾

Organic solar cells or organic photovoltaics are an application where organic polymers or small molecules cannot yet compete and replace the inorganic based solar cells. It is reported that the efficiency (conversion of photons absorbed into an electric current) of an inorganic solar cell can achieve the value of 20%, where the efficiency for the OSC is currently around 10%.²⁸⁾ The solar cell, organic and inorganic based, operates following the photovoltaic effect which can be described as the generation of a voltage difference at the junction between two different materials in response to an incident visible radiation. Inside a solar cell the conversion of the sunlight to electric current can be seen as a three step process where 1) is the generation of the current by the incident radiation, 2) is the separation of the charge carriers and 3) is the collection of the charge carriers at the right electrodes to produce the electrical current. The composition and the structure of an or-

organic solar cell is presented in Figure 27. The organic solar cell can be described as normal or inverted depending on the direction of the charge flow. In the normal geometry the positive electrode is attached to the substrate and the light shines on them before being absorbed in the active layer (situation of Figure 27) while in the inverted geometry the two electrodes and the charge selective layers are switched around.

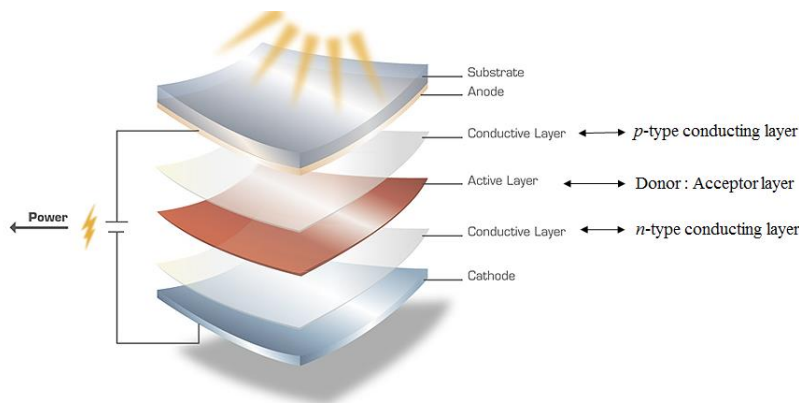


Figure 27. Schematic composition of an organic solar cell.

The active layer is formed from a donor component (polymer or small molecule) that absorbs the light and generates excitons (electron-hole pairs); the electrons are then pushed towards the acceptor (usually a C_{60} fullerene derivatives) then travel through the electrons conductive layer (n -type material) and then to the electrode to be converted in electrical current. The hole transport layer (p -type material) can be made of PEDOT: PSS and metal oxide (MoO_x) while the electron conductive layer can be of PCBM and ZnO .

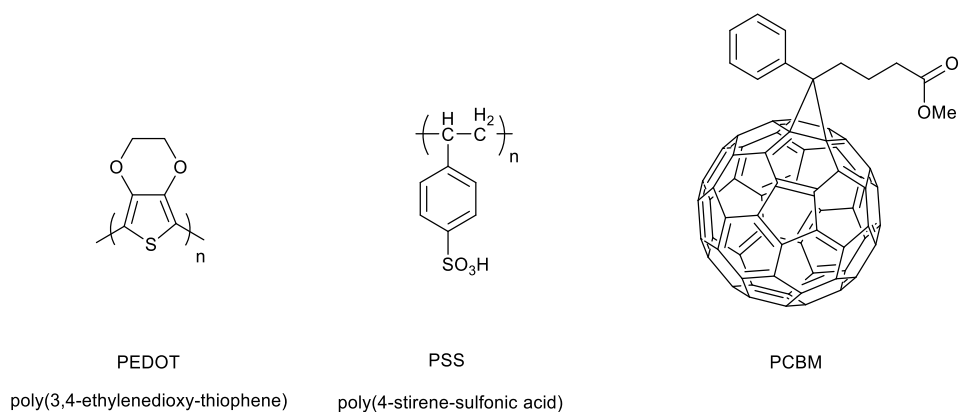


Figure 28. PEDOT and PSS polymer and the fullerene derivative PCBM.

1.2.5. The SQUID ³³).

The SQUID has been already mentioned in the paragraph 1.2.2 as an application of superconducting materials. This device is the most sensitive available to detect magnetic

field and the measurement of the magnetic field from the sample is actually measured indirectly and not directly by the SQUID itself. The sample moves through a system of superconducting detection coils which are located outside the sample chamber and at the centre of the magnet. As the sample moves its magnetic moment induces a current in the detection coils. The detection coils, the superconducting connection wire which connects detection coils and the SQUID input coil can be imagined as a superconducting loop, so any change in the magnetic flux in the detection coils produces a change in the current in the superconducting loop which is proportional to the change in magnetic flux. This variation in the current produces a variation in the SQUID output voltage which is proportional to the magnetic field of the sample. It is as if the SQUID was an extremely sensitive current to voltage converter.

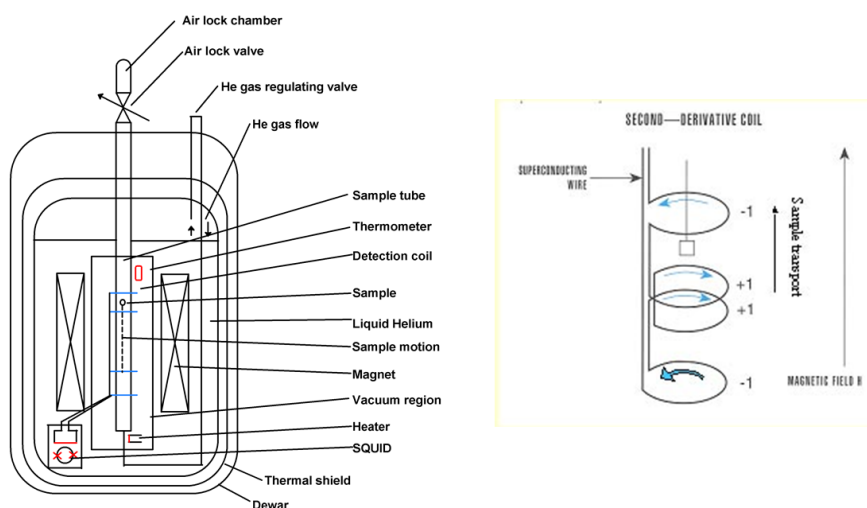


Figure 29. Schematic illustration of the SQUID components.

1.2.6. Conductivity measurements.

The most widely used system for measuring the conductivity of a single crystal is the four-probe method outlined schematically in Figure 30. This method has replaced the two-probe method which is another way of measuring the resistivity across a sample. The main advantage of using a four-probe method is that the recorded value does not contain small resistivity values intrinsic in the system such as the probe resistance and the contact resistance between each probe and the sample analysed. These values may be small but if the resistivity of the sample is very small too, the value recorded may be significantly different from the “true” resistivity value. The four probes numbered 1, 2, 3 and 4, are placed in contact with the surface of the sample and between the contact 1 and 4 is applied a constant current measured by an ammeter. Between the probe 2 and 3 is measured the

drop of potential as the current flows along the sample. The voltage drop is measured by a voltmeter. The resistance of the sample is obtained by the voltage / current ratio and the resistivity from the formula

$$\rho = (R/l) A;$$

where l is the distance between probes 2 and 3 and A is cross-sectional area.

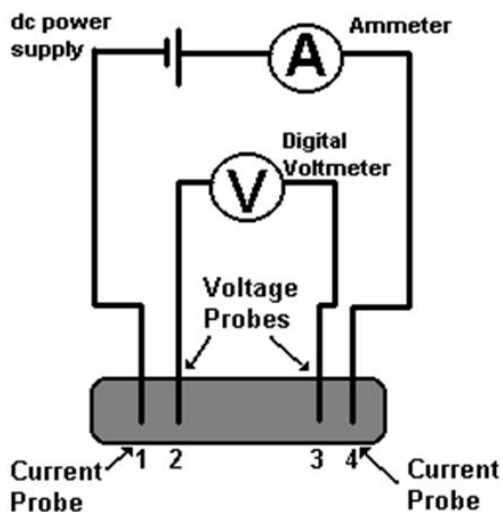


Figure 30. Schematic representation of the four-probe method to measure the resistivity of a sample.

1.2.7. Electrocrystallisation ³⁴⁾.

The electrocrystallisation method is a technique to synthesise high quality crystals of stable radical cation salts of donor systems. The apparatus is represented in Figure 31 and as the name says the redox process is made possible by the current flow. The glassware in use is commonly called an H-shaped cell. The presence of the frit filter in the middle of the cell allows a slow diffusion of the two solutions into each other. For a successful synthesis the solvent and the reagents must be of high purity and the glassware is usually washed after every experiment with acid and rinsed with plenty of water before drying. In a typical experiment a few milligrams of the donor molecule are placed on one side of the H-cell and a solution of a $n\text{Bu}_4\text{N}$ salt of a particular anion (to provide charge carriers and counter ion for salt) is added on both sides to an equal level. At this point the platinum electrodes are inserted into the H-cell and the system is left to equilibrate before connecting the electrodes with the cathode and the anode (donor side) of the power supply and then a constant current is left to flow through the system. The initial value of the current is usually around $0.5 \mu\text{A}$ and may be increased if no crystals are formed after few days.

The solvent choice is determined by its ability to solubilise both donor and charge carrier bearing in mind that it is desirable that the crystals formed would be insoluble in that solvent. Often the solvent is a high boiling point non-typical organic solvent such as chloro benzene, bromo benzene, benzonitrile or 1,1,2-trichloroethane which seem to partially solubilise the donor.

The crystallisation process is sensitive to factors such as solvent, temperature and concentration of charge carriers and donor species so a right combination of all these factors is required to maximise the efficiency of the entire process in terms of number and quality of crystals.

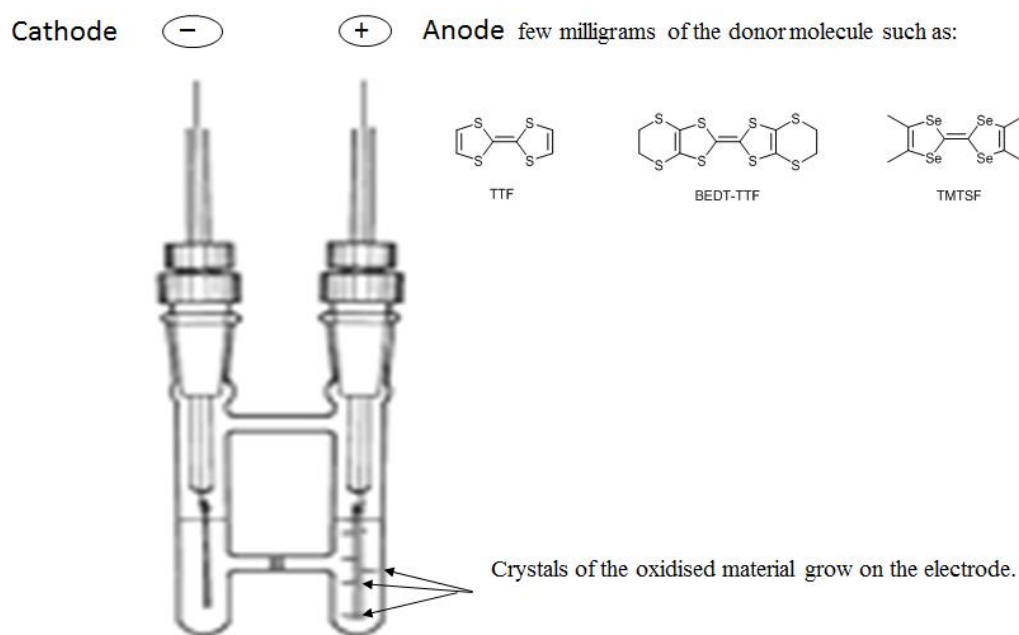


Figure 31. Typical electrocrystallisation experiment apparatus.

1.3 Magnetism.^{14,15)}

A brief introduction to the magnetic properties of solids is given due to the presence of magnetic measurements in Chapter 4. Magnetic behaviour is a property generally encountered in inorganic or organometallic compounds where transition metal or lanthanides species are involved. The magnetic behaviour arises when there are unpaired electrons in the outer shell. This means that the magnetic moment of the electron is not cancelled out and this determines the presence of a magnetic moment in the molecule and the property of being attracted to or repelled from an external magnetic field. Generally the most common magnetic atoms are the ones with *d* and *f* electrons, but many other elements can show magnetic behaviour. The materials in which none of the constituent atoms contain a permanent magnetic moment are called diamagnetics while materials which contain atoms with a permanent magnetic moment are classified as paramagnetic, ferromagnetic, antiferromagnetic or ferrimagnetic. The former magnetic behaviour can be distinguished from the other three due to the random orientation of its electron magnetic moments at all temperatures when there is no external magnetic field applied. The difference is also shown in figure 31 when the orientation of the magnetic moments is compared. In a ferromagnetic material the magnetic moments are orientated parallel to each other, while for an antiferromagnetic material the orientation is antiparallel to one another. In a ferrimagnetic compound the tendency is to an antiparallel orientation where the number or the size of magnetic moments in one orientation is much larger than in the other direction.

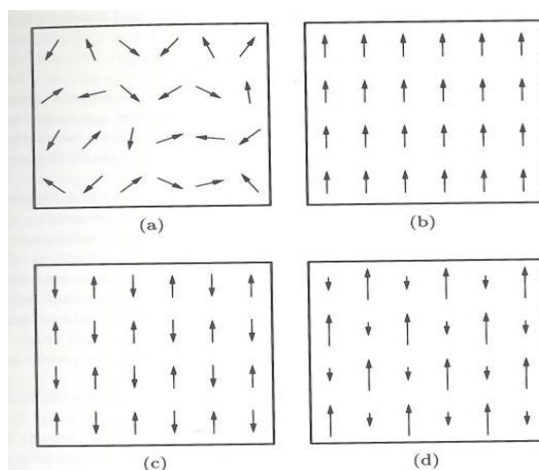


Figure 32. Orientation of magnetic moments a) in paramagnetic materials at all temperatures, b) in ferromagnetic, c) antiferromagnetic and d) ferrimagnetic materials at low temperatures.

Diamagnetic substances are repelled by a magnetic field, and as a consequence of this superconductor materials show perfect diamagnetism and are repelled by a magnetic field (levitation phenomenon). Paramagnetic substances are attracted by a magnetic field, and

in particular this attraction is stronger for ferromagnetic materials and weaker for antiferromagnetic substances. The two most important parameters to characterise the magnetic properties of a material are μ (magnetic permeability) or χ (magnetic susceptibility) which are both dimensionless. The relation between them is given by the equations presented below:

$$B = H + 4\pi I;$$

where $4\pi I$ is the sample contribution and I is the magnetic moment of the sample per unit volume;

The permeability, μ , is defined as :

$$\mu = B/H = 1 + 4\pi \cdot (I/H)$$

The susceptibility, χ , is defined as:

$$\chi = (I/H) \cdot (1/m) \cdot F;$$

where F is the molecular weight of the sample and m is the mass.

The parameter commonly used to describe the magnetic behaviour is the susceptibility χ , which is the parameter used to express the results in Chapter 4. Using the magnetic susceptibility it is important to describe its dependence on the temperature. Many paramagnetic materials follow the Curie law at high temperature, and this means that the susceptibility is inversely proportional to the temperature as stated in the Curie's law equation:

$$\chi = C / T;$$

where T is the temperature and C is called Curie constant.

Although the Curie's law is widely accepted, a better fit with the experimental data recorded is given by the Curie-Weiss law where the relation between χ and the temperature is adjusted by a constant as the equation below shows:

$$\chi = C / (T - \theta);$$

where θ is known as Weiss constant. The two laws are compared in the Figure 33 where χ^{-1} is plotted against the temperature, T .

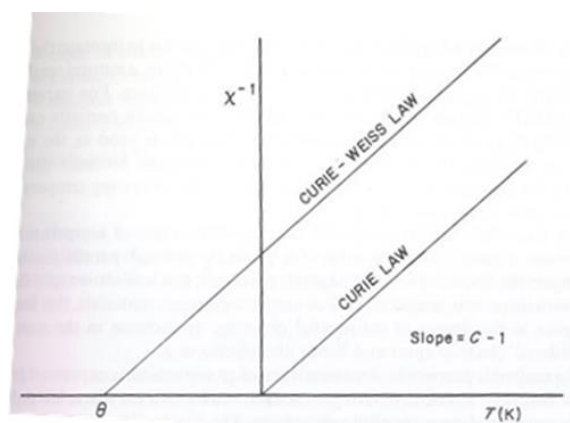


Figure 33. $1/\chi$ plotted against Temperature for Curie and Curie-Weiss law.

The behaviour of ferromagnetic and antiferromagnetic materials with temperature is more complex. In Figure 34 the plot of susceptibility against the temperature for paramagnetic, ferromagnetic and antiferromagnetic materials is compared.

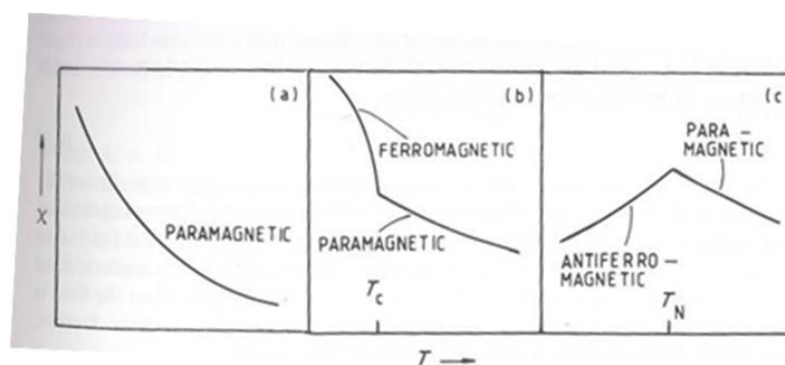


Figure 34. Plot of χ against T for a) a paramagnetic material, b) a ferromagnetic and c) antiferromagnetic materials at low temperatures.

A ferromagnetic material, Figure 34 b), has a very large susceptibility at low temperature due to cooperative interactions between magnetic species, and when the temperature starts to increase the value of χ starts to decrease rapidly until a critical temperature known as Curie temperature, T_c , above which the material presents a typical paramagnetic behaviour predicted by the Curie-Weiss law. For an antiferromagnetic material, Figure 34 c), at low temperature the susceptibility has a small value and on increasing the temperature its value increases rapidly up to a critical temperature called the Néel temperature, T_N above which the material behaves like paramagnetic. The experimental magnetic measurements conducted on the metal complexes presented in Chapter 4 have been carried out at Brock University, Canada, by a member of Dr. Pilkington's research group by using the SQUID technique. The prediction for the expected value of $\chi(T)$ at high temperature for the given metallic centre (transition metal centre or lanthanide) is given by:

$$\chi(T) = g^2/8 \cdot J(J+1);$$

where g is the gyromagnetic ratio and J is the total angular momentum quantum number.

The experimental $\chi(T)$ value at each temperature is calculated using the follow equation:

$$\chi(T) = (M/H) \cdot (1/m) \cdot MW;$$

where M is the magnetisation, the data measured by the instrument), H is the magnetic field, m is the mass of the sample in grams and MW is the molecular weight of the compound analysed. H is known and m is the amount of sample introduce in the capsule.

1.4 Organic conductors.

1.4.1. Carbon based molecules.

The beginning of the carbon based conductor field can be dated to around 1950 when Inokuchi and Akamatsu³⁵⁾ published a paper on the electrical resistivity on Violanthrone (**16**) (10^{-12} - 10^{-13} $\Omega \cdot \text{cm}$ applied voltage of 1V). This first experimental evidence that organic compounds could act as semiconductors was also supported by the elucidation of the band structure of graphene by the studies of Coulson³⁶⁾ and Wallace³⁷⁾. A few years later, in 1954, Inokuchi reported also the photoconductive behaviour of a thin film of Violanthrone.³⁸⁾ The same Japanese group also measured the electrical resistivity of Isoviolanthrene (**17**) under pressure and a value of 10^7 $\Omega \cdot \text{cm}$ was recorded³⁹⁾.

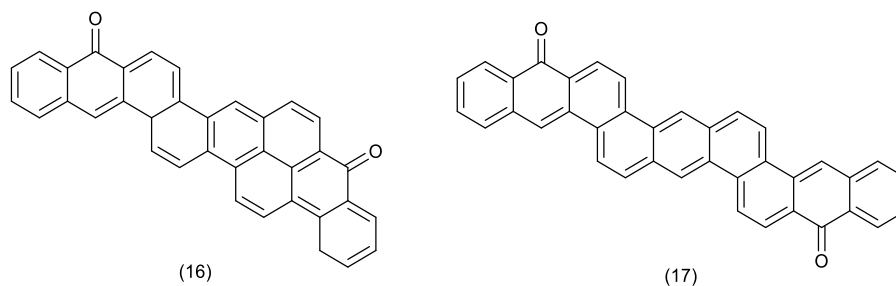


Figure 35 Violanthrene (**16**) and Isoviolanthrene (**17**).

The breakthrough in organic conductors was the observation of the high conductivity of the perylene-bromine charge transfer salt by Akamatsu *et al.* which registered a resistivity value of 10^0 $\Omega \cdot \text{cm}$ ⁴⁰⁾. More experiments of this kind were then performed and various conducting charge transfer salts were prepared and analysed⁴¹⁾. The table below summarise the result published.

Table 1. Charge transfer organic semiconductors prepared by doping polycyclic compounds.

Complex	ρ ($\Omega \cdot \text{cm}$)	ΔE (eV)
Perylene-bromine	7.8	0.13
Pyranthrene-bromine	220	0.20
Violanthrene-bromine	66	0.20
Violanthrene-iodine	44	0.15

After the preparation of the TTF-TCNQ charge transfer salt the focus for preparing organic conductors shifted to the organo-sulphur building block, but it is worth mentioning that polycyclic compounds like pentacene or naphthacene are still under investigation for

use as semiconducting layers in transistors. Examples of acene-based materials can be found in recent papers and reviews ⁴²⁾. Recently many effort are directed on the graphene and carbon nanotubes ⁴³⁾ as sources for conductive materials not only from universities but also under the guidance of the EU which founded a multi-million project recognised as one of the largest ever European research initiatives ⁴⁴⁾.

1.4.2. Polymers.

The expression organic polymer in terms of conductive materials where electrons can flow along the polymer skeleton would be possible only in the presence of a conjugated system which allows the electrons to flow from one monomer to another. So it is easy to realise how, for example, polyacetylene can show some electrical conductivity (10^{-9} - 10^{-5} ohm⁻¹ cm⁻¹) while polyethylene behave as an insulator as outlined in the Figure 36. Conjugated organic polymers can be either insulators or semiconductors and their importance increased massively since 1990 when a really important discovery allowed their use in light emitting diodes. In general when the expression organic polymer is mentioned it is intended as “intrinsic conducting polymer” (ICP) or “synthetic metal” due to the intrinsic need of doping the polymers to achieve the desired result (electrical conductivity) ⁴⁵⁾. In 1977 MacDiarmid, Heeger and co-workers ⁴⁶⁾ measured the electrical conductivity of polyacetylene doped with an electron acceptor such as Br₂, SbF₅, WF₆ or H₂SO₄ or b) with electron donors such as alkali metals and recorded a conductivity of 10^3 ohm⁻¹ cm⁻¹ for the *trans* polyacetylene.

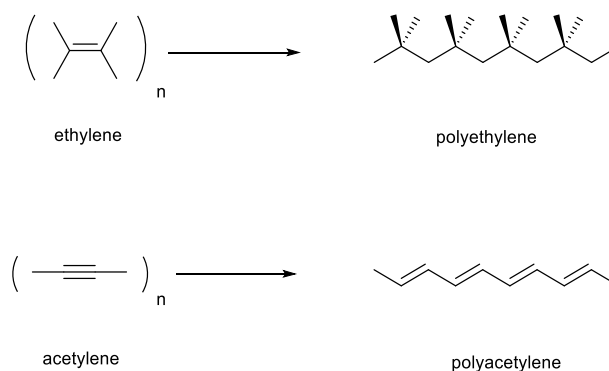


Figure 36. Bond connectivity in polyethylene and polyacetylene. Unsaturation in polyacetylene allow electron to flow through the polymer.

This discovery dramatically changed not only the conductivity of that specific polymer but the entire concept of conjugated polymers. By doping a semiconductor with a small

amount of known dopants (< 10%) it is possible to dramatically change its electrical conductivity and other properties. The doping process is reversible and produces little or no degradation of the original polymer. There are also various ways in which a polymer can be doped and also it is possible to selectively *p*-dope or *n*-dope the polymer of interest and create a blended polymer to optimise the final compound based on the properties required. Doped polymers of polyaniline (**18**), polypyrrole (**19**), polythiophene (**20**) and polyfuran (**21**) are also known.

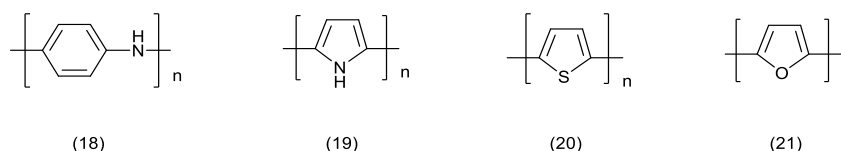


Figure 37. Example of known doped conductive polymers.

For their discoveries of metallic conductivity in organic polymers Alan MacDiarmid, Alan Heeger and Hideki Shirakawa were awarded the Noble Prize for Chemistry in the year 2000 ⁴²⁾. From the historical point of view it is worth to say that the first conductive polymer discovered was polyaniline back in 1862 by H. Letherby in London while investigating two fatal poisoning accidents. The results were published in *The Journal of Chemical Society* but like many experimental evidences of oxidation of aniline before and after 1862 remained unknown or of marginal interest. Then in the 1960s came the discovery of the first conducting poly-heterocycle, polypyrrole. This was found to conduct after doping with iodine and subject to thermolysis by D. E. Weiss and B.A. Bolto *et al.* in Australia in 1963 (conductivity 1 S cm^{-1}) ⁴⁷⁾ and later in 1968-69 by electrical oxidation of pyrrole to black pyrrole by Dall'Olio (Parma, Italy) in which the observed conductivity reached 7.45 S cm^{-1} ⁴⁸⁾. In the 1980s a type of polymer well-known for its conductive property was the poly (3-alkyl-thiophenes) but they were unstable, especially in contact with humid air. The fundamental contribution that opened the way to solve the problem came from two Bayer researchers Friederich Jona and Gerhard Heywang which expanded the thiophene to a bicyclic ring structure. The preparation of few monomers such as MDOT (**22**), EDOT (**23**) PDOT (**24**) was achieved and polymerisation of (**23**) immediately resulted in a high conductivity and stability for the polymer obtained. Then shortly after, from a collaboration between Bayern AG and Agfa Gevaert, was born the complex PEDOT:PSS in response to the request of new antistatics for photographic films ⁴⁹⁾. Indeed the new complex PEDOT:PSS was found to be processable from its stable micro-dispersion in water and in the early 1990s the manufacturing process of this complex started as antistaic agent and photographic material. Still nowadays the complex is

one of the most used conductive polymers in terms of applications and also for theoretical studies on conductive materials.⁵⁰⁾

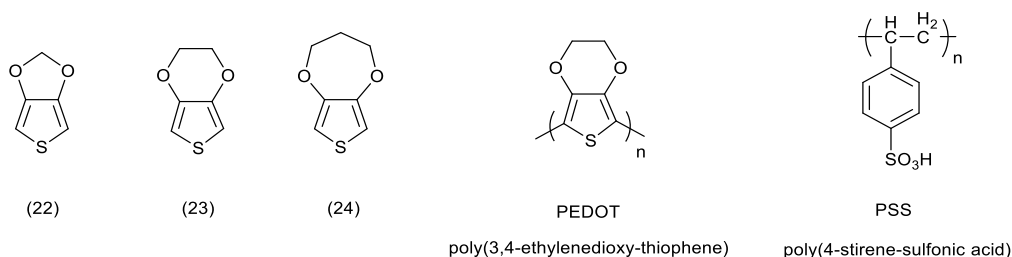


Figure 38. Monomers of dialkyloxythiophene and the PEDOT and PSS polymers.

There are also polymers based on TTF building blocks and early work in this field involved incorporation of TTF units onto the backbone of polyurethane, polyamide, polyesters and polysulfonates⁵¹⁾. There are many example of introducing TTF unit on the side chain of a polymer such as the work presented by Green and Allen which achieved preparation of a vinyltetrathiafulvalene polymer (**25**)⁵²⁾. Other examples are the polymerisation of (*p*-vinylphenyl)tetrathiafulvalene **26** by Kaplan *et al.*⁵³⁾ and the polymerisation of *p*-(2-tetrathiafulvalenyl)phenylmetacrylate (**27**) by Pitmann Jr *et al.*⁵⁴⁾ (Figure 39). All the described polymers had solubility issues and it was found problematic to characterise them properly.

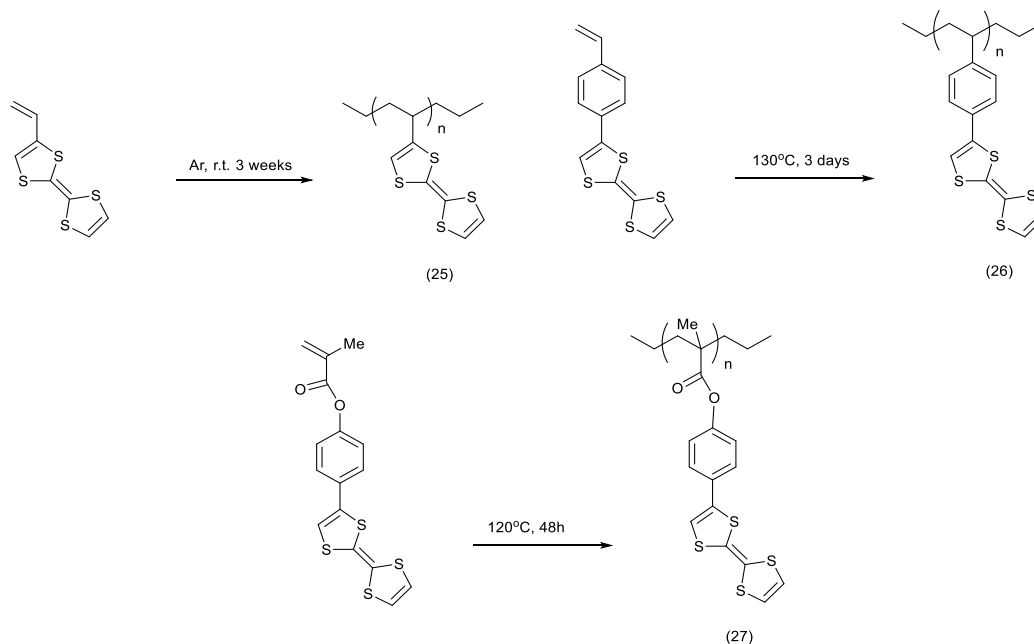


Figure 39. A few examples of TTF-based polymers.

Other examples are the direct attachment of TTF units to a polyacetylene backbone prepared by polymerising 2-ethynyl-TTF by Shimizu and Yamamoto to give polymer (**28**) which turned out to be insoluble in common solvents. The incorporation of an ether bridge between the alkene chain and the TTF increased the solubility of polymer (**29**).⁵⁵⁾

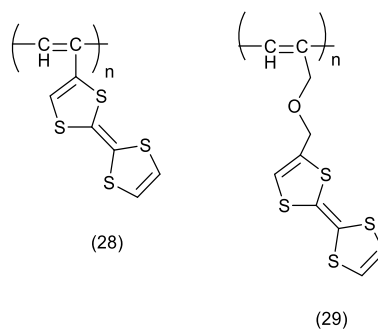


Figure 40. TTF-based polymers prepared by Shimizu and Yamamoto.

There are examples of TTF-based polymers where the TTF is incorporated in the main chain, such as in **(30)** and **(31)** prepared by Müllen and co-workers which showed conductivity values of 0.55 S cm^{-1} for **(30)** after doping with iodine (I_3^- , 60%) and of $1.5 \cdot 10^{-2} \text{ S cm}^{-1}$ (I_3^- , 55%) for polymer **(31)**.⁵⁶⁾

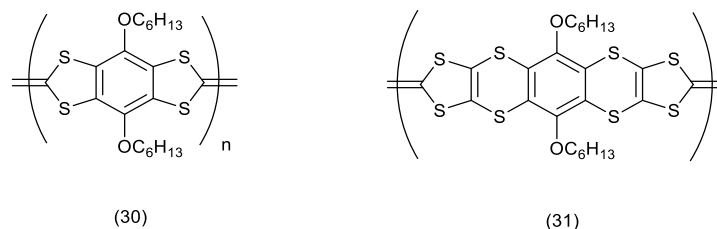
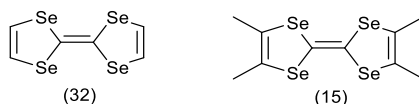


Figure 41. Examples of a TTF-based polymer where TTF is in the main chain.

1.4.3. Overview of TTF substituted donors for conducting materials and some of their applications.

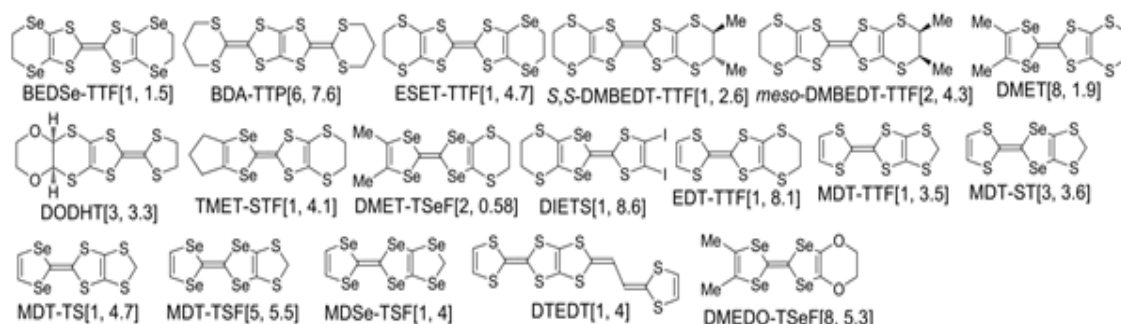
After the preparation of the TTF-TCNQ complex mentioned in the paragraph 1.1 and the discovery of its metallic behaviour, the search for better conducting (semiconducting and superconducting) organic molecules have seen TTF as the most widely used building block. After this discovery chemists all around the world produced a huge effort in the search for conducting organic materials with performances as good as metals or with lower T_c temperature (superconductors). This effort produced an enormous amount of TTF derivatives where sulphurs were replaced by other chalcogen atoms such as oxygen, selenium and tellurium or nitrogen or by varying the substituent on the TTF molecule.

The first fundamental milestones after the complex TTF-TCNQ and its metallic behaviour were tetraselenafulvalene (TSF) **(32)** and its derivative tetramethyl-tetraselenafulvalene (TM-TSF) **(15)** presented below.

Figure 42. TSF (**32**) and TM-TSF (**15**) donors.

A series of (TM-TSF)₂X (X = PF₆⁻, AsF₆⁻, SbF₆⁻, TaF₆⁻, NbF₆⁻, NbO₄⁻, ClO₄⁻, ReO₄⁻ and FSO₃⁻) salts was realised by Bechgaard *et al.*⁵⁷⁾ in 1980 and some were found to be superconductors ($T_c = 1-2$ K) and since then are known as Bechgaard salts. In particular the perchlorate was a superconductor at ambient pressure while the others showed the same characteristic but under pressure (5-12 kbar). Analysis of the perchlorate structure determined by XRD showed the presence of the perchlorate anions in channels between stacks of donors and showing short O---H interactions. From this moment the search for superconductors based on the TTF molecule and the understanding of the role of non-covalent interactions became even stronger. The TTF analogue salts of (TM-TTF)₂X (X = PF₆⁻, SbF₆⁻, BF₄⁻, Br⁻) displayed superconductivity behaviour with $T_c < 3$ K under pressure in the range 2.6 - 9 GPa⁵⁸⁾.

Another very productive building block for making superconductors is the BEDT-TTF donor which gave around 60 superconductors⁵⁹⁾, where the most relevant are salts of general formula (BEDT-TTF)₂X such as (BEDT-TTF)₂[Cu(CN)₂Br]⁶⁰⁾ ($T_c = 11.6$ K at r.t.), or (BEDT-TTF)₂ICl₂⁶¹⁾ ($T_c = 14.2$ K at 8.2 GPa). Both of these salts are arranged in a κ -type packing. Another of BEDT-TTF superconductor is (BEDT-TTF)₂I₃ (first quasi-2D organic superconductor at ambient pressure) which has $T_c = 1.4-1.6$ K at ambient pressure⁶²⁾, or (BEDT-TTF)₂IBr₂ a mixed polyhalide with $T_c = 2.7$ K at ambient pressure⁶³⁾. In addition to TM-TSF, TM-TTF and BEDT-TTF a summary of all the TTF derivatives presenting superconductor behaviour are summarised in the figure below with the number of superconductor species and T_c in bracket.

Figure 43⁵²⁾. Donor molecules giving superconducting salts with the number of superconductor species and the highest T_c recorded in brackets.

In addition to the donors containing sulphurs or selenium in the inner or outer ring it is also possible to find nitrogen and oxygen atoms in the outer ring. These donors are less

common but are among the molecules prepared and studied to achieve better performances in semiconductors and higher T_c in superconducting materials. Indeed there are very few examples of oxygen substituted TTFs where the atom is in the inner ring. The first example of this kind of donor is DBTOF (**33**) which was clearly reported only in the year 2000⁶⁴⁾ although its preparation was achieved in 1988⁶⁵⁾. The main example of the oxygen substituted TTF derivatives is the BEDO-TTF (BO) (**34**) where oxygen atoms are in both of the outer rings.

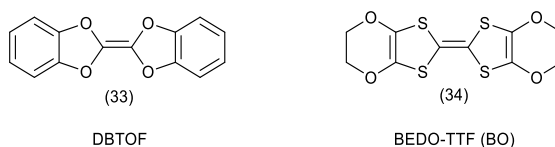


Figure 44. Oxygen based donors.

The BO donor was prepared in 1989 by Wudl *et al.*⁶⁶⁾ based on the recent discovery of the copper oxide superconductors⁶⁷⁾ where according to theory the species responsible for the mixed valence was not the $\text{Cu}^{\text{II}} / \text{Cu}^{\text{III}}$ couple but the oxygen radical cations⁶⁸⁾. Wudl and co-workers decided to prepare the BO donor to see if it was possible to observe metallic or even superconducting behaviour in oxygen containing donors. Indeed BEDO-TTF generated charge transfer salts with I_3^- , $\text{Cu}(\text{SCN})_2^-$ and ReO_4^- , which showed metallic behaviour⁶⁹⁾.

Another boost to the synthesis of novel and more complex TTF based conducting materials came when in 1974 Aviram and Ratner⁷⁰⁾ proposed that theoretically a single system based on Donor-spacer-Acceptor (D-s-A), such as (**35**) where the spacer is a saturated linker, would behave as a molecular rectifier where the current flows in one particular direction only between the two electrodes (Figure 45). The first experimental evidence of this was revealed by Metzger *et al.*⁷¹⁾ with compound (**36**) where neither TTF nor TCNQ were involved.

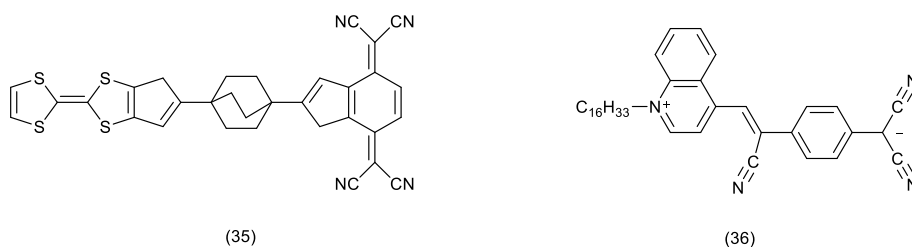


Figure 45. The molecular rectifiers proposed by Aviram and Ratner (**35**) and prepared by Metzger *et al.* (**36**).

1.4.4 Fullerene-based polymers and oligomers for photovoltaic applications.

The C₆₀ fullerene was discovered in 1985 as a stable compound derived from laser irradiation of graphite by H. W. Kroto, R.F. Curl and R. E. Smalley⁷²⁾. It was then made on preparative scale in 1990 by resistive heating of graphite by D. Hoffmann *et al.*⁷³⁾ and from that moment the C₆₀ fullerene has been one of the most studied acceptor molecule for applications in materials chemistry such as for photovoltaic devices^{74,75)}. In 1996 the three scientists who discovered it were awarded the Nobel Prize in Chemistry. From the organic photovoltaics point of view the C₆₀ fullerene is highly regarded as an excellent electron acceptor due to the large number of unsaturations present on its surface. C₆₀ fullerene has been involved also in the preparation of polymers and adducts with electron donor TTF and its derivatives to achieve the preparation of better donor-acceptor systems. A few examples of oligomers are presented (Figure 46). In particular the compound **(37)** is the first TTF-C₆₀ fullerene adduct reported back in 1996⁷⁶⁾. Many more examples of expanded-TTF- C₆₀ fullerene systems, such as **(38)**⁷⁷⁾, are studied for application in photovoltaic cells. Compound **(39)**, known as PCBM, made by Wudl *et al.* in 1995⁷⁸⁾, is one of the most studied and the most successful fullerene derivative for preparing solar cells.

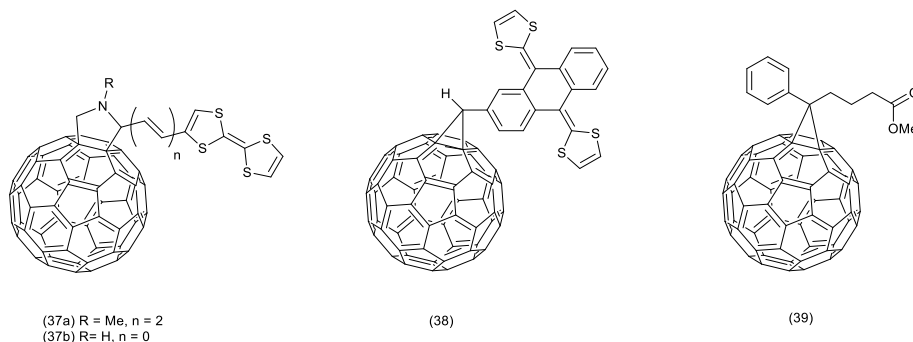


Figure 46. Examples of substituted C₆₀ fullerene oligomers.

One of the latest trends in fullerene chemistry is the realisation of molecular dumbbells which have shown improved photovoltaic performances⁷⁹⁾. In this kind of derivatives two fullerenes are at the side of the electron donor such as in compound **(40)** (Figure 47). Indeed it has been recently demonstrated by Blom and co-workers⁸⁰⁾ that the performance of a photovoltaic device depends on the C₆₀ content.

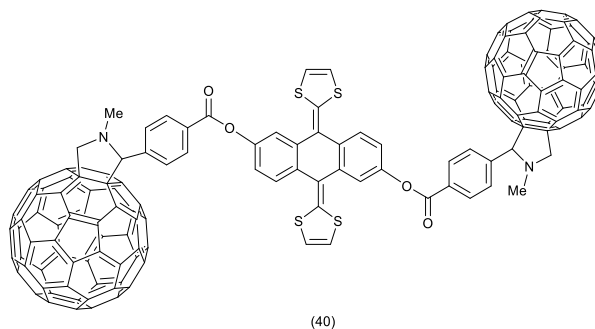


Figure 47. Example of molecular dumbbell system.

1.4.5 TTF as a building block for molecular switches, receptors, molecular machine and its use in organic synthesis.

One of the most interesting uses of TTF outside of conductive materials is as receptors for ionic (cationic and anionic) and neutral guests⁸¹. The host-guest interaction can be detected as a change in the redox behaviour of the TTF unit and this can be revealed by a cyclic voltammetry measurement. The host, in this particular field, is a TTF unit which is substituted with a macrocycle (crown ether or calixarene) who is responsible for binding the guest. These kind of macromolecules are usually classified in terms of the guest's charge and a few examples of cationic, anionic and neutral guest receptors. In the case of the former a major contribution came from J. Becher and co-workers who prepared and characterised many TTF-based receptors such as **(41)**⁸².

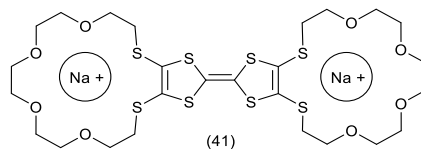


Figure 48. Example of a TTF-crown-ether receptor with high sensitivity for sodium.

Becher and co-workers developed a very reliable and high yielding method for preparation of *mono*-, *bis*-, *ter*- and *tetra*-substituted TTF donors by using bromopropionitrile and caesium hydroxide as protection/deprotection method⁸³ for its chemistry preparations as outlined below.

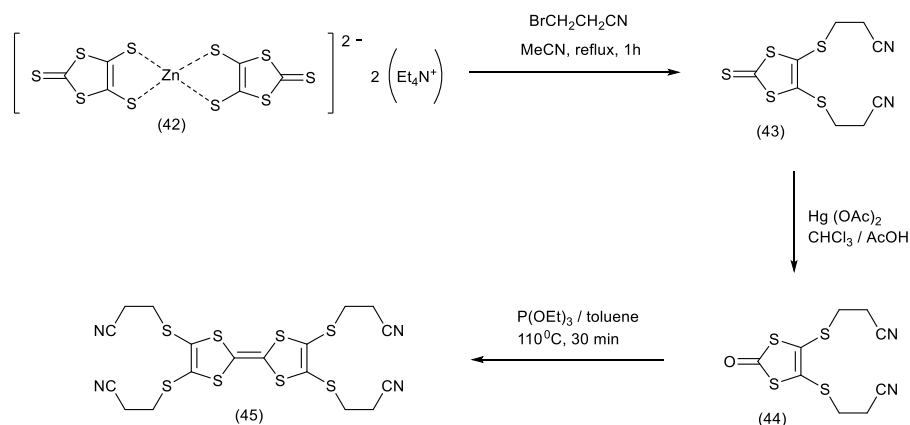
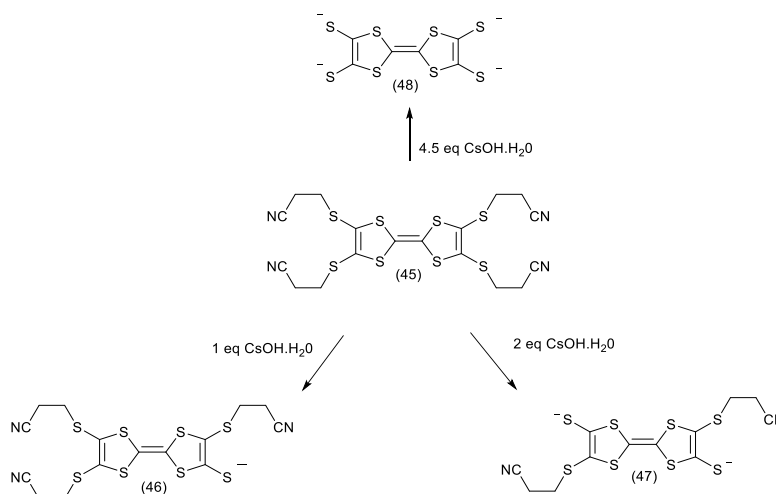


Figure 49. Standard preparation of tetrasubstituted TTF donor (45).

Then once the donor molecule (45) has been prepared, it is possible to deprotect the desired number of sulphurs in order to create the monothiolate (46), the dithiolate (cis/trans) (47) or the tetrathiolate (48) species (Scheme 5).



Scheme 5. Preparation of the mono-, bis- or tetra-thiolate species from donor (45).

Many efforts have been made in order to build systems where the complexity of the macrocycle and/or of the donor core would allow easier host-guest interaction of redox processes as shown in the examples below where calix[4]arene was used for binding cations such as in (49)⁸⁴ (Figure 50) or the donor core was modified by extending its π -conjugation as shown for compounds (50), (51) and (52)⁸⁵ (Figure 51).

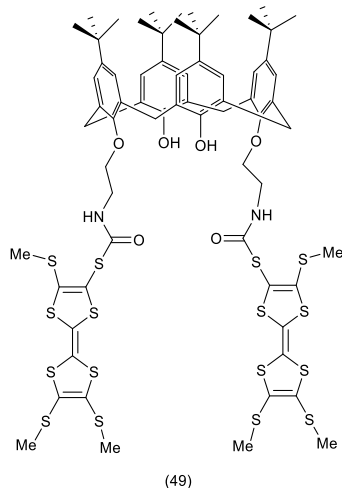


Figure 50. Example of cationic receptor based on a calix[4]arene with amide substituted TTF donor.

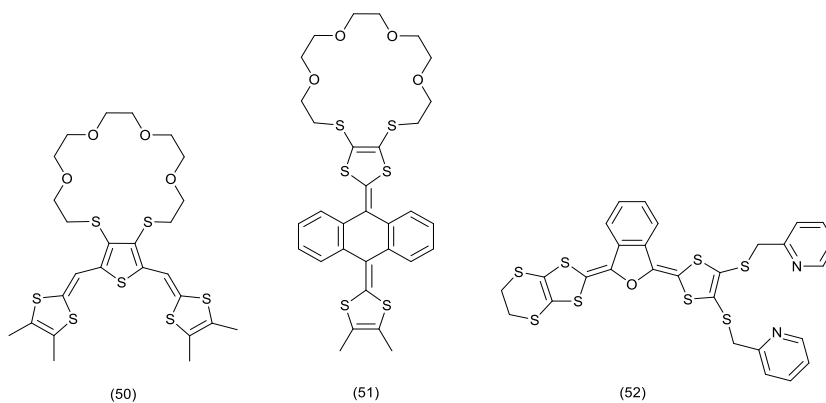


Figure 51. Examples of TTF substituted receptors with a conjugated core.

Substituted TTF molecules have been found to be good receptors for anions, such as in the specific case of compound **(53)** whose sensitivity and selectivity are very high for binding fluoride.⁸⁶⁾

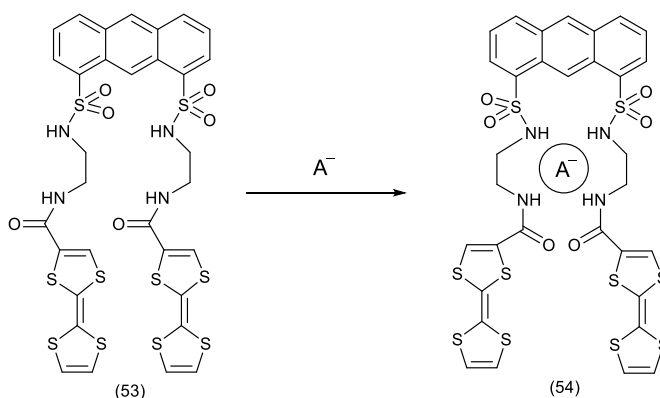


Figure 52. Anion receptor based on substituted TTF.

Another example of how TTF-macrocycles can be used for anion detection is presented by the calix[4]pyrrole core of compound **(55)** which has a high ability for binding halide

anions. In particular this compound showed one of the highest affinity for X^- anions among the non-strapped calix[4]pyrrole.⁸⁷⁾

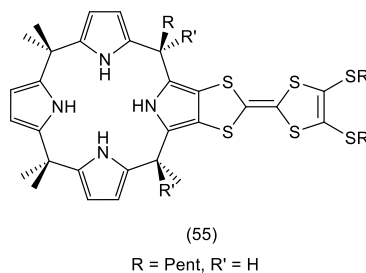


Figure 53. Example of a calix[4]pyrrole reported in the literature.

There also examples of systems able to bind neutral guests such as compound **(56)** capable of detecting saccharides through a change in its luminescence behaviour. The compound **(56)** was found really effective for detection of D-fructose.⁸⁸⁾

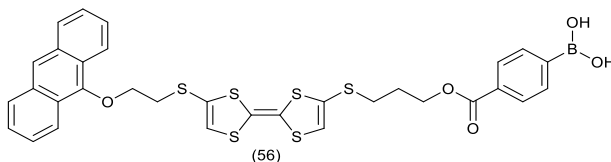


Figure 54. Example of a disubstituted TTF as a receptor for neutral guest.

Another interesting application utilising a TTF-macrocycle is as molecular switches sensitive to multiple external stimuli. An example is the CT complex between the TTF derivative and the bipyridyl macrocycle recently reported by Chiu *et al.*⁸⁹⁾. In the complex reported the author emphasise the importance of the electron donor in order to stabilise interactions for the complex formation. The diphenylglycouril functionalised TTF can be seen as molecular switch for binding/releasing of guest in response to external stimulations such as the presence of metal cations and their change in concentration and other chemicals (Figure 55).

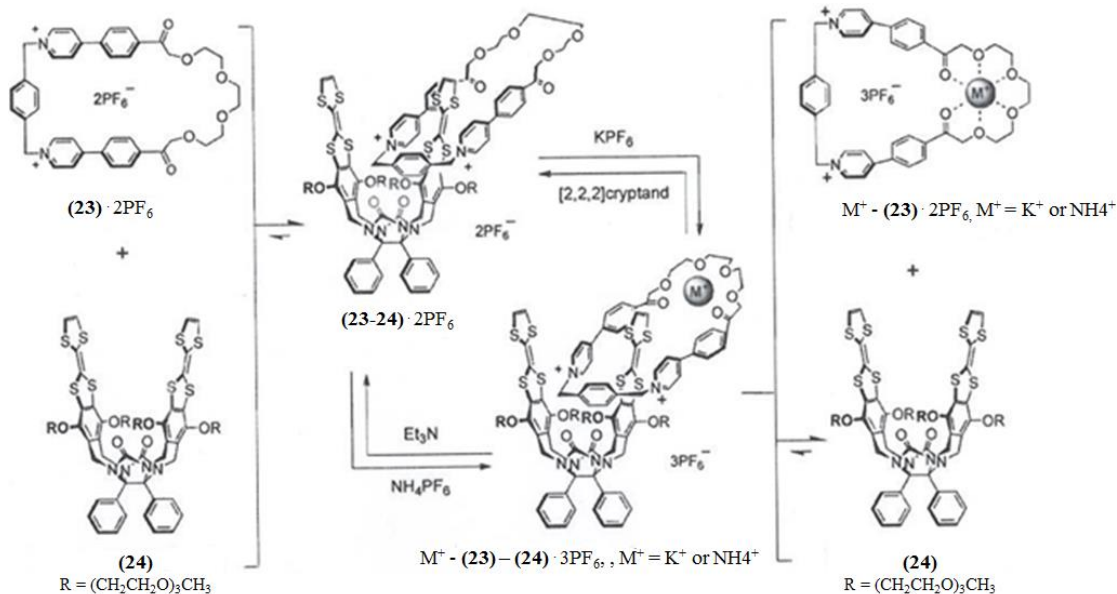


Figure 55⁸²⁾. Example of how the two units can assemble and act as a molecular machine.

Another interesting application of the TTF donor is in a sequence of reactions called “radical polar crossover” which was investigated and studied by J.A. Murphy *et al.* in the synthesis of polycyclic core molecules such as the alkaloids *Aspidosperma*⁹⁰⁾.

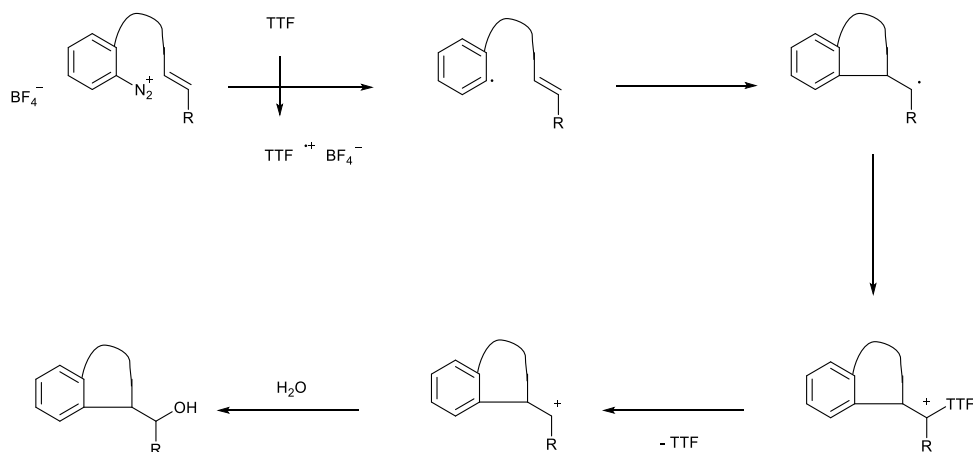


Figure 56. Radical polar crossover reaction mechanisms.

The TTF behaves as a reducing agent under mild conditions such as at r.t., in acetone and using the catalytic amount necessary to mimic the behaviour of samarium iodide, SmI_2 , which is widely used in total synthesis to prepared multicyclic compounds⁹¹⁾.

1.5 Bibliography.

1. F. Wudl, G. Smith and E. Hufnagel, *J. Chem. Soc. Chem. Comm.*, 1970, **21**, 1453
2. F. Wudl, D. Wobschall and E. J. Hufnagel, *J. Am. Chem. Soc.*, 1972, **94**, 670.
3. D. O. Cowan and F. Kaufman, *J. Am. Chem. Soc.*, 1970, **92**, 6198.
4. M. J. Minot and J. H. Perlstein, *Phys. Rev. Lett.*, 1971, **26**, 371.
5. D. S. Acker and W. R. Hertler, *J. Am. Chem. Soc.*, 1962, **84**, 3370-3374, R. J. Crawford, *J. Org. Chem.*, 1983, **48**, 1366.
6. J. Ferraris, D. Cowan, V. t. Walatka and J. Perlstein, *J. Am. Chem. Soc.*, 1973, **95**, 948.
7. H. Prinzbach, H. Berger and A. Lüttringhaus, *Angew Chem. Int. Ed.-Eng.*, 1965, **4**, 435.
8. S. Hünig, H. Schlaf, G. Kießlich and D. Scheutzow, *Tetrahedron Lett.*, 1969, **10**, 2271.
9. M. Mizuno, A. F. Garito and M. P. Cava, *J. Chem. Soc. Chem. Comm.*, 1978, 18-19; G. Saito, T. Enoki, K. Toriumi and H. Inokuchi, *Solid State Commun.*, 1982, **42**, 557.
10. J. Yamada and T. Sugimoto, *TTF Chemistry: Fundamentals and Applications of Tetrathiafulvalene; with 47 Tables*, Springer, 2004.
11. M. R. Bryce, *Journal of Materials Chemistry*, 2000, **10**, 589. P. Batail, *Chem. Rev.*, 2004, **104**, 4887; R. P. Shibaeva and E. B. Yagubskii, *Chem. Rev.*, 2004, **104**, 5347; M. Bendikov, F. Wudl and D. F. Perepichka, *Chem. Rev.*, 2004, **104**, 4891. J. D. Wallis and J. Griffiths, *J. Mater. Chem.*, 2005, **15**, 347.
12. N. Martín, *Chem. Comm.*, 2013, **49**, 7025.
13. S. Parkin, M. Ribault, D. Jerome and K. Bechgaard, *J. Phys. C: Solid State Physics*, 1981, **14**, 5305; S. De Soto, C. Slichter, A. Kini, H. Wang, U. Geiser and J. Williams, *Phys. Rev. B*, 1995, **52**, 10364.
14. G. Parker, *Introductory semiconductor device physics*, Prentice Hall, 1994, b) B. Bleaney and B. Bleaney, *Electricity and Magnetism, Volume 1*, Oxford University Press, 2013, c) B. I. Bleaney, B. I. Bleaney and B. Bleaney, *Electricity and Magnetism, Volume 2*, Oxford University Press, 2013.
15. A. R. West, *Solid state chemistry and its applications*, John Wiley & Sons, 2013.
16. H. K. Onnes, *Comm.Phys.Lab.Univ.Leiden*, 1911, **122**.

17. [http://cds.cern.ch/journal/CERNBulletin/2011/16/News Articles/](http://cds.cern.ch/journal/CERNBulletin/2011/16/News%20Articles/)
18. W. Meissner and R. Ochsenfeld, *Naturwissenschaften*, 1933, **21**, 787.
19. J. Bardeen, L. N. Cooper and J. R. Schrieffer, *Phys. Rev.*, 1957, **108**, 1175.
20. B. D. Josephson, *Phys. Lett.*, 1962, **1**, 251.
21. L. Schneemeyer, J. Waszczak, T. Siegrist, R. Van Dover, L. Rupp, B. Batlogg, R. Cava and D. Murphy, *Nature*, **328**, 1987, 601.
22. E. Maxwell, *Phys. Rev.*, 1950, **78**, 477.
23. C. Reynolds, B. Serin and L. Nesbitt, *Phys. Rev.*, 1951, **84**, 691.
24. H. Frohlich, *Proc. Royal Society of London. Series A. Mathematical and Physical Sciences*, 1954, **223**, 296.
25. <http://www.superconductors.org/history.html>.
26. <http://www.oled-info.com/>.
27. <http://energy.gov/eere/sunshot/organic-photovoltaics-research>.
28. <http://www.bbc.co.uk/schools/gcsebitesize/design/electronics/switchesrev3.shtml>.
29. <http://news.bbc.co.uk/1/hi/sci/tech/488394.stm>.
30. http://www.st-andrews.ac.uk/~www_pa/Scots_Guide/info/comp/passive/diode/pn_junc/pn_junc.htm
31. <http://electronics.howstuffworks.com/oled.html>.
32. <http://plasticphotovoltaics.org/lc/lc-polymersolarcells/lc-how.html>; “Organic electronics for a better tomorrow: Innovation, accessibility and sustainability” CS3 summit-September 2012.
33. D. C. Jiles, *Introduction to magnetism and magnetic materials*, CRC Press, 1998.
34. P. Batail, K. Boubekour, M. Fourmigué and J. P. Gabriel, *Chemistry of materials*, 1998, **10**, 3005.
35. H. Akamatsu and H. Inokuchi, *J. Chem. Phys.*, 1950, **18**, 810.
36. C. Coulson, *Nature*, 1947, **159**, 265.
37. P. R. Wallace, *Phys. Rev.*, 1947, **71**, 622.
38. H. Akamatsu and H. Inokuchi, *J. Chem. Phys.*, 1952, **20**, 1481; H. Inokuchi, *Bull. Chem. Soc. Jpn.*, 1954, **27**, 22.
39. H. Inokuchi, *Bull. Chem. Soc. Jpn.*, 1955, **28**, 570.
40. H. Akamatsu, H. Inokuchi and Y. Matsunaga, *Nature*, 1954, **173**, 168.

41. H. Akamastu, H. Inokuchi and Y. Matsunaga, *Bull. Chem. Soc. Jpn.*, 1956, **29**, 213; H. Inokuchi, *Organic electronics*, 2006, **7**, 62.
42. F. G. Brunetti, R. Kumar and F. Wudl, *J. Mater. Chem.*, 2010, **20**, 2934.
43. V. Georgakilas, K. Kordatos, M. Prato, D. M. Guldi, M. Holzinger and A. Hirsch, *J. Am. Chem. Soc.*, 2002, **124**, 760.
44. <http://graphene-flagship.eu/>
45. A. G. MacDiarmid, *Angew. Chem. Int. Ed-Eng.*, 2001, **40**, 2581 and reference therein.
46. C. K. Chiang, C. Fincher Jr, Y. Park, A. Heeger, H. Shirakawa, E. Louis, S. Gau and A. G. MacDiarmid, *Phys. Rev. Lett.*, 1977, **39**, 1098.; C. Chiang, M. Druy, S. Gau, A. Heeger, E. Louis, A. G. MacDiarmid, Y. Park and H. Shirakawa, *J. Am. Chem. Soc.*, 1978, **100**, 1013.
47. R. McNeill, R. Siudak, J. Wardlaw and D. Weiss, *Aust. J. Chem.*, 1963, **16**, 1056; B. A. Bolto and D. Weiss, *Aust. J. Chem.*, 1963, **16**, 1076; B. A. Bolto, R. McNeill and D. Weiss, *Aust. J. Chem.*, 1963, **16**, 1090.
48. A. Dall'Olio, G. Dascola, V. Vacara and V. Bocchi, *CR Acad.Sci.Paris*, 1968, **267**, 433.
49. F. Jonas and L. Schrader, *Synth. Met.*, 1991, **41**, 831; G. Heywang and F. Jonas, *Adv Mater*, 1992, **4**, 116;
50. A. Elschner, S. Kirchmeyer, W. Lovenich, U. Merker and K. Reuter, *PEDOT: principles and applications of an intrinsically conductive polymer*, CRC Press, 2010.
51. C. U. Pittman, Y. Liang and M. Ueda, *Macromolecules*, 1979, **12**, 355; C. U. Pittman Jr, Y. Liang and M. Ueda, *Macromolecules*, 1979, **12**, 541.
52. D. C. Green and R. W. Allen, *J. Chem. Soc., Chem. Commun.*, 1978, **19**, 832.
53. M. Kaplan, R. Haddon, F. Wudl and E. Feit, *J. Org. Chem.*, 1978, **43**, 4642.
54. C. U. Pittman Jr, M. Ueda and Y. F. Liang, *J. Org. Chem.*, 1979, **44**, 3639.
55. T. Shimizu and T. Yamamoto, *Inorg. Chim. Acta*, 1999, **296**, 278.
56. S. Frenzel, S. Arndt, R. M. Gregorious and K. Müllen, *J. Mater. Chem*, 1995, **5**, 1529; S. Frenzel, M. Baumgarten and K. Müllen, *Synth. Met.*, 2001, **118**, 97.
57. D. Jerome, A. Mazaud, M. Ribault and K. Bechgaard, *Journal de Physique Letters*, 1980, **41**, 95.

58. D. Jérôme and H. Schulz, *Adv. Phys.*, 1982, **31**, 299; K. Bechgaard, *Mol. Cryst. Liq. Cryst.*, 1982, **79**, 357.; M. Sakata, Y. Yoshida, M. Maesato, G. Saito, K. Matsumoto and R. Hagiwara, *Mol. Cryst. Liq. Cryst.*, 2006, **452**, 103.
59. G. Saito and Y. Yoshida, in *Unimolecular and Supramolecular Electronics I*, ed., Springer, 2012, 67.
60. A. M. Kini, U. Geiser, H. H. Wang, K. D. Carlson, J. M. Williams, W. Kwok, K. Vandervoort, J. E. Thompson and D. L. Stupka, *Inorg. Chem.*, 1990, **29**, 2555.
61. H. Taniguchi, M. Miyashita, K. Uchiyama, K. Satoh, N. Môri, H. Okamoto, K. Miyagawa, K. Kanoda, M. Hedo and Y. Uwatoko, *J. Phys. Soc. Jpn*, 2003, **72**, 468.
62. K. Bender, I. Hennig, D. Schweitzer, K. Dietz, H. Endres and H. J. Keller, *Mol. Cryst. Liq. Cryst.*, 1984, **108**, 359.
63. J. M. Williams, H. H. Wang, M. A. Beno, T. J. Emge, L. Sowa, P. Copps, F. Behroozi, L. Hall, K. D. Carlson and G. Crabtree, *Inorg. Chem.*, 1984, **23**, 3839.
64. K. Tanaka, K. Yoshida, T. Ishida, A. Kobayashi and T. Nogami, *Adv Mater*, 2000, **12**, 661.
65. O. Safiev, D. Nazarov, V. Zorin and D. Rakhmankulov, *Khim. Get-erotsikl. Soedin*, 1988, **6**, 852.
66. T. Suzuki, H. Yamochi, G. Srdanov, K. Hinkelmann and F. Wudl, *J. Am. Chem. Soc.*, 1989, 111, 3108.
67. J. G. Bednorz and K. A. Müller, *Zeitschrift für Physik B Condensed Matter*, 1986, **64**, 189.
68. V. Emery, *Phys. Rev. Lett.*, 1987, **58**, 2794; G. Chen and W. A. Goddard 3rd, *Science*, 1988, **239**, 899
69. F. Wudl, H. Yamochi, T. Suzuki, H. Isotalo, C. Fite, H. Kasmai, K. Liou, G. Srdanov and P. Coppens, *J. Am. Chem. Soc.*, 1990, **112**, 2461; M. A. Beno, H. H. Wang, A. M. Kini, K. D. Carlson, U. Geiser, W. Kwok, J. E. Thompson, J. M. Williams, J. Ren and M. H. Whangbo, *Inorg. Chem.*, 1990, **29**, 1599; S. Khasanov, B. Z. Narymbetov, L. Zorina, L. Rozenberg, R. Shibaeva, N. Kushch, E. Yagubskii, R. Rousseau and E. Canadell, *Eur. Phys J. B.*, 1998, **1**, 419.
70. A. Aviram and M. A. Ratner, *Chem. Phys. Lett*, 1974, **29**, 277.

71. R. M. Metzger, B. Chen, U. Höpfner, M. Lakshmikantham, D. Vuillaume, T. Kawai, X. Wu, H. Tachibana, T. V. Hughes and H. Sakurai, *J. Am. Chem. Soc.*, 1997, **119**, 10455.
72. H. W. Kroto, J. R. Heath, S. C. O'Brien, R. F. Curl and R. E. Smalley, *Nature*, 1985, **318**, 162.
73. J. Wragg, J. Chamberlain, H. White, W. Krätschmer and D. R. Huffman, *Nature*, 1990, **348**, 623.
74. N. Martín, L. Sánchez, M. A. Herranz, B. Illescas and D. M. Guldi, *Acc. Chem. Res.*, 2007, **40**, 1015 and reference therein
75. D. M. Guldi and M. Prato, *Acc. Chem. Res.*, 2000, **33**, 695; J. L. Segura, N. Martín and D. M. Guldi, *Chem. Soc. Rev.*, 2005, **34**, 31; F. Giacalone and N. Martin, *Chem. Rev.*, 2006, **106**, 5136; D. M. Guldi, B. M. Illescas, C. M. Atienza, M. Wielopolski and N. Martín, *Chem. Soc. Rev.*, 2009, **38**, 1587.
76. N. Martín, L. Sánchez, C. Seoane, R. Andreu, J. Garín and J. Orduna, *Tetrahedron Lett.*, 1996, **37**, 5979; M. Prato, M. Maggini, C. Giacometti, G. Scorrano, G. Sandona and G. Farnia, *Tetrahedron*, 1996, **52**, 5221.
77. N. Martín, L. Sánchez and D. M. Guldi, *Chem. Comm.*, 2000, 113.
78. J. C. Hummelen, B. W. Knight, F. LePeq, F. Wudl, J. Yao and C. L. Wilkins, *J. Org. Chem.*, 1995, **60**, 532.
79. L. Sánchez, M. Á. Herranz and N. Martín, *J. Mater. Chem.*, 2005, **15**, 1409.
80. V. D. Mihailetschi, L. J. A. Koster, P. W. Blom, C. Melzer, B. de Boer, J. K. van Duren and R. A. Janssen, *Adv. Funct. Mater.*, 2005, **15**, 795.
81. J. L. Delgado, P. Bouit, S. Filippone, M. Á. Herranz and N. Martín, *Chem. Comm.*, 2010, **46**, 4853.
82. T. Jørgensen, T. K. Hansen and J. Becher, *Chem. Soc. Rev.*, 1994, **23**, 41; M. B. Nielsen, C. Lomholt and J. Becher, *Chem. Soc. Rev.*, 2000, **29**, 153.
83. N. Svenstrup, K. M. Rasmussen, T. K. Hansen and J. Becher, *Synthesis*, 1994, **8**, 809.
84. B. Zhao, M. Blesa, N. Mercier, F. Le Derf and M. Sallé, *New J. Chem.*, 2005, **29**, 1164.
85. G. Trippé, D. Canevet, F. Le Derf, P. Frère and M. Sallé, *Tetrahedron Lett.*, 2008, **49**, 5452; S. Dolder, S. Liu, F. Le Derf, M. Sallé, A. Neels and S. Decurtins, *Org. Lett.*, 2007, **9**, 3753-3756; M. R. Bryce, A. S. Batsanov, T.

- Finn, T. K. Hansen, A. J. Moore, J. A. Howard, M. Kamenjicki, I. K. Lednev and S. A. Asher, *Eur. J. Org. Chem.*, 2001, **2001**, 933.
86. H. Lu, W. Xu, D. Zhang, C. Chen and D. Zhu, *Org. Lett.*, 2005, **7**, 4629.
87. K. A. Nielsen, J. O. Jeppesen, E. Levillain and J. Becher, *Angew. Chem. Int. Ed-Eng.*, 2003, **42**, 187.
88. Z. Wang, D. Zhang and D. Zhu, *J. Org. Chem.*, 2005, **70**, 5729.
89. P. Chiang, P. Cheng, C. Lin, Y. Liu, C. Lai, S. Peng and S. Chiu, *Chem. Eur. J.*, 2006, **12**, 865.
90. J. A. Murphy and S. J. Roome, *J. Chem. Soc., Perkin Trans. I*, 1995, 1349; J. Murphy and S. Roome, *J. Chem. Soc., Perkin Trans. I*, 1998, 2341.
91. K. E. Nicolaou, S. P. Ellery and J. S. Chen, *Angew. Chem. Int. Ed-Eng*, 2009, **48**, 7140.

Chapter 2

**Attempted synthesis of BEDT-TTF
dimers and related substituted
BEDT-TTF donors obtained.**

2.1 Introduction.

The TTF dimers and oligomers have been extensively studied in the last forty years and are still attracting a lot of interest from the academic community. The systems are electron donors linked together and can be explained and compared based on two major classifications which differ from each other only in terms of how the units (two or more) are connected to one another ¹⁾. The first classification is based on the number and position of the linkage of the spacer group and it can be divided into four groups: ^{1c)}

- Single-linkage such as the type **(57)**;
- Double-linkage such as the type **(58)-(60)**;
- Triple-linkage such as the type **(61)** ;
- Quadruple-linkage such as the type **(62)-(63)**;

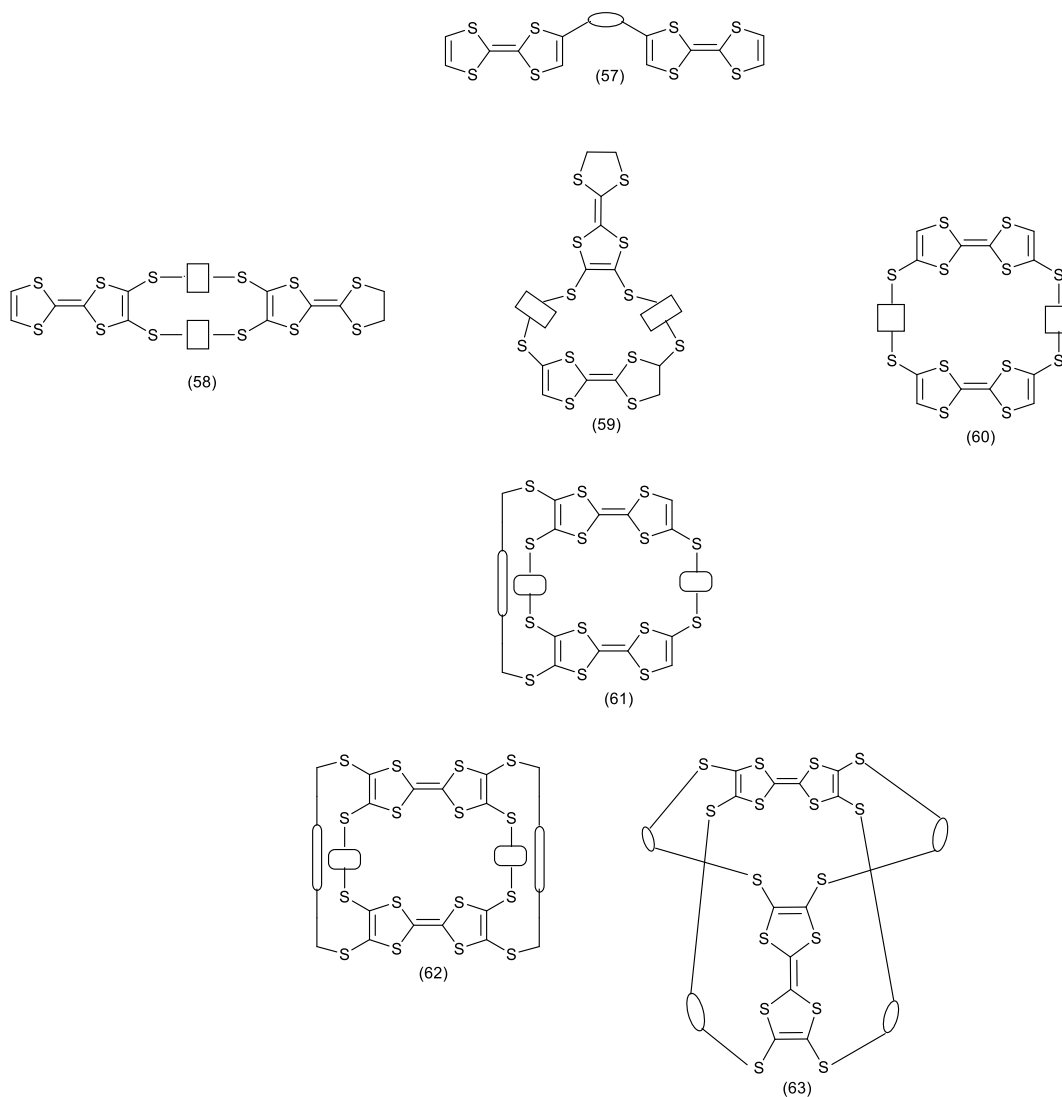


Figure 57. Example of various types of TTF dimer depending on the linkage between the two units.

A second classification can be made by considering the type of bond which connects the two donor molecules.

- π -conjugated systems as for **(64)**;
- heteroatoms linked systems as for **(65)**; (where X is the heteroatom)
- σ -bond linked systems as for **(66)**;

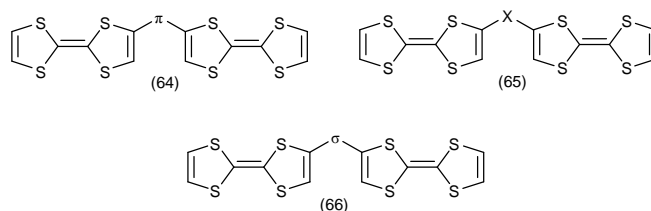


Figure 58. Classification of the TTF dimers depending on the spacer in between the two TTF units.

The condensed type of TTF dimers **(67)**, **(68)** and **(69)** have also been prepared and studied but are not included in the two classifications reported.¹⁾

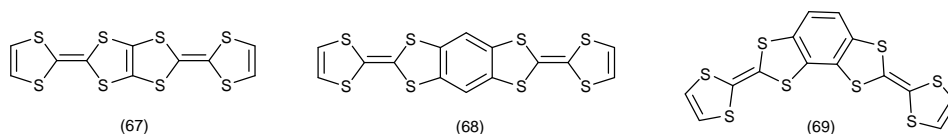


Figure 59. Different types of condensed TTF donors.

The linker between the two units may also be the source of intra-molecular through bond interactions such as in the case of **(64)** and **(65)** or of intra-molecular through space interactions for dimer **(66)**. The intra-molecular interaction through bond can be established in a head to tail connectivity; while the intra-molecular through space can be originated from the face to face stack of the TTF units.¹⁾

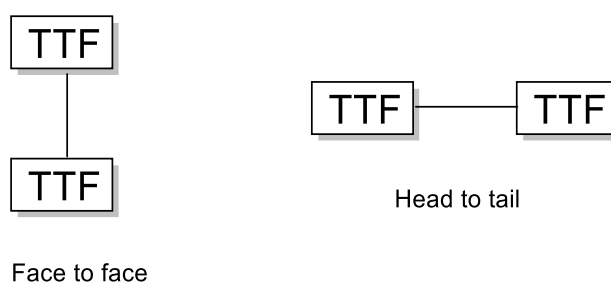


Figure 60. The two different connections for the TTF unit to interact with each other.

As a result of this intra-molecular interaction dimeric TTFs may display multistage redox behaviour which would lead to unique properties and structures in their charge-transfer or ion radical salts.¹⁾

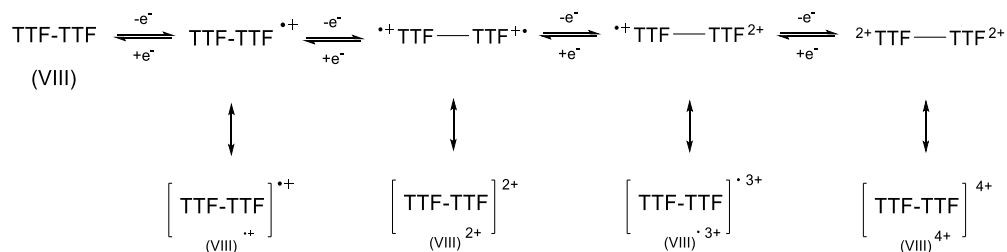


Figure 61. Redox processes for a TTF dimer and formation of radical cations and multi-cationic species.

Another important aspect of TTF dimers is the enhancement of dimensionality that the resulting structure can achieve. Various strategies have been defined like *i*) replacement of sulphurs by chalcogens with larger orbitals such as selenium and tellurium such as for TSF (**68a**), *ii*) increasing the number of sulphur atoms as in the case of BEDT-TTF (**69**), or *iii*) increase the size and spatial extension of the donor molecules such as in the case of TM-TTF (**67a**) and TM-TSF (**68b**) to stabilise the donor in its cationic state and to allow more inter- and intra-molecular interaction between donors.²⁾ All three approaches can be visualised in Figure 62.

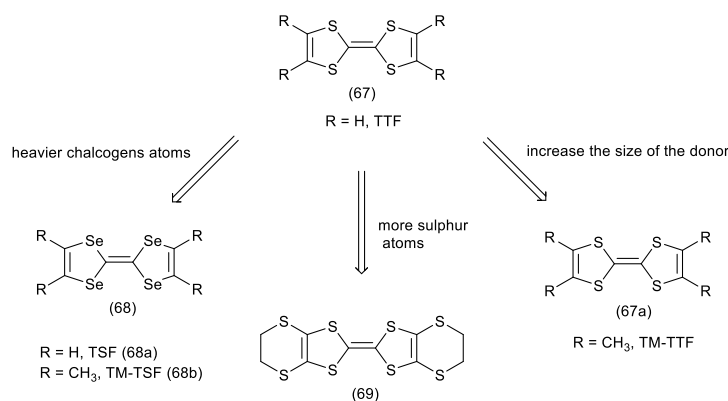


Figure 62. Examples of the strategies that can be adopted to enhance dimensionality.

The BEDT-TTF (**69**) (in blue and black) comes from the simple introduction of ethylene-dithio bridges on each side of the TTF (**67**) (in black) and it is a good example of how to increase the dimensionality by adding extra chalcogen atoms. The peripheral ethylene units are flexible allowing the molecule to adopt slightly different conformations. This is revealed in the crystal structure by showing some disorder in the structure.

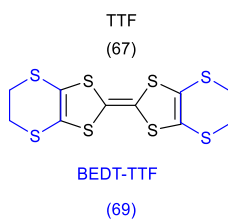
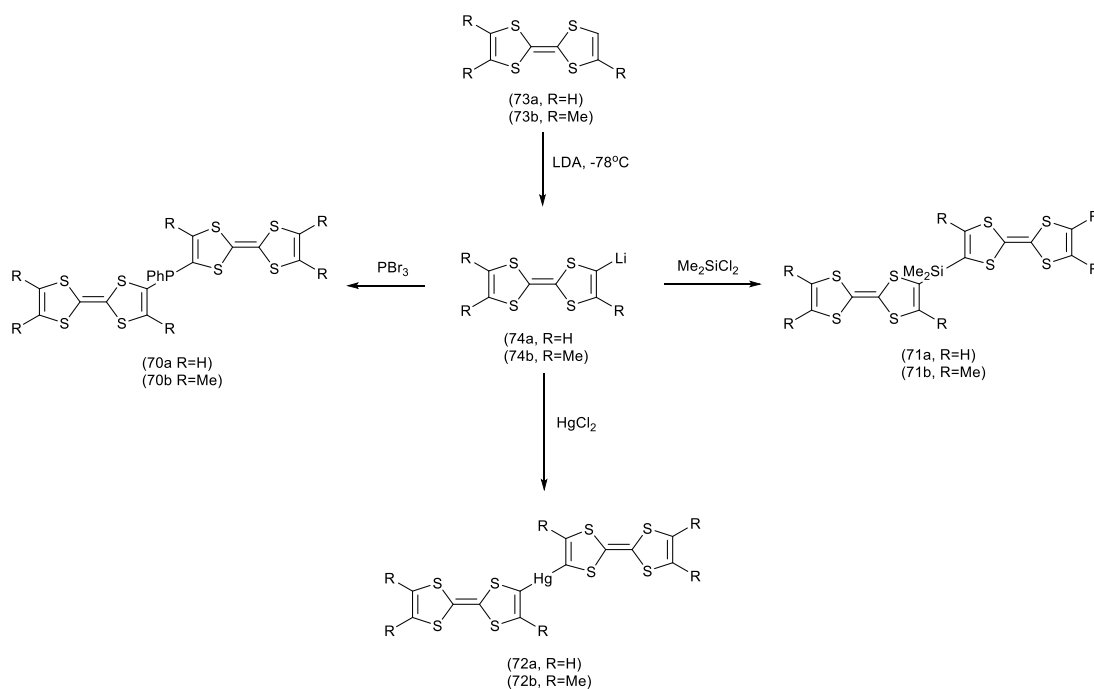


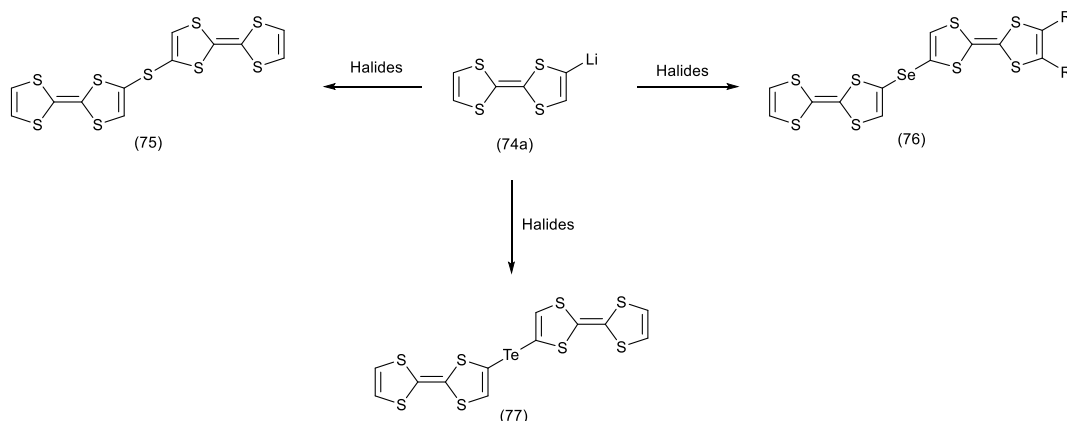
Figure 63. Emphasis on the difference between TTF and BEDT-TTF.

The study of the radical cation salts derived from BEDT-TTF with inorganic anions has been really productive leading to the discovery of several superconductors at temperatures below *ca.* 12K³⁾ and most metallic BEDT-TTF salts are quasi two-dimensional (2D) conductors with conductivity essentially isotropic in the plane of a 2D non-bonded S---S network. In parallel with the move from TTF to BEDT-TTF other forms of dimeric TTFs were prepared and studied. The incorporation of heteroatoms in TTF systems, in the sense of BEDT-TTF or in the linker for dimers or higher oligomers, have the potential to increase the intermolecular orbital overlap in the solid state. This results in high-dimensional networks and would suppress the Peierls distortion⁴⁾ for a metal-insulator transition, which is characteristic for a one-dimensional conducting system. There are more than a few examples in the literature of TTF dimers or oligomers linked by phosphorus (70), silicon (71) and mercury (72).⁵⁾ The first common step is the lithiation of the substrate (73) to generate mono-lithiated TTF (74) (Scheme 6).



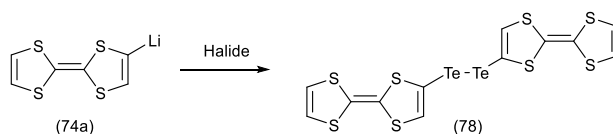
Scheme 6. TTF dimers linked by different heteroatoms. The lithiation of substrate is the starting point to generate the desired dimer.

Analogous examples have been prepared and reported with the chalcogen atoms sulphur (**75**), selenium (**76**) and tellurium (**77**).⁶⁾



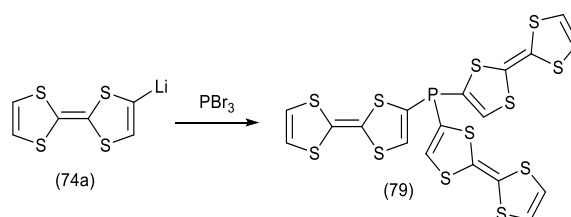
Scheme 7 Dimers linked by different chalcogen atoms.

The dimers prepared have been also analysed by X-ray crystallography showing a two dimensional network through S---S and X---X (where X is the heteroatom) contacts, such as in the case of (**75**) and (**77**). Due to the chalcogen-heteroatom interaction some of the TTF dimers prepared have shown high conductivity, as in the case of dimer (**78**) which presents a conductive behaviour ($5 \times 10^{-5} \text{ S cm}^{-1}$) in the neutral state.⁶⁾



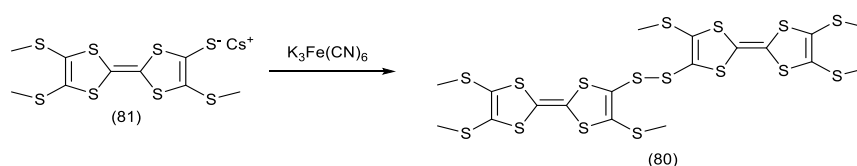
Scheme 8. Conductive Te-Te bridged TTF dimer.

Formigue and Batail also reported the preparation of a trimeric TTF (**79**) by reacting lithiated TTF (**74a**) with PBr_3 .⁷⁾



Scheme 9. TTF-trimer linked by a phosphorus atom.

Another interesting dimer is (**80**) which contains a di-sulfide bridge was reported in the literature by Becher *et al.*⁸⁾ This compound has been synthesised by oxidative homo-coupling of the thiolate (**81**) with potassium hexacyanoferrate(III).



Scheme 10. TTF dimer linked by a two sulphur atoms bridge.

These examples reported on the work carried out in the field of TTFs dimer and higher oligomers do not include the work based on conjugated TTFs and its evolution into π -extended TTFs. This particular kind of compound has been extensively studied and there is a huge amount of literature about different kinds of conjugated systems prepared and studied⁹⁾. The simplest example is the direct linked dimer (**82**) and its selenium analogue (**83**) is also reported.

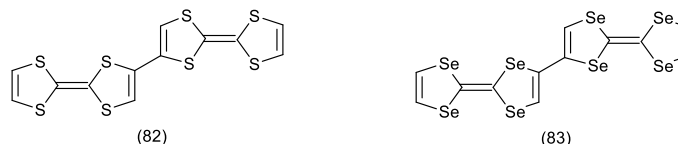


Figure 64. Conjugated TTF dimers based on sulphur and selenium network atoms.

The synthesis of (**82**) has been reported in the literature many times using different strategies which include transition metal catalysed coupling as the most efficient.¹⁰⁾ The same strategy has been applied for the preparation of (**83**).¹¹⁾ Examples of dimers linked by ethylene (**84**) and acetylene (**85**) bridges have also been prepared and reported.¹²⁾

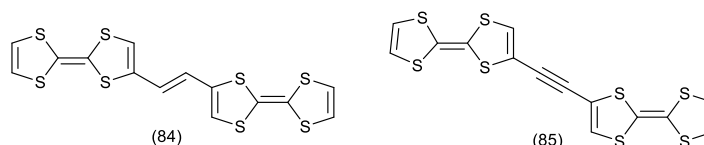


Figure 65. Examples of conjugated dimers with an unsaturation in the linker.

Recently the attention moved towards the so-called π -extended-TTF systems, which are based on an anthraquinone unit fused with a TTF molecule of which (**86**) is the simplest example. Preparation and properties of this molecule have been prepared by Miyashi *et al.*¹³⁾ The parent compound (**87**) bearing a *bis*-(ethylenedithio) bridge and analogue (**88a**) were reported by Bryce *et al.*¹⁴⁾, while benzo compound (**88b**) was prepared by Akiba *et al.*¹⁵⁾

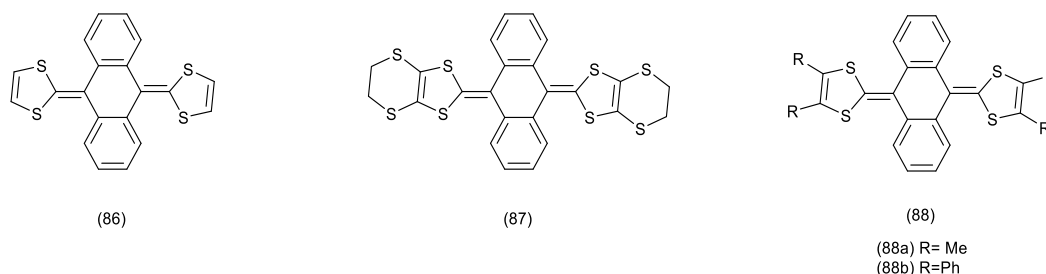


Figure 66. Different examples of π -extended-TTF systems.

Conjugated –TTF and π -extended-TTF systems were not, anyway, the topics approached during this PhD. There is thus a wide literature on dimeric TTF systems.¹⁾ In contrast there are hardly any poly-BEDT-TTF systems reported. The work presented in this chapter was aimed at preparing such molecules for developing new organic conductors.

2.2 Background.

During this PhD the work has been focused on linking two BEDT-TTF units together aiming to achieve the preparation of the kind of system presented in Figure 67. The linker has been represented as X in order to indicate a generic heteroatom or a chain containing a heteroatom.

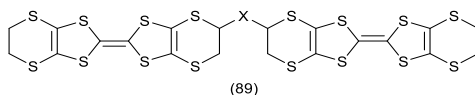
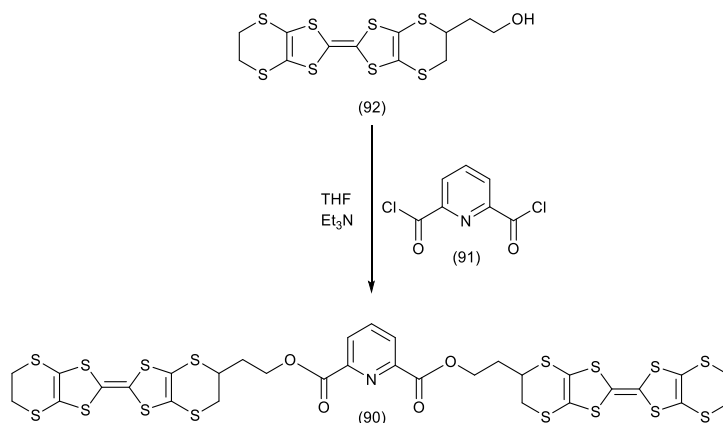


Figure 67. Generic desired targeted BEDT-TTF dimer.

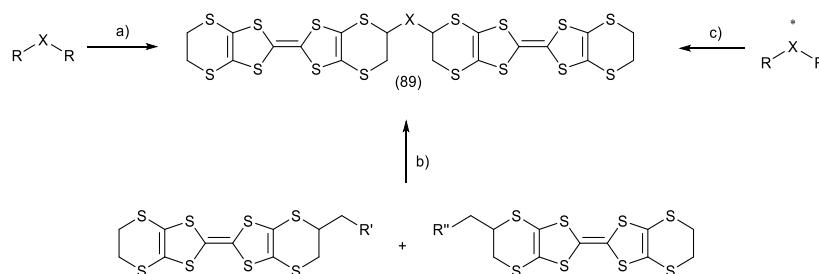
The reason for choosing this kind of system, BEDT-TTF rather than TTF, is the large amount of work, published and unpublished, that has been carried out in the Wallis group for decades on BEDT-TTF, in order to use established knowledge, expertise and functionalised donors made and reported in these years. One dimer has already been prepared in the Wallis laboratory, and has also been reported in the literature ¹⁶⁾. The donor (90) was prepared using the following strategy: commercially available pyridine di-carbonyl chloride (91) was reacted with the hydroxy-ethyl-BEDT-TTF (92) in THF in the presence of trimethylamine (Scheme 11). The final purpose of the compound was to bind metals to generate metal complexes which can show more than one property in order to increase the knowledge in the field of hybrid organic-inorganic multifunctional materials. It is worth mentioning that this was not the purpose of the work presented in this chapter.



Scheme 11. Preparation of donor (90) which represent an example of dimeric ET compound and metal ligand.

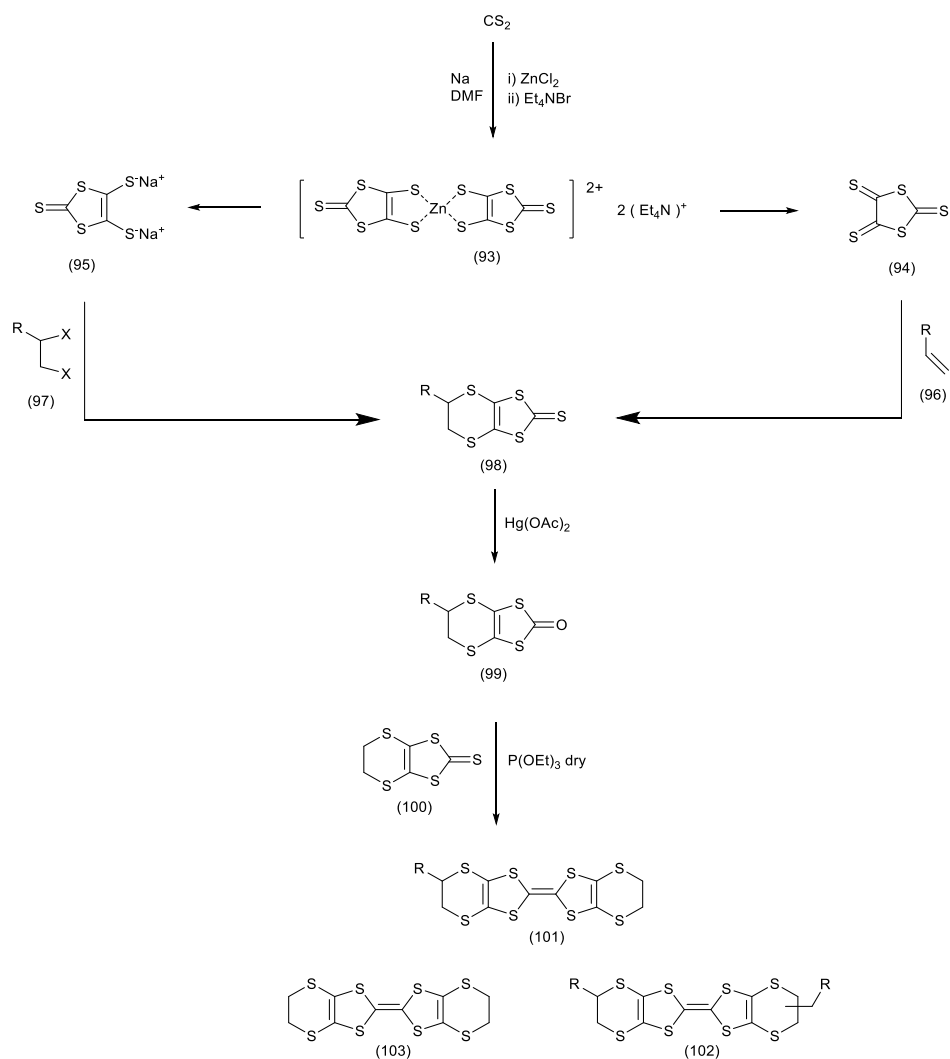
The purpose of the work presented in this chapter is to generate systems like donor (90), where two BEDT-TTF molecules are connected together by a central spacer. Different strategies, different central linkers and different mono-substituted BEDT-TTF donors have been involved, each one presenting different properties. The approach behind the preparation of donor (90) was to react a novel donor such as hydroxyl-ethyl-BEDT-TTF

(**92**) with a pyridine derivative in order to include a tridentate site for coordinating metal centres. The work undertaken here in the attempt to realise BEDT-TTF dimers started initially with the formation of the donor around the central linker (paragraph 2.3.1). The second approach studied was to react two suitable mono-substituted BEDT-TTF donors together (paragraph 2.3.2), while the third approach presented was to generate BEDT-TTF dimers around a central spacer which presents optical activity (paragraph 2.3.3).



Scheme 12. The three different strategies designed to reach targeted dimer (**89**).

The general synthetic pathway which lead to a substituted BEDT-TTF donor is presented in the scheme below.

Scheme 13. General preparation of cross-coupled (**101**) and homo-coupled (**102**) donors.

The starting point for the synthesis of every substituted thione (**98**), oxo-compound (**99**), cross-coupled donor (**101**) and homo-coupled donor (**102**) presented in this work is the synthesis of the zinc complex of 2-thioxo-1,3-dithiole-4,5-dithiolate (**93**). This reaction is a single electron reduction of carbon disulphide (CS_2) with metallic sodium. The reaction is carried out in dimethylformamide (DMF), from 0°C to 20°C and the resulting suspension is left stirring overnight, until all the sodium has been consumed. This step is crucial because it represents the construction of the building block of the sulphurs network. The proposed mechanism for the reduction mentioned has been put forward by Bryce *et al.*¹⁷ The Bryce mechanism leads to the formation of the dithiolate (**95**) and the sulphur heterocycle (**104**).

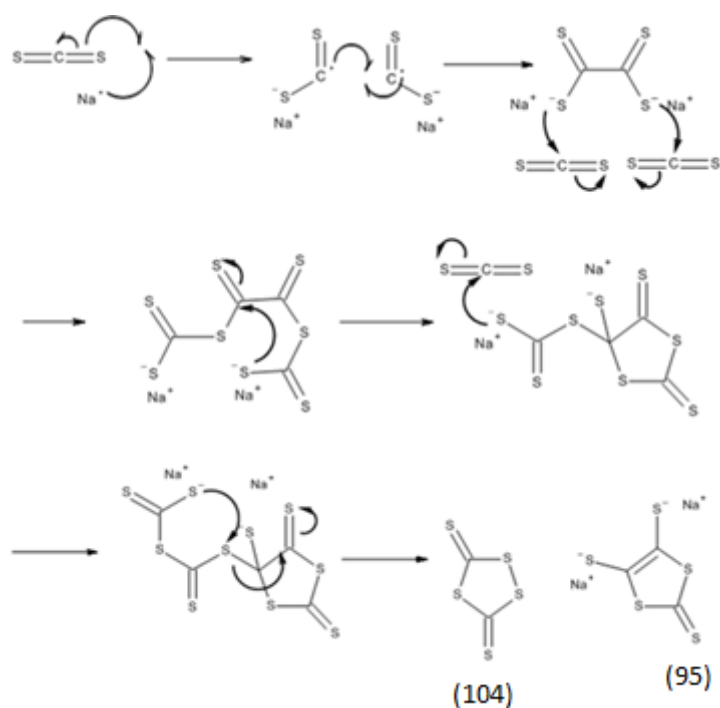
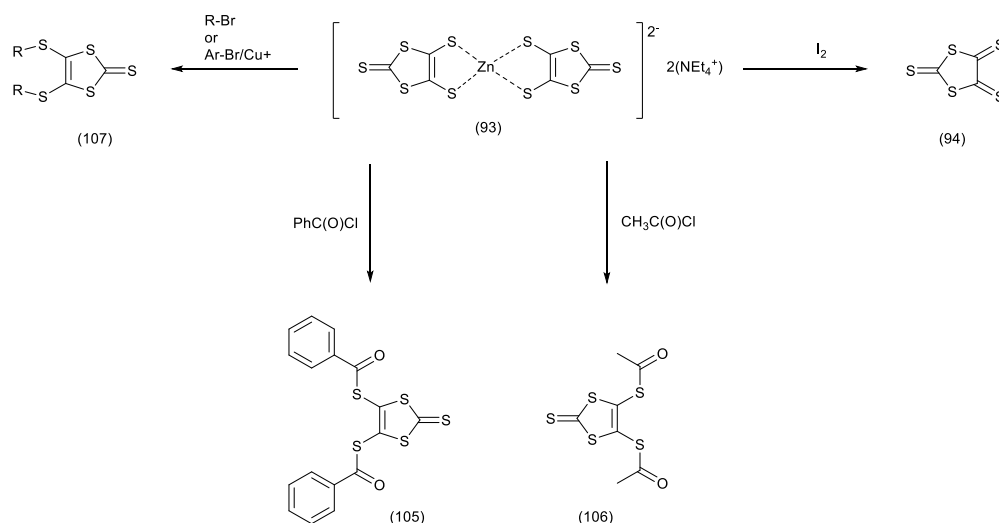


Figure 68. Proposed mechanism for the single electron reduction reaction between carbon disulphide and metallic sodium in DMF.

The dithiolate (**95**) produced in the last step of the proposed mechanisms is trapped out as a zinc-complex (**93**) by the addition of zinc chloride and tetraethylammonium bromide solutions to the reaction mixture which is left to stir overnight. A red precipitate of the tetraethyl salt of the 1:2 complex of zinc with the dithiolate is formed and after filtration and drying is recovered in 76% yield. This complex represents the starting material for every synthetic route towards the preparation of BEDT-TTF and TTF derivatives presented in this work. The zinc-complex (**93**) can be further reacted on in three main ways, either *a*) by reaction with benzoyl chloride¹⁸⁾ to form di-benzoyl protected thione (**105**) or by reaction with acetyl chloride¹⁹⁾ to form the di-acetyl protected thione (**106**), where both these compounds can be seen as precursors of dithiolate (**95**) or *b*) by oxidation with iodine in acetone/ethanol mixture at -78°C to afford the oligomeric trithione (**94**) which on heating undergoes a thermal depolymerisation to give a *vic*-dithione which undergoes many Diels-Alder type [4+2] cycloaddition reactions²⁰⁾ or *c*) by direct reaction of the zinc complex with electrophiles to give thiones such as (**107**).



Scheme 14. Different ways to react zinc-complex (93) to furnish protected thiones (105), (106) or (107) or trithione (94).

All three compounds (105), (106) and (94) provide valuable intermediates for the construction of mono-substituted BEDT-TTF donors. The next step in the generic scheme 13, after preparing the zinc-complex and its intermediates, is the preparation of thione (98). It can be generated by reaction of trithione (94) with the appropriate substituted alkene (96) by a [4+2] cyclo-addition. At this stage purification of the desired compound, by flash chromatography, is necessary to obtain the monosubstituted compound (98) from the polymeric material formed by reaction of trithione (94) with itself. Alternatively, thione (98) can be prepared from the sodium salt of the dithiolate (95) by reaction with a *vic*-dibromide (97)²¹⁾ or a cyclic sulphate ester.²²⁾ In the next step the thione sulphur atom in (98) is exchanged for oxygen using mercury (II) acetate to give the oxo compound (99). The donor synthesis is completed by double bond formation between oxo compound (99) and the unsubstituted thione (100) using the standard methodology involving freshly distilled triethyl or trimethyl phosphite. The unsubstituted thione (100) can be easily generated by reaction of the zinc complex (93) with 1, 2-dibromoethane in dry acetonitrile by refluxing the mixture for 8 hours. The desired product can be isolated by filtration and is ready to use without any further purification. In the phosphite mediated coupling reaction purification of the desired compound is necessary to separate the mono-substituted compound (101) from BEDT-TTF (103) and di-substituted compound and its isomers (102).²³⁾ The mechanisms for the sulphur-oxygen exchange (Figure 69) and the phosphite mediated coupling (Figure 70) are shown. For simplicity both mechanisms are described using un-substituted thione (100). This mechanism can be applied to every generic thione, (98), that undergoes exchange of sulphur for oxygen and phosphite mediated coupling reactions. In the case of thione (100) the exchange led to the oxo-compound (108).

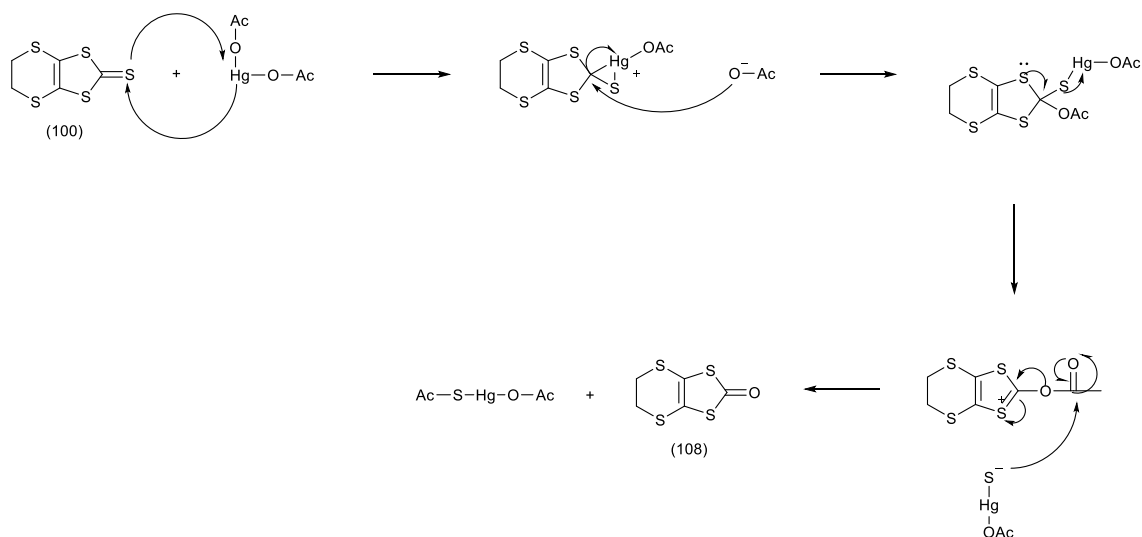


Figure 69. Mechanism of the exchange sulphur-oxygen reaction on substrate (100) using mercury (II) acetate.

The phosphite mediated coupling reaction proposed mechanism is developed by reacting (100) with its analogue oxo-compound (108) to furnish, in this case, BEDT-TTF (103). To be noticed that the alkyl chain in the phosphite is represented as R due to the fact that the coupling can be performed using different phosphites such as trimethyl ($\text{P}(\text{OMe})_3$), triethyl ($\text{P}(\text{OEt})_3$), or tri-isopropyl-phosphite ($\text{P}(\text{Oi-Pr})_3$).¹⁷⁾

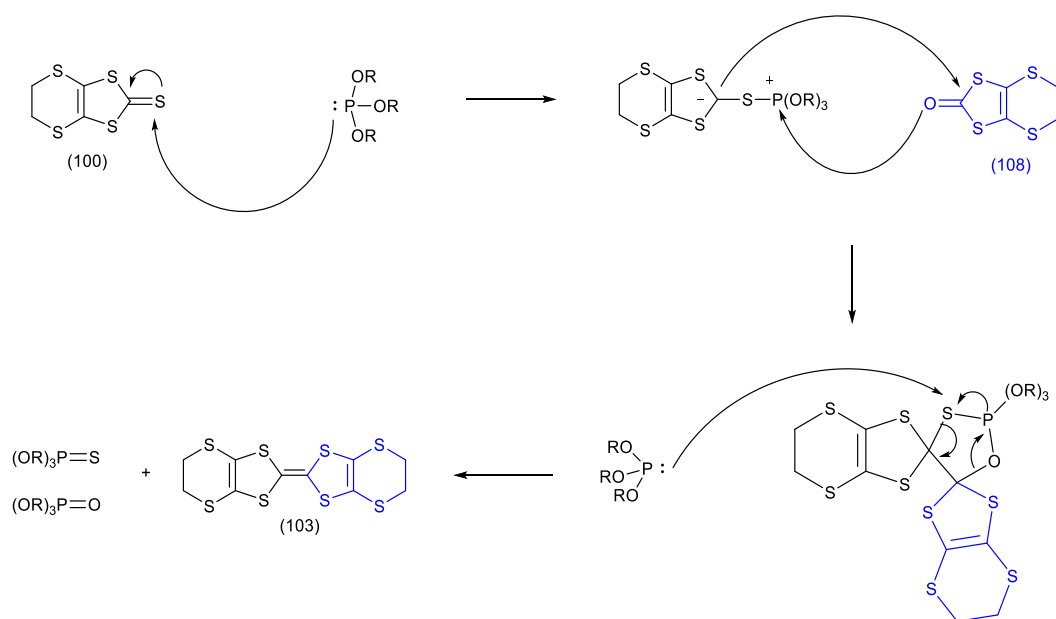


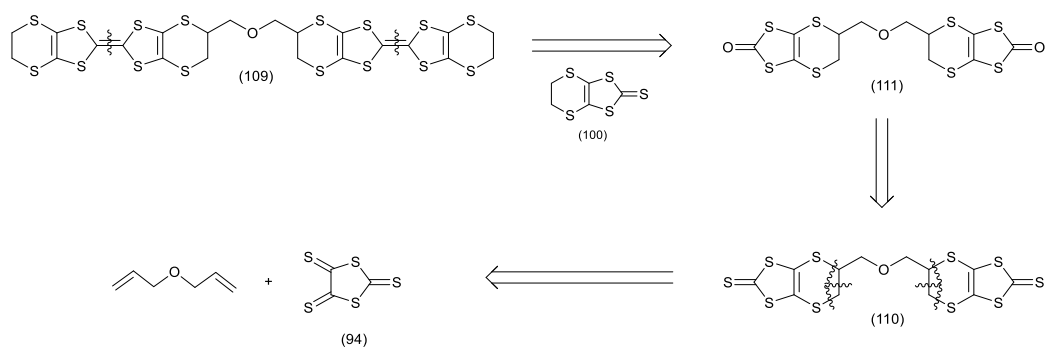
Figure 70. Mechanism of the phosphite mediated coupling to furnish the BEDT-TTF building block.

2.3 Result and Discussion

2.3.1 Ether and thio-ether bridged BEDT-TTF dimers.

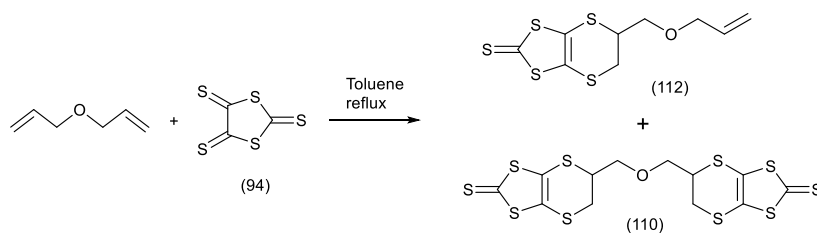
2.3.1.1 Preparation of dimeric BEDT-TTF by using di-allyl-ether and di-allyl-sulphide as starting materials.

The first synthetic approach designed to prepare the target donor (**109**), containing an ether bridge, is presented in scheme below:



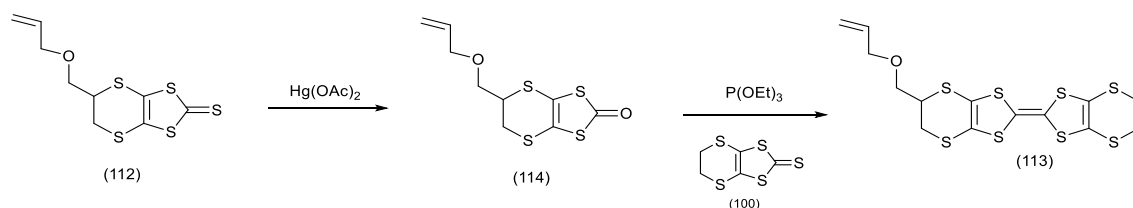
Scheme 15. Retrosynthetic approach considered to generate the desired dimer (**109**).

The strategy involves the use of di-allyl-ether that provides two terminal alkenes suitable for two cyclo-addition sites with the trithione (**94**) to give dithione (**110**), with the ether functionality to act as a linker. Following the standard procedure, developed and optimized in the Wallis laboratory, the next step would be the exchange of sulphurs for oxygens which is expected to give the product (**111**). The last step is represented by the phosphite mediated coupling by reacting the *bis*-oxo compound (**111**) and the un-substituted thione (**100**) in freshly distilled triethyl phosphite to give the target compound (**109**). Unfortunately the first step gave only a very small yield (6%) of the desired *bis*-(thione) (**110**) after purification and separation of the components in the mixture by flash chromatography. The main product, in 68% yield, was the mono-cyclised product (**112**) (Scheme 16) whose identity is supported by the presence of the alkene carbon resonances at 133.7 (-CH) and 117.8 (CH₂) ppm as well as hydrogen resonances at 5.85 ppm, multiplet for -CH, and two double quartets at 5.27 and 5.20 ppm for the *trans* and *cis* protons of the terminal -CH₂ with a major coupling constant of J = 17 and 10 Hz respectively. The problem appears to be the low reactivity of the alkene of the mono-addition product towards the second cyclo-addition reaction.



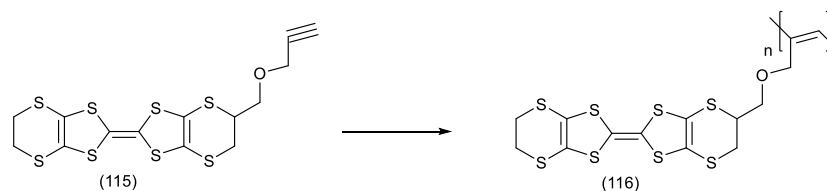
Scheme 16. Mixture of compound (110) and (112) purified by column chromatography after the first step.

The same reaction was attempted changing conditions such as the trithione: di-allyl-ether ratio, solvent and time but none of these changes gave the desired compound (110) in a better yield. Given that thione (112) could be prepared in good yield, it was then used to prepare a novel BEDT-TTF donor (113) which, to our knowledge, is the first with an alkene side chain. Exchange of thione sulphur for oxygen yielded oxo-compound (114) in 83% yield, and subsequent phosphite mediated coupling of (114) with the thione (100) gave the new donor (113) in 52% yield (Scheme 17). The resulting red oil was recrystallized from acetonitrile to yield a red solid which was used to generate single crystals of radical cation salts by diffusion with oxidants and/or by electro-crystallisation experiments.²²⁾



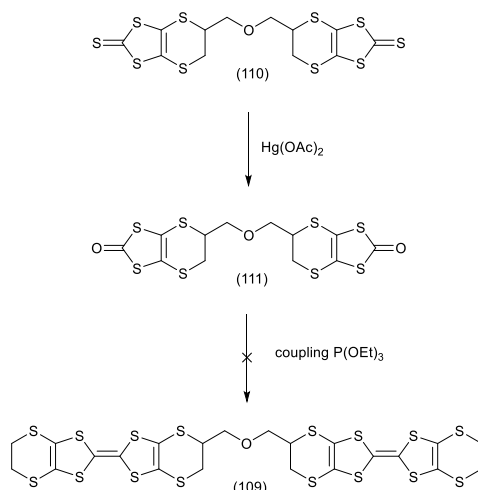
Scheme 17. Standard methodology followed to generate donor (113).

It is worth mentioning that an alkyne substituted donor (115), similar to donor (113), has been prepared and reported in the literature by Zhu *et al.*^{1c, 23)} Donor (115) was polymerised to yield a polyalkyne, (116), which showed electrical conductivity of $1.95 \times 10^{-5} \text{ S cm}^{-1}$ if doped with iodine vapour, or a weaker conductive behaviour, $7.3 \times 10^{-9} \text{ S cm}^{-1}$ if oxidised by iodine solution.

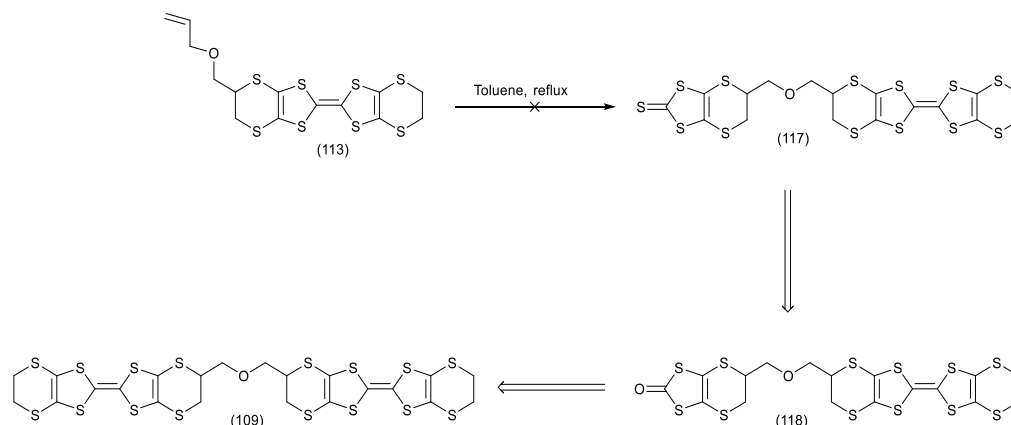


Scheme 18. Polymerisation of alkyne substituted donor (115) to furnish a weakly conductive polymer (116).

After the preparation of novel donor (113), the focus shifted to the conversion of bis-thione (110) in order to generate the desired dimeric BEDT-TTF system (109). The procedure and reactants involved were exactly the same used in the case of thione (112). The planned transformations are presented (Scheme 19).

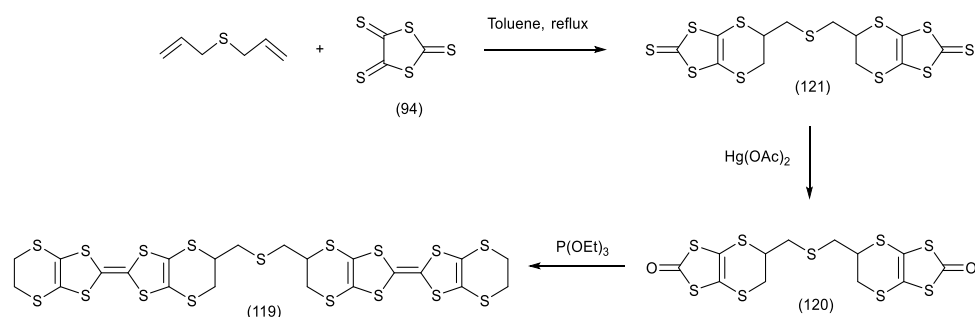
Scheme 19. Steps involved for the preparation of donor **(109)**.

The second step, the exchange of sulphur for oxygen, presented no difficulties and the oxo-compound **(111)** was obtained in excellent yield (91%). As expected the thio-carbonyl carbon resonance at 207.5 ppm was replaced by a carbonyl resonance at 187.9 ppm, and the alkene carbon atoms at the fusion of the rings shifted up-field as expected. However, the coupling of this *bis*-(oxo compound) **(111)** with an excess of the unsubstituted thione **(100)** using freshly distilled triethyl phosphite did not lead to the desired dimeric BEDT-TTF derivative **(109)**. After purification by flash chromatography the materials which gave an orange spot on the tlc, usually identified as the donor formed, appeared not to be the desired compound but a reaction product of the thione **(100)** with triethyl phosphite itself. The compound could not be clearly identified although MS analysis and NMR spectra were collected. Due to the failure of the first strategy it was decided to apply the usual donor construction methodology to donor **(113)** with the aim of building a second donor on to the alkene functionality as shown below (Scheme 20).

Scheme 20. Proposed alternative strategy to generate dimeric donor **(109)** from donor **(113)**.

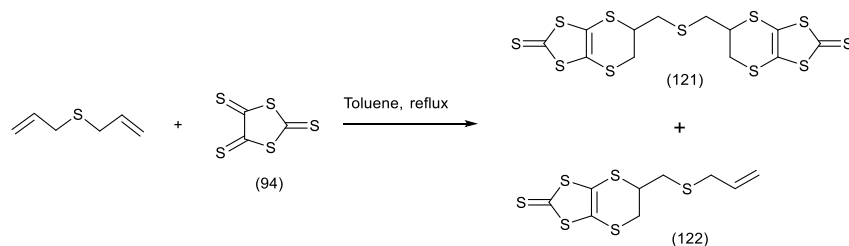
The designed procedure involved the reaction of donor **(113)** with trithione **(94)** in refluxing toluene. The next step would involve the exchange sulphur for oxygen with mercury

acetate in chloroform at r.t, followed by the final coupling with freshly distilled triethyl or trimethyl phosphite to afford, after purification, the desired donor (**109**). Unfortunately during the monitoring of the reaction between donor (**113**) and trithione (**94**), the tlc showed that the starting material was consumed, however there was no obvious new product. The reaction mixture was purified by flash chromatography and the most intense spots separated and analysed by NMR spectroscopy but the desired compound (**117**) was not identified. As the allyl-oxo-donor (**113**) disappeared during the reaction, according to tlc, a possible explanation is that a retro-Diels-Alder reaction of donor (**113**) was taking place. To verify this possibility a solution of (**113**) in toluene was refluxing overnight, but no changes were seen by tlc. The synthesis of the corresponding donor (**119**), which is an analogue of desired donor (**109**), was also explored.



Scheme 21. Procedure to generate targeted donor (**119**) from di-allylsulfide.

The first step is, as before, the formation of the two six-membered rings at the ends of the di-allyl sulphide to generate *bis*-thione (**121**) which is more likely to be found in low yield.

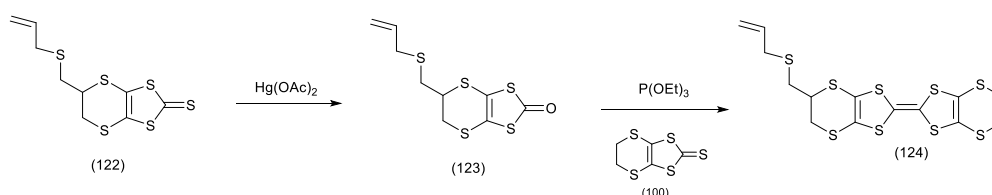


Scheme 22. Mixture of products formed during the first step.

The synthetic route involved exactly the same transformations presented before for the di-allyl ether, so exchange of sulphurs for oxygen to give compound (**120**) is the second step, followed by coupling with freshly distilled triethyl phosphite and un-substituted thi-one (**100**) to generate the desired dimer (**119**). Following the standard procedure, the Diels-Alder step, reaction between *bis*-allyl sulphide and (**94**), was even more problematic than the one previously performed. As before the reaction was monitored by tlc and the presence of two yellow spots was detected. After purification by column chromatography and characterisation of products by NMR spectroscopy the faster moving yellow

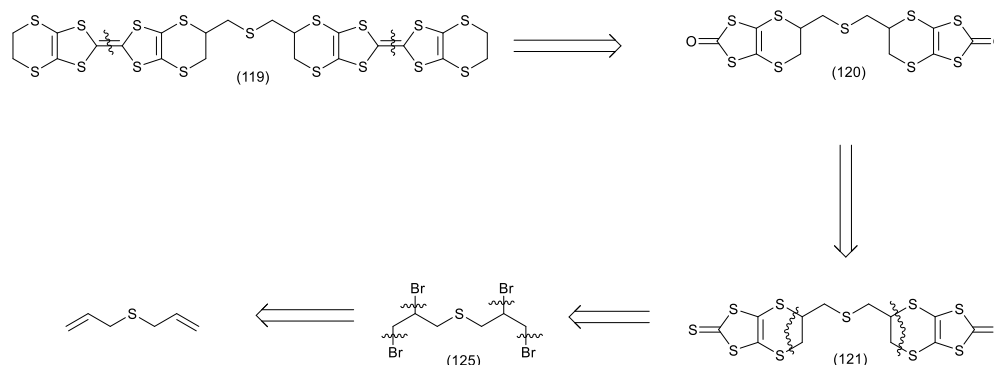
spot was identified as the mono-adduct (**122**), while the slower moving yellow spot needed more investigations. Thione (**122**) was recovered as an orange-red oil, in 30% yield, which is far lower than the 68% obtained from the di-allyl-ether reaction with trithione (**94**). The lower yield afforded may be partially due to the difference in the electronegativity of sulphur compared to the oxygen, which made di-allyl sulphide a worse substrate, than di-allyl ether, for a Diels-Alder reaction. The $^1\text{H-NMR}$ presented characteristic double bond peaks such as a multiplet for the $=\text{CH}$ at 5.74 ppm and two overlapping doublets at 5.11 and 5.08 ppm for the terminal $=\text{CH}_2$. The coupling constant for the *trans* and *cis* proton are $J = 14.2$ and 9.9 MHz respectively and the small coupling between the two protons in the terminal $-\text{CH}_2$ with $J = 1$ Hz. The identification of thione (**122**) was also supported by the presence in the carbon resonance of the peak at 207.8 ppm ($\text{C}=\text{S}$), and peaks at 133.7 and 118.2 ppm for the double bond. Indeed the MS analysis confirmed the identity of compound. The second fraction contained according to the NMR spectra, a mixture of *bis*-thione (**121**) and thione (**122**) which could not be separated. This could be indicative of a tendency for the *bis*-thione (**121**) to undergo a retro cycloaddition reaction.

Given that only thione (**122**) could be prepared in an acceptable yield, it was then converted to the corresponding final donor (**124**) by following the standard methodology. From thione (**122**) the usual exchange sulphur-oxygen was achieved in 60% yield, followed by a phosphite mediated coupling. Donor (**124**) was obtained after purification by column chromatography as a red solid in 31% yield and used to generate single crystals of radical cation salts by electro-crystallisation method or charge-transfer salts by diffusion.

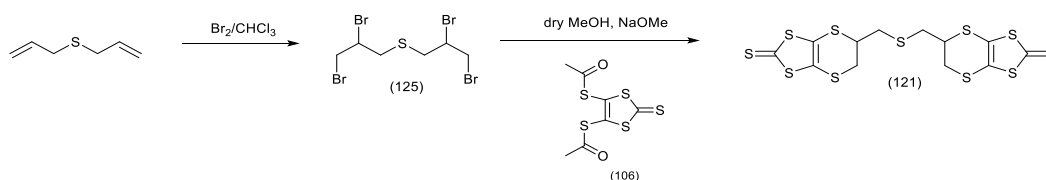


Scheme 23. Standard methodology followed for the preparation of novel donor (**124**).

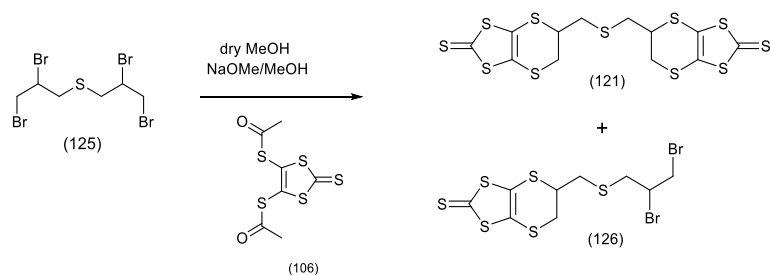
Since the preparation of *bis*-thione (**121**) was problematic and it was not possible to obtain it pure, the synthetic work moved on to a different strategy which is explain in the scheme below.

Scheme 24. Second strategy applied to prepare *bis*-thione (**121**) through tetrabromo compound (**125**).

Due to the low reactivity of the di-allyl-sulphide towards the formation of *bis*-thione (**121**) it was decided to avoid the Diels-Alder reaction and to attempt the generation of the six-membered ring using a different substrate. Tetrabromo compound (**125**) was identified as a good starting material to undergo a cyclisation reaction in the presence of a dithiolate species generated from protected thione (**106**) as outlined below (Scheme 25).

Scheme 25. Alternative route to achieve the preparation of *bis*-thione compound avoiding a Diels-Alder reaction.

The first step involved the reaction between di-allyl sulphide and bromine in chloroform at -20°C . The residue was purified by column chromatography to give relatively pure tetrabromide (**125**). The characterisation by proton NMR showed a pattern in accordance with the expected one, while the carbon resonance showed the presence of three major peaks, as expected, but also several small peaks close to the main three which may belong to a different stereo-isomer of the product formed. The pale-yellow oil revealed a molecular ion peak at m/z 434.7263 in accordance with the theoretical m/z 434.7268 in the mass spectrum. The second step involved the acetyl protected thione (**106**) as a source of dithiolate. The reaction involved the initial deprotection of thione (**106**) in dry MeOH at 0°C by slow addition of NaOMe/MeOH (25% in weight) solution. When the mixture resulted in a dark-red/purple colour then the tetrabromo compound (**125**) was added dropwise. The reaction was stirred for three hours before a yellow spot was detected on tlc. The temperature was increased to 50°C and then to reflux but no second product was detected by tlc. The crude product was isolated and characterised by NMR. Based on the ^1H and ^{13}C spectra the crude material seemed to be a mixture of starting material and mono-thione (**126**) and/or bis-thione (**121**).



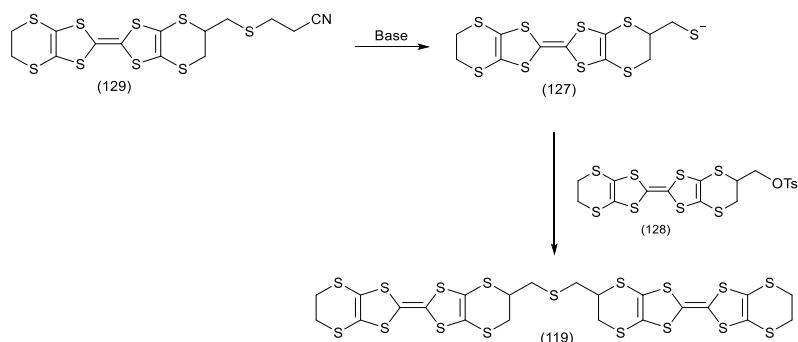
Scheme 26. Mixture of product which may have been formed from the substitution reaction performed.

The mixture was also analysed by mass-spectrometry but no peak was detected for any of the two possible thiones that may be formed. As a result of this the identification of the product formed was inconclusive and more investigation is needed.

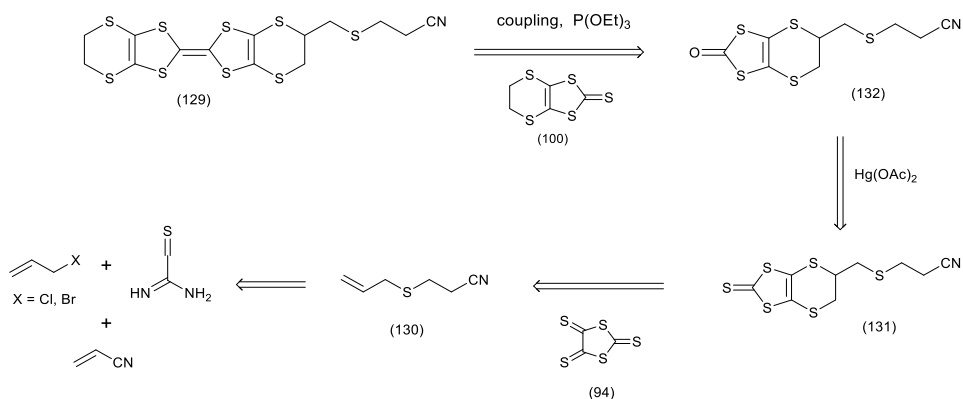
2.3.2 Attempted preparation of dimeric BEDT-TTF system by reacting two substituted ET donors together.

2.3.2.1 Preparation of a novel BEDT-TTF donor with a cyano-ethyl protecting group on a sulphur atom.

The challenge of preparing a dimeric BEDT-TTF has seen another attempt using a partially new strategy, by reacting two donors together as in the case presented in Scheme 27. A novel donor was prepared bearing a suitable protecting group on a side chain sulphur atom, in order to deprotect it and react the thiolate (**127**) formed with a second donor containing a suitable leaving group such as (**128**). The targeted donor for this purpose is the compound (**129**), where a cyano-ethyl functionality is protecting the sulphur atom which is the constituent of our central linker in donor (**119**). This protecting group has been extensively used in the literature by Becher *et al.*^{8,24} in TTF chemistry.

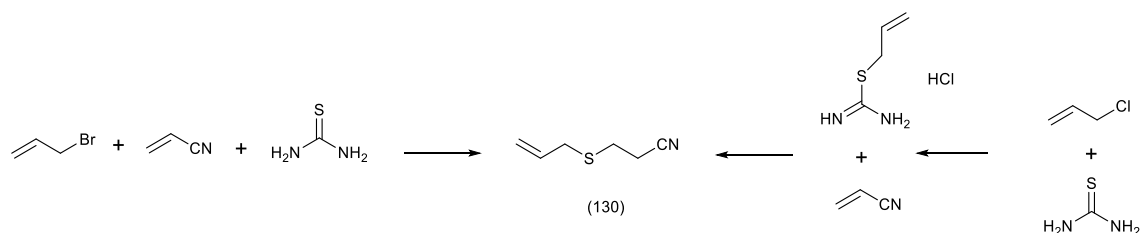
Scheme 27. Strategy planned to prepare donor (**119**) from novel donor (**129**).

The initial strategy was to deprotect the donor (**129**) using caesium hydroxide or sodium methoxide then to add a solution of donor (**128**) to displace the tosyl group and form a dimer. The novel donor (**129**) was prepared using commercially and easily available starting materials as shown below (Scheme 28).



Scheme 28. Proposed route to achieve preparation of donor (**129**).

The planned strategy involved cyclo-addition between trithione (**94**) and 3-(allyl-thio)propanitrile (**130**), which was synthesised following two different literature methods²⁵. Both these procedures involved thiourea, allyl chloride or bromide and acrylonitrile using either PEG or ethanol. Both procedures gave a good yield of product (**130**).



Scheme 29. The two methods to synthesis alkene (**130**).

After preparation of dienophile (**130**), the following step was the formation of the six-membered ring by reacting trithione (**94**) and (**130**). Thione (**131**) was isolated by flash chromatography in 46% yield. The isolated compound was analysed by NMR spectroscopy where the appearance in the $^1\text{H-NMR}$ spectrum of peaks at 3.76 ppm and 3.39 ppm related to the six membered ring formed and in the $^{13}\text{C NMR}$, of peaks at 207.4 ppm for $-\text{C}=\text{S}$ and at 122.6 and 121.6 ppm for the sp^2 carbons of the five membered ring were evidence of the successful transformation. The identification was supported by the CHN analysis. The exchange of thione sulphur for oxygen was carried out using the standard methodology involving mercury (II) acetate and chloroform to give oxo-compound (**132**) in 97% yield. Its identity was confirmed especially by carbon resonance due to the shift from 207.4 ppm ($\text{C}=\text{S}$) to 188.8 ppm ($\text{C}=\text{O}$) and the shift of the sp^2 carbons to 113.4 and 112.3 ppm. The triethyl phosphite mediated coupling between oxo-compound (**132**) and

Chapter 2 Attempted synthesis of BEDT-TTF dimer and related substituted BEDT-TTF donors obtained unsubstituted thione (**100**) was carried out at 90°C using freshly distilled phosphite under inert atmosphere to give the desired cross-coupled donor (**129**) in 30% yield after purification by flash chromatography. The characterisation by ^1H and ^{13}C -NMR, agreed in the identification of donor (**129**), which was also confirmed by the CHN analysis. Once the desired donor had been obtained the strategy was to deprotect the side chain sulphur atom using a strong base to remove the cyanoethyl group and to react the resulting thiolate with tosyloxymethyl-BEDT-TTF^{7,8}) as reported above (Scheme 27). The deprotection was attempted using a number of strong bases such as sodium *tert*-butoxide, sodium methoxide, tetrabutylammonium hydroxide (TBA-OH), caesium hydroxide, sodium hydride and n-BuLi. The tlc plates have been scanned and attached to provide evidence which support the theoretical explanation which have been given to these unsuccessful attempts. Below (Figure 71 and 72) is reported the situation encountered in four different reactions, starting with sodium hydride and caesium hydroxide (Figure 71).

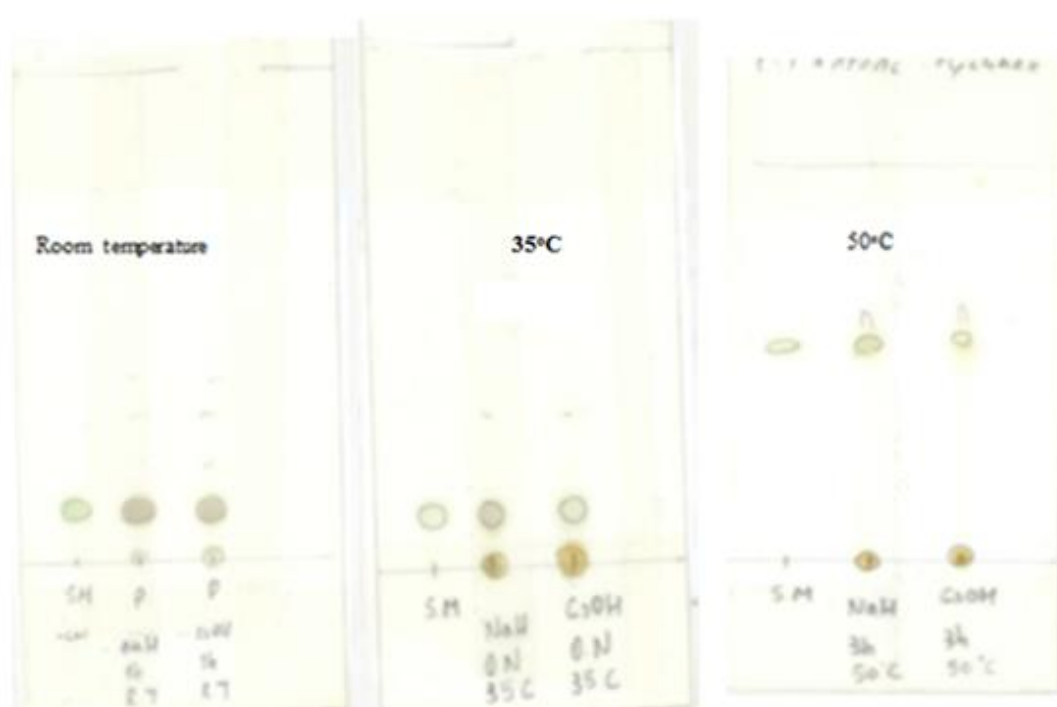
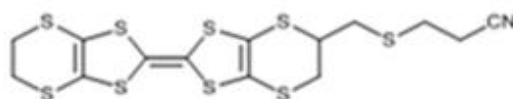
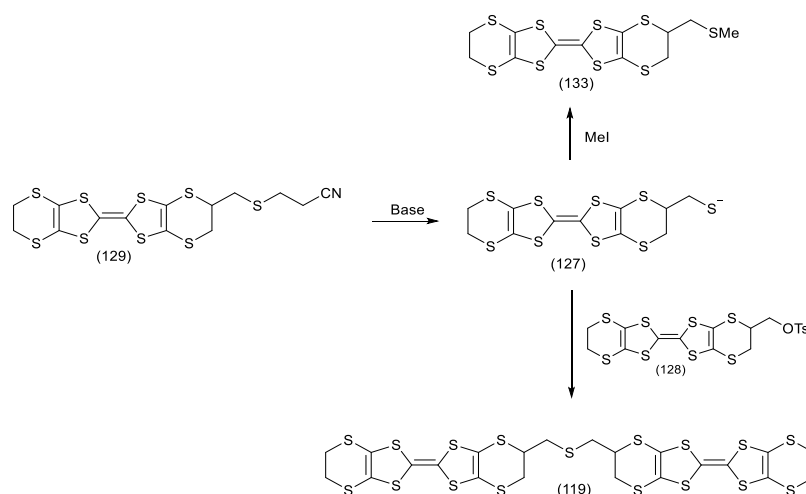


Figure 71. Comparisons of the tlc plates developed at different conditions for the attempted deprotection of donor (**129**) with NaH and CsOH.

From the figure above it is clearly visible that despite different conditions, such as 20°C, 30°C and then 50°C the starting material is still present as the main component of the reaction mixture. This is a strong evidence that the bases used are not strong enough to

displace, completely, the cyano-ethyl group from the ET derivate. The spot at the bottom is surely due to the base. Addition of methyl iodide did not lead to any secondary reaction to provide methylthio-methyl-BEDT-TTF (**133**).



Scheme 30. Consequences of addition of methyl iodide in case of successful deprotection of donor **(129)**.

The same results have been reported in the cases of lithium-dimethyl-amide and n-BuLi. The starting material is the main and only component in the product's mixture after addition of the base.

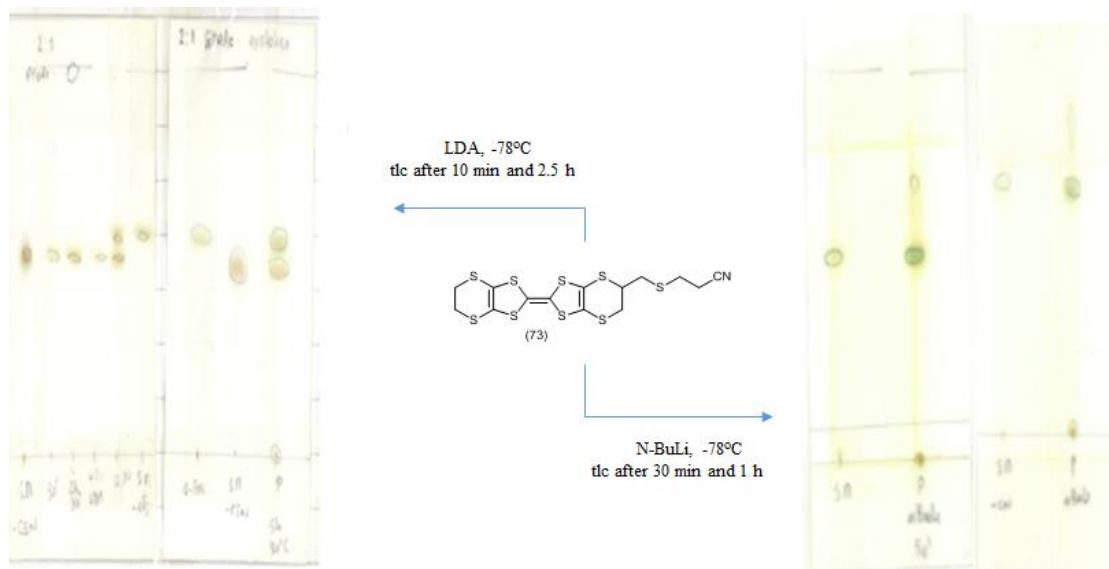


Figure 72. Comparison between the tlc plates developed for the two different methodology.

The evidence shown above define how hard is the deprotection of the sulphur atom. Moreover the use of this protecting group in TTF chemistry has been widely reported in research papers, review articles and books. The common factor in the references found so far is that the sulphur atom is attached directly to an sp^2 carbon atom ^{1,8)} as in Figure 73 and unlike the current situation presented in this work (Figure 74). A closer look at the

two kind of systems considered here shows that the substrate used in the literature is more reactive than the one involved in this work.

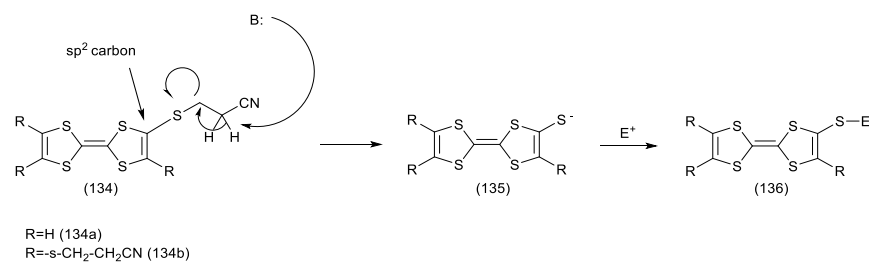


Figure 73. Proposed mechanism for the displacement of cyano-ethyl group.

The substrate involved in this research presented the carbon hybridisation as sp^3 , not only for the carbon directly attached to the sulphur, but also for the neighbouring carbon.

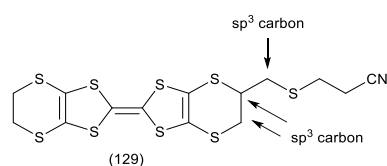


Figure 74. Hybridisation of carbon next to the sulphur in the system investigated.

A possible explanation is that the conjugation in the system presented in Figure 73 stabilises the dithiolate so it become more reactive towards its deprotection. The conjugation is not present in the system in Figure 74 and it does not play its part. Going back to the reaction performed it become even clearer that the addition of an electrophilic species, such as tosyl-oxo-methyl-BEDT-TTF (**128**) is not leading to any sort of reaction. Indeed the two spots are clearly visible even if they run very close to each other (Figure 75). Unusual chemistry in BEDT-TTF systems has been observed before, and there may be a contribution from the tendency of the donor molecules to stuck together in solution making the side chains less accessible.

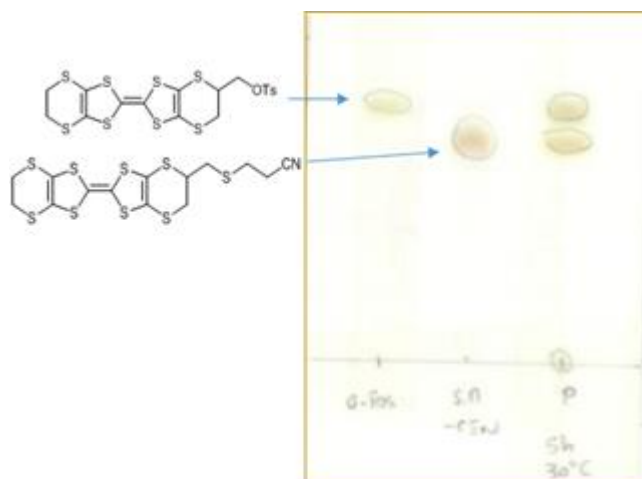


Figure 75. Identification of the reagents involved on the developed TLC plate.

When the reaction shown in Scheme 30 was performed a second parallel reaction was in progress. In this case a different electrophile was added, 1,3,5-trichloro-triazine (**137**), and the mixture was monitored at r.t., 35°C and in refluxing THF without, even in this case, any evidence of reaction observed on the tlc plate.

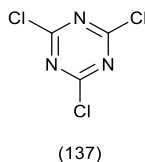
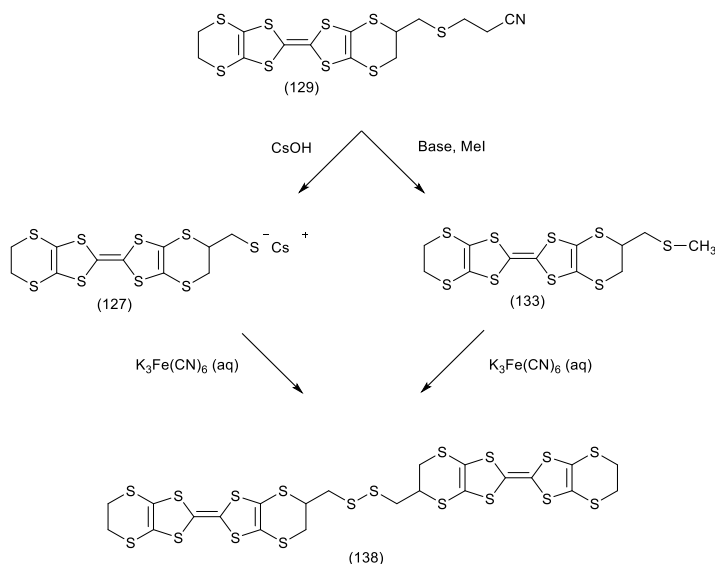


Figure 76. The second electrophile added to the reaction mixture.

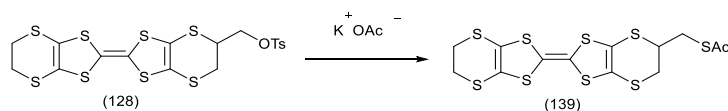
At last acetic acid was added to quench the reactions involving sodium hydride and caesium hydroxide and ¹H-NMR of the residues were recorded. The spectra obtained were of a really difficult interpretation and no useful information have been found on it. Even this strategy was abandoned and the challenge of preparing a dimeric BEDT-TTF derivative moved on to a different type of linkage. In the eventuality that the thiolate would have been formed another alternative strategy had been considered to generate a dimeric BEDT-TTF system. The method, reported in the literature,⁸⁾ would consist of the oxidation of the caesium salt of dithiolate (**127**) or in the oxidation of the methyl-thio-methyl-ET (**78**) to generate the disulphide (**84**) unit using K₃Fe(CN)₆. However, this reaction has not been performed due to the failure of the deprotection methods attempted.



Scheme 31 Further strategy to generate a disulphide bridged dimer after deprotection of donor (**129**).

A final attempt of preparing a dimeric BEDT-TTF linked by an alkyl chain containing an heteroatom was made using a donor with a more labile sulphur protecting group. The synthesis of the S-acetyl protected donor (**139**) was undertaken. Tosyl-oxymethyl-BEDT-

TTF (**128**)²⁶⁾ was reacted with potassium thioacetate in THF, to give the S-acetyl protected donor in 65% yield as a brown solid.



Scheme 32 Reaction to generate acetyl protected thiol (**139**) from donor (**128**).

The ¹H and ¹³C-NMR spectra show clearly the acetyl's methyl group at 2.31 ppm and the carbonyl at 194.90 ppm, and the high resolution mass spectrum confirms the molecular composition with an *m/z* of 472.8439 against the theoretical *m/z* value of 472.8447. The final step was the deprotection of novel donor (**139**) and reaction of the thiolate group with a second donor containing an electrophilic carbon.

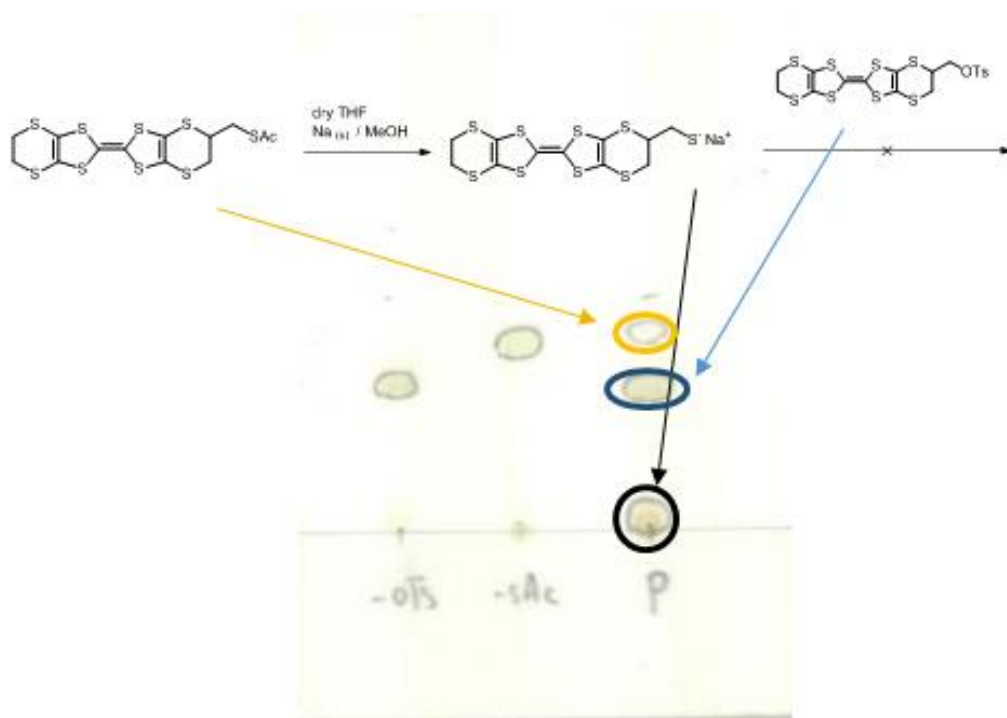


Figure 77. Identification of the reagents involved onto the tlc plate developed for monitoring of the reaction.

The donor (**139**) was deprotected with sodium methoxide and the tosyloxy-methyl-BEDT-TTF (**128**) added. However though tlc confirmed deprotection no subsequent reaction occurred. A second electrophile, 1,3,5-trichloro-triazine (**137**) was added but this did not lead to any new product. A final quench with acetic acid was done in the attempt to generate the thiol (**140**) but no material could be recovered.

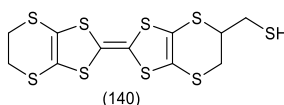
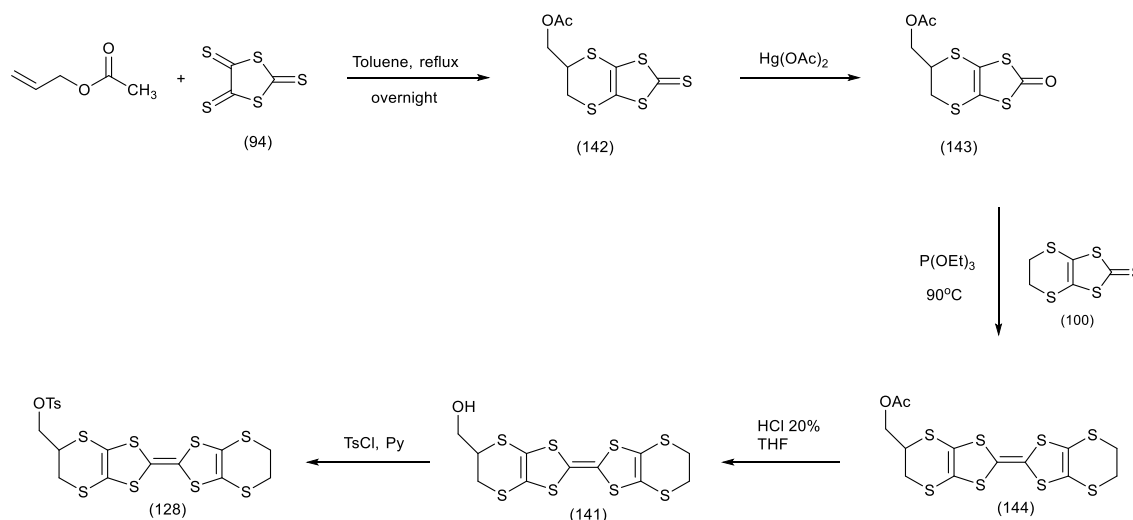


Figure 78. Quenching the reaction with AcOH should led to the formation of donor (**140**).

The synthesis of dimeric BEDT-TTF systems using alkylic chains containing heteroatoms was abandoned and the synthesis moved on to consider a different kind of bridge.

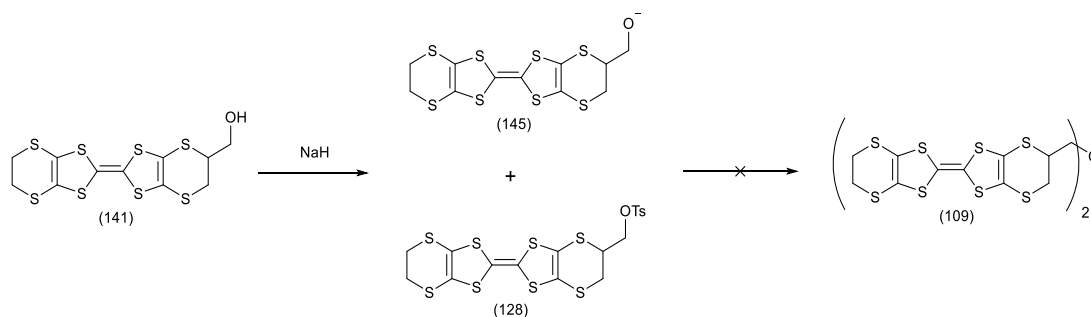
2.3.2.2 Preparation of *exo*-methylene-BEDT-TTF, and further linking strategies.

A new strategy was to make the ether link between two suitable BEDT-TTF substituted units by reacting hydroxyl-methyl-BEDT-TTF (**141**)²⁶⁾ with tosyl-oxy-methyl-BEDT-TTF (**128**) in the presence of a base. The preparation of the two donors involved is presented in Scheme 33. The hydroxy-methyl-BEDT-TTF (**141**) was prepared following the route developed in the Wallis laboratory, in four steps, and the tosyl-oxy-methyl-BEDT-TTF (**128**) was prepared by reaction of hydroxymethyl-BEDT-TTF (**141**) with 7 equivalents of tosyl chloride; the need for 7 equivalents being an example of the unusual chemistry of BEDT-TTF derivatives.

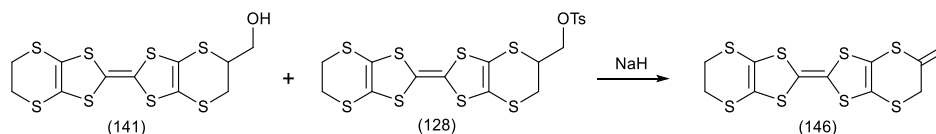


Scheme 33. Preparation of donor (**128**) and (**141**).

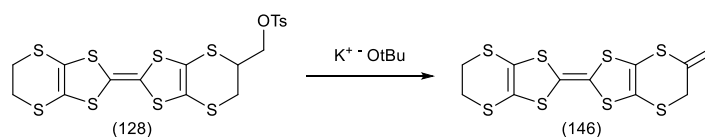
The idea was to deprotonate the hydroxylic group using sodium hydride and then to add to the alkoxide (**145**) formed a species containing an electrophilic carbon bearing a good leaving group such as in donor (**128**) to give the desired dimer (**109**). A possible complication was competition between the deprotonated species acting as a base, to eliminate tosic acid rather than substitute the tosyl group.

Scheme 34. Desired product (**109**) was not isolated by reacting together donor (**128**) and (**141**).

Interestingly, when donors (**128**) and (**141**) were reacted together the tosyl-oxy-methyl-BEDT-TTF (**128**) undergoes completely the elimination reaction and no trace of the substituted product was found. This led to a new donor (**146**) in 92% yield and as shown in the Scheme 35 the alkene group lies in a side chain and is not in the six-membered ring. This is supported by the NMR spectra. The two alkene hydrogens give singlet signals at 5.22 and 5.13 ppm in the ^1H -NMR spectrum. The ^{13}C -NMR showed alkene peaks at 137.4 ppm for 5-C and at 111.0 ppm for the terminal $=\text{CH}_2$. In addition there is the presence of peaks for the bis-ethylene-dithio bridge at 30.1 ppm and the 6-C carbon peak at 36.5 ppm.

Scheme 35. Product obtained by reacting donors (**128**) and (**141**) together.

Donor (**146**) could be easily obtained from tosyl-oxy-methyl-BEDT-TTF (**128**) using a strong base such as sodium *tert*-butoxide as it shown in Scheme 36:

Scheme 36. Elimination reaction on tosyl-oxy-methyl BEDT-TTF to give donor (**146**).

Interestingly for donor (**146**) the mass spectrometry analysis recorded an m/z value of 391.2835 (100%). However $\text{C}_{11}\text{H}_8\text{S}_8$ requires a nominal mass of 396. The observed m/z ratio is difficult to explain because it requires the loss of four hydrogens which is not easily understandable. Probably it is due to some sort of rearrangement or the machine was incorrectly calibrated. Despite this donor (**146**) has been analysed using different techniques and there are no doubts about this compound as the NMR spectroscopy and the CHN analysis confirmed the structure. In the literature²⁷⁾ the isomer of donor (**146**), donor (**147**) is reported (Figure 78). In fact the two structures are tautomers.

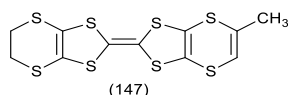


Figure 79. Donor (147) reported in the literature which is an isomer of donor (146).

The ¹H-NMR spectrum for donor (147) shows a singlet at 2.30 ppm or 2.11 ppm²⁷⁾ depending on the deuterated solvent used. This characteristic peak for a methyl group is missing in the NMR spectrum of donor (146). This evidenced the correct identification of the donor obtained. Several radical cation salts have been characterised from (146), as described later. Due to the failure of this approach with regards to the dimer preparation a few more different strategies have been considered and are reported. In a further attempt to generate a dimer of the same kind of donor (109), but with a longer spacer, the focus moved to donor (148).

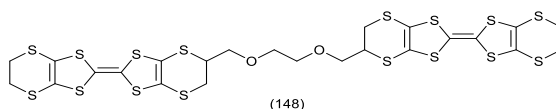
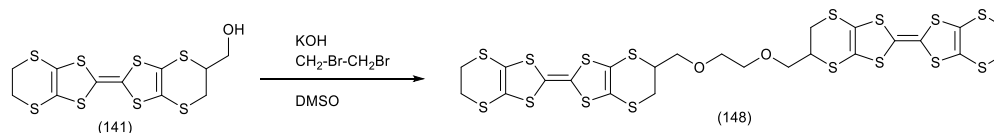


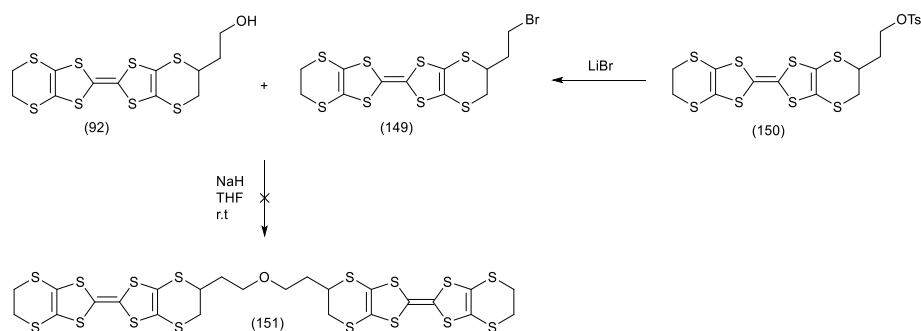
Figure 80. New targeted dimeric BEDT-TTF system.

One strategy was the alkylation of hydroxyl-methyl-BEDT-TTF (141) with a dibromide. Thus, donor (141) was reacted with 1, 2-dibromoethane in the presence of powdered potassium hydroxide (excess) in DMSO (Scheme 37).



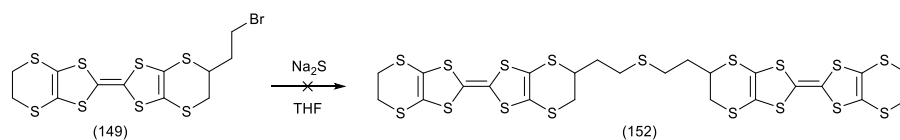
Scheme 37. Reaction performed to attempt the generation of donor (148).

However, the desired product was not isolated and the residue, analysed by NMR spectroscopy was not fully identified. A second strategy for the preparation of dimeric BEDT-TTF involved the reaction between donors (149) and (141) (Scheme 38). Donor (149) is a novel compound and was prepared from tosyl-oxo-ethyl-ET (150) by treatment of the former with an excess of LiBr and obtained in 60% yield.



Scheme 38. Preparation of donor (149) and attempted synthesis of dimer (151).

Unfortunately even in this case the desired compound (151) was not obtained. A possible improvement could be to increase the temperature up to reflux to see if any sort of reaction is detected. In an attempt to make the corresponding donor with a thio-ether linkage (152), the novel donor (149) was reacted with sodium sulphide. However no product could be isolated.

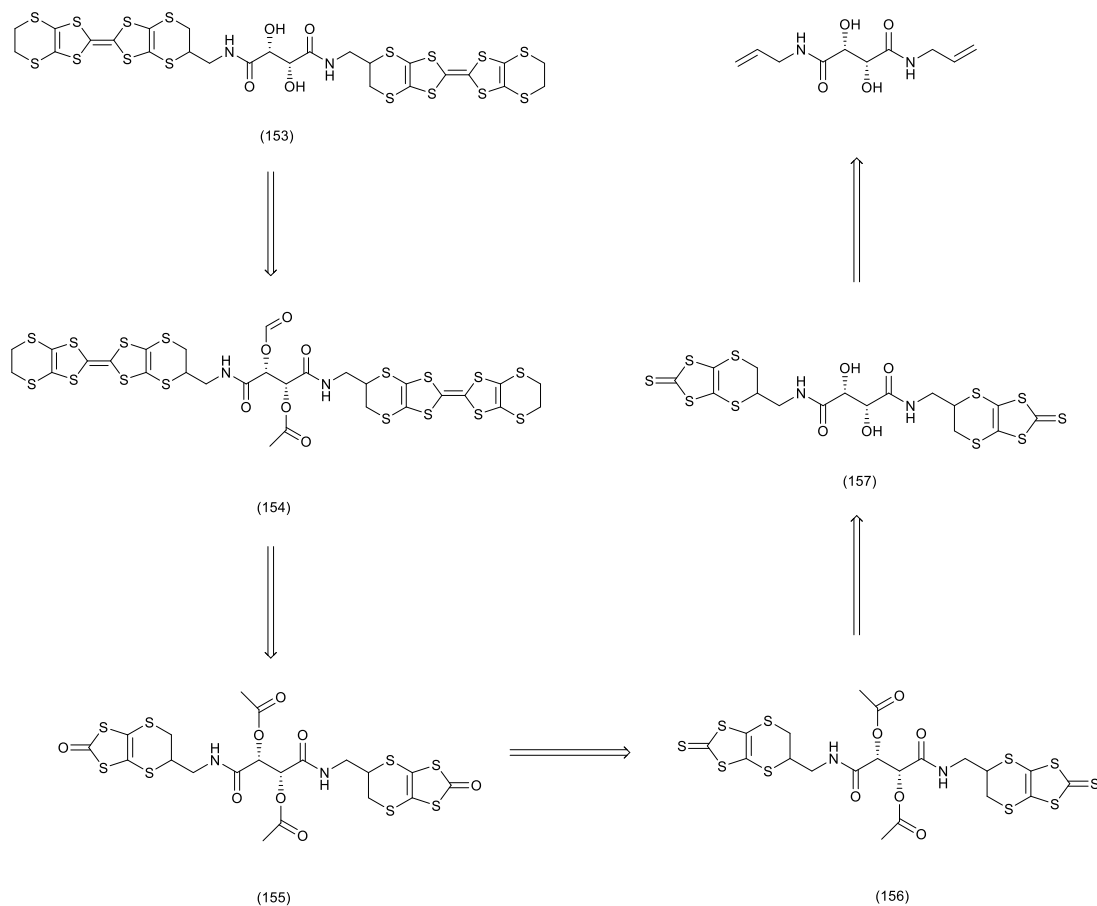


Scheme 39. Attempted reaction for the preparation of dimer (152).

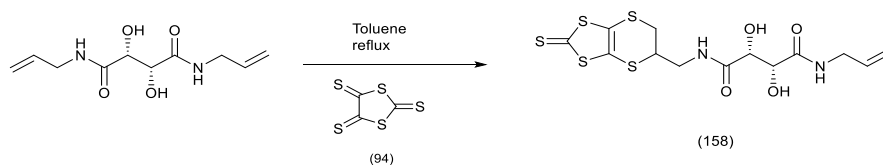
2.3.3 Attempting the synthesis of dimeric BEDT-TTF systems using optically active linkers.

2.3.3.1 Progress in the preparation of chiral BEDT-TTF dimer using (+)-*N,N'*-diallyltartramide as central linker.

The strategy involved using (+)-*N,N'*-diallyltartramide, a suitable starting material that is commercially available and relatively cheap. The targeted donor (153) has the potential to form multiple hydrogen bonding interactions because of the presence of amide and alcohol functional groups. The planned route to generate the desired compound (153) is presented (Scheme 40).

Scheme 40. Planned route to achieve formation of desired donor (**153**).

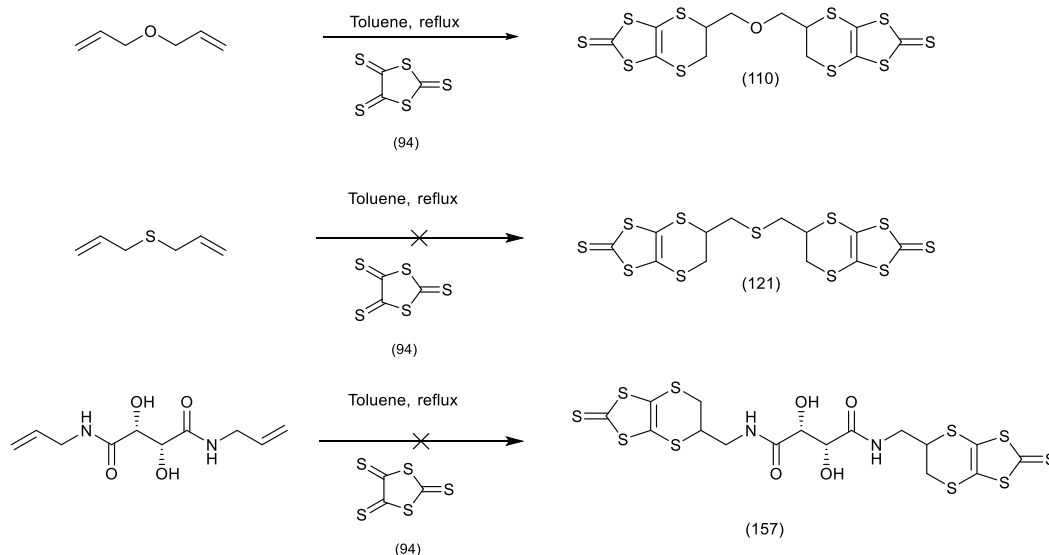
The first step involved the reaction of (+)-*N, N'*-diallyltartramide with trithione (**94**) to form a six-membered ring on each side of the enantiopure amide. It was decided to try the cyclisation without protecting the amide or the alcohol functionalities. This first step was performed by refluxing trithione (**94**) and (+)-*N, N'*-diallyltartramide in toluene under a nitrogen atmosphere overnight. The tlc plate showed the presence of a single yellow spot, which means probably only one double bond reacted to give cyclisation.



Scheme 41. Cyclisation reaction of the started material only occurred on one of the two terminal double bonds.

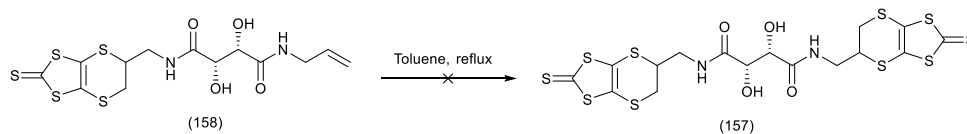
The purification of the reaction mixture by column chromatography led to the isolation of a single product which was analysed by ^1H and ^{13}C -NMR. The spectra were not perfectly clean and did not lead to an absolute identification. Mass spectrometry gave an m/z value of 424.9787 against a theoretical m/z of 424.9786, supportive of structure (**158**), the 1:1 adduct.

At this point it is possible to compare the three reactions performed so far by refluxing trithione (**94**) and a dienophile, such as diallyl ether, diallyl sulphide and (+)-*N,N'*-diallyltartramide in toluene. Only the former compound gave the *bis*-thione targeted even if in really low yield while in all three cases the mono-cyclised thione was isolated. This is further evidence of the low reactivity of the mono-cyclised products towards the second cyclisation.



Scheme 42. General scheme to emphasize the reactivity of substrates involved towards a double cyclisation.

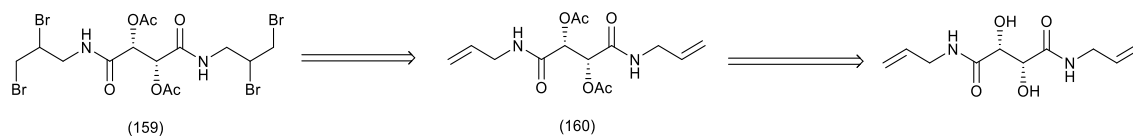
Due to the lack of reactivity of dienophile (+)-*N,N'*-diallyltartramide to generate the targeted *bis*-thione compound (**157**), it was decided to attempt the second cyclisation using mono-thione (**158**). The reaction of the mono-cyclised compound with trithione (**94**) in refluxing toluene failed to generate the desired compound. From $^1\text{H-NMR}$ the crude mixture showed mainly the starting material and no trace of the *bis*-thione (**157**).



Scheme 43. Attempted reaction to generate the *bis*-thione (**157**) from the *mono*-thione (**158**).

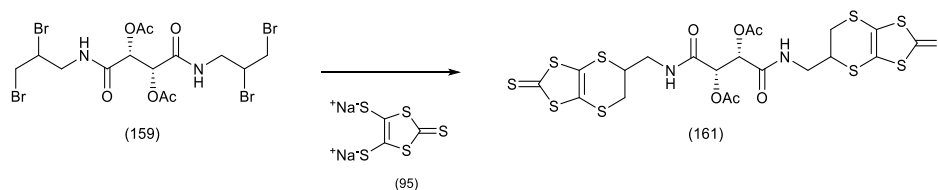
Two possible explanations for the failure of this double Diels-Alder reaction are *a*) the high insolubility of the mono-adduct and/or *b*) a highly favoured retro Diels-Alder reaction of the bis-adduct. The new approach designed was aimed to avoid the Diels-Alder reaction and involved the preparation of the *tetra*-bromo-*bis*-acetyl protected tartramide (**159**). The protection of the hydroxyl groups took place in the first step by reacting (+)-*N,N'*-diallyltartramide with acetic anhydride and pyridine for twenty hours from 0°C to r.t. to afford acetyl protected compound (**160**). Characterisation by ^1H and $^{13}\text{C-NMR}$ show acetyl peaks at 2.10 ppm in the proton resonance and the carbonyl and methyl peaks

at 169.2 and 20.6 ppm in the carbon spectrum. The following step involved the bromination of compound (**160**) by a solution of bromine (3 eq) in chloroform. The isolation of the product furnished a pale yellow solid in 74% yield. The characterisation by ^1H and ^{13}C -NMR spectroscopy showed no double bond peaks and new peaks at 3.80 (doublet), 3.50 ppm (multiplet) in the proton resonance related with new peaks at 43.9 and 35.7 ppm in the carbon spectrum.



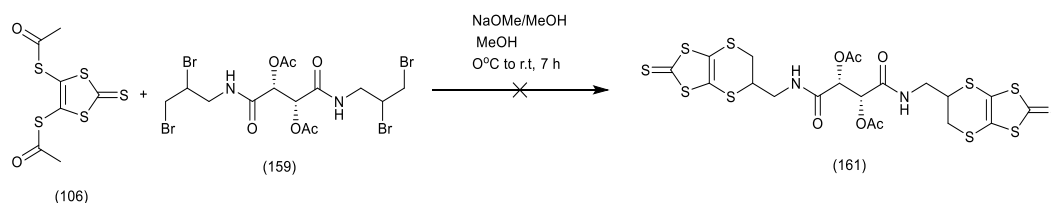
Scheme 44. Retrosynthetic pathway to generate tetrabromo compound (**160**).

The following step would be to react (**159**) with dithiolate (**95**) to form the six membered ring on both sides to furnish (**161**) as shown in the scheme. In this way the [4+2] cyclisation is replaced by a double nucleophilic substitution. This strategy is certainly longer but it may be found more effective.



Scheme 45. Alternative strategy to achieve preparation of protected *bis*-thione (**161**) avoiding [4+2] cyclisation reaction.

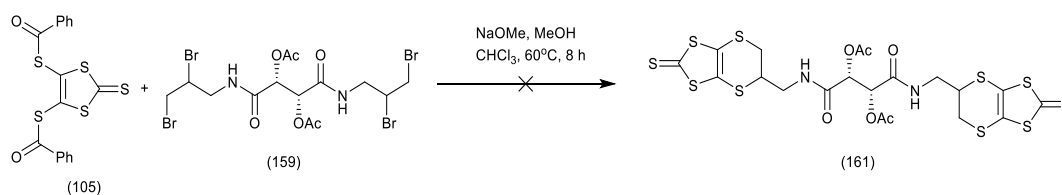
The first reaction was carried out using acetyl protected thione (**106**). A suspension of thione (**106**) in dry MeOH at 0°C was treated with NaOMe/MeOH (2 eq) until the appearance of a dark-red/purple solution. At this stage tetrabromo compound (**159**) was added and the resulting suspension was left to stir and warmed up to r.t. for 7 hours. The reaction mixture was monitored by tlc without showing any substantial change.



Scheme 46 Reaction performed to attempt the preparation of bis-thione (**161**).

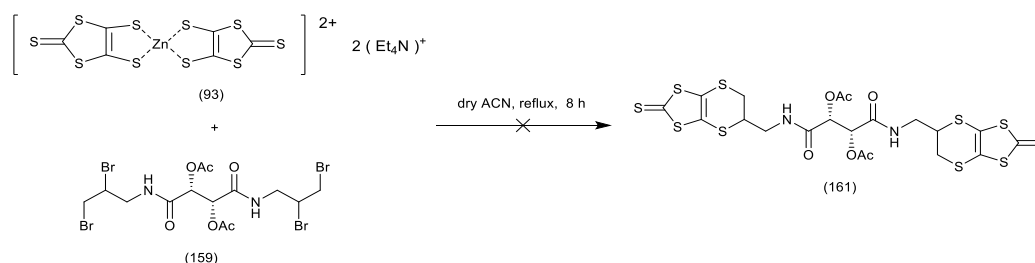
Due to the experience gained over the years this kind of reaction decomposes if left overnight, so the mixture was quenched with methyl iodide and immediately a change in colour was seen. A second attempt was performed using benzoyl protected thione (**105**). The dithiolate generate in situ using NaOMe/MeOH (25% in weight) solution was transferred

by cannula into a second 3-neck round-bottomed-flask containing a solution of tetrabromo compound (**159**) in chloroform at 60°C under a nitrogen atmosphere. The reaction mixture was left stirring for 8 hours.



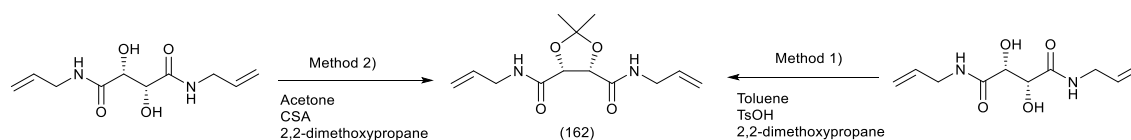
Scheme 47. Second attempt to prepare of bis-thione (**161**) by increasing the temperature.

After purification by column chromatography the desired compound was not identified. The third and last attempt used the zinc-complex (**93**) as a source of dithiolate (**95**). The protected tetrabromo compound (**159**) and zinc complex (**93**) were refluxed in dry acetonitrile for 8 hours and the reaction was monitored by tlc.



Scheme 48. Third attempt performed to prepare of bis-thione (**161**) by using zinc complex and higher temperature.

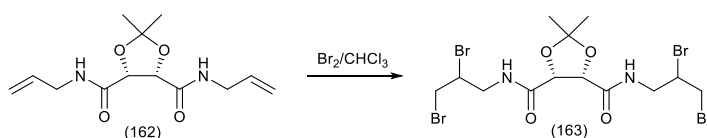
No substantial changes were seen and no product was isolated. The strategy involving the acetyl protected tartramide was abandoned due to the lack of reactivity of the acetyl protected tetrabromo compound to undergo nucleophilic substitution. In order to attempt the generation of the targeted *bis*-thione a different protecting group was considered. The choice fell on the acetonide group to protect the –OH's present in the starting material. A reference in the literature had been found²⁸⁾ but it was decided to modify it due to the presence of benzene as a solvent. Two different standard methods were involved in order to select the more efficient of the two. Both are reported in the scheme below and explained afterwards.



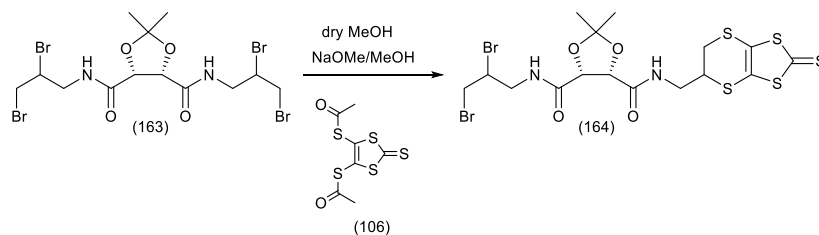
Scheme 49. Reactants and reagents involved in the two different methods attempt to generate acetonide (**162**).

In detail method 1) was taken directly from the reference cited, using a catalytic amount of tosic acid (0.1 eq) and 2,2-dimethoxypropane (1.1eq) with the only difference of replacing benzene with toluene for obvious health and safety reasons; while method 2) is a

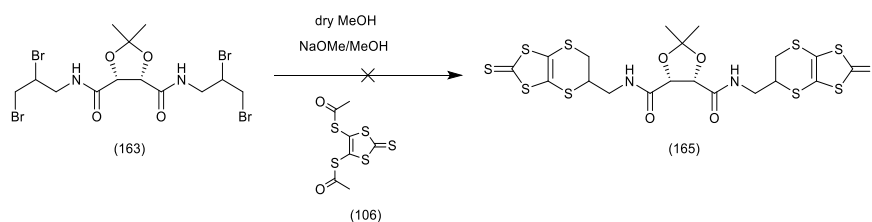
standard procedure for preparation of acetonides involving a catalytic amount of camphorsulfonic acid (CSA) (0.1 eq), 2,2-dimethoxypropane (2.2 eq) and acetone as solvent²⁹). After isolation of the product the best yield 92% was given by method 2). The acetonide protected compound (**162**) was recovered as a pale-yellow oil. The following step was the bromination of compound (**162**) by excess of bromine (3 eq) in a chloroform solution at 0°C for 1 hour when monitoring by tlc revealed all starting materials was gone. The solution was quenched with sodium thiosulfate solution (10%) and left to stir for an additional thirty minutes. After the work-up a yellow-brown oil was isolated in 64%. Characterisation of the oil by ¹H and ¹³C-NMR showed the desired tetrabromide (**163**) which needed no further purification.

Scheme 50. Bromination of acetonide (**162**).

Reaction between the tetrabromoacetonide (**163**) with dithiolate (**95**), generate in situ by treatment of thione (**106**) with NaOMe/MeOH (25% in weight), was carried out in dry MeOH at 50°C for 3 hours. After purification by column chromatography and characterisation by ¹H and ¹³C-NMR the spectra appeared to be a mixture of starting material (**163**) and a new compound which was identified as the mono-thione (**164**) by mass spectrometry analysis which revealed a peak at m/z 622.8455 when $C_{16}H_{20}O_4N_2Br_2S_5+H$ requires m/z 622.8466.

Scheme 51. Compound (**164**) was the only product from the reaction performed identified by MS analysis.

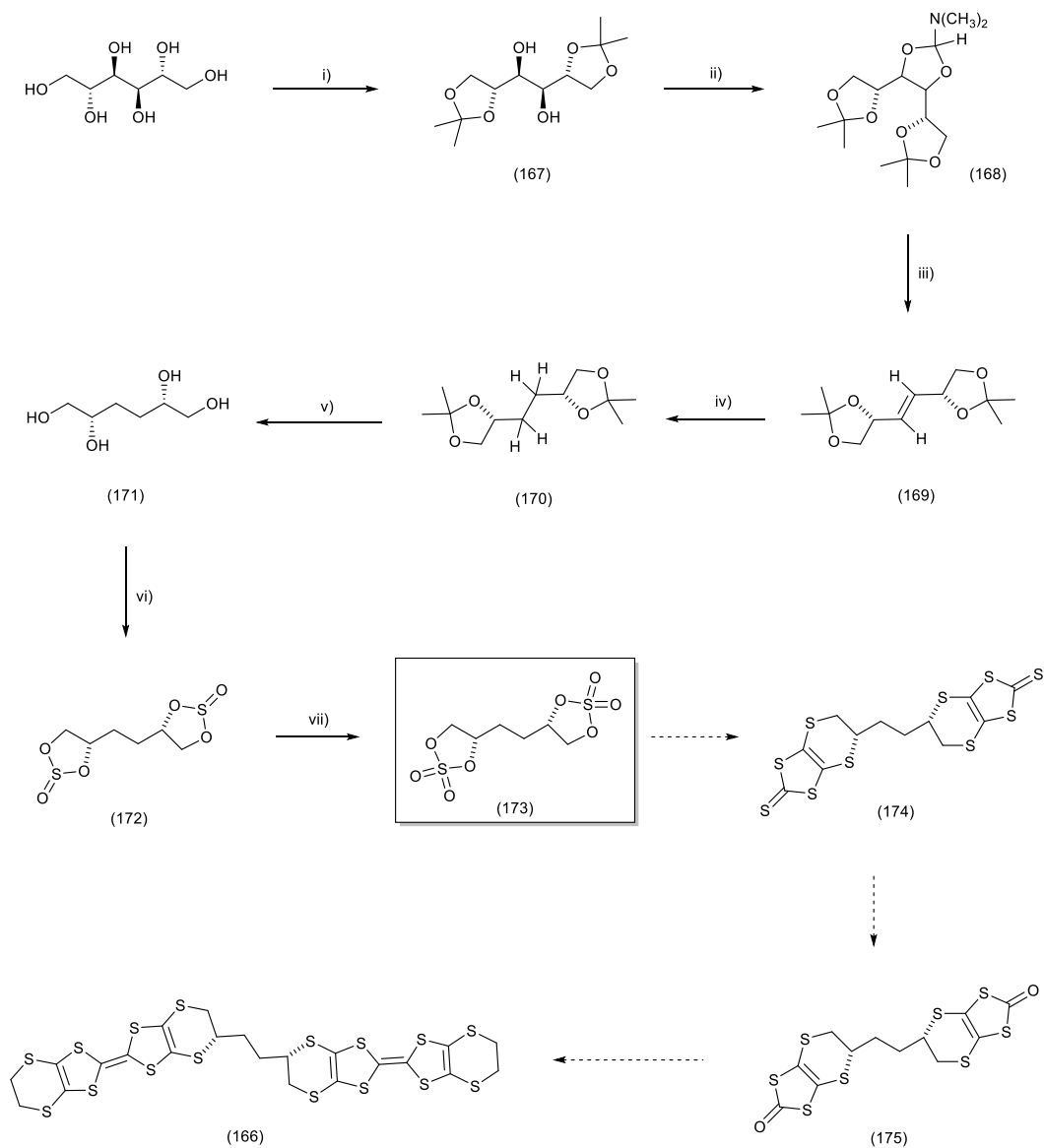
No trace of the acetonide protected *bis*-thione (**165**) was found in the same spectrum. A possible solution could be to leave the reaction on longer and under refluxing condition.

Scheme 52. Desired bis-thione (**165**) was not found in the residue isolated.

An alternative strategy could be to attempt the reaction by using the zinc complex (**93**) which is soluble in acetonitrile. This could be refluxed at higher temperature than methanol and this could give a little bit more energy maybe necessary to generate desired compound. This latter strategy was adopted but no trace of the desired product was revealed. In summary, it appears very difficult indeed to prepare the *bis*-thione compounds.

2.3.3.2 Preparation of dimeric BEDT-TTF system starting from D-mannitol.

The use of *D*-mannitol as a starting material to generate a BEDT-TTF donors has already found application in the Wallis laboratory and some examples are reported in the literature.^{30, 31)} The aim of the synthesis was to achieve the preparation of an optically active dimeric BEDT-TTF such as (**166**). The full synthetic route to achieve the preparation of targeted compound is presented below (Scheme 53). The work established during this PhD stopped at *bis*-sulphate (**173**). The steps completed were all already reported in the literature^{30,31,32,33)} and the procedures were followed carefully. The cyclic sulphate ester chemistry was adopted to retain the stereochemistry on the inner hydroxylic groups. The *bis*-cyclic sulphite esters compound (**172**) was obtained as a colourless oil in 80% yield. The ¹H-NMR spectrum was really complex due to the fact that three different stereoisomers have been formed. This is due to the additional chirality at the sulphite sulphur atom. The oxidation to *bis*-sulphite (**172**) yielded a white crystalline solid in 92% yield and characterisation by ¹H-NMR showed a pattern which is consistent with the one reported in the literature.³³⁾ The rest of the synthetic route would follow the series of transformations which have been already reported in the BEDT-TTF derivatives discussion. It is also worth mentioning that an analogue of the targeted compound (**166**) has already been prepared and reported in the literature³⁴⁾ but, according to our understanding, it is different from the desired target (**166**). The dimer reported does not present any element of stereochemistry due to the strategy applied for its preparation. The paper copy of the published material was not obtained but on the Scifinder database³⁵⁾ it is clear that the compound has been made from 1,2,5,6-tetrabromo hexane probably obtained from hexa-1,5-diene. No stereochemistry is specified due to the nature of the bromination reaction.

Scheme 53. Procedure for preparation of desired optically active dimer (**166**).

2.3.4 Progress in the preparation of bis-substituted BEDT-TTF donors.

2.3.4.1 Attempted synthesis of *bis*-(*exo*-methylene)-BEDT-TTF as a substrate for further cyclisation reactions.

With the preparation of donor **(146)**, which presents a double bond directly attached to the six-membered ring, a new idea arose, which was to try to develop donors capable of further cyclisation. The (*exo*-methylene)-BEDT-TTF **(146)** is shown as an example but the new target compound was the *bis*-(*exo*-methylene)-BEDT-TTF **(176)**.

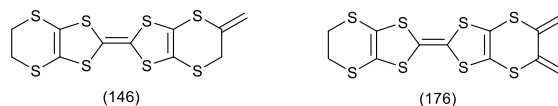
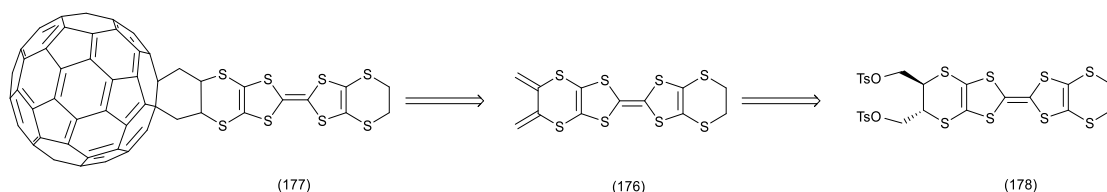


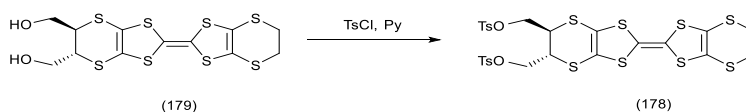
Figure 81. New targeted donor **(176)** able to undergo further cyclisation reaction.

The new donor **(176)** would have the potential for [4+2] cyclisation reaction even with C₆₀ fullerene to give donor **(177)** whose designed preparation is presented below (Scheme 54). The planned synthesis involves the preparation of the *bis*-*exo*-methylene-BEDT-TTF **(176)**, which can be the product of a double elimination reaction on substrate **(178)** in the presence of a strong base, such as potassium *tert*-butoxide. The same strategy has been applied, successfully, for the preparation of donor **(146)**.



Scheme 54. Designed retrosynthetic approach to prepare donor **(177)**.

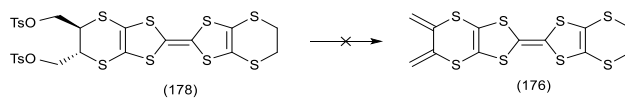
The preparation of the *bis*-tosyl-oxy-methyl-BEDT-TTF **(178)** was a standard transformation to convert the two –OH groups in the donor **(179)** into a better leaving group. This reaction was performed by reacting **(179)** with tosyl chloride and pyridine at 0°C overnight. Isolation of product yielded the desired donor **(178)** in 90 % yield as an orange solid.



Scheme 55. Preparation of donor **(178)**.

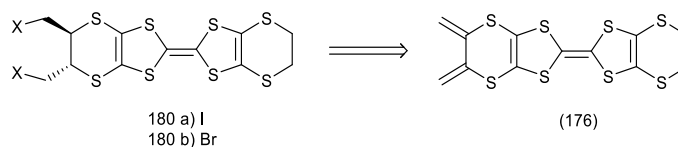
The characterisation by ¹H and ¹³C-NMR showed the expected pattern. The CHN analysis and the FT-IR spectrum completed the full characterisation of the new donor obtained. In the donor **(178)** the two side chains adopted the *trans* configuration due to the stereochemistry of the starting material used; the *trans*-1,4-dibromo-but-2-ene. The *cis*-isomer of donor **(178)** had already been prepared in the Wallis laboratory and reported in previous works.¹⁸⁾ as well as donor **(179)**.³⁶⁾ After the preparation of desired compound **(178)** the planned strategy was applied. According to it the base would attack on the carbon in position 5 and 6 to lead to the elimination of two tosylates resulting in the formation of

the double bond. The *bis*-tosylate (**178**) was dissolved in dry DMF under a nitrogen atmosphere. To this was added a solution of sodium *tert*-butoxide (2.1 eq) in dry MeOH. The reaction mixture was left to stir at r.t. and monitored by tlc and after two hours the starting material was consumed and a new spot was detected. The crude product was isolated and characterised by NMR spectroscopy which provided no evidence of the desired product.



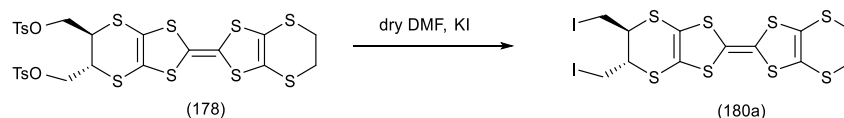
Scheme 56. Generation of *bis*-*exo*-BEDT-TTF was not achieved by using donor (**123**).

The reaction would have been tried also with *bis*-iodo (**180a**) and *bis*-bromo (**180b**) derivatives, but they proved to be difficult to prepare.



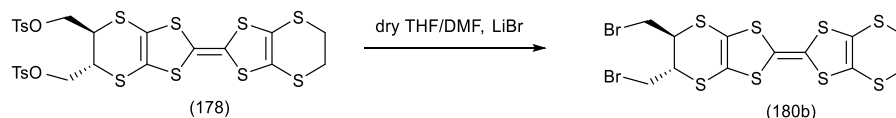
Scheme 57. Halogen substituted ET donor (**180**) was designed as a starting material to generate donor (**176**).

The first attempt involved the reaction between donor (**178**) and an excess of potassium iodide (2.5 eq) in DMF. However, under a variety of conditions, the reaction failed to yield the desired donor.



Scheme 58. Attempted reaction to prepare *Bis*-iodo-methyl-BEDT-TTF (**180a**).

To make the dibromo derivative (**180b**) a solution of (**178**) in dry THF was treated with an excess of LiBr (10 eq). No signs of completion were seen at room temperature nor in refluxing THF, so dry DMF was added and the temperature was increased up to 75°C for 48 hours. Monitoring of the reaction by tlc shown starting materials was consumed and a new spot was detected. The crude compound was isolated and analysed by ¹H-NMR which showed a proton pattern that needs more investigation.



Scheme 59. Performed reaction to obtain donor (**180b**).

The *bis*-bromo-methyl-ET (**180b**) and *bis*-iodo-methyl-BEDT-TTF (**180a**) could have been suitable substrates to use in the generation of desired *bis*-*exo*-methylene-BEDT-TTF

(176), but also interesting donors to be tested in diffusion and electro-crystallisation experiments.

2.3.4.2 Preparation of a donor containing two thiocyanate groups.

The preparation of new donors for diffusion and/or electro-crystallisation experiments has always been a priority in the attempt to develop a favourite building block which can lead to the generation of a family of conducting salts. The targeted donor was the *bis*-(thiocyanate-methyl)-BEDT-TTF (**181**).

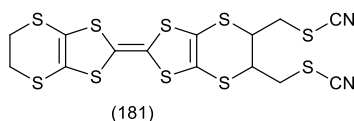


Figure 82. Targeted compound for diffusion and electrocrystallisation experiments.

To achieve the preparation of the desired donor the choice of the reagent was important to ensure the thiocyanate anion reacted at the sulphur and not at the nitrogen atom.

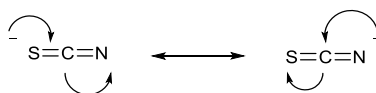


Figure 83. Resonance of the negative charge in the thiocyanate anion.

The reagent selected was potassium thiocyanate.³⁷⁾ A THF solution of donor (**178**) was reacted with an aqueous solution of an excess of potassium thiocyanate (6.5 eq) at reflux for 25 hours. The desired product was isolated as a yellow solid. The characterisation by ¹³C NMR showed the presence of the nitrile at 109.1 ppm among the *sp*² carbons of the sulphur network and the FT-IR which showed a strong intense band is present at 2151.6 cm⁻¹. The purity of the compound was confirmed by the elemental analysis. The donor is currently under investigation in electrocrystallisation experiments.

2.3.5 Progress in the preparation of new substituted donors from allyl-oxo-methyl-BEDT-TTF (**113**).

The synthesised donor allyl-oxo-methyl-BEDT-TTF (**113**) can be useful as a starting material for further reaction, especially due to the presence of the terminal double bond. For this purpose developing its chemistry means performing reactions on the alkene without

interfering with the BEDT-TTF building block, especially avoiding strong oxidants and too strong acidic or basic conditions. The main idea was to generate an alcohol or a halide. Several strategies have been considered and investigated for example *i*) addition of bromine, *ii*) reaction with *m*CPBA, *iii*) hydroboration and *iv*) oxymercuration-demercuration.

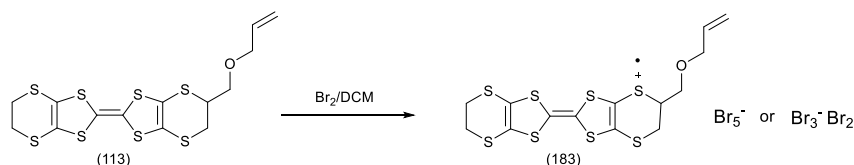
i) Addition of bromine:

The addition of bromine to the terminal alkene was attempted by slow addition of bromine to a solution of the donor (**113**) in dichloromethane at -10°C .³⁸⁾



Scheme 60. Procedure for the preparation of donor (**182**).

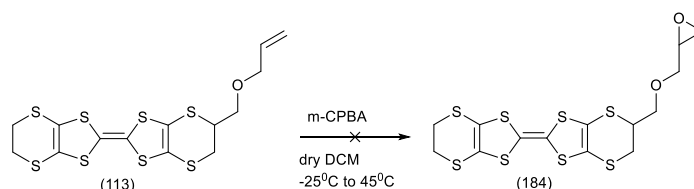
This reaction was investigated to test whether addition to the double bond would be preferred to charge transfer salt formation. Immediately after the addition a large amount of dark solid formed suggesting a charge-transfer salt formation. The crude NMR spectra evidenced the presence of a free double bond and the CHN analysis was consistent with (144) Br^{5-} where the anion is either a combination of bromine and Br_3^- anion. Presence of penta-bromide anion has been found in the literature³⁹⁾ and few example are reported in the Cambridge Structural Database⁴⁾.



Scheme 61. CT salt (**183**) obtained by adding bromine to donor (**113**).

ii) Reaction with *m*-CPBA:

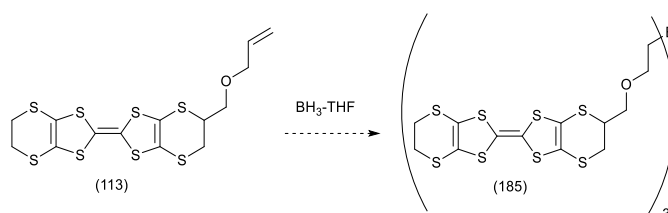
The strategy behind the attempted reaction with *m*-CPBA was to generate an epoxide which could react with a nucleophile in a second step to open the ring and generate an more substituted side chain. This reactant was considered due to its wide application in organic synthesis for epoxides formation even if there are alternatives⁴¹⁾.

Scheme 62. Designed preparation of donor (**184**) by reacting m-CPBA and donor (**113**).

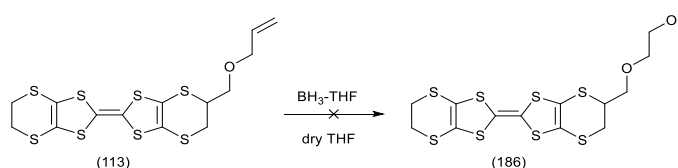
The reaction was carried out by adding m-CPBA (1.5 eq) to a solution of donor (**113**) in dry dichloromethane at -20°C under a nitrogen atmosphere. The reaction was left to stir and monitored by tlc. After 45 min was stopped and the residue was purified by column chromatography. Although tlc showed a number of new products, the starting material was isolated as the major component. Few of these new products were analysed by ^1H and ^{13}C -NMR and only starting material could be seen. One of the residue obtained was analysed by mass spectrometry in search of an adduct of the donor (**113**) with oxygen, but the spectrum revealed only starting material.

iii) Hydroboration;

A double bond can react with borane, $\text{BH}_3\cdot\text{THF}$. This reaction was performed for a double purpose: *a*) to furnish an alcohol by quenching the reaction with hydrogen peroxide and sodium hydroxide and *b*) to prepare a triborane. The second, and more intriguing aim, would have been an extremely interesting compound with three substituted BEDT-TTF units around a central boron atom.

Scheme 63. Triborane formation by reacting donor (**113**) and $\text{BH}_3\cdot\text{THF}$.

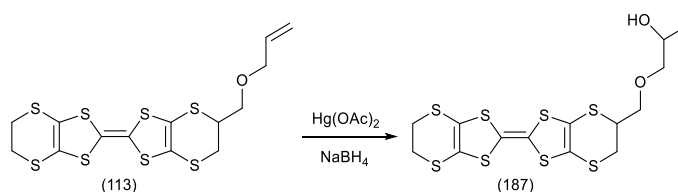
The focus was towards the preparation of the alcohol. The reaction was performed dissolving donor (**113**) in dry THF and cooling to 0°C . The complex $\text{BH}_3\cdot\text{THF}$ (1.1 eq) was added dropwise. The reaction was then monitored at different temperature (up to reflux) without seen any change on the tlc plate. It was concluded that the boron coordinated one of the sulphur atoms.

Scheme 64. Hydroboration failed to give desired alcohol (**186**).

The reactions previously reported have seen the use of reagents which could potentially oxidise the substrate such as peracid and bromine or coordinate the sulphurs, as in the case of borane –tetrahydrofuran complex. The double bond was a spectator during these transformations and was not affected. Due to this evidence it was decided to involve a different option.

iv) Oxymercuration/Demercuration:

The reagent involved in oxymercuration is mercury (II) acetate which is not a threat for the donor (**60**) and the same is for the de-mercuration reagent, sodium borohydride, a reducing agent which should not be involved in any kind of reaction with the sulphur network.



Scheme 65. Oxymercuration/Demercuration reaction product (**187**).

The reaction was performed by adding mercury (II) acetate, two equivalents, to a solution of donor (**60**) in THF and H₂O at 0°C. The mixture was left to stir and warmed up to reflux for three hours. The reaction was quenched with sodium borohydride and after aqueous work-up and purification by column chromatography alcohol (**187**) was isolated as a red solid in 20% yield. Under all conditions tried, there was always unreacted donor (**113**) present, indicating the difficulties of BEDT-TTF reactions. The protons of the methyl group resonated at 1.08 ppm (doublet) and the corresponding carbon was seen at 18.6 ppm. The carbon connected with the –OH group showed a signal at 66.3 ppm. The FT-IR spectrum helped the identification by showing a characteristic stretching at 3343 cm⁻¹ (large-broad band) and finally the CHN analysis confirmed the identity of the compound as the desired donor (**187**).

2.3.6 Preparation of radical cation and charge transfer salts by electrocrystallisation and diffusion experiments.

2.3.6.1 Cyclic voltammetry of the new donors synthesised.

The cyclic voltammeteries of some of the new donors prepared were measured using a three electrode set-up method (reference, working and counter electrodes). All the measurements are relative to Ag/AgCl at platinum electrode. A recorded amount of the desired donor was added into a 0.1 M solution of *n*-BuN₄PF₆ in dichloromethane which was used as carrier charge.

Table 2. Cyclic voltammetry potentials for the new substituted ET donors.

Donor	E ₁ (V)	E ₂ (V)
BEDT-TTF (103)	0.52	0.94
(113)	0.53	0.94
(124)	0.53	0.94
(129)	0.54	0.94
(146)	0.56	0.97
(181)	0.58	0.94
(187)	0.53	0.93

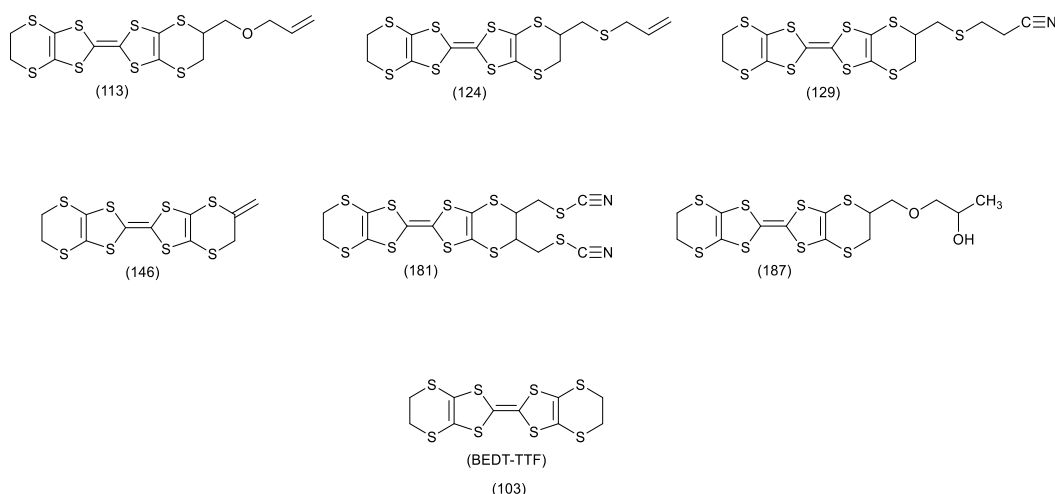
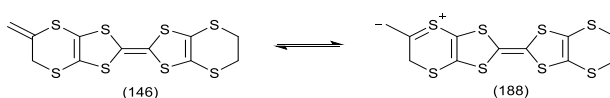


Figure 84. Donors analysed by C.V.

All the measured donors presented a two reversible oxidation-reduction behaviour which is characteristic of the BEDT-TTF molecules and its derivatives. The values recorded are very similar to each other. Only the exo-methylene functionalised donor (**146**) presents a slightly different potential, comparison with the BEDT-TTF, which is due to the effect of the extra conjugation in the external ring.

Figure 85. Conjugation effect which contribute to the slightly different behaviour of the donor (**146**).

2.3.6.2 Electrocristallisation and diffusion experiment involving *exo*-ET (92).

Electrocristallisation experiments on *exo*-(methylene) BEDT-TTF (**146**) in the presence of various anions were carried out. The most successful was with tetrabutylammonium-perchlorate which gave thin black crystals of a 1:1 radical cation salt. The experiment was carried in an H-shaped electrochemical cell fitted with a glass frit and in the anodic side was placed donor (**146**) and on the cathodic side tetrabutylammonium perchlorate. The solvent used was chlorobenzene and its levels were allowed to equilibrate on either side. A constant current of 2 μA was applied and the short needle-like black crystals were collected after three days. Diffusion of iodine into a solution of *exo*-(methylene) BEDT-TTF led to a 2:2:1 salt of the donor monocation with triiodide and iodine. A solution of the donor (**146**) in dichloromethane and a solution of iodine in benzonitrile were left to diffuse into each other in the dark for 3 days and then crystals were collected and analysed. The structures of both salts were determined by X-ray crystallography. Attempts to grow crystals of the neutral donor were unsuccessful.

A crystal of the 1:1 salt with perchlorate was measured at the EPSRC National Crystallographic Service at Southampton using MoK α X-radiation at 100 K. The crystal system is monoclinic in space group P2₁/c with one donor cation and one anion in the asymmetric unit (Figure 86). The crystals are twinned and there is some orientational disorder of the perchlorate ion, as well as some of the commonly observed conformational disorder in the unsubstituted dithiin ring leading to a rather high R-factor of 11%. The donor cations are organised in centrosymmetric pairs, and these are packed in the *bc* plane along with the anions (Figure 87) which isolate pairs from one another. However, there are short contacts between pairs which lie side by side in the *a* direction (Figure 88). In the donor cation the effect of the exocyclic alkene is a shortening of the bonds connecting it to its S and C neighbours to 1.758(17) and 1.457(2) Å. The alkene bond length is 1.315(2) Å but the shortness may be due to some slight positional disorder of the terminal methylene group. The conformation of the substituted dithiin ring is an envelope with the sp³ carbon atom at the envelope's flap. The exocyclic sp² methylene group lies to the opposite side. Within a dimer the shortest S...S contacts are between the TTF sulphur atoms (3.375(2) and 3.504(2) Å). Between dimers the shortest contacts are between a dithiin S and dithiole S (3.460(4) and 3.481(4) Å), thus providing a possible route for conduction of electrons

Chapter 2 Attempted synthesis of BEDT-TTF dimer and related substituted BEDT-TTF donors obtained through the structure. Unfortunately the crystals were too brittle to attach electrodes for conductivity measurements.

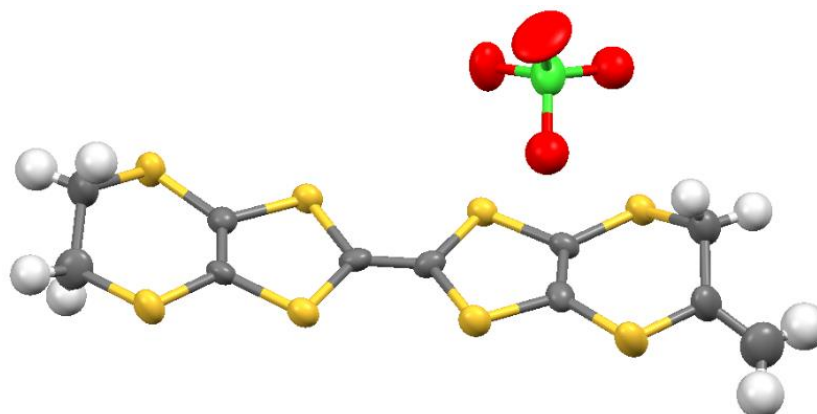


Figure 86. Molecular structure of the salt **(146)**ClO₄ with anisotropic displacement parameters drawn at the 50% level, and only one orientation of the disordered anion shown.

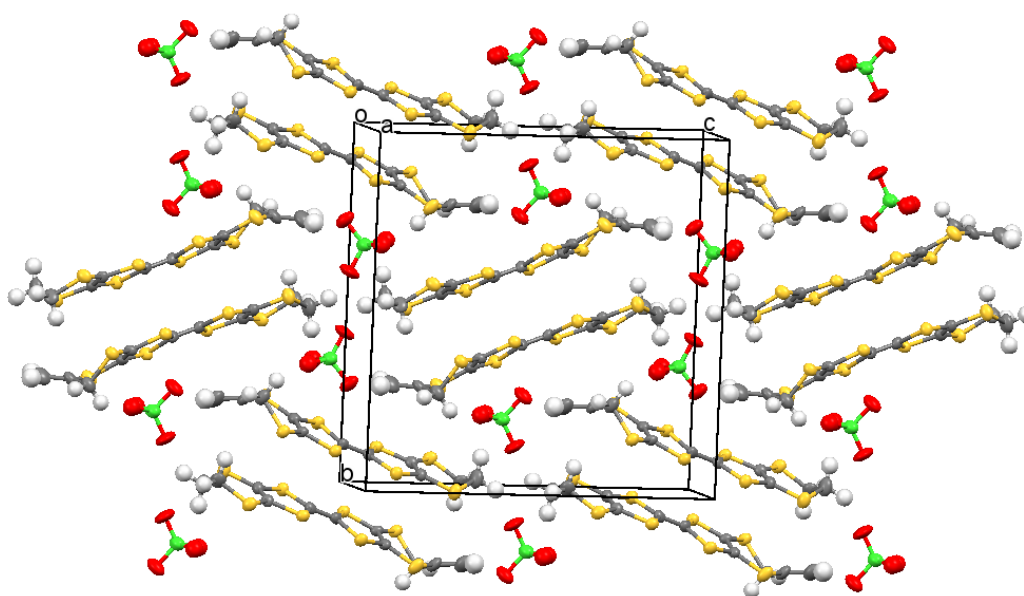


Figure 87. Crystal packing of the salt **(146)**ClO₄

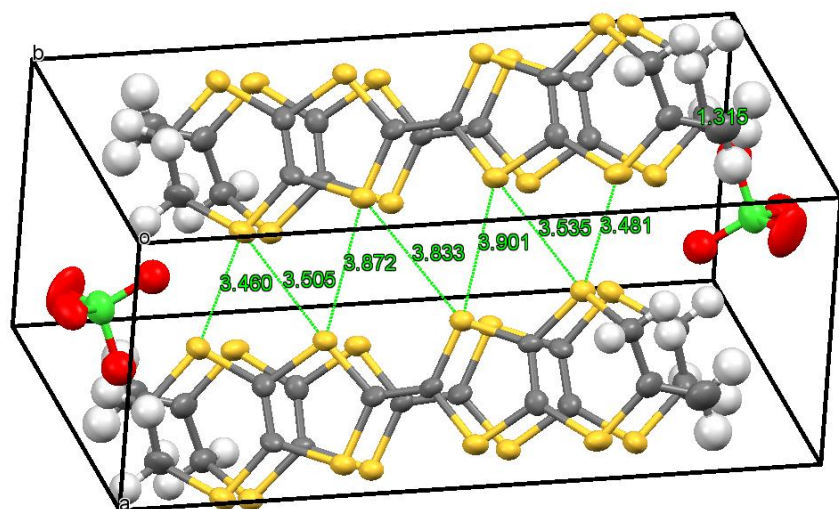


Figure 88. Inter-dimer S...S contacts in the salt **(146)**·ClO₄.

The crystal structure of the salt obtained by diffusion with iodine is shown in Figure 89. The data was measured at the EPSRC National Crystallographic Service at Southampton using MoK α X-radiation at 296 K. The crystal system is triclinic and the space group is P-1. The structure refined to an R-factor of 0.0487. The asymmetric unit is composed of one donor cation, one triiodide and half of an iodine molecule, since the iodine molecule lies on a centre of symmetry. The donor cations are organised in face to face pairs, which are almost surrounded by iodine molecules and triiodide anions (Figures 89 and 90). However, there are side to side contacts between adjacent pairs of donor cations in the *a* direction (Figure 90). The lengths of the I-I bonds are 2.805(1) Å in the iodine molecule and 2.873(9) and 2.953(9) Å in the triiodide anion, and the two species approach each other at 85° with a I...I contact of 3.379(1) Å between them. Lines of triiodide anions run through the structure between the donor cation pairs, with head to tail I...I contacts between triiodides of 3.427(1) and 3.839(1) Å. Within the radical cation pairs there are four short S...S contacts between the S atoms of the TTF core all of length 3.396(4) Å. The S...S contacts between adjacent cation pairs are longer and lie in the range 3.462(4)-4.021(4) Å.

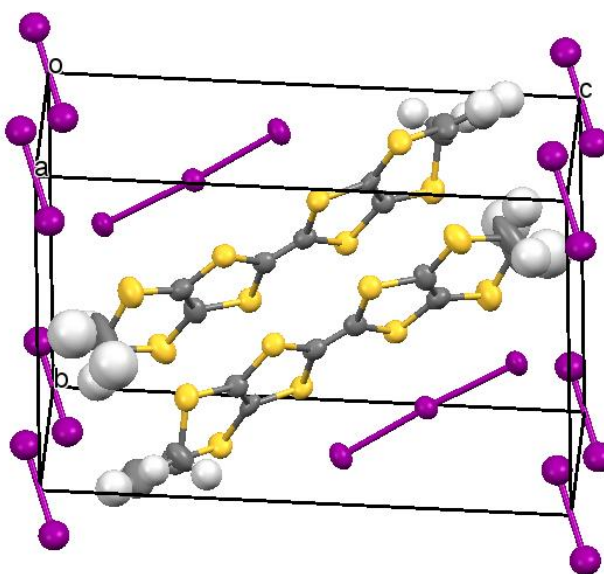


Figure 89. Face to face radical cation pair surrounded by triiodide anions and iodine molecules in the crystal structure of **(146)**·I₃·0.5I₂. Anisotropic displacement parameters are drawn at the 50% level.

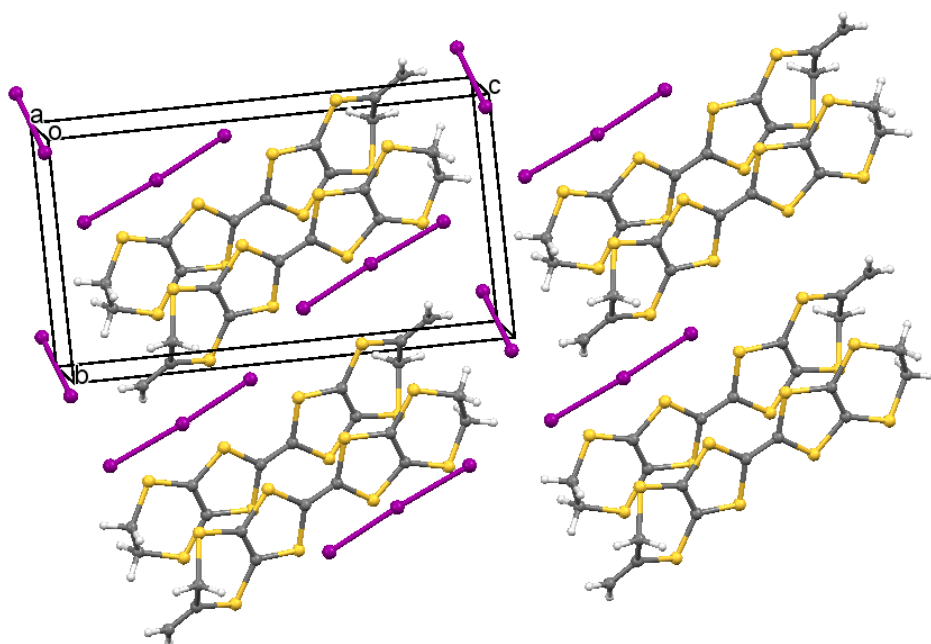


Figure 90. The crystal structure of **(146)**·I₃·0.5I₂ showing the lines of triiodide anions lying between donor cation pairs and cross linked with iodine molecules.

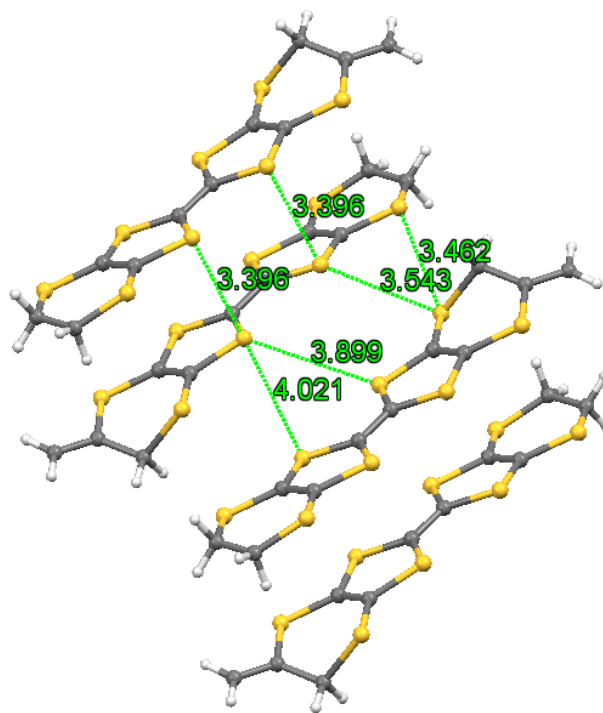
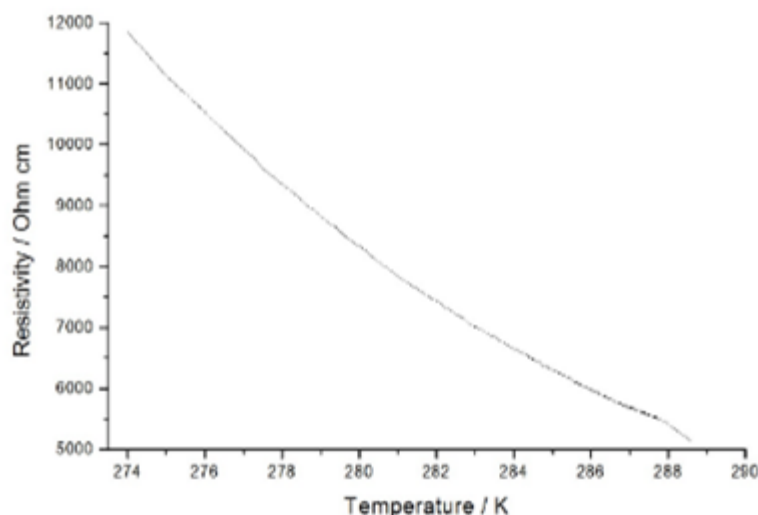
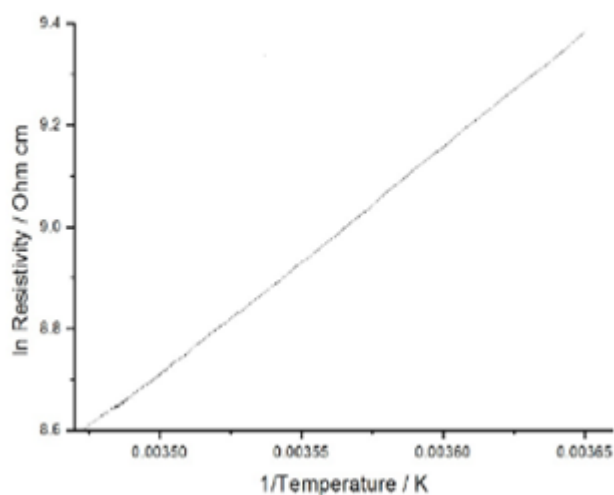


Figure 91. S...S contacts within a radical cation pair and between adjacent pairs in the crystal structure of (146) $\cdot\text{I}_3\text{O.5I}_2$.

This salt showed semiconducting properties. Figure 92 shows the change of resistivity (Ohm/cm) against the change in temperature (K). As for a typical semiconductor on decreasing the temperature the resistivity of the crystal increases in an exponential way. This is the response of the electron flow from the valence band to the conduction band when the energy provided is decreased. The second graph is the log of resistivity (Ohm/cm) against $1/\text{temperature}$ (K) and here the relation is linear, and for an increase of the $1/T$ value there is a linear response of the log R value. The recorded room temperature conductivity was $1.89 \times 10^{-4} \text{ S cm}^{-1}$ and its activation energy 0.373 eV. The activation energy is half the energy required for an electron to be promoted from the valence band to the conductive band.

Figure 92. Resistivity response to the temperature changes of the crystal of $(\mathbf{92})\text{I}_3/0.5\text{I}_2$.Figure 93. Resistivity response to the $1/\text{temperature}$ changes of the crystal of $(\mathbf{92})\text{I}_3/0.5\text{I}_2$.

2.3.6.3 Electrocrystallisation and diffusion experiment involving allyloxo-methyl-ET-(113).

The oxidation potentials of the allyloxymethyl and allyl thiomethyl-BEDT-TTF donors, **(113)** and **(124)**, were similar to those of BEDT-TTF with oxidation potentials of 0.53 and 0.94 V relative to the Ag/AgCl electrode. Electrocrystallisation experiments on allyloxo-methyl-BEDT-TTF **(113)** in the presence of various oxidising agents were carried out. The most successful was with tetrabutylammonium perchlorate which gave thin dark green crystals of a 1:2 radical cation salt. The crystal growth was carried at r.t. in an H-shaped electrochemical cell fitted with a glass frit in chlorobenzene. A constant current

Chapter 2 Attempted synthesis of BEDT-TTF dimer and related substituted BEDT-TTF donors obtained of 0.5 μA was applied for a period of four weeks and the short needle-like green crystals isolated by filtration.

The crystal structure, measured at 100 K, is monoclinic in space group $P2_1$ and there are two donor cations, each bearing a charge of 2^+ , and four perchlorate anions in the unit cell. The unit cell packing is shown in Figure 94 and its expansion is shown in Figure 95. Attempts to grown crystals of the neutral donor were unsuccessful.

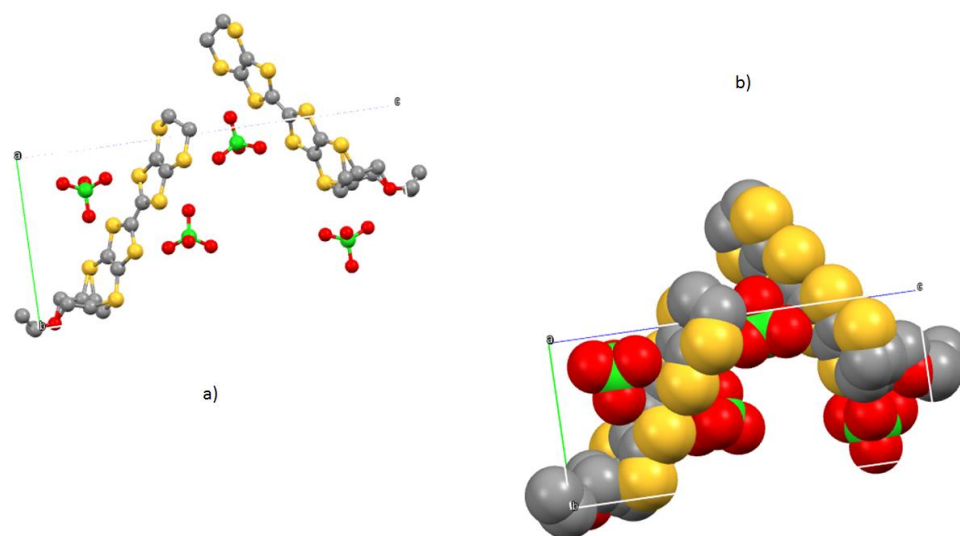


Figure 94. Packing in the unit cell as a) ball and stick and b) spacefill viewed down to the a axis.

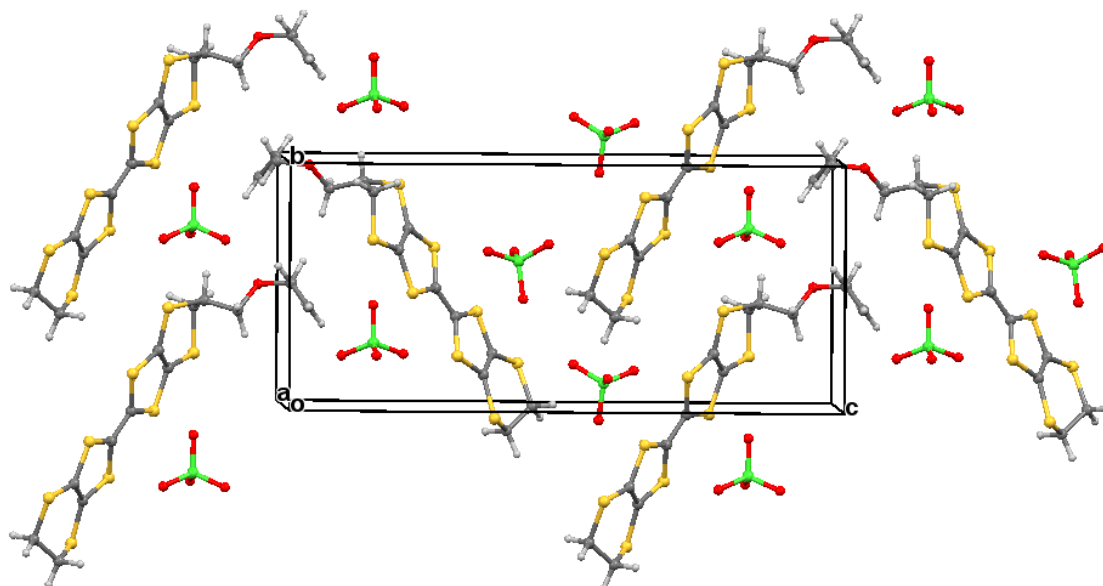


Figure 95. Crystal structure of $(113)2\text{ClO}_4$ viewed down the a axis.

The donor dication shows the typically very long bond between dithiole units of 1.441(19) \AA , and the four central C-S bonds, shortened by the 2^+ charge, lie in the range 1.676(18)-

1.717(19) Å. The monosubstituted donor is disordered between two orientations, which are roughly related by a 2 fold rotation about the long axis of the molecule. The orientations differ mainly in the point of attachment of the side chain to the dithiin ring, however the side chains lie so that the two structures have a common position for the terminal allyloxy group. This is achieved by the dithiin ring in the two structures adopting an approximate envelope conformation with the side chain attached to the “flap” methine carbon and oriented in a pseudo-axial manner (Figure 96).

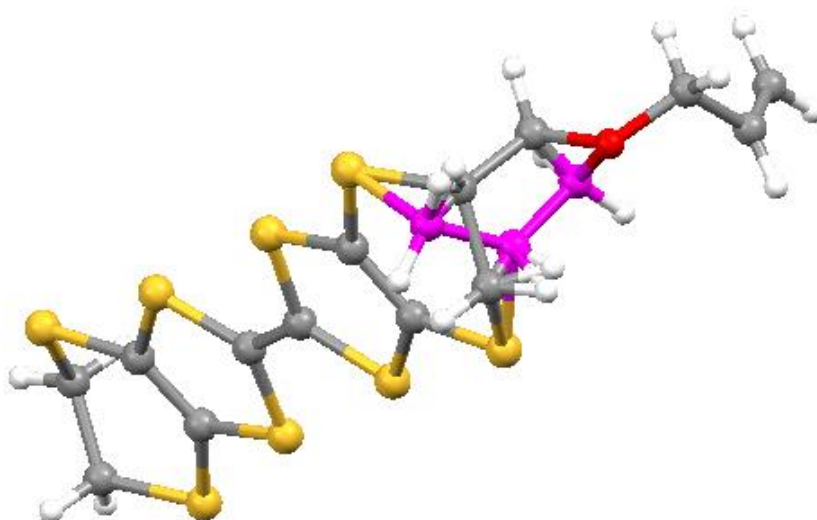


Figure 96. View of the donor cation of (**113**) showing the two disordered orientations of the side chain and how they overlap.

There is no stacking of donor dications, but there are lines of dications along the *b* axis organised so that the molecules are strongly slipped relative to each other so that the only, rather long, S...S contacts (3.728(7) and 3.785(7) Å) are between sulfurs from the unsubstituted end of one donor and sulfurs from the substituted end of the next donor. The perchlorate anions are distributed among the donor dications, and each donor has S...O contacts to four anions (Figure 97). Although donor stacking with segregated anions is common in BEDT-TTF radical cation salts, the larger donor charge in this case leads to anion contacts with the organosulfur residue.

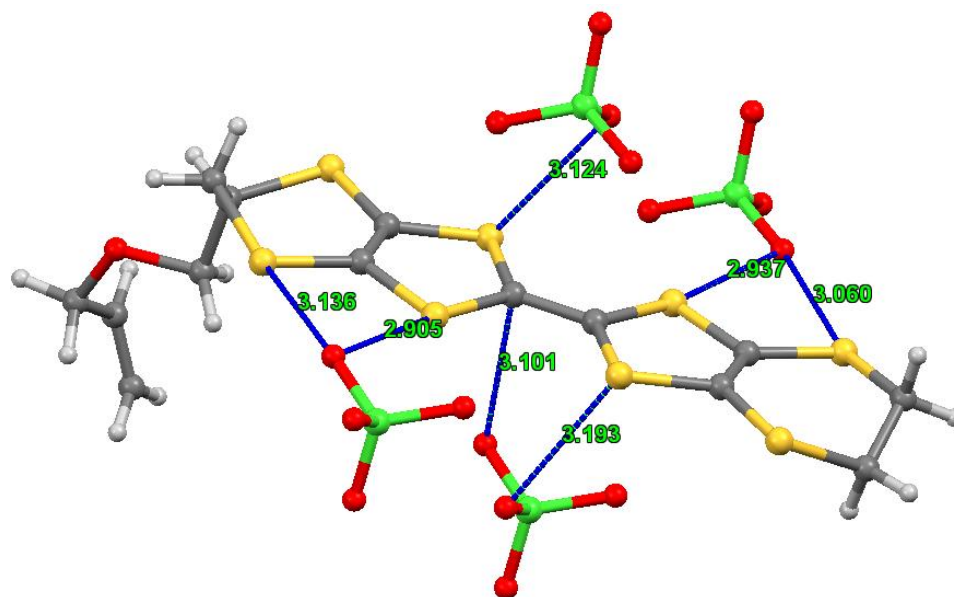


Figure 97. Contacts (Å) between the donor dication and perchlorate anions.

Diffusion of a solution of iodine into a solution of allyl-oxo-methyl-BEDT-TTF (**113**) was attempted using different solvents but no complete structure was achieved from XRD data collection. The ET skeleton of carbons and sulphurs is clearly visible, as well as the iodine and triiodide but the full identification of the side chains was found to be really problematic. Up to date no crystal structure has been completed due to the disorder in the side chain of the donor molecule. The crystals were found to be electrically insulating.

2.4 Conclusions and Future work.

To conclude the work described in chapter 2 new donors have prepared, in particular with alkene functionality on the side chain, and fully characterised. Indeed donor (**113**) and (**146**) produced single crystals after electrocrystallisation and/or diffusion experiments and the conductivity measurement of the salt (**146**) $I_3 \cdot 0.5I_2$ evidenced its semiconducting nature at r.t. Indeed more experiments to obtain single crystals will be performed and more conductivity measurements on single crystals obtained are ongoing.

With regards to the dimer formation of BEDT-TTF different alternatives have been tested and the reactivity towards the *bis* cyclisation reaction has been very low and it was the main obstacle for the formation of bridged *bis*-BEDT-TTF such as in the case of *bis*-oxo-compound (**113**), or tetra-bromo sulphide (**125**), or tetra-bromo compounds (**159**) and (**163**) which failed to furnished the desired *bis*-thione and no dimer could be prepared. The alternative route under investigation is outlined below (Figure 98) and involves the use of carboxylic acid derivative such as (**188**) which would be converted to a series of amide, such as (**190**), using the mix anhydride method.

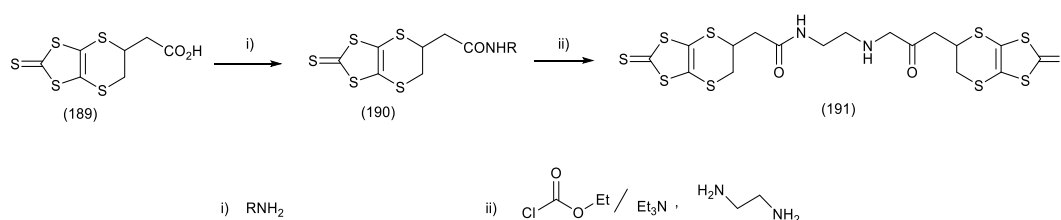


Figure 98. Future strategy to realise bridged-BEDT-TTF dimers.

The donors which present the terminal alkene functionality such as (**113**) and (**124**) and (**146**) can be of interest for future polymerisation experiments.

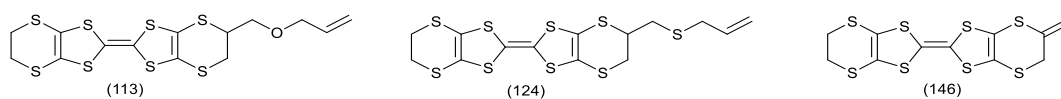
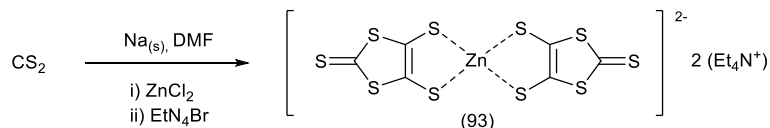


Figure 99. Some of the new donors prepared which could be polymerise

In term of preparation of *bis*-BEDT-TTFs all the attempts failed and up to date the possibility still to be explored is to conclude the synthesis of donor (**173**) where only a few steps are left.

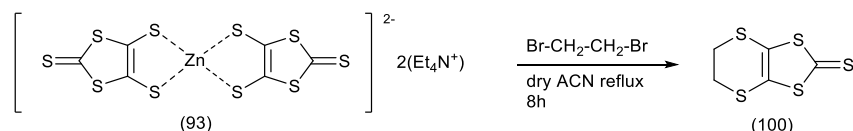
2.5 Experimental Part

2.5.1 Synthesis of bis (tetraethylammonium)-bis (1,3-dithiole-2-thione-4,5-dithiol) zincate (**93**).



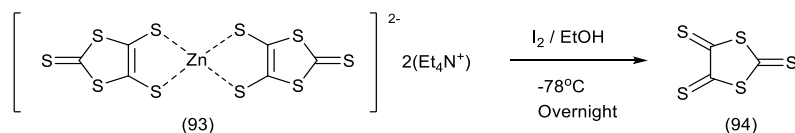
To degassed DMF (480 ml) was added carbon disulphide (240 ml) and the mixture was cooled down to 0°C under a nitrogen atmosphere. Sodium metal (14.5 g, 630 mmol) was cut into fine pieces under cyclohexane, then added to the solution over 20 min. Stirring was continued for 8 h, until all the sodium was consumed. The unreacted sodium was destroyed by addition of MeOH. Separate solutions of (i) ZnCl₂ (21.3 g) in water (100 ml) and NH₃ 35% (360 ml) and (ii) Et₄NBr (66.0 g) in water (500 ml) were added consecutively in approximate equivolume portions over 20 min. A red precipitate is formed. The mixture was stirred overnight, and the product isolated by filtration *in vacuo* and sequentially washed with *i*-PrOH (3 x 250 ml) and ether (250 ml) to afford the compound (**93**) (84.6 g, 74%) as a red powdery solid; m.p. 209-211°C, (lit ¹⁷) m.p. 205-207°C).

2.5.2 Synthesis of 5, 6-dihydro-[1,3]dithiolo[4,5-b][1,4]dithiine-2-thione (**100**).



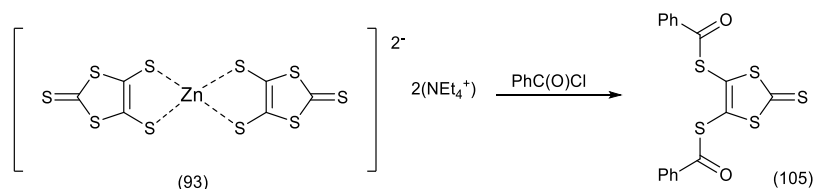
Zinc salt (**93**) (15.25 g, 21.21 mmol) was dissolved in dry CH₃CN (150 ml) and a dark-red solution was formed. 1,2-dibromoethane (8.24 g, 44.1 mmol) was added and the mixture was left refluxing for 6 h. The suspension was allowed to cool down to r.t., and the product collected by filtration and washed with cold methanol to afford thione (**100**) as a bright yellow-green solid (4.42 g, 93%); δ_H (400 MHz, CDCl₃): 3.38 (4H, s, 5-,6-*H*₂); δ_C (100MHz, CDCl₃): 208.2 (C=S), 123.5 (3a-, 7a-C), 29.6 (5,6-C); found C, 26.81; H, 1.84%, C₅H₄S₅ requires C, 26.78, H, 1.78%.

2.5.3 Synthesis of 1, 3-dithiolane-2,4,5-trithione (**94**).



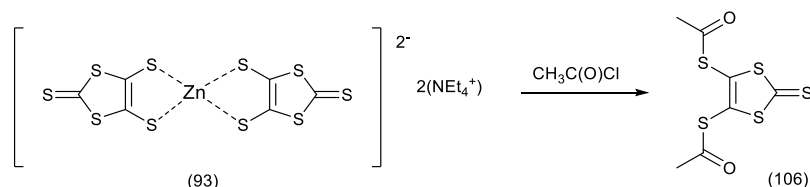
A solution of zinc salt **(93)** (15.1 g, 21.0 mmol) in acetone (105 ml) was cooled down to -78°C using a CO_2 /acetone bath and then a solution of iodine (10.9 g, 43.1 mmol) in EtOH (300 ml) was added over 1.5 h. The suspension was left stirring overnight. A yellow mustard suspension was formed. The product was isolated by filtration and washed in this following order with acetone (2 x 50 ml), water (2 x 50 ml), EtOH (2 x 50 ml) and Et_2O (3 x 50 ml) and left to dry in a vacuum oven at 70°C for 6 h. A yellow-orange solid was obtained (9.83 g). The yield corresponds to $> 100\%$, due to a presence of impurities such as ZnI_2 .

2.5.4 Synthesis of 4, 5-bis (benzoylthio)-1,3-dithiole-2-thione (**105**).



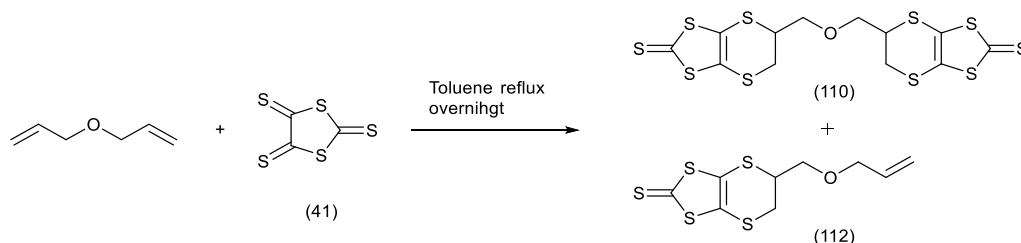
Benzoyl chloride (10 ml, 83.5 mmol) was added dropwise with stirring to a solution of zinc complex **(93)** (15.0 g, 20.9 mmol) in acetone AR (100 ml). After the addition was complete and stirring had continued for 5 min, the orange precipitate was collected by filtration *in vacuo*. To the crude material was added chloroform (100 ml) and the mixture stirred for 10 min before filtration. The solid was slurried with further portions of chloroform until the washings ran clear. Combined washings and filtrate were concentrated *in vacuo* to 150 ml and the solution boiled. After 5 min methanol (150 ml) was added to precipitate the product from solution. The product was isolated by filtration *in vacuo* and washed with cold methanol (50 ml) to afford **(105)** (14.9 g, 88%) as a bright yellow solid; δ_{H} (400 MHz, CDCl_3): 7.91 (4H, m, 2 x Ar- H_2), 7.64 (2H, m, Ar- H_2), 7.48 (4H, m, 2 x Ar- H_2); δ_{C} (100 MHz, CDCl_3): 221.3 (C=S), 185.3 (2 x C=O), 134.9, 133.6, 129.1, 127.9 (Ar- C_{12} , 4-,5-C).

2.5.5 Synthesis of 4,5 -bis (acetylthio)-1,3-dithiole-2-thione (**106**).



To a stirring solution of zinc complex **(93)** (16.20 g, 22.4 mmol) in acetone AR (150 ml) at 0°C was added dropwise acetyl chloride (15.9 ml, 224.4 mmol) and the solution was left stirring overnight. The orange suspension was washed with water (300 ml) and then extracted with diethyl ether (3 x 150 ml). The organic layers were collected and washed with water (3 x 100 ml) and brine (100 ml) and dried over MgSO₄. Evaporation of the diethyl ether yielded the protected thione **(106)** as a yellow solid. (5.40 g, 85%) m.p. 75-77°C; δ_H (400 MHz, CDCl₃): 2.39 (6H, s, 2 x -CH₃); δ_C (100 MHz, CDCl₃): 211.9 (C=S), 189.1 (2 x C=O), 132.9 (4-, 5-C), 30.0 (2 x -CH₃).

2.5.6 Synthesis of racemic and *meso* mixture of 5,5'-(oxy-bis(methylene))bis(5,5',6,6'-tetrahydro-[1,3]dithiolo[4,5-b][1,4]dithiine-2-thione) (**110**) and of 5-(allyloxymethyl)-5,6-dihydro-[1,3]dithiolo[4,5-b][1,4]dithiine-2-thione (**112**).

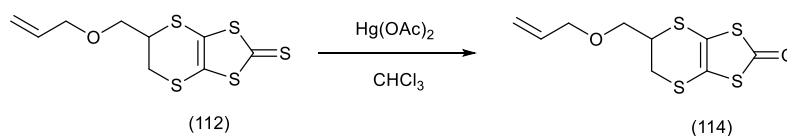


A suspension of trithione **(94)** (2.90 g, 15.0 mmol) and allyl ether (0.50 g, 5.0 mmol) in toluene (50 ml) was heated to reflux with stirring overnight. The suspension formed was allowed to cool down to r.t. and filtered. The solid residue was washed with toluene and the combined filtrates collected. The solvent was evaporated and the residue purified by flash chromatography on silica (6:1 = cyclohexane: ethyl acetate) (R_f 0.75) to yield compound **(112)** (0.99 g, 68%) as a red oil. δ_H (400 MHz, CDCl₃): 5.85 (1H, m, -CH=CH₂), 5.27 (1H, dd, J=17.3, 1.6 Hz, -CH=CHH-*trans*), 5.20 (1H, dd, J=10.1, 1.6 Hz, -CH=CHH-*cis*), 4.01 (2H dt, J= 5.7 Hz, -O-CH₂-CH=CH₂), 3.86 (1H, m, 5-*H*), 3.77 (1H, t, J=8.5 Hz, 5-*CH_a*), 3.60 (1H, dd, J= 9.5, 5.5 Hz, 5-*CH_β*), 3.31(2H, m, 6-*H₂*); δ_C (100 MHz, CDCl₃): 207.7 (C=S), 133.7 (-CH=CH₂), 123.5, 122.1 (3a-,7a-C), 117.8 (-CH=CH₂), 72.3 (5-CH₂-O-), 70.6 (-O-CH₂-CH=CH₂), 42.6 (5-C), 31.3 (6-C); ν_{max} 2848, 1644, 1486, 1096 (C-O-

C), 1056 (C=S), 924, 786, 514; *HRMS*: (ASAP) found: 294.9403 (100%), C₉H₁₀O₁S₅ + H requires: 294.9408; found C, 36.86; H, 3.46%, C₉H₁₀O₁S₅ requires C, 36.73; H, 3.40%.

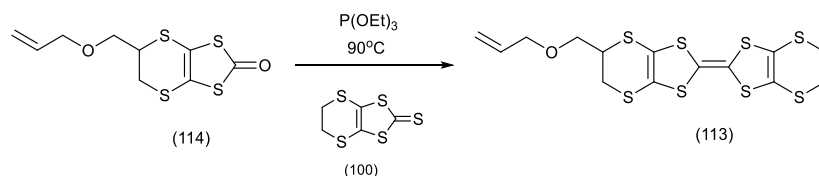
Purification by flash chromatography on silica (6:1 = cyclohexane:ethyl acetate) (*R_f* 0.35) also yielded compound (**110**) as the slowest moving fraction (0.15 g, 6%) as a brown solid, m.p. 116-117 °C (dec). δ_H (400 MHz, CDCl₃): 3.84 (4H, m, -CH₂-O-CH₂-O-), 3.67 (2H, m, 5-, 5'-H), 3.26 (4H, br d, J = 3.8 Hz, 6-6'-H₂); δ_C (100MHz, CDCl₃): 207.5 (2 x C=S), 122.8, 121.9 (4 x sp²-C), 76.7 (-CH₂-O-CH₂-). 42.1 (5, 5'-C), 31.2 (6-, 6'-C); ν_{max} 2847, 1478, 1404, 1261, 1112, 1054, 868, 517; *HRMS*:(ASAP) found 490.8003 C₁₂H₁₀O₁S₁₀ + H requires 490.8011; found C, 29.48; H, 2.15%, C₁₂H₁₀O₁S₁₀ requires C, 29.38; H, 2.04%. Over a period of time the compound appeared to decompose.

2.5.7 Synthesis of 5-(allyloxymethyl)-5, 6-dihydro-[1,3]dithiolo[4,5-b][1,4]dithiin-2-one (**114**).



To a solution of thione (**112**) (2.10 g, 7.3 mmol) in CHCl₃ (100 ml) was added mercury (II) acetate (5.70 g, 17.9 mmol) and the suspension was left stirring for 4 h. at r.t. under a nitrogen atmosphere. The solid obtained during the reaction was filtered and washed with CHCl₃. The combined filtrates were collected and neutralised with saturated aqueous NaHCO₃ (5 x 50 ml). The organic layer was collected and washed with water (100 ml) and brine (100 ml) and dried over MgSO₄. The solvent was evaporated to give the desired compound (**114**) (2.70 g, 83%) as a yellow-brown oil; δ_H (400 MHz, CDCl₃): 5.82 (1H, m, -CH=CH₂), 5.23 (1H, dd, J= 17.2, 1.4 Hz -CH=CHH-*trans*), 5.23 (1H, dd, J= 10.4, 1.6 Hz, -CH=CHH-*cis*), 3.97 (2H, dd, J= 5.7, 1.3 Hz, -CH₂-O-CH=CH₂), 3.84 (1H, m, 5-H), 3.75 (1H, t, J= 9.6 Hz, 5-CH_a), 3.57 (1H, dd, J= 9.6, 5.6 Hz, 5-CH_β), 3.27 (2H, m, 6-CH₂); δ_C (100 MHz, CDCl₃): 188.7 (C=O), 133.8 (-CH=CH₂), 117.7 (CH=CH₂), 113.9, 112.5 (3a-, 7a-C), 72.3 (5-CH₂-O), 70.7 (O-CH₂-CH=CH₂), 44.3 (6-C), 32.4 (5-C); ν_{max} 2918, 2853, 1673 (C=O), 1621, 1509, 1241, 1093 (C-O-C) 825, 763, 542; *HRMS*: (ASAP) found: 278.9632 (100%), C₉H₁₀O₂S₄ + H requires: 278.9636; found C, 38.69; H, 3.48%, C₉H₁₀O₂S₄ requires C, 38.85; H, 3.60%.

2.5.8 Synthesis of 5-(allyloxymethyl)-(BEDT-TTF) (**113**).



To a solution of oxo compound **(114)** (1.10 g, 3.9 mmol) in freshly distilled triethyl phosphite (30 ml) was added unsubstituted thione **(100)** (1.70 g, 7.8 mmol) and the solution was left stirring for 5 h. at 90°C under a nitrogen atmosphere. The BEDT-TTF formed was filtered off and the triethyl phosphite was distilled off by using a Kugelrohr oven. The residue was purified by flash chromatography (3:1=cyclohexane:ethyl acetate) affording the desired product **(113)** as an orange solid (0.94 g, 53%). m.p. 82.5-84°C; δ_H (400 MHz, CDCl_3): 5.81 (1H, m, $-\text{CH}=\text{CH}_2$), 5.22 (1H, dd, $J=16.9, 1.8$ Hz, $-\text{CH}=\text{CHH}_{trans}$), 5.14 (1H, dd, $J=10.5, 1.8$ Hz, $-\text{CH}=\text{CHH}_{cis}$), 3.95 (2H, d, $J=5.5$ Hz, $-\text{O}-\text{CH}_2-\text{CH}=\text{CH}_2$), 3.73 (1H, m, 5-*H*), 3.67 (1H, t, $J=9.2$ Hz, 5- CH_α), 3.50 (1H, dd, $J=9.2, 5.0$ Hz, 5- CH_β), 3.22 (4H, s, 5'-6'- H_2), 3.16 (2H, m, 6- H_2); δ_C (100 MHz, CDCl_3): 134.0 ($-\text{CH}=\text{CH}_2$), 117.7 ($\text{CH}=\text{CH}_2$), 114.1, 113.7, 113.3, 111.6 (2-, 2'-, 3a-, 7a-, 3'a-, 7'a-C), 72.3 (5- CH_2), 71.0 ($\text{O}-\text{CH}_2-\text{CH}=\text{CH}_2$), 43.05 (5-C), 32.1 (6-C), 30.1 (5'-, 6'-C); ν_{max} 3075, 2847, 1643, 1512, 1408, 1283, 1094, 986, 907, 770, 500; HRMS:(ASAP) found: 454.8881 (100%), $\text{C}_9\text{H}_{10}\text{O}_2\text{S}_4 + \text{H}$ requires: 454.8883; found C, 36.91; H, 3.15%, $\text{C}_{14}\text{H}_{14}\text{O}_1\text{S}_8$ requires C, 37.00; H, 3.08%.

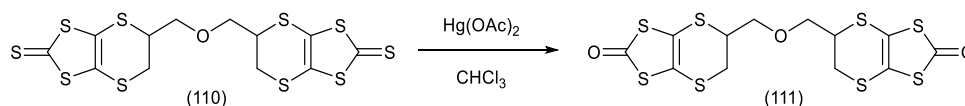
Preparation of **(113)**·(ClO_4)₂.

Electrocrystallisation of **(113)** (10 mg) in a solution of tetrabutylammonium perchlorate (120 mg) in chlorobenzene (40 ml) using a constant current of 0.5 μA over four weeks gave small black needles of **(113)**·(ClO_4)₂.

Crystal data for **(113)**·(ClO_4)₂: $\text{C}_{14}\text{H}_{14}\text{OS}_8 \cdot 2\text{ClO}_4$, $M_r = 653.63$, monoclinic, $a = 5.9156(4)$, $b = 9.5177(7)$, $c = 21.3112(16)$ Å, $\beta = 97.871(4)^\circ$, $V = 1188.58(13)$ Å³, $Z = 2$, $P2_1$, $D_c = 1.826$ g cm⁻³, MoK α ($\lambda = 0.6889$ Å), $\mu = 0.942$ mm⁻¹, $T = 100(2)$ K, 9058 unique reflections ($R_{int} = 0.08$), $R(F, F^2 > 2\sigma) = 0.079$, $R_w(F^2, \text{all data}) = 0.22$. Absolute structure parameter = 0.14(15). The data were collected using synchrotron X-ray radiation ($\lambda = 0.6889$ Å) at the Diamond Light Source, UK using Beamline I19 situated on an undulator insertion device with a combination of double crystal monochromator, vertical and horizontal focussing mirrors and a series of beam slits (primary white beam and either side of the focussing mirrors). The experimental hutch (EH1) is equipped with a Crystal Logic

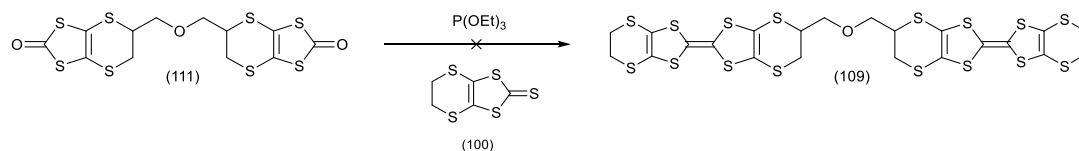
4-circle kappa geometry goniometer with a Rigaku Saturn 724 CCD detector and an Oxford Cryosystems Cryostream plus cryostat (80-500K). Data reduction, cell refinement and absorption correction were performed using *CrystalClear-SM Expert 2.0 r5*.⁴²⁾ The structure was solved with *SUPERFLIP*⁴³⁾ and refined with *SHELXL2013*⁴⁴⁾ within OLEX2 Graphics in *OLEX2*⁴⁵⁾. The structure was refined as a 2-component twin; twin law (1 0 0 / 0 -1 0 / -1 0 -1) corresponding to 2-fold rotation about the 1 0 0 direction. Twin law identified using ROTAX⁴⁶⁾ and hklf5 file generated through WINGX.⁴⁷⁾ Twin scale factor refined to 0.394(4). Disorder was present in the sp³ carbon atoms of the substituted dithiin ring and the first methylene carbon of the side chain, and these were modelled over two half occupied sites. Distance restraints were applied and atoms were refined with isotropic displacement parameters. All geometric analyses were performed using PLATON⁴⁸⁾ and all illustrations were made with MERCURY.⁴⁹⁾

2.5.9 Synthesis of racemic and *meso* mixture of 5,5'-(oxy-bis(methylene))bis(5,5',6,6'-tetrahydro-[1,3]dithiolo[4,5-b][1,4]dithiin-2-one) (**111**).



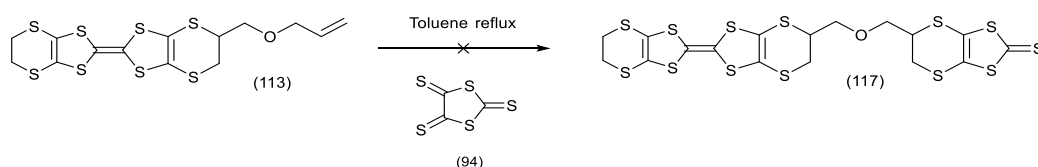
To a solution of (**110**) (0.75 g, 1.53 mmol) in CHCl₃ (60 ml) was added mercury (II) acetate (1.71 g, 5.36 mmol) and the suspension was left stirring at r.t. for 5 h. The solid was filtered off and the solution was neutralised with saturated aqueous NaHCO₃ (5 x 50 ml). The organic phase was collected, washed with water (50 ml) and brine (50 ml) and dried over MgSO₄. The evaporation of the solvent gave the desired product (**111**) as a brown solid (0.64 g, 91%), m.p. 122-123.5°C; δ_H (400 MHz, DMSO-d₆): 4.17 (2H, m, 5-, 5'-H), 3.86 (2H, m) and 3.70 (2H, m) (-CH₂-O-CH₂-), 3.48 (2H, dd, J=13.6, 3.4 Hz) and 3.39 (2H, dd, J=13.6, 6.3 Hz) (6-, 6'-H₂); δ_C (100 MHz, DMSO-d₆): 187.9 (2 x C=O), 114.2, 112.7 (4 x sp²-C), 71.4 (CH₂-O-CH₂-), 44.4 (5-, 5'-C), 32.0 (6-, 6'-C); ν_{max} : 2850, 1614, 1498, 1408, 1100, 768, 463; HRMS: (ASAP) found 458.8489 C₁₂H₁₀O₁S₁₀ +H requires 458.8468; found C, 31.54; H, 2.29%, C₁₂H₁₀O₃S₈ requires C, 31.44; H, 2.18%.

2.5.10 Attempted coupling reaction of *bis* (BEDT-TTF-methyl) ether (**109**).



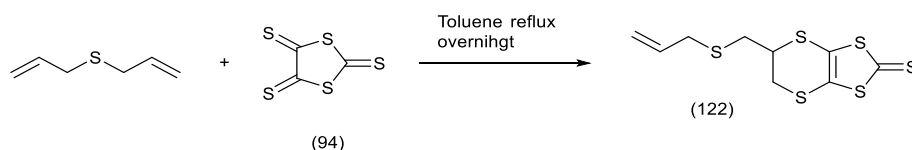
A solution of oxo compound (**111**) (0.24 g, 0.53 mmol) and unsubstituted thione (**100**) (0.29 g, 1.29 mmol) in freshly distilled triethyl phosphite (8 ml) was left stirring for 15 h. at 90°C under nitrogen. The solid formed during the reaction was filtered, washed with CHCl₃ and the combined filtrates were evaporated. The triethyl phosphite was distilled off by using a Kugelrohr oven. The obtained oil was dried over silica powder and purified by flash chromatography (1:1=cyclohexane: DCM) but the desired product was not identified.

2.5.11 Attempted cyclisation reaction of 5-allyloxy-methyl-BEDT-TTF (**113**) with trithione (**94**).



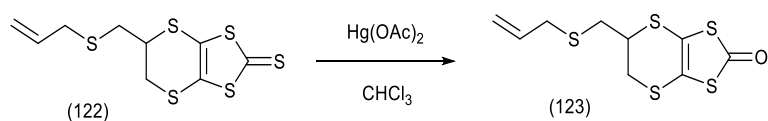
A suspension of 5-(allyloxymethyl)-BEDT-TTF (**113**) (0.48 g, 1.05 mmol) and trithione (**94**) (1.88 g, 9.59 mmol) was refluxed in toluene (50 ml) overnight. The reaction was followed by tlc and the addition of trithione (**94**) was terminated only when compound (**113**) was completely consumed. The solid formed was filtered and the filtrate purified by flash chromatography (9:1=cyclohexane: ethyl acetate). The solid and the fractions collected were analysed by NMR spectroscopy but the desired product was not found. As the NMR showed no trace of the free double bond present in (**113**), initially it was thought that this compound undergoes a retro-Dies-Alder, but no evidence of this was found when a toluene solution of the donor (**113**) was refluxed under the same conditions.

2.5.12 Synthesis of 5-(allylthiomethyl)-5,6-dihydro-[1,3]dithiolo[4,5-b][1,4]dithiine-2-thione (**122**).



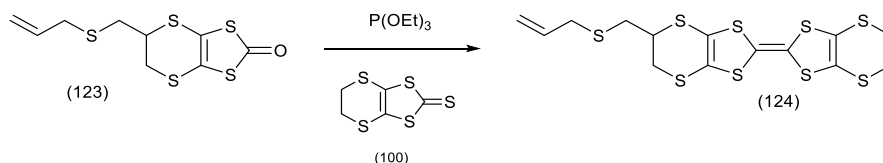
A suspension of trithione (**94**) (5.82 g, 29.7 mmol) and allyl sulphide (1.42 g, 11.9 mmol) in toluene (160 ml) was heated to reflux overnight. The suspension was allowed to cool down to r.t. and filtered. The solid residue was washed with CHCl_3 and the combined filtrates collected. The solvent was evaporated and the residue purified by flash chromatography on silica (3:1 = cyclohexane:ethyl acetate) (R_f 0.75) to yield compound (**122**) (1.14 g, 31%) as a red oil. δ_H (400 MHz, CDCl_3): 5.74 (1H, m, $-\text{CH}=\text{CH}_2$), 5.11 (2H, br d, $J=9.6$ Hz, $-\text{CH}=\text{CHH-cis}$), 5.08 (2H, dd, $J=17.1, 1.4$ Hz, $-\text{CH}=\text{CHH-trans}$), 3.68 (1H, m, 5- H), 3.35 (2H, m, 6- H_2), 3.14 (2H, d, $J=7.2$ Hz, $-\text{S}-\text{CH}_2-\text{CH}=\text{CH}_2$), 2.86 (1H, dd, $J=14.0, 8.9$ Hz, 5- CH_α), 2.80 (1H, dd, $J=14.0, 5.9$ Hz, 5- CH_β); δ_C (100 MHz, CDCl_3): 207.8 ($\text{C}=\text{S}$), 133.7 ($-\text{CH}=\text{CH}_2$), 123.1, 121.7 (3a-,7a- sp^2C), 118.2 ($-\text{CH}=\text{CH}_2$), 42.5 (5- C), 35.3 ($-\text{CH}_2-\text{S}-\text{CH}_2$), 34.8 ($-\text{S}-\text{CH}_2-\text{CH}=\text{CH}_2$), 32.9 (6- C); ν_{max} 2905, 1631, 1484, 1403, 1054 ($\text{C}=\text{S}$), 917, 574; *HRMS*:(ASAP) found: 310.9179 (100%), $\text{C}_9\text{H}_{11}\text{S}_6 + \text{H}$ requires: 310.9180.

2.5.13 Synthesis of 5-(allythiomethyl)-5,6-dihydro-[1,3]dithiolo[4,5-b][1,4]dithiin-2-one (**123**).



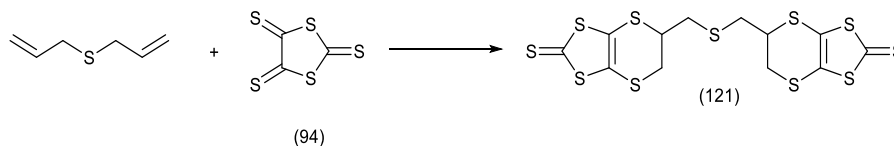
To a solution of thione (**122**) (1.10 g, 3.5 mmol) in CHCl_3 (25 ml) under a nitrogen atmosphere was added mercury (II) acetate (3.00 g, 9.4 mmol) and the suspension was left stirring for 2 h. at r.t. The solid obtained was filtered and washed with CHCl_3 until washes ran clear. The combined filtrates were washed with saturated solution of NaHCO_3 (5 x 20 ml). The organic layer was collected and washed with water (30 ml) and brine (30 ml) and dried over MgSO_4 . The solvent was evaporated to give the desired compound (**123**) (0.60 g, 53%) as a pink-red oil; δ_H (400 MHz, CDCl_3): 5.72 (1H, m, $-\text{CH}=\text{CH}_2$), 5.13 (1H, br d, $J=10.0$ Hz, $-\text{CH}=\text{CHH-cis}$), 5.09 (1H, br d, $J=17.5, 1.3$ Hz, $-\text{CH}=\text{CHH-trans}$), 3.72 (1H, m, 5- H), 3.40 (1H, dd, $J=13.4, 3.1$ Hz, 6- CH_α), 3.40 (1H, dd, $J=13.4, 3.1$ Hz, 6- CH_α), 3.33 (1H, dd, $J=13.4, 6.0$ Hz, 6- CH_β), 3.14 (2H, d, $J=7.3$ Hz, $-\text{CH}_2-\text{CH}=\text{CH}_2$), 2.89 (1H, dd, $J=13.9, 9.0$ Hz, 5- CH_α), 2.81 (1H, dd, $J=13.9, 5.8$ Hz, 5- CH_β); δ_C (100 MHz, CDCl_3): 188.9 ($\text{C}=\text{O}$), 133.8 ($-\text{CH}=\text{CH}_2$), 118.2 ($\text{CH}=\text{CH}_2$), 113.5, 112.3 (3a-,7a- C), 44.4 (5- C), 35.4 ($-\text{CH}_2-\text{S}-\text{CH}_2$), 34.9 ($-\text{S}-\text{CH}_2-\text{CH}=\text{CH}_2$), 34.2 (6- C); ν_{max} 2910, 1670, 1628, 1503, 1405, 1226, 988, 916, 888, 754; found C, 36.60; H, 3.51%, $\text{C}_9\text{H}_{10}\text{O}_1\text{S}_5$ requires C, 36.73; H, 3.40%.

2.5.14 Synthesis of 5-(allyl-thio-methyl)-(BEDT-TTF) (**124**).



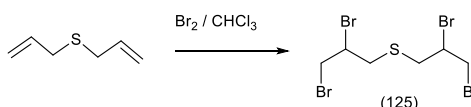
To a solution of oxo compound (**123**) (0.60 g, 2.05 mmol) in freshly distilled triethyl phosphite (30 ml) under a nitrogen atmosphere was added unsubstituted thione (**100**) (0.92 g, 4.1 mmol) and the solution was left stirring for 5h at 90°C. The solid formed was filtered off and washed with cold chloroform until washes ran clear. The chloroform was then removed at the rotary evaporator and the phosphite was distilled off by using a Kugelrohr oven. The crude red oil was purified by flash chromatography (6:1=cyclohexane: ethyl acetate) affording the donor (**124**) as an orange-red solid (0.29 g, 31%), m.p. 107-109°C; δ_H (400 MHz, $CDCl_3$): 5.72 (1H, m, $-CH=CH_2$), 5.08 (1H, br d, $J=10.8$ Hz, $-CH=CH_{H_{cis}}$), 5.07 (1H, dq, $J=16.4, 1.3$ Hz, $-CH=CH_{H_{trans}}$), 3.61 (1H, m, 5- H), 3.24 (2H, m, 6- H_2), 3.22 (4H, s, 5',6'- CH_2), 3.12 (2H, d, $J=7.2$ Hz, $-S-CH_2-CH=CH_2$), 2.82 (1H, dd, $J=14.0, 9.2$ Hz, 5- CH_α), 2.75 (1H, dd, $J=14.0, 5.8$ Hz, 5- CH_β); δ_C (100 MHz, $CDCl_3$): 133.7 ($-CH=CH_2$), 117.9 ($CH=CH_2$), 113.7, 112.8, 111.8, 111.6 (6 x sp^2-C), 42.9 (5-C), 35.3 ($-S-CH_2-CH=CH_2$), 34.9 ($-CH_2-S-$), 33.6 (6-C), 30.1 (5', 6'-C); ν_{max} 2915, 1633, 1517, 1399, 1287, 1203, 913, 882, 772; found C, 35.81; H, 2.93%, $C_{14}H_{14}S_9$ requires C, 35.74, H, 2.98%.

2.5.15 Synthesis of racemic and *meso* mixture of 5,5'-(oxy-bis(methylene))bis(5,5',6,6'-tetrahydro-[1,3]dithiolo[4,5-b][1,4]dithiine-2-thione) (**121**).



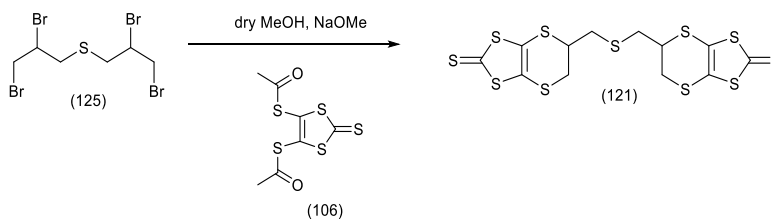
The compound (**121**) was obtained following the same procedure which furnished compound (**122**). Purification by flash chromatography on silica (6:1 = cyclohexane: ethyl acetate) (R_f 0.35) yielded a mixture of mono-thione (**122**) and desired bis-thione (**121**). The evidence of the compound (**122**) was gained from observation of 1H -NMR spectrum which shows presence of terminal alkene peaks while the presence of the desired bis-thione (**121**) was only revealed by mass spectrometry analysis. HRMS: (ASAP) found 506.7779 $C_{12}H_{10}S_{11} + H$: requires 506.7783.

2.5.17 Synthesis of *bis*(2,3-dibromopropyl)sulfide (**125**).



To a solution of allyl sulphide (1.18 g, 10.35 mmol) in carbon tetrachloride (30 ml) cooled down to -20°C was added dropwise a solution of bromine (1.60 ml, 31.05 mmol) in carbon tetrachloride (10 ml) and the yellow solution was left to stir for 2 h. at -20°C. The solution was then quenched with 10 % solution of sodium thiosulfate in water (10 ml) and left to stir for an additional 30 min. Chloroform was added to the mixture (25 ml). The organic layer was separated and washed with water (50 ml) and brine (50 ml) and dried over Na₂SO₄. Evaporation of solvent gave desired compound (**125**) a yellow oil (2.4g, 53%). δ_H (400 MHz, CDCl₃): 4.30 (2H, m, 2 x -CHBr), 3.86 (2H, m, -CHHBr), 3.78 (2H, m, -CHHBr), 3.29 (1H, m, -CH_αS), 3.21 (2H, m, -CH_βS); δ_C (100 MHz, CDCl₃): 50.14 (-CH-Br), 39.0 (2 x CH₂-S-), 35.1 (CH₂Br) for one diastereoisomer, and 48.2 (-CH-Br), 37.5 (2 x CH₂-S-), 34.5 (CH₂Br) for the other diastereoisomer. HRMS: (ASAP) found 430.7304 C₆H₁₀S₁Br₄ +H requires 430.7309.

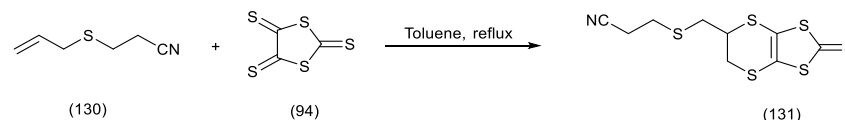
2.5.18 Attempted synthesis of 5,5'-(oxy-bis (methylene)) bis (5,5',6,6'-tetrahydro-[1,3]dithiolo[4,5-b][1,4]dithiine-2-thione) (**121**)-method B.



To a suspension of acetyl protected thione (**106**) (2.19 g, 7.7 mmol) in dry MeOH (40 ml) cooled down to 0°C under a nitrogen atmosphere was added sodium methoxide/methanol (25% in weight) solution (15.5 mmol, 3.55 ml). The solution turned to a dark-red/purple colour and was left stirring for additional 30 min. Then tetra-bromo compound (**125**) (1.68 g, 3.9 mmol) was added dropwise and the suspension was left to stir and warm up to r.t. for 2.5 h. Monitoring the reaction by tlc showed the appearance of a yellow spot, so a further 0.58 g of (**125**) were added and temperature was set at 50°C. After two additional hours the tlc showed two spots and the temperature was increased up to reflux for 1 h. Methyl iodide was added to quench unreacted dithiolate.

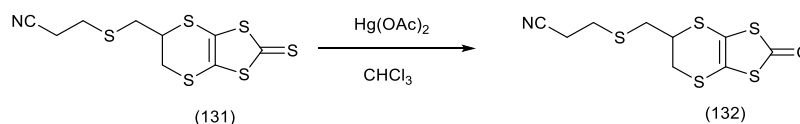
The reaction was allowed to cool down to r.t. and methanol was evaporated. DCM was added to the residue and washed with water (50 ml) and brine (50 ml) and dried over Na_2SO_4 . The residue was characterised by $^1\text{H-NMR}$ but the identity of the *bis* thione (**121**) could not be verified.

2.5.19 Synthesis of 3-((2-thioxo-5,6-dihydro-[1,3]dithiolo[4,5-b][1,4]dithiin-5-yl)methylthio)propanenitrile (**131**).



To a suspension of thione (**94**) (3.77 g, 19.2 mmol) in toluene (100 ml) was added alkene (**77**) (1.63 g, 12.8 mmol) and the mixture was refluxed under a nitrogen atmosphere for 5 h. The dark brown solution obtained was allowed to cool to r.t. The solid formed was filtered, washed with CHCl_3 (300 ml) and the combined filtrates were evaporated. The residue was purified by flash chromatography (1:1=hexane: ethyl acetate) to give the desired thione (**131**) as a brown oil (1.91 g, 46%) δ_{H} (400 MHz, CDCl_3): 3.76 (1H, m, 5-*H*), 3.39 (2H, d, $J = 4.4$ Hz, 5- CH_2), 3.07 (1H, dd, $J = 13.9, 8.8$ Hz, 6- H_{α}), 2.97 (1H, dd, $J = 13.9, 6.1$ Hz, 6- H_{β}), 2.83 (2H, m, - S-CH_2 -), 2.65 (2H, m, - $\text{CH}_2\text{-CN}$); δ_{C} (100 MHz, CDCl_3): 207.4 ($\text{C}=\text{S}$), 122.6, 121.6 (3a-,7a-*C*), 117.9 ($\text{C}\equiv\text{N}$), 42.3 (5-*C*), 36.5 (5- $\text{CH}_2\text{-S}$), 32.7 (6-*C*), 28.3 (- S-CH_2 -), 19.0 (- $\text{CH}_2\text{-CN}$); ν_{max} 2922, 2248 ($\text{C}\equiv\text{N}$), 1484, 1411, 1053 ($\text{C}=\text{S}$), 791, 732; *HRMS*: (ASAP) found: 322.9050 (10%), $\text{C}_9\text{H}_9\text{N}_1\text{S}_6^+$: requires: 322.9054; found C, 33.55; H, 2.93; N, 4.25%, $\text{C}_9\text{H}_9\text{N}_1\text{S}_6$ requires C, 33.44; H, 2.79; N, 4.33%.

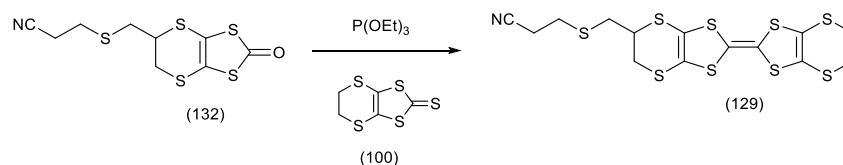
2.5.20 Synthesis of 3-((2-oxo-5,6-dihydro-[1,3]dithiolo[4,5-b][1,4]dithiin-5-yl)methylthio)propanenitrile (**132**).



To a solution of thione (**131**) (1.18 g, 3.65 mmol) in CHCl_3 (50 ml) was added an excess of mercury (II) acetate (2.91 g, 9.12 mol) and the suspension was left stirring for 4h.at r.t. The solid formed was filtered and washed with CHCl_3 until washes ran clear. The combined filtrates were washed with NaHCO_3 saturated solution (3 x 100 ml), water (100

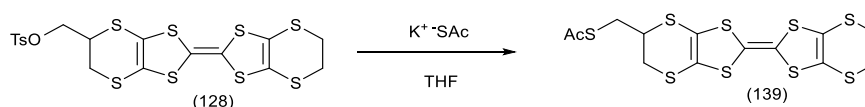
ml) and brine (100 ml). The organic phase was collected, dried over MgSO_4 and evaporation of the solvent furnished oxo-compound (**132**) as a yellow-brown oil (1.09 g, 97%). δ_H (400 MHz, CDCl_3): 3.75 (1H, m, 5- H), 3.42 (1H, dd, $J = 13.5, 3.1$ Hz, 5- CH_a), 3.36 (1H, dd, $J = 13.5, 5.7$ Hz, 5- CH_b), 3.10 (1H, dd, $J = 13.8, 9.0$ Hz, 6- H_a), 2.98 (1H, dd, $J = 13.8, 5.9$ Hz, 6- H_b), 2.83 (2H, m, -S- CH_2 -), 2.65 (2H, m, - CH_2 -CN); δ_C (100 MHz, CDCl_3): 188.8 (C=S), 113.2, 112.3 (3a-,7a-C), 117.9 (C \equiv N), 43.8 (5-C), 36.6 (5- CH_2 -S), 33.8 (6-C), 28.3 (-S- CH_2 -), 19.0 (- CH_2 -CN); ν_{max} 2980, 2921, 2250 (C \equiv N), 1614 (C=O), 1497, 1404, 1201, 761; HRMS: (ASAP) found: 307.9361 (50%), $\text{C}_9\text{H}_9\text{N}_1\text{S}_5+\text{H}$: requires: 307.9360; found C, 35.07; H, 2.95; N, 4.64%, $\text{C}_9\text{H}_9\text{N}_1\text{S}_5$ requires C, 35.18; H, 2.93; N, 4.56%.

2.5.21 Synthesis of 5-(3-methylthio-propanenitrile)-BEDT-TTF (**129**).



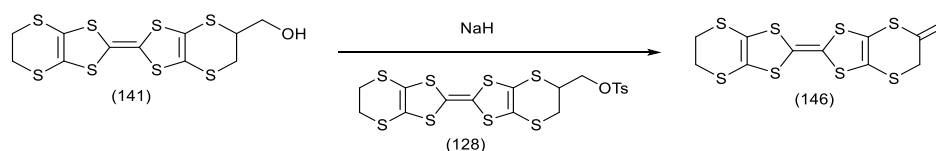
Oxo-compound (**132**) (0.31 g, 1.01 mmol) and unsubstituted thione (**100**) (0.68 g, 3.03 mmol) were left stirring in freshly distilled triethyl phosphite (15 ml) overnight at 90°C under a nitrogen atmosphere. The solid formed was filtered. The triethylphosphite was distilled off by using a Kugelrohr oven and the residue purified by flash chromatography (1:1= cyclohexane: ethyl acetate) to give the desired donor as a yellow solid (0.59 g, 30%) m.p. $122\text{--}123^\circ\text{C}$ dec; δ_H (400 MHz, $\text{DMSO-}d_6$): 4.03 (1H, m, 5- H), 3.38 (4H, s, 5',6'- CH_2), 3.37 (2H, m, 5- CH_2), 2.98 (1H, dd, $J = 14.0, 8.0$ Hz, 6- H_a), 2.90 (1H, dd, $J = 14.0, 7.0$ Hz, 6- H_b), 2.83 (2H, m, - CH_2 -S), 2.48 (2H, m, - CH_2 -CN); δ_C (100 MHz, $\text{DMSO-}d_6$): 119.4 (C \equiv N), 112.8, 112.1, 110.4 (6 x sp^2 C), 42.9 (5-C), 35.1 (5- CH_2 -S-), 33.1 (6-C), 29.5 (5', 6'-C), 26.6 (-S- CH_2), 18.0 (- CH_2 -CN) ν_{max} 2915, 2244 (C \equiv N), 1404, 1288, 1211, 998, 884, 774; found C, 34.69; H, 2.72(5); N, 2.91%, $\text{C}_{14}\text{H}_{13}\text{N}_1\text{S}_9$ requires C, 34.78; H, 2.69; N, 2.90%.

2.5.22 Synthesis of Acetylthiomethyl-BEDT-TTF (**139**).



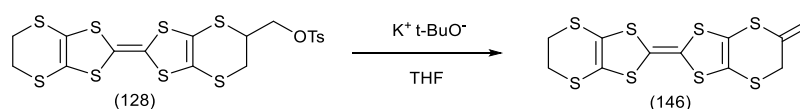
To a solution of compound (**128**) (0.26 g, 0.46 mmol) in dry THF (5 ml) under a nitrogen atmosphere was added potassium thioacetate (0.10 g, 0.92 mmol) and the suspension was left stirring overnight under reflux. The reaction vessel was allowed to cool down to r.t. and the THF evaporated. DCM was added to the residue and the suspension was washed with water (3 x 20 ml) and brine (20 ml) and dried over Na₂SO₄. The solvent was evaporated and the residue purified by flash chromatography (1:1= cyclohexane:diethyl ether) to give donor (**139**) as an orange solid (0.14g, 65%). δ_H (400 MHz, CDCl₃): 3.66 (1H, m, 5-*H*), 3.17 (6H, m, 5', 6', 6-*H*₂), 2.31 (3H, s, -CH₃); δ_C (100 MHz, CDCl₃): 194.9 (-C=O), 113.8, 112.5, 110.9 (2-, 2', -3a-, 7a-, 3'a-, 7'a-C), 42.6 (5-C), 33.7, 33.4 (-CH₂-S, 6-C), 30.6 (-CH₃), 30.1 (5', 6'-C); ν_{max} 2913, 1691 (C=O), 1124, 925, 771; HRMS:(ASAP) found: 472.8439 (100%), C₁₃H₁₂O₁S₉ +H: requires: 472.8447.

2.5.23 Synthesis of *exo*-BEDT-TTF (**146**)-method A.



To a solution of hydroxy-methyl-BEDT-TTF (**141**) (0.11 g, 2.70 mmol) in THF (8 ml) was added NaH (0.68 g, 2.86 mmol) and the resulting suspension was left stirring for 5 min. Then tosyl-oxymethyl-BEDT-TTF (**128**) (0.20 g, 0.35 mmol) was added and the solution was left stirring at 50°C for 48 h. After this time the tlc showed a new spot. To neutralise the excess of sodium hydride, i-PrOH and iced water were added to the solution. The solid formed was filtered, washed with diethyl ether and characterised by NMR spectroscopy. The filtrate was dried over silica powder and purified by flash chromatography (6:1=cyclohexane: ethyl acetate) to give, not the desired compound, but the donor (**146**) as an orange solid (0.10 g, 92%) m.p. 165-166°C (dec). δ_H (400 MHz, CDCl₃): 5.22 (1H, s, -C=CHH _{α}), 5.13 (1H, s, -C=CHH _{β}), 3.52 (2H, s, 6-*H*₂), 3.23 (4H, s, 5'-6'-*H*₂); δ_C (100 MHz, CDCl₃): 137.4 (5-C), 117.1, 114.6, 113.7 (2-, 2', -3a-, 7a-, 3'a-, 7'a-C) 111.0 (=CH₂), 36.5 (6-C), 30.1 (5', 6'-C); ν_{max} 3357, 2958, 2921, 1693, 1598, 1407, 1259, 1124, 1093, 1020, 875, 768; found C, 33.45; H, 2.09%, C₁₁H₈S₈ requires C, 33.33; H, 2.08%.

2.5.24 Synthesis of *exo*-BEDT-TTF (**146**)-method B.



To a solution of tosyl-oxymethyl-BEDT-TTF (**128**) (0.103 g, 0.18 mmol) in dry THF (5 ml) was added t-BuOK (27 mg, 0.28 mmol). The solution was stirring at r.t. under a nitrogen atmosphere for 3 h. as a new spot was seen. The solvent was evaporated, DCM was added and the mixture washed with water. The organic phase was collected and dried over Na₂SO₄. The product was purified by flash chromatography (3:1=hexane: ethyl acetate) to yield product (**146**) as an orange solid (0.10 g, 97%) m.p 165-166°C (dec). δ_H (400 MHz, CDCl₃): 5.22 (1H, s, -C=CHH _{α}), 5.13 (1H, s, -C=CHH _{β}), 3.52 (2H, s, 6-H₂), 3.23 (4H, s, 5'-6'-H); δ_C (100 MHz, CDCl₃): 137.4 (=CH₂), 117.1, 114.6, 113.7 (2-, 2'-, 3a-, 7a-, 3'a-, 7'a-C) 111.0 (5-C), 36.5 (6-C), 30.1 (5', 6'-C); ν_{max} 3357, 2958, 2921, 1693, 1598, 1407, 1259, 1124, 1093, 1020, 875, 768; found C, 33.45; H, 2.09%, C₁₁H₈S₈ requires C, 33.33; H, 2.08%.

Preparation of (**146**)·(ClO₄)₂.

Electrocrystallisation of (**146**) (5 mg) in a solution of tetrabutylammonium perchlorate (47 mg) in chlorobenzene (40 ml) using a constant current of 0.5 μ A over four weeks gave small black needles of (**146**)·(ClO₄)₂.

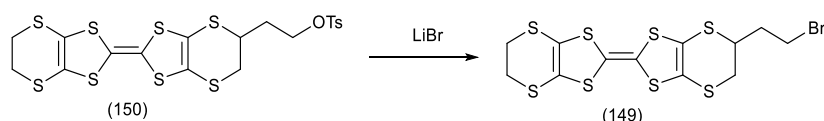
Crystal data for **146**·ClO₄: C₁₁H₈S₈·ClO₄, M_r = 496.10, monoclinic, a = 6.401(2), b = 16.234(5), c = 16.417(5) Å, β = 95.579(9)°, V = 1697.9(9) Å³, Z = 4, $P2_1/c$, D_c = 1.941 g cm⁻³, MoK α (λ = 0.71073 Å), μ = 1.224 mm⁻¹, T = 100(2) K, 12665 unique reflections (R_{int} = 0.16), 8291 with $F^2 > 2\sigma$, $R(F, F^2 > 2\sigma)$ = 0.11, $R_w(F^2, \text{all data})$ = 0.16. The data were measured at the National Crystallography Centre, Southampton University on a Rigaku AFC12 diffractometer equipped with enhanced sensitivity (HG) Saturn724+ CCD detector mounted at the window of an FR-E+ *SuperBright* molybdenum rotating anode generator (Mo K α , λ = 0.71075 Å) with VHF *Varimax* optics (70 μ m focus) using Crystal Clear software⁴²⁾ for data collection and reduction. The structure was solved with SHELXS97⁵⁰⁾ and refined with SHELX2013⁴⁴⁾ within OLEX2⁴⁵⁾. Data were collected from a twinned crystal. ROTAX⁴⁶⁾ was used to identify the twin law, corresponding to a 2-fold rotation about the 1 0 0 direction: twin law [1.000 0.000 0.000] [0.000 -1.000 0.000][-0.498 0.000 -1.000] and the twin component fraction refined to 0.71. Disorder or more probably high thermal motion, in the ClO₄ anion was modelled with two of the oxygen sites split over two sites with the occupancy refined competitively, 0.63/0.37(3), and isotropic atomic displacement parameters for partially occupied atoms. Distance restraints were applied to the Cl-O distances.

Preparation of (**146**)·I₃·0.5I₂

A solution of donor (**146**) (10 mg) in dichloromethane (10 ml) was slowly diffused into a solution of iodine (10 mg) in benzonitrile (10 ml) and was kept in the dark over a period of one week to furnish black crystals of (**146**) \cdot I₃ \cdot 0.5I₂.

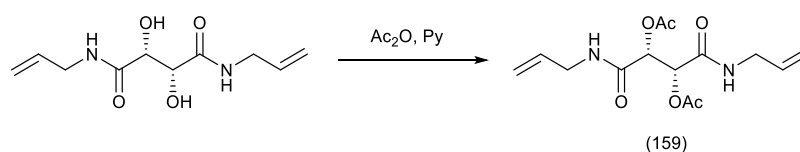
Crystal data for **146** \cdot I₃ \cdot (I₂)_{0.5}: C₁₁H₈S₈ \cdot I₃ \cdot 0.5I₂, $M_r = 904.28$, triclinic, $a = 8.2014(15)$, $b = 9.1986(16)$, $c = 15.637(3)$ Å, $\alpha = 86.967(10)$, $\beta = 86.049(10)$, $\gamma = 72.972(7)^\circ$, $V = 1124.6(4)$ Å³, $Z = 2$, $P-1$, $D_c = 2.670$ g cm⁻³, MoK α ($\lambda = 0.71073$ Å), $\mu = 6.281$ mm⁻¹, $T = 296(2)$ K, 4911 unique reflections ($R_{int} = 0.026$), 3208 with $F^2 > 2\sigma$, $R(F, F^2 > 2\sigma) = 0.049$, $R_w (F^2, \text{all data}) = 0.15$. Data were collected at room temperature using a Rigaku Mercury II CCD configured with the Rigaku MicroMax-007HF generator and VariMax confocal mirror using Crystal Clear software⁴²⁾ for data collection and reduction. The structure was solved by SIR92⁵¹⁾ and refined with SHELX2013⁴⁴⁾ using the Rigaku CrystalStructure[®] software package.

2.5.25 Synthesis of bromo-ethyl-BEDT-TTF (**149**).



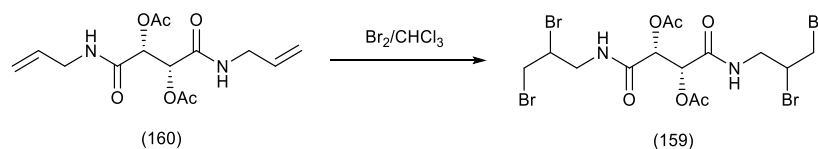
To a solution of tosyloxy-ethyl-BEDT-TTF (**150**) (0.21 g, 0.36 mmol) in dry THF (10 ml) was added lithium bromide (0.22 g, 2.52 mmol) and the solution was left stirring at reflux under a nitrogen atmosphere overnight. The reaction was stopped and allowed to cool down to r.t. and then the THF was evaporated. Ethyl acetate was added (15 ml) and washed with water (10 ml) and brine (10 ml) and dried over Na₂SO₄. Evaporation of the solvent under reduced pressure afforded donor (**149**) as an orange solid. (0.11 g, 60%); δ_H (400 MHz, CDCl₃): 3.78 (1H, m, 5-*H*), 3.66 (4H, m, -CH₂-CH₂-Br), 3.37 (1H, dd, $J=13.3, 3.4$ Hz, 6-*H α*), 3.22 (4H, s, 5',6'-*H $_2$*), 3.02 (1H, dd, $J=13.3, 5.5$ Hz, 6-*H β*); δ_C (100 MHz, CDCl₃): 113.8, 112.9, 111.9 (2-,2'-,3a-,7a-,3'a-,7'a-*C*), 41.8 (5-*C*), 39.4, 36.7, 34.9 (5-CH₂-CH₂-Br, 6-*C*), 30.1 (5'-, 6'-*C*); found C, 29.33; H, 2.42%, C₁₂H₁₂BrS₈ requires C, 29.27; H, 2.44%.

2.5.26 Synthesis of 2*R*,3*R*-*N,N'*-diallyl-*O,O'*-diacetyl tartramide (**160**).



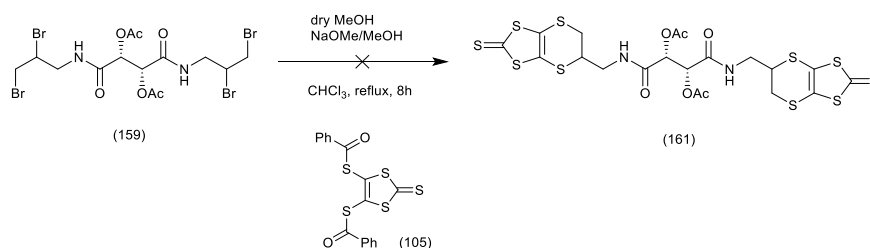
To (+)-*N,N'*-diallyltartramide (1.02 g, 4.5 mmol) was added pyridine (10 ml) and the solution was cooled down to 0°C. Acetic anhydride (1.0 ml, 11.2 mmol) was added dropwise to the solution and the mixture was left to stir and warm up to r.t for 21 h. Iced water (50 ml) was added and the reaction mixture was washed with DCM (3 x 20 ml). The organic layers were collected and washed with 2M HCl (5 x 30 ml), water (30 ml), brine (30 ml) and dried over MgSO₄. Evaporation of DCM afforded a white crystalline solid (0.93g, 67%) identified as desired compound (**160**), m.p 208-210°C; δ_H (400 MHz, CDCl₃): 6.31 (2H, t, J= 5.5 Hz, 2 x -NH), 5.73 (2H, m, 2 x -CH=CH₂), 5.59 (2H, s, 2 x -CH(OAc)), 5.12 (4H, m, 2 x -CH=CH₂), 3.87 (2H, m, 2 x -CH_oH-NH), 3.76 (2H, m, 2 x -CH_βH-NH), 2.10 (6H, s, 2 x -CH₃); δ_C (100 MHz, CDCl₃): 169.2 (2 x CO(NH)), 165.9 (2 x COCH₃), 133.3 (2 x -CH=CH₂), 116.8 (2 x -CH=CH₂), 72.3 (2 x CH(OAc)), 41.8 (2 x -CH₂-NH), 20.6 (2 x -CH₃); ν_{max} 3163 (NH), 1663 (C=OCH₃), 1589 (C=ONH), 1449, 1282, 1215, 1156, 695; HRMS: (ASAP) found: 313.1388 (25%), C₁₄H₂₁O₆N₂+H: requires: 313.1394; $^{297}[\alpha]_D = 114.85^\circ$ (c = 1.01, MeOH).

2.5.27 Synthesis of *N,N'*-(2'',3'')-dibromopropyl)-2*R*,3*R*-diacetoxybutanediamide (**159**).



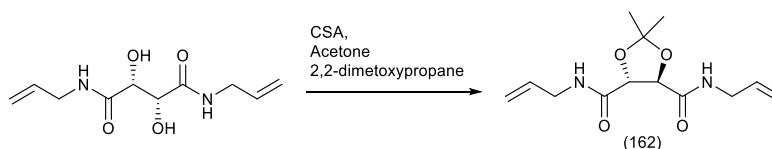
To a solution of bis alkene (**160**) (0.15 g, 0.45 mmol) in CHCl₃ (3 ml) at -5°C was added dropwise a solution of Br₂ (0.07 ml, 1.4 mmol) in CHCl₃ (1 ml) and the resulting mixture was left stirring in ice for 1h. Monitoring by tlc showed no starting material left and the reaction was quenched with a 10% solution of Na₂S₂O₃ (10 ml) and left stirring for further 15 min. The suspension was extracted with chloroform (10 ml) and the organic layer was collected and washed with water (10 ml) and brine (10 ml) and dried over MgSO₄. Evaporation of the solvent gave compound (**159**) as a pale yellow solid (0.23 g, 74%) m.p 151-152°C (dec.); δ_H (400 MHz, CDCl₃): 8.45 (2H, m, 2 x -NH), 5.45 (2H, s, 2 x -CH(OAc)), 4.33 (2H, m, 2 x -CHBr), 3.80 (4H, d, J= 5.7 Hz, 2 x -CH₂Br), 3.50 (4H, m, 2 x -CH₂N), 2.04 (6H, t, J= 5.6 Hz, 2 x -CH₃); δ_C (100 MHz, CDCl₃): 169.3 (2 x O=C(NH)), 166.1 (2 x O=CCH₃), 71.9 (2 x CH(OAc)), 51.5 (2 x -CH₂N) 43.9(2 x -CHBr) , 35.8 (2 x -CH₂Br), 20.7 (2 x -CH₃); ν_{max} 3321 (NH), 1748 (C=OCH₃), 1659 (C=ONH), 1542, 1424, 1373, 1201, 1058, 961; HRMS: (ASAP) found: 628.8128 (33%), C₁₄H₂₀N₂O₆Br₄+H: requires: 628.8128.

2.5.28 Attempted synthesis of (2*R*,3*R*)-*N,N'*-[2-thioxo-5,6-dihydro-[1,3]dithiolo[4,5-*b*][1,4]dithiin-5-yl)methyl] O,O'-diacetyl tartramide (**161**).



A solution of dibenzoyl compound (**105**) (0.34 g, 0.85 mmol) in dry MeOH (10 ml) was cooled down to 0°C and NaOMe/MeOH (25% in weight) solution (0.41 ml, 1.78 mmol) was added. After the usual change in colour (from yellow to deep-red/purple) the solution was left to stir for additional 30 min and then a solution of tetrabromo compound (**159**) (0.30 g, 0.47 mmol) in chloroform (10 ml) was added. The reaction mixture was left stirring at r.t for 3 h and monitoring by tlc showed no sign of reaction. The temperature was increased up to 60°C, initially for 1 h, and then to reflux for another 7 h but still without any change on the tlc. The reaction was quenched with methyl iodide and stopped. The desired product (**161**) was not synthesised due to the lack of reactivity of compound (**159**) towards the dithiolate under the reported conditions.

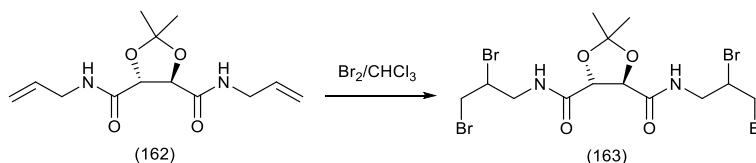
2.5.29 Synthesis of 4*R*,5*R*-(*N,N'*-diallyl)-2,2-dimethyl-1,3-dioxolane-4,5-dicarboxamide (**162**).



To a solution of (+)-*N,N'*-diallyltartramide (1.60 g, 6.9 mmol) in acetone AR (25 ml) was added camphor-sulfonic acid (0.66 mmol, 0.16 g) and 2,2-dimethoxypropane (2.1 mmol, 2.7 ml) and the suspension was stirring at 50°C for 24 h. The reaction was monitored by tlc (1:1= cyclohexane: THF) until all starting material disappeared. Acetone was evaporated under reduced pressure and ethyl acetate (40 ml) was added to the residue. The organic layer was washed with saturated NaHCO₃ solution (3 x 20 ml), water (30 ml) and brine (30 ml) and dried over MgSO₄. Evaporation of the solvent yielded the desired compound (**162**) as a yellow oil (1.70 g, 92%) δ_H (400 MHz, CDCl₃): 7.17 (2H, t, J= 5.2 Hz, 2 x -NH), 5.75 (2H, m, 2 x -CH=CH₂), 5.14 (2H, dq, J= 17.2, 1.2 Hz, 2 x -CH=CHH_{trans}),

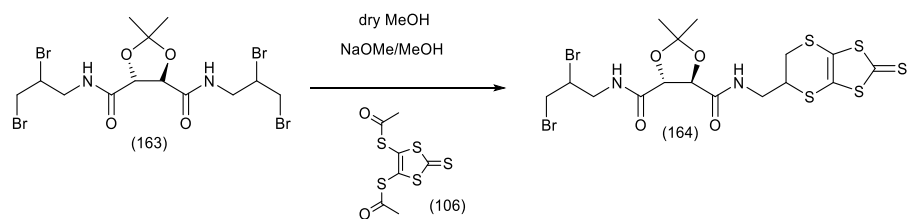
5.07 (2H, dq, $J = 10.3, 1.2$ Hz, 2 x $-\text{CH}=\text{CHH}_{\text{cis}}$), 4.51 (2H, s, 4-,5- H), 3.86 (2H, dt, $J = 5.8, 2.8$ Hz, 2 x $-\text{CHH}_{\alpha}\text{-NH}$), 3.86 (2H, dt, $J = 5.7, 2.8$ Hz, 2 x $\text{CHH}_{\beta}\text{-NH}$), 1.41 (6H, s, 2 x $-\text{CH}_3$); ν_{max} 3398 (NH), 1681 (O=CNH), 1542, 1426, 1347, 1085, 866, 752; HRMS: (ASAP) found: 269.1496, $\text{C}_{13}\text{H}_{20}\text{N}_2\text{O}_4+\text{H}$: requires: 269.1496; $^{298}[\alpha]_{\text{D}} = 139.60^\circ$ ($c = 1.01$, MeOH).

2.5.30 Synthesis of 4*R*,5*R*-*N,N'*-bis(2,3-dibromopropyl)-2,2-dimethyl-1,3-dioxolane-4,5-dicarboxamide (163).



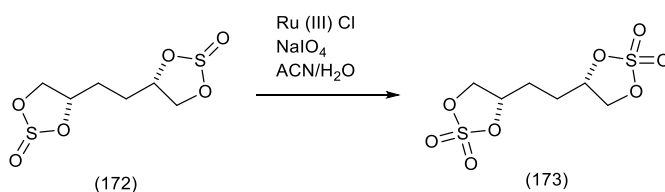
To a solution of **(162)** (0.89 g, 3.3 mmol) in chloroform (5 ml) at 0°C was added dropwise a solution of Br_2 (10 mmol, 0.5 ml) in chloroform (3 ml) and the solution was left stirred for 1h. The brown solution was quenched with a solution of 10% $\text{Na}_2\text{S}_2\text{O}_3$ solution (30 ml) and left stirring for further 15 min. The resulted suspension was extracted with chloroform (20 ml). The organic layer was collected and washed with water (30 ml) and brine (30 ml) and dried over MgSO_4 . Evaporation of the solvent gave compound **(163)** as a sticky pale brown oil (1.24 g, 64%). δ_{H} (400 MHz, CDCl_3): 7.35 (1H, t, $J = 4.4$ Hz, $-\text{NH}$), 7.30 (1H, t, $J = 5.9$ Hz, $-\text{NH}$), 4.58 (2H, s, 4-, 5- H), 4.32 (2H, m, 2 x $-\text{CHBr}$), 3.97 (4H, m, 2 x $-\text{CH}_2\text{Br}$), 3.77 (2H, m, 2 x $-\text{CHH}_{\alpha}\text{-NH}$), 3.61 (2H, m, 2 x $-\text{CHH}_{\beta}\text{NH}$), 1.46, 1.43 (6H, 2 x $-\text{CH}_3$); δ_{C} (100 MHz, CDCl_3): 169.8 (2 x $\text{CO}(\text{NH})$), 112.6 (2- C), 76.8 (4-,5- C), 50.3 (2 x $-\text{CH}_2\text{N}$) 43.7 (2 x $-\text{CHBr}$), 33.2 (2 x $-\text{CH}_2\text{Br}$), 26.0 (2 x $-\text{CH}_3$); ν_{max} 3148 (NH), 1662 (O=CNH), 1583, 1518, 1449, 1280, 1214, 1155, 697; HRMS:(ASAP) found: 584.8232 $\text{C}_{13}\text{H}_{20}\text{Br}_4\text{N}_2\text{O}_4+\text{H}$: requires: 582.8229. The compound is a mixture of two isomers.

2.5.31 Synthesis of 4*R*,5*R*-*N*-(2',3'-dibromopropyl)-*N'*-((2''-thioxo-5'',6''-dihydro-[1'',3'']dithiolo[4'',5''-b][1'',4'']dithiin-5''-yl)methyl) 2,2-dimethyl-1,3-dioxolane-4,5-dicarboxamide (164).



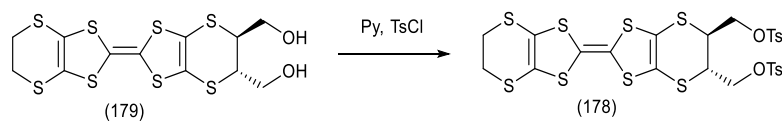
To a solution of acetyl compound (**106**) (0.93 g, 3.3 mmol) in dry MeOH (20 ml) at 0°C under a nitrogen atmosphere was added NaOMe/MeOH (25% in weight) solution (0.41 ml, 1.78 mmol). After the usual change in colour (from yellow to deep-red/purple) the solution was left to stir for additional 30 min and then tetrabromo compound (**163**) (0.97 g, 1.65 mmol) was added. The reaction mixture was left to stir at r.t for 1.5 h and monitoring by tlc showed no sign of reaction. The temperature was increased up to 50°C for 7 h before a new yellow spot appeared on the tlc. The reaction vessel was allowed to cool down to r.t. and methanol was evaporated. DCM was added to the residue and washed with water (50 ml) and brine (50 ml) and dried over Na₂SO₄. Characterisation by ¹H and ¹³C-NMR evidenced the presence of a mixture of compounds which included the starting material (**163**). By MS analysis it was proven that the other compound was monothione (**164**). HRMS: (ASAP) found: 622.8455 C₁₆H₂₀Br₂N₂O₄S₅+H: requires: 622.8466; No separation of the two compounds has been successful up to date.

2.5.32 Synthesis of ethane-1,2-bis-4'-R-1',3',2'-dioxathiolate-2',2'-dioxide) (**173**).



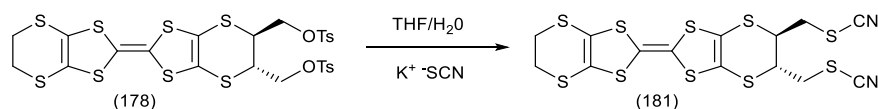
To a biphasic mixture of cyclic sulphite (**172**) (0.26 g, 1.10 mmol) in acetonitrile: water (10 ml: 10 ml) were added ruthenium (III) chloride (9 mg, 0.04 mmol) and sodium periodate (0.74 g, 3.5 mmol) and the resulting mixture was left stirring vigorously at r.t. overnight. The mixture was diluted with DCM (30 ml) and the organic layer collected and washed with water (30 ml), sodium hydrogen carbonate saturated solution (30 ml) and brine (30 ml) and dried over MgSO₄. The evaporation of the solvent furnished a black solid to which was added DCM and filtered over celite. Evaporation of the solvent furnished cyclic sulphate (**173**) as a white solid (0.28 g, 92%); δ_H (400 MHz, CDCl₃): 5.20 (2H, m, 2 x 4-H), 4.91 (2H, dd, J = 9.1, 6.1 Hz, 2 x 5'-H_a), 4.54 (2H, dd, J = 9.1, 7.5 Hz, 2 x 5'-CH_β), 2.05 (4H, m, 2 x 1-,2-H₂); δ_C (100 MHz, CDCl₃): 83.8 (2 x 4'-C), 74.0 (2 x 5'-C), 2.05 (2 x (1-,2-C));

2.5.33 Synthesis of *trans*-bis(tosyloxomethyl)-BEDT-TTF (**178**).



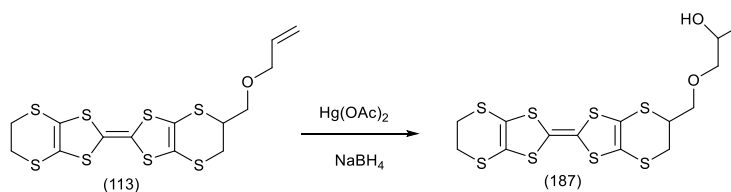
To a solution of *trans*-bis-(hydroxyl-methyl)-BEDT-TTF (**179**) (0.31 g, 0.69 mmol) in pyridine (33 ml) at 0°C was added tosyl chloride (1.33 g, 6.9 mmol) and the reaction mixture was left to stir overnight. The reaction mixture was quenched with iced water (150 ml) and the suspension was washed with DCM (5 x 30 ml). Organic layers were collected and washed with 2M HCl (5 x 30 ml), water (1 x 30 ml), brine (1 x 30ml) and dried over Na₂SO₄. Evaporation of solvent afforded the tosylated donor (**178**) (0.47 g, 90%) as an orange solid m.p. 159-160°C. δ_H (400 MHz, CDCl₃): 7.70 (4H, d, J = 8.3 Hz, 2 x Ar-*H*₂), 7.29 (4H, d, J = 8.1 Hz, 2 x Ar-*H*₂), 4.08 (4H, m, 2 x -CH₂-O-), 3.63 (2H, m, 5-, 6-*H*), 3.21 (4H, s, 5'-, 6'-*H*₂), 2.38 (6H, s, 2 x -CH₃); δ_C (100 MHz, CDCl₃): 145.5, 131.9, 130.1, 127.9 (Ar-*C*₁₂), 113.7, 108.6 (2-, 2'-, 3a-, 7a-, 3'a-, 7'a-*C*), 68.7 (2 x -CH₂-O-Ts), 39.1 (2 x 5-, 6-*C*), 30.2 (5'-, 6'-*C*), 21.7 (2 x -CH₃); found C, 41.59; H, 2.93%, C₂₆H₂₄O₆S₁₀ requires C, 41.49; H, 3.19%.

2.5.34 Synthesis of *trans*-bis(cyanothiomethyl)-BEDT-TTF (**181**).



To a solution of donor (**178**) (0.14 g, 0.19 mmol) in THF:H₂O (20:5 ml) was added potassium thiocyanate (0.07 g, 0.58 mmol) and the solution was refluxed for 25 h. The reaction was stopped and allow to cool down to r.t. The THF was evaporated under reduced pressure to yield a precipitate which was filtered and washed with ether (5 x 15 ml) to furnish a yellow solid identified as desired donor (**181**) (0.06 g, 60%); δ_H (400 MHz, CDCl₃): 3.89 (2H, m, 5-,6-*H*), 3.49 (2H, dd, J= 18.4, 6.4 Hz, 5-,6-*CH*_α-S), 3.31 (4H,s, 5'-,6'-*H*₂), 3.24 (2H, dd, J= 18.8, 11.2 Hz, 5-,6-*CH*_β-S)); δ_C (100 MHz, CDCl₃): 112.9, 112.1, 109.2 (2-, 2'-, 3a-, 7a-, 3'a-, 7'a-*C*, 2 x -C≡N), 42.0 (5, 6-*C*), 35.8 (2 x -CH₂-SCN), 27.7 (5', 6'-*C*); ν_{max} 3390, 2984, 2917, 2151 (-CN), 2076, 1632, 1406, 1285, 1262, 1191, 998, 880; found C, 31.86; H, 1.83; N, 5.41%, C₁₄H₁₀N₂S₁₀ requires C, 31.94; H, 1.90; N, 5.32%.

2.5.35 Synthesis of a diastereomeric mixture of 5-(2''''-hydroxypropoxymethyl)-BEDT-TTF (**187**).



Donor (**113**) (0.13 g, 0.3 mmol) was dissolved in THF (3 ml), mercury (II) acetate (0.01 g, 0.31 mmol) and water (2 ml) were added and the solution was left stirring for 6 h. Sodium borohydride (0.11 mg, 0.31 mmol) was added to quench the reaction. After evolution of gas was completed the suspension was concentrated *in vacuo* and DCM (20 ml) was added. The organic layer was collected, washed with water (20 ml) and brine (20 ml) and dried over MgSO₄. Evaporation of solvent under reduced pressure yielded compound (**187**) as a red-orange solid (0.03 g, 20%); m.p. 89-91°C δ_H (400 MHz, CDCl₃): 3.90 (1H, m, -CH(OH)), 3.75 (2H, m, 5-CH_α, 5-H), 3.55 (1H, m, 5-CH_β) 3.41(1H, m, -O-CH_α-CH), 3.24 (2H, m, -O-CH_β-CH), 3.22 (4H, s, 5',6'-H₂), 3.16 (2H, m, 6-H₂), 1.08 (3H, d, J = 6.4 Hz, -CH₃); δ_C (100 MHz, CDCl₃): 113.9, 113.7, 108.7 (2-, 2'-, 3a-, 7a-, 3'a-, 7'a-C), 77.0 (1''''-C), 72.1, 72.0 (5-CH₂), 66.3 (2''''-C), 43.0, 42.8 (5-C), 32.0, 32.1 (6-C), 30.1 (5'-, 6'-C), 18.7 (3''''-C); ν_{max} : 3343 (OH), 2936, 2857, 1407, 1097, 770; found C, 35.54; H, 3.44%, C₁₄H₁₆O₂S₈ requires C, 35.59; H, 3.39%.

2.6 Bibliography.

1. M. Iyoda, M. Hasegawa and Y. Miyake, *Chem. Rev.*, 2004, **104**, 5085, b) J. Yamada and T. Sugimoto, *TTF Chemistry: Fundamentals and Applications of Tetrathiafulvalene*, Springer, 2004, c) G. Schukat and E. Fanghänel, *Sulfur reports*, 2003, **24**, 1, d) L. Ouahab and E. Yagubskii, *Organic Conductors, Superconductors and Magnets: From Synthesis to Molecular Electronics: From Synthesis to Molecular Electronics*, Springer, 2004.
2. M. R. Bryce, *J. Mater. Chem.*, 1995, **5**, 1481; b) J. Roncali, *J. Mater. Chem.*, 1997, **7**, 2307.
3. M. Kini, U. Geiser, H. H. Wang, K. D. Carlson, J. M. Williams, W. Kwok, K. Vandervoort, J. E. Thompson and D. L. Stupka, *Inorg. Chem.*, 1990, **29**, 2555.
4. M. Cardona and Y. Y. Peter, *Fundamentals of semiconductors*, Springer, 2005.
5. M. Fourmigué and P. Batail, *Bull. Soc. Chim. Fr.*, 1992, **129**, 29; b) J. Y. Becker, J. Bernstein, M. Dayan and L. Shahal, *J. Chem. Soc., Chem. Commun.*, 1992, **15**, 1048; c) M. Fourmigue and Y. S. Huang, *Organometallics*, 1993, **12**, 797.
6. J. Y. Becker, J. Bernstein, S. Bittner, J. A. Sarma and L. Shahal, *Tetrahedron Lett.*, 1988, **29**, 6177; b) M. R. Bryce, G. Cooke, A. S. Dhindsa, D. J. Ando and M. B. Hursthouse, *Tetrahedron Lett.*, 1992, **33**, 1783; c) J. D. Martin, E. Canadell, J. Y. Becker and J. Bernstein, *Chem. Mater.*, 1993, **5**, 1199.
7. M. Fourmigué and P. Batail, *J. Chem. Soc., Chem. Comm.*, 1991, **19**, 1370.
8. P. Leriche, M. Giffard, A. Riou, J. Majani, J. Cousseau, M. Jubault, A. Gorgues and J. Becher, *Tetrahedron Lett.*, 1996, **37**, 5115.
9. F. G. Brunetti, J. L. López, C. Atienza and N. Martín, *J. Mater. Chem.*, 2012, **22**, 4188.
10. Y. N. Kreitsberga, A. Edzhinya, R. Kampare and O. Y. Neiland, *Zhurnal Organiskeoi Khimii*, 1989, **25**, 1456; b) M. Iyoda, Y. Kuwatani, M. Oda, Y. Kai, N. Kaneshisa and N. Kasai, *Angew. Chem. Int. Ed.- Eng*, 1990, **29**, 1062, c) A. Miyazaki, K. Enomoto, K. Okabe, H. Yamazaki, J. Nishijo, T. Enoki, E. Ogura, K. Ugawa, Y. Kuwatani and M. Iyoda, *J. Solid State Chem.*, 2002, **168**, 547.
11. M. Iyoda, K. Hara, C. R. Venkateswara Rao, Y. Kuwatani, K. Takimiya, A. Morikami, Y. Aso and T. Otsubo, *Tetrahedron Lett.*, 1999, **40**, 5729; b) J. Yamada and T. Sugimoto, *TTF Chemistry: Fundamentals and Applications of Tetrathiafulvalene*, Chapter 5, Springer, 2004 and reference therein.

12. T. Otsubo, Y. Kochi, A. Bitoh and F. Ogura, *Chem. Lett.*, 1994, **11**, 2047.
13. Y. Yamashita, Y. Kobayashi and T. Miyashi, *Angew. Chem. Int. Ed.-Eng.*, 1989, **28**, 1052,
14. A. S. Batsanov, M. R. Bryce, M. A. Coffin, A. Green, R. E. Hester, J. A. Howard, I. K. Lednev, N. Martín, A. J. Moore and J. N. Moore, *Chem. Eur. J.*, 1998, **4**, 2580.
15. K. Ishikawa, K. Akiba and N. Inamoto, *Bull. Chem. Soc. Jpn.*, 1978, **51**, 2684; M. R. Bryce and A. J. Moore, *Synth. Met.*, 1988, **27**, 557; A. J. Moore and M. R. Bryce, *Synthesis*, 1991, **1991**, 26.
16. J. Griffiths, R. J. Brown, P. Day, C. J. Matthews, B. Vital and J. D. Wallis, *Tetrahedron Lett.*, 2003, **44**, 3127.
17. C. Wang, A. S. Batsanov, M. R. Bryce and J. A. Howard, *Synthesis*, 1998, **11**, 1615.
18. J. Griffiths, PhD Thesis, Nottingham Trent University, 2004.
19. S. A. Amelichev, V. V. Popov, L. S. Konstantinova, S. P. Golova, V. V. Novikov, E. D. Lubuzh, L. V. Mikhalechenko, V. P. Gul'tyai and O. A. Rakitin, *Mendeleev Commun.*, 2010, **20**, 80.
20. Y. Neiland, Y. Y. Katsens and Y. N. Kreitsberga, *Zhurnal Organicheskoi Khimii*, 1989, **25**, 658.
21. G. Steimecke, H. Sieler, R. Kirmse and E. Hoyer, *Phosphorus and Sulfur and the Related Elements*, 1979, **7**, 49.
22. J. D. Wallis, A. Karrer and J. D. Dunitz, *Helv. Chim. Acta*, 1986, **69**, 69.
23. J. Yamada and T. Sugimoto, *TTF Chemistry: Fundamentals and Applications of Tetrathiafulvalene*, Chapter 1, Springer, 2004 and reference therein.
24. P. Batail, K. Boubekeur, M. Fourmigué and J. P. Gabriel, *Chem. Mater.*, 1998, **10**, 3005.
25. W. Qin, D. Zhu, *Gaofenzi Xuebao*, 1997, **1**, 121.
26. N. Svenstrup, K. M. Rasmussen, T. K. Hansen and J. Becher, *Synthesis*, 1994, **1994**, 809.
27. Y. Zhao, Z. Ge, T. Cheng and R. Li, *Synlett*, 2007, **2007**, 1529; b) H. Firouzabadi, N. Iranpoor and M. Abbasi, *Tetrahedron*, 2009, **65**, 5293.
28. Q. Wang, P. Day, J. Griffiths, H. Nie and J. D. Wallis, *New J. Chem.*, 2006, **30**, 1790.
29. F. Turksay, J. D. Wallis, U. Tunca and T. Ozturk, *Tetrahedron*, 2003, **59**, 8107.

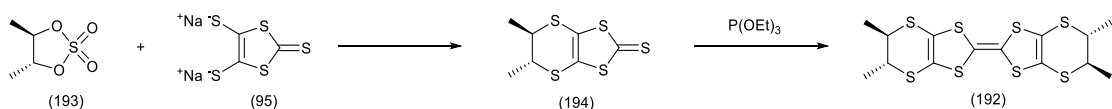
30. B. Koppenhoefer, H. Allmendinger and B. Peters, *Liebigs Ann. Chem.*, 1987, 991.
31. P. J. Kocienski, *Protecting groups*, Thieme, 2005.
32. J. Wallis, *J. Chem. Soc., Perkin Trans. 1*, 1997, 3173.
33. F. Eastwood, K. Harrington, J. Josan and J. Pura, *Tetrahedron Lett.*, 1970, **11**, 5223; b) R. S. Tipson and A. Cohen, *Carbohydr. Res.*, 1968, **7**, 232; c) J. Holz, R. Stürmer, U. Schmidt, H. Drexler, D. Heller, H. Krimmer and A. Börner, *Eur. J. Org. Chem.*, 2001, **2001**, 4615; d) R. J. Brown, A. C. Brooks, J. Griffiths, B. Vital, P. Day and J. D. Wallis, *Org. Biomolec. Chem.*, 2007, **5**, 3172.
34. M. Marzi, P. Minetti and D. Misiti, *Tetrahedron*, 1992, **48**, 10127.
35. N. Machinaga and C. Kibayashi, *Synthesis*, 1992, **1992**, 989; b) Y. Gao and K. B. Sharpless, *J. Am. Chem. Soc.*, 1988, **110**, 7538; c) B. M. Kim and K. B. Sharpless, *Tetrahedron Lett.*, 1989, **30**, 655.
36. X. Yang, P. Wu, D. Zhu, *Hecheng Huaxue*, 1993, **1**, 141.
37. SciFinder Scholar Database Copyright © 2014 American Chemical Society.
38. S. Bouquillon and J. Muzart, *Eur. J. Org. Chem.*, 2001, **2001**, 3301.
39. N. N. Greenwood and A. Earnshaw, *Chemistry of the Elements*, Elsevier, 1997.
40. B. S. Furniss, *Vogel's Textbook of Practical Organic Chemistry*, Pearson Education India, 1989.
41. V. Vitske, H. Herrmann, M. Enders, E. Kaifer and H. Himmel, *Chem. Eur. J.*, 2012, **18**, 14108.
42. <http://webcsd.csd.rsc.org/index.php>.
43. M. Chas, M. Lemarié, M. Gulea and N. Avarvari, *Chem. Comm.*, 2008, **2**, 220.
44. *CrystalClear-SM Expert 2.0 r5*, Rigaku Ltd, 2010.
45. SUPERFLIP. L. Palatinus, G. Chapuis, *J. Appl. Cryst.* 2007, **40**, 786.
46. SHELX2013. G.M. Sheldrick, University of Göttingen, Germany, 2012.
47. OLEX2. O.V. Dolomanov, L.J. Bourhis, R.J. Gildea, J.A.K. Howard, H. Puschmann, *J. Appl. Cryst.*, 2009, **42**, 339.
48. ROTAX. S. Parsons, R.O. Gould, R.I. Cooper, D.J. Watkin, *J. Appl. Crystallogr.*, 2002, **35**, 168.
49. WINGX. L.J. Farrugia, *J. Appl. Cryst.*, 2012, **45**, 849.
50. PLATON. A.L. Spek, *Acta Crystallogr.* 2009, **D65**, 148.
51. MERCURY. C.F. Macrae, P.R. Edgington, P. McCabe, e.Oidcock, G.P. Shields, R. Taylor, M. Towler, J. van de Streek, *J. Appl. Crystallogr.* 2006, **39**, 453.
52. SHELX97. G.M. Sheldrick, *Acta Crystallogr.*, 2008, **A64**, 112.

53. SIR92. A. Altomare, M.C. Burla, G. Camalli, G. Cascarano, C. Giacovazzo, A. Gualiardi, G. Polidori, *J. Appl. Crystallogr.*, 1994, **27**, 435.

Chapter 3
Preparation of novel enantiopure
TTF derivatives.

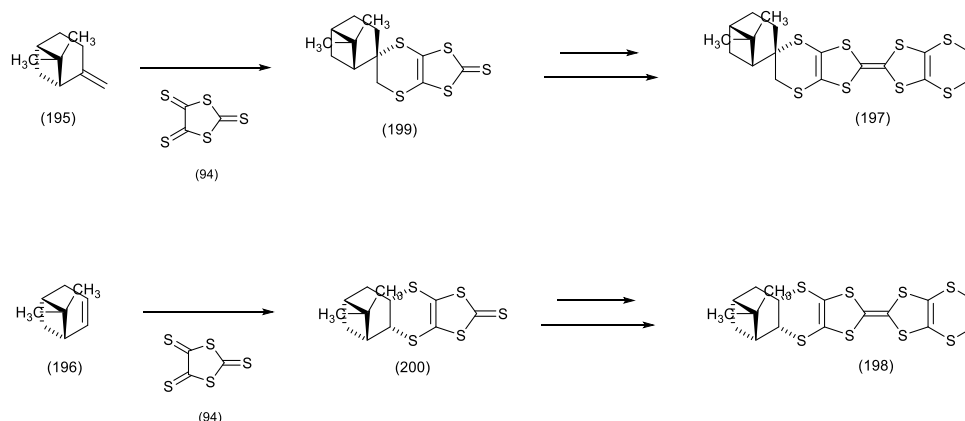
3.1 Introduction.

The preparation and characterisation of TTF derivatives as multifunctional materials has always been an interesting field where the energies of researchers have been focused since the discovery of the TTF molecule and its properties ¹⁾. The ultimate goal is to combine, inside the same material, more than one property such as conductivity and chirality or conductivity and magnetism (Chapter 4) ²⁾. Numerous compounds have been prepared and investigated in the last three decades in order to realise such a material where the two or more property can act independently or by affecting each other. These efforts have been recently reviewed ³⁾. The introduction of chirality has been even more intriguing after the publication in 2002 by Rikken *et al.* ⁴⁾ of the experimental evidence of the effect of chirality on the resistance of chiral carbon nanotubes. The absolute configuration of the nanotubes involved had a direct influence on their conductivity when an applied magnetic field is parallel to the direction of the current. The effect was called electrical magneto-chiral anisotropy, known as EMCA. This discovery has boosted the interest in the preparation of chiral donors although the intriguing question about the possible effect of chirality on the material properties had risen long before ⁵⁾. Only recently the experimental evidence of this phenomenon have been found by Avarvari *et al.* in a tetrathiafulvalene based donor ⁶⁾. In the same field experimental evidence of the Hall effect ⁷⁾ is currently also an interest topic of research ⁸⁾. The introduction of chirality has another effect which is to avoid a potential degree of disorder that a racemic molecule has, due to the presence of both enantiomers. A more ordered crystal structure can create a better pathway for the electrons to flow through the molecules ⁹⁾. Due to the fact that the majority of organic conductors known are based on TTF derivatives ¹⁰⁾, the academic community has been focusing on introducing chirality into this sulphur-rich building block. Dunitz *et al.* ⁵⁾ prepared and characterised the first enantiopure donor, (*S,S,S,S*)-tetramethyl-ET (**192**) by reacting together the cyclic sulphate ester (**193**) and the dithiolate (**95**) in order to furnish enantiopure thione (**194**). The phosphite mediated coupling was then performed to achieve preparation of chiral donor (**192**) which is still studied and reported in the literature as radical cation salt with interesting properties ¹¹⁾. The strategy is described in the Scheme 66.



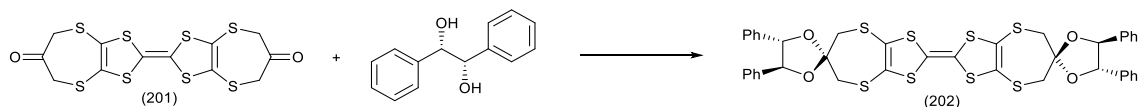
Scheme 66. Synthesis of the first enantiopure donor (**192**).

The use of cyclic sulphate ester chemistry is not the only strategy adopted for the preparation of chiral TTF derivatives. Introduction of chirality on a carbon atom of the TTF building block has been achieved by diastereoselective cycloaddition between trithione **(94)** and a dienophile, such as **(195)** or **(196)**, containing a chiral centre as reported by Wallis *et al.*¹²⁾. The preparation of chiral donors **(197)** and **(198)** with (-)- β -pinene **(195)** and apopinene **(196)** respectively is shown below.



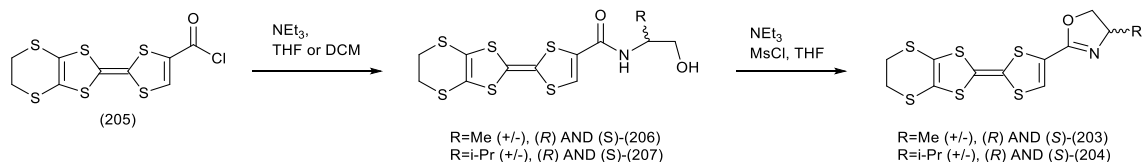
Scheme 67. Synthesis of chiral donors **(197)** and **(198)** by reacting trithione **(94)** and alkenes **(195)** and **(196)**.

Another strategy to generate chiral TTF derivatives is to react an achiral donor with a chiral moiety for example by ketalisation of the two carbonyl groups in donor **(201)** by (*S,S*)-1,2-diphenylethane-1,2-diol to give donor **(202)** (Scheme 68).¹³⁾



Scheme 68. Alternative strategy to include chiral in a TTF derivatives.

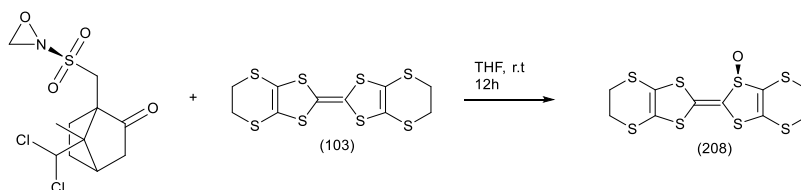
From the previous few examples is clear that the introduction of chirality on the carbon atom can be achieved in a number of different ways. A particularly successful TTF chiral derivative generated following the latter strategy is the EDT-TTF-Me-oxazoline series **(203)**-**(204)** prepared in the racemic and both enantiopure forms by Avarvari and Formigué.¹⁴⁾ Reaction of chloride **(205)** with a chiral β -amino-alcohol gave donors **(206)**-**(207)** which were cyclised to generate compounds **(203)**-**(204)** by using triethylamine and methyl-chloride.



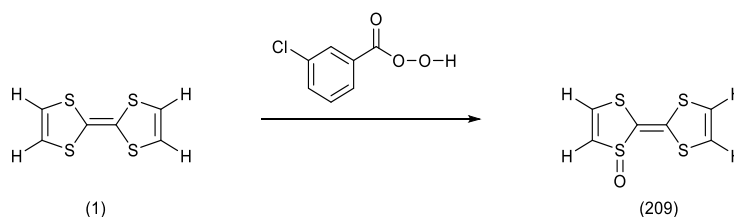
Scheme 69. Preparation of TTF-oxazolines in racemic and both enantiopure forms.

A series of **(203)**₂AsF₆ salts was prepared and fully characterised and the radical cation salts showed metallic behaviour down to 230K with a conductivity at r.t. of 100 S cm⁻¹ for the enantiopure salts and 10 S cm⁻¹ for the racemic compound ¹⁴).

Avarvari *et al.* ¹⁵) also reported the synthesis of the chiral organo-sulphur donor **(208)** where one of the sulphurs in the internal five- membered ring has been oxidised to a mono-sulfoxide. The reaction performed involved BEDT-TTF **(103)** and the chiral compound (+)-8, 8-dichlorocamphoryl-sulfonyl-oxaziridine as an oxidizing agent and furnished the inner monosulfoxide **(208)** with an enantiomeric excess of 44% after purification by column chromatography ¹⁵).

Scheme 70. Preparation of the chiral BEDT-TTF sulfoxide **(208)**.

It is worth to mention that at the time of the preparation of the chiral TTF-sulfoxide **(208)** a similar kind of TTF-S-oxide had been already reported in the literature by Garito ,Cava *et al.* ¹⁶) who prepared racemic compound **(209)** by reacting the TTF molecule **(1)** with *m*-CPBA in a biphasic system.

Scheme 71. Preparation of sulfoxide **(209)**.

An alternative strategy to introduce chirality into a BEDT-TTF salt, without modifying the structure of the donor itself, is by chiral induction, such as crystallising the donor and the acceptor molecules from a chiral solvent. Martin *et al.* ¹⁷) reported the preparation of the first chiral BEDT-TTF-tris-(oxalate)-metallate (III) by using Na₃Cr(C₂O₄)₃ in dichloromethane-acetonitrile-*R*-(-)-carvone as supporting electrolyte in the electro-crystallisation of BEDT-TTF. The salt obtained had the composition (BEDT-TTF)₃NaCr(C₂O₄)₃CH₂Cl₂. By using a simple mixture of dichloromethane-acetonitrile

as electrolyte in absence of the chiral solvent the same electro-crystallisation experiment was repeated and the resulting salt was α''' -(BEDT-TTF)₉[Cr(C₂O₄)₃]₈Na₁₈(H₂O)₂₄. The two compounds crystallised in two different space groups and revealed two different packing of donor and acceptor molecules. The key point is that in the salt (BEDT-TTF)₃NaCr(C₂O₄)₃·CH₂Cl₂ there is only a single enantiomer of Cr(C₂O₄)³⁻ throughout the structure and this introduces chirality to all the lattice ¹⁷⁾. Conducting salts containing anions such as [M(ox)₃]³⁻ (where M=Fe³⁺, Cr³⁺, Ga³⁺ and ox= oxalate), ^{2b,18)} [Cr(2,2'-bipy)(ox)₂]⁻ ¹⁹⁾ or [Fe(croc)₃]³⁻ (croc = croconate), ²⁰⁾ have been reported in the literature before with the difference that the anions were present as both of their enantiomers Δ and Λ in equal amounts. The first example of using chiral anions to introduce chirality in to BEDT-TTF salts during the electro-crystallisation process was reported by Coronado, Galan-Mascaros *et al.* ²¹⁾ who synthesised the complex (BEDT-TTF)₃[Sb₂(L-tart)₂]₂·CH₃CN by electro-crystallisation of BEDT-TTF and K₂[Sb₂(L-tart)₂] in a mixture of acetonitrile and benzonitrile. Conductivity measurements on a single crystal showed semiconducting behaviour at r.t. (1 S cm⁻¹). The experiment was repeated using the K₂[Sb₂(D-tart)₂] without mentioning any reference to its conductive behaviour. Recently Formigué *et al.* ²²⁾ prepared the organic metal (EDT-TTF-I₂)₂(D-camphorsulfonate)·(H₂O) by combining in an electrocrystallisation experiment a *bis*-halogenated-TTF derivative such as (**210**) with a chiral anion from TBA-*D*-camphorsulfonate (**211**), in 1,1,2-trichloroethane. The conductivity of the crystal obtained was measured at r.t. and a value of 3-5 S cm⁻¹ was recorded, while a metallic behaviour was shown above 200 K.

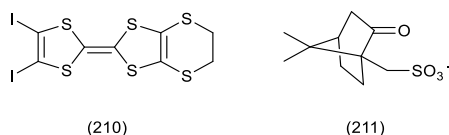
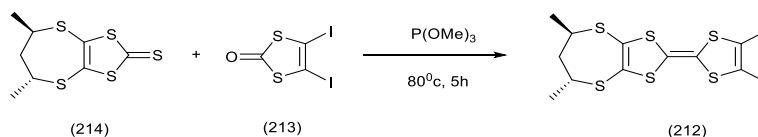


Figure 100. Chiral anion and TTF derivate donor electrocrystallised together.

More recently Formigué *et al.* ²³⁾ described the preparation of the asymmetric donor (**212**) by reacting the oxo-compound (**213**) and thione (**214**) together as presented below. This donor had been realised combining two different aspects that two different research groups postulated based on their experience in the TTF field. On the thione (**214**) side Wallis *et al.* ²⁴⁾ postulated that introducing chirality on an outer seven-membered ring would create the opportunity for a chair conformation to occur. This could lead to the observation of a helical stack of donors (**212**) in the solid state, which has been investigated as an efficient way of generating chirality in supramolecular systems ²⁵⁾.

Scheme 72. Phosphite mediated coupling to generate donor **(212)**.

The second aspect involves the oxo-compound **(213)** where the introduction of a non-covalent interaction such as halogen bonding can help to transfer the chirality from the anion to the donors stack together in the solid state.^{22,23} Donor **(212)** was electrocrystallised in the presence of chloride anion and led to a crystal of **(212)₂Cl** which showed conductive behaviour at room temperature with $\sigma = 0.04 \text{ S cm}^{-1}$ and an activation energy of 0.086 eV. Continuing with the introduction of chirality by chiral anions, Avarvari and Madalan *et al.*²⁶) reported the preparation of radical cation salts of BEDT-TTF **(103)**, the TTF-oxazoline donors **(215)** and the enantiopure tetramethyl-BEDT-TTF donors **(216)** and **(192)** with the chiral anion *tris*(tetrachlorobenzenediolato)phosphate(V) **(217)** called TRISPHAT. The electrocrystallisation experiments involved both racemic and single enantiomer TRISPHAT anions yielded single crystals whose crystallographic analysis revealed that both enantiomers of the anion were present despite the preparation conditions being carefully checked.

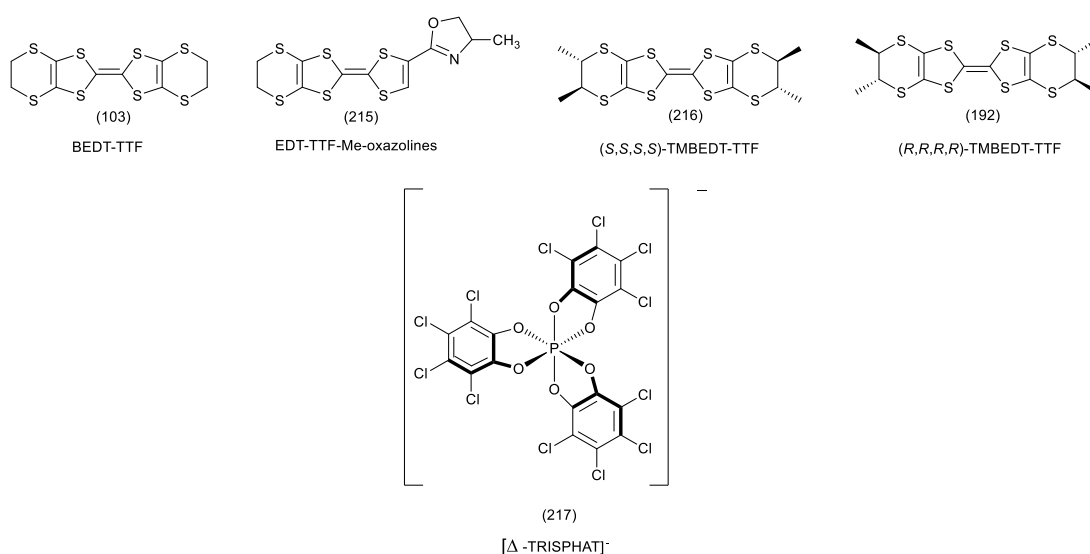
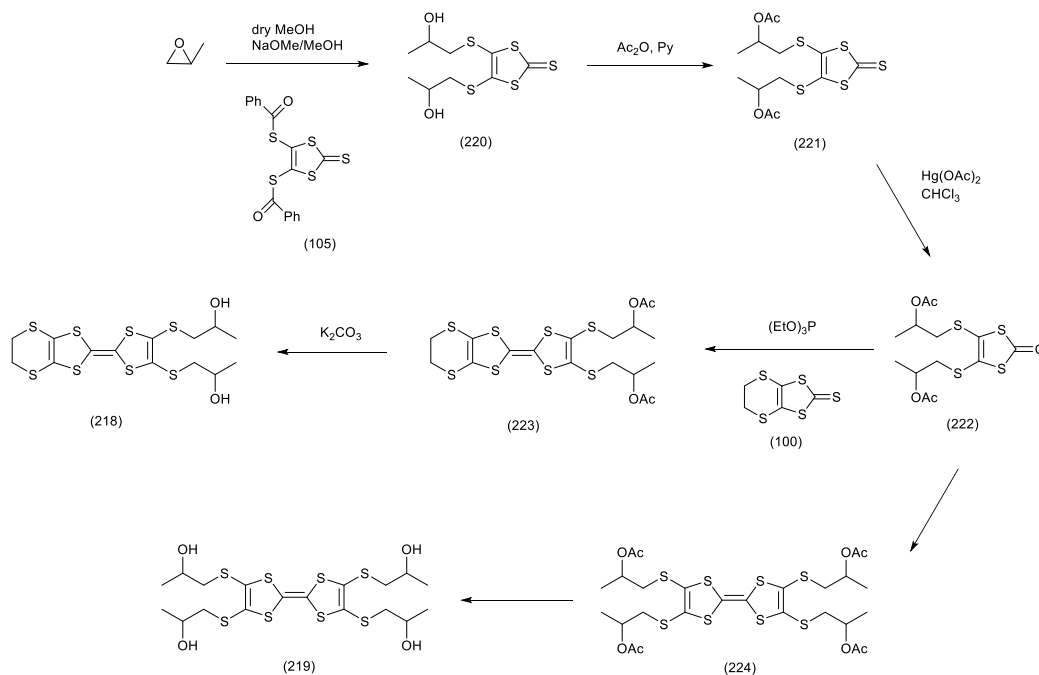


Figure 101. A few examples of the donors involved in the electrocrystallisation with chiral anion (TRISPHAT).

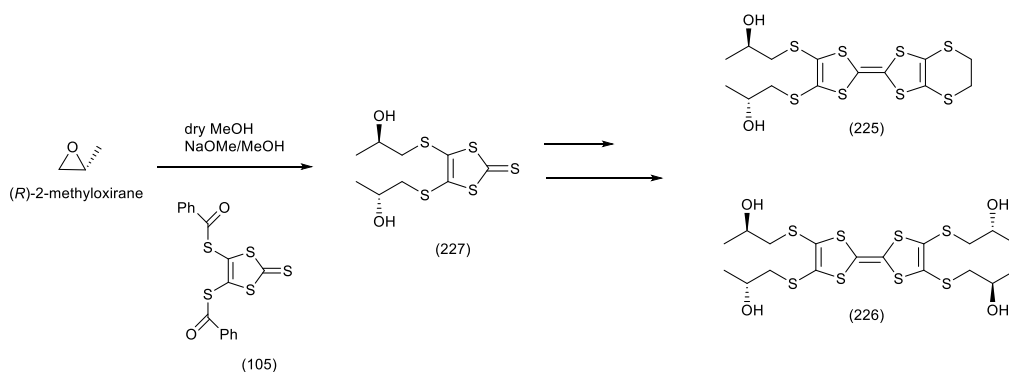
3.2 Background.

As explained in paragraph 3.1 recently the theme of introduction of chirality in organic conductors has emerged strongly after the experimental evidence collected by Rikken *et al.*⁴⁾ of the electrical magneto-chiral anisotropy effect. In addition to this discovery another trend to guide the crystal packing of donor-acceptor systems is the introduction of hydrogen bonding or halogen bonding²⁷⁾ functionalities onto the donor and/or acceptor skeleton. The design of the organic donors in order to guide the way they interact to each other in the solid state and the interactions with the anions take its origin from the crystal engineering vision postulated by Desiraju²⁸⁾ in order to provide a rational way to design a molecule by looking at the properties of the desirable compound. These two themes have been also the focus of the research in the Wallis group which led to the preparation of various novel single enantiomer donors which are reported in the literature²⁹⁾. Recently the synthesis of a novel family of donors has been reported in both enantiomers (*R,R*) and (*S,S*) together with a mixture of the racemic and *meso* compounds which were unseparable³⁰⁾. These donors contain the 2-hydroxypropylthio side chains which are capable of making hydrogen bonding interactions in the solid state. In the scheme below is presented the synthetic route undertaken to prepare the racemic cross coupled (**218**) and homo-coupled (**219**) compounds from the racemic starting material (\pm)-propylene-oxide.



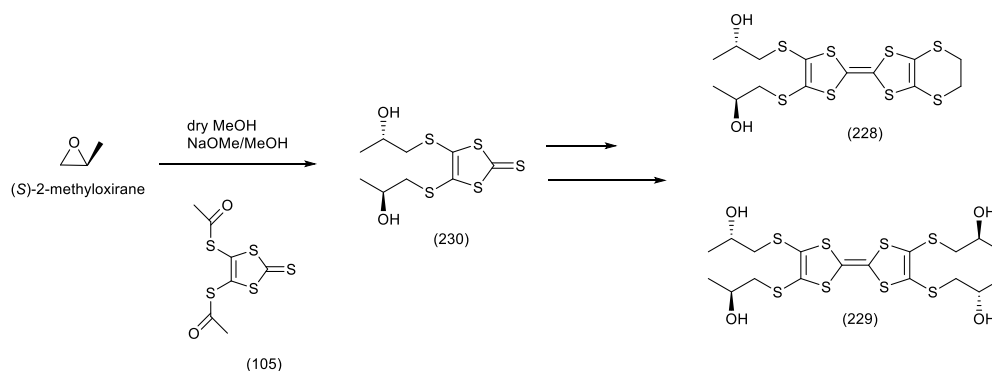
Scheme 73. Preparation of the racemic cross-coupled and homo-coupled donors.

In the schemes below is summarised the preparation of the enantiopure donors (*R,R*)-**(225)**, (*R,R,R',R'*)-**(226)** (Scheme 74) from the enantiopure starting material (*R*)-propylene oxide respectively.



Scheme 74. Preparation of the enantiopure diol **(225)** and tetrol **(226)**. The thione and final products are presented.

The preparation of enantiopure donors (*S,S*)-**(228)** and (*S,S,S',S'*)-**(229)** (Scheme 75) from the enantiopure starting material (*S*)-propylene oxide is reported below.



Scheme 75. Preparation of the enantiopure diol **(228)** and tetrol **(229)**. The thione and final products are presented.

Electrocrystallisation of donor **(228)** with $(\text{NH}_4)_4\text{Fe}(\text{III})_2\text{tris}(\text{oxalate})_5$ gave a salt whose asymmetric cell contains four donors and one $[\text{Fe}(\text{III})_2(\text{oxalate})_5]^{4-}$ anions. The crystal packing of the $(\text{225})_4\text{Fe}(\text{III})_2(\text{oxalate})_5$ is shown below.

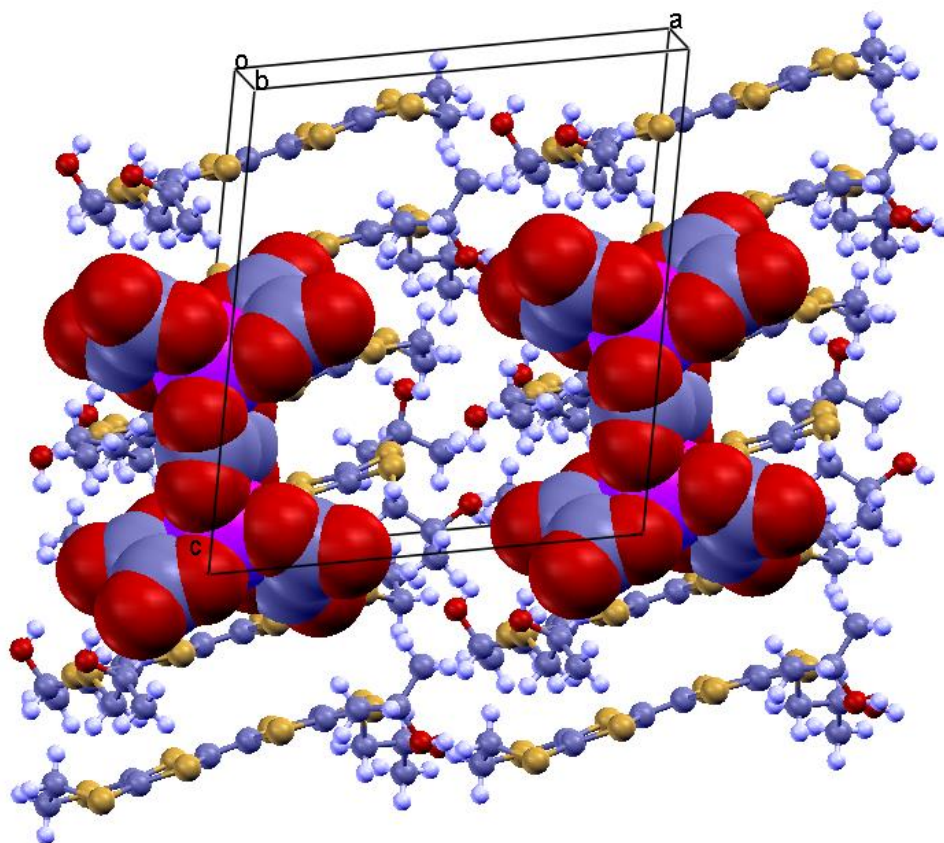
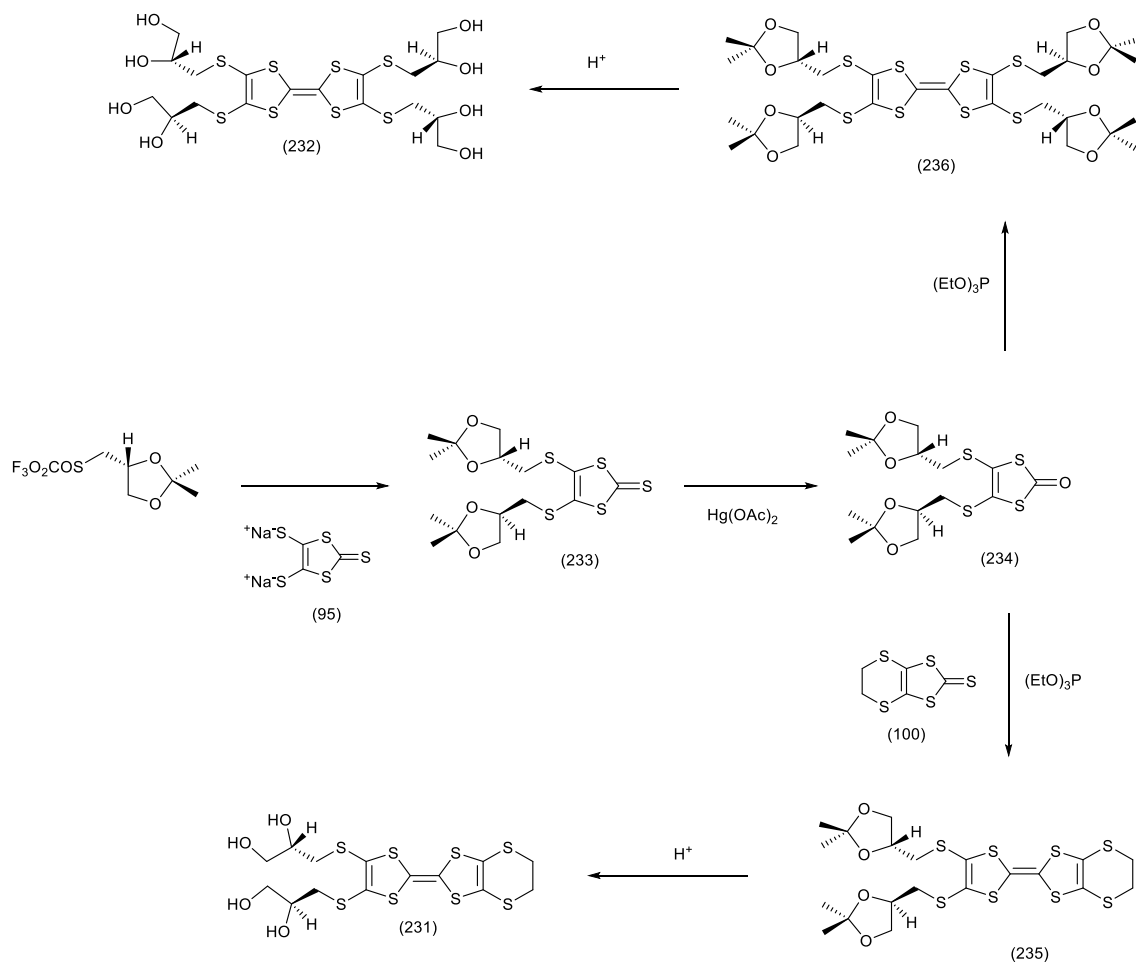


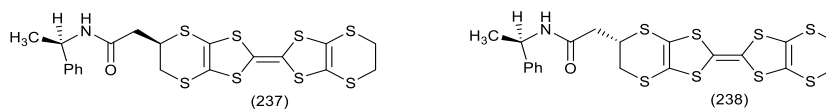
Figure 102. Crystal packing of $(\mathbf{225})_4\text{Fe(III)}_2(\text{oxalate})_5$ with oxalate bridges in evidence.

The interesting feature in this salt is that the chirality at the two metal centres are opposites (Δ and Λ) and this was the first example of a charge transfer salt with chiralities on both donor and anion species. No conductivity measurement could be performed due to the fragility of crystals obtained. The same donor generated a 1:1 charge transfer salt with TCNQ-F₄ by diffusion which was an insulator. Indeed the three donors (*R,R*, *S,S* and *meso*/racemic species) gave the first family of charge transfer salts with the anion BF₄⁻ where all three crystals measured were found to be semiconductors^{30a)}.

More interesting donors have been prepared recently^{30a)} to gain further knowledge and evidence of how the hydrogen bonding interactions can determine novel crystal packing arrangements which could lead to an improvement in the electrical conductivity. Cross-coupled donor (**231**) and homo-coupled donor (**232**) present four and eight hydroxyl groups respectively. In the Scheme 76 the syntheses of these novel donors are presented.

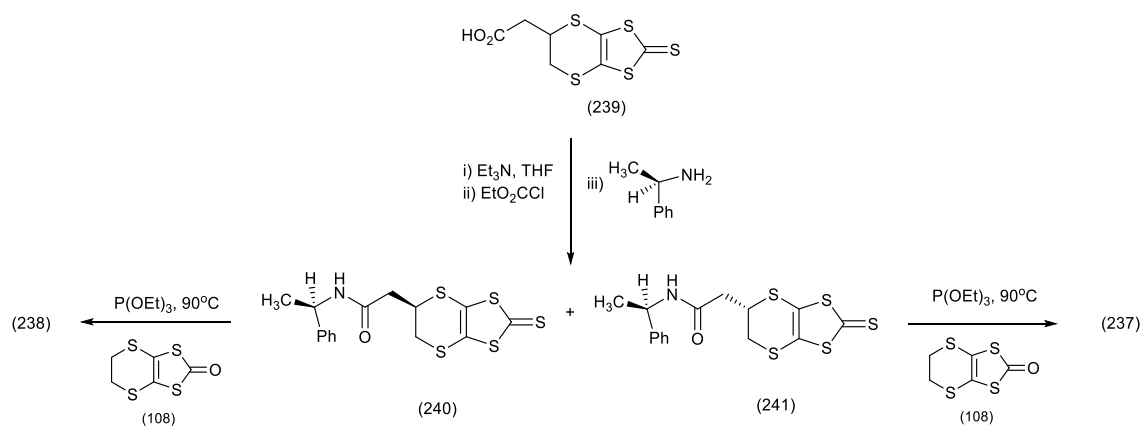
Scheme 76. Preparation of tetra-ol and octa-ol (**231**) and (**232**).

The homo-coupled compound (**232**) generated a crystal of a 1:1 salt with I_3^- by diffusion of iodine into a DCM solution. The material showed semiconducting behaviour with a room temperature resistivity of $3.61 \Omega \cdot \text{cm}^{-1}$ and an activation energy of 22.5 meV. Enantiopure amide donors (**237**) and (**238**) have been prepared and are currently under investigation by electrocrystallisation and diffusion experiments.



Scheme 77. Chiral donor prepared from enatiopure amides.

The thione (**239**) was obtained by reacting together trithione (**94**) and vinyl acetic acid. In the next step the reaction between the enantiopure amine *R*- α -phenylethylamine and thione (**239**) furnished the two enantiopure amide substituted thiones (**240**) and (**241**) which have been separated by chromatography and both analysed by X-ray crystallography which allowed the identification of the compound's absolute configurations. The two enantiopure donors were obtained by reacting unsubstituted oxo-compound (**242**) and thiones (**237**) and (**238**) in freshly distilled triethyl phosphite (Scheme 78).



Scheme 78. Preparation of chiral amide-substituted BEDT-TTF.

Another example of chiral donors prepared in the Wallis laboratory is presented below by *bis*-pyrrolo-TTFs (**242**), (**243**) and (**244**)³¹. The strategy adopted is based on the approach that Becher developed to prepare *bis*-pyrrolo-TTFs.³²

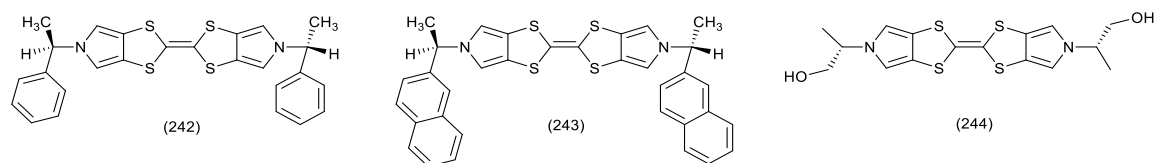


Figure 103. Example of bis-pyrrolo-TTF's.

3.3 Results and discussion.

3.3.1 Preparation of novel enantiopure donors capable of hydrogen-bonding interactions at different levels.

The aim of the work presented in this chapter was to prepare new enantiopure organosulfur donors bearing hydrogen-bonding functionalities on the side chain as substrates for preparing radical cation salts which would show evidence of EMCA. The work can be divided into three parts depending on the different starting materials used. In the first part is described the preparation of donors from substituted epoxides such as in the case of compounds (245)-(250). In detail the side chain presents the –OH group in every donor and a second functional group inserted to evaluate its potential influence on the donor's properties in the solid state. For donors (245)-(248) the introduction of aromatic rings has been chosen to influence the self-assembly of donors in a helical rearrangement³³⁾ which can induce the EMCA phenomena. The presence of the aromatic rings could enhance the π - π stacking interactions, outside the usual stacking between the carbon and sulphur network of the dithiin and dithiole rings, since it is very important to maximise the π -overlap among donors to optimise the conductive behaviour of the oxidised material³⁴⁾. For donors (249)-(250) a methoxy group acts as hydrogen bond acceptor in addition to the donor property of the hydroxyl group.

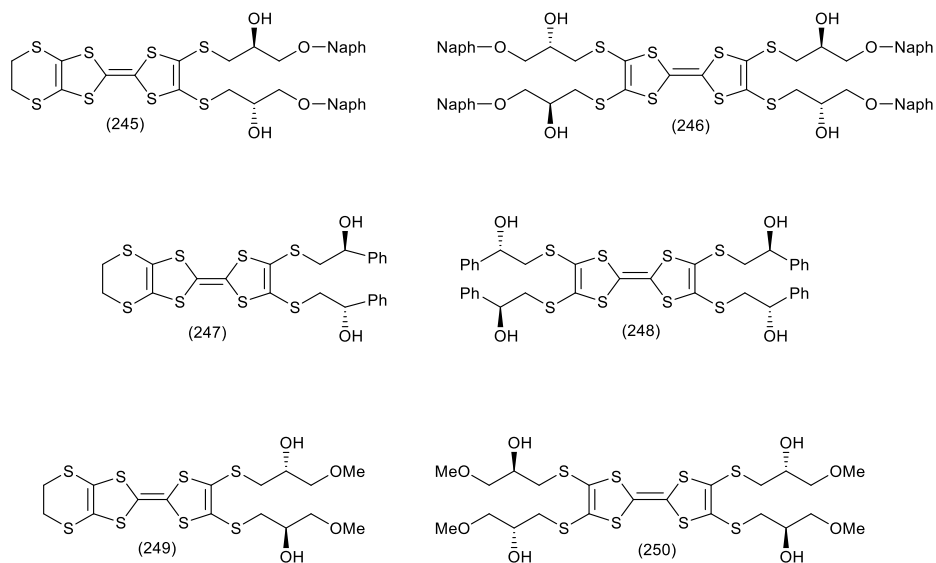


Figure 104. Target donors from substituted epoxides as starting materials.

Following these new molecules is the preparation of a mixed organosulfur donor (251) bearing different number of hydroxyl groups on the side chains to encourage a deviation

from the standard planar face to face stack between donors, and to provide multiple interactions between the –OH groups and acceptors/anions involved in their salts. Finally the attempt to prepare donors (252)-(253) is described in order to compare their properties with a similar, recently prepared, donor with one less methylene group per side chain.

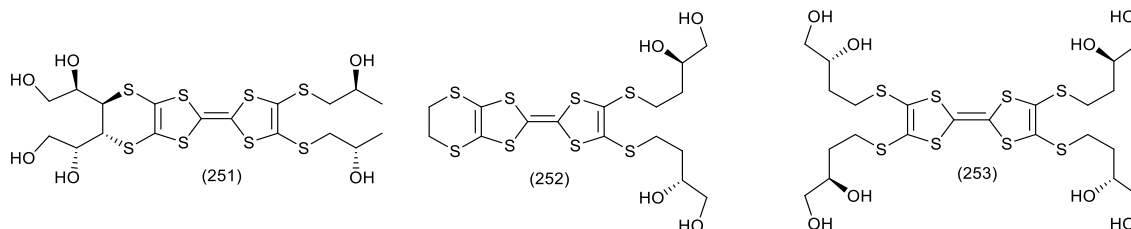


Figure 105. Targeted mixed donor (251), tetrol (252) and octol (253).

The synthesis of these new donors is, anyway, only the first step and more effort is needed to generate good quality crystals of the oxidised materials to compare their crystal packings and electrical conductivities and so increase knowledge in the field of chiral conductive materials.

3.3.2 Preparation of racemic and enantiopure donors where hydrogen-bonding is coupled with enhanced π - π stacking interactions.

The aim of this part of the work was to synthesise a series of donors which included on their side chains two sources of non-covalent interaction: hydrogen bonding and additional π - π stacking. The hydrogen bonding functionality is represented by the introduction of a hydroxyl groups. The additional π - π stacking interaction will be introduced in two different ways: *a*) by introduction of a naphthalene group and *b*) by introduction of a phenyl ring. The ultimate goal is to compare the crystal packing and the electrical properties of the donors realised to gain more knowledge of the better substituent and side chain to improve the chiral packing in the donor salts. One of the most popular substituents to introduce chirality and maximise the π -overlap is the binaphthyl group which is reported in the literature in a few examples.³⁵⁾ The reason behind the effort is due to their restricted rotation about the aryl-aryl bond. The aim is to produce a helical rearrangement of donors in a radical cation salt. Here we use a combination of a single naphthyl group and a chiral centre to promote the electrical chiral anisotropy effect⁴⁾.

3.2.2.1 Preparation of enantiopure donors from (*S*)-(1'-naphthoxymethyl)oxirane.

The targeted donors for studying the two noncovalent interactions together are presented in Figure 106.

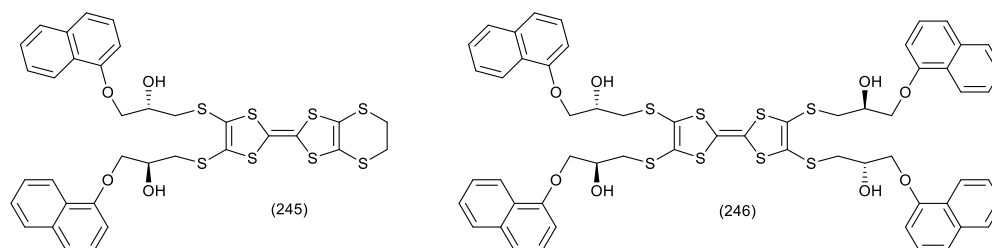
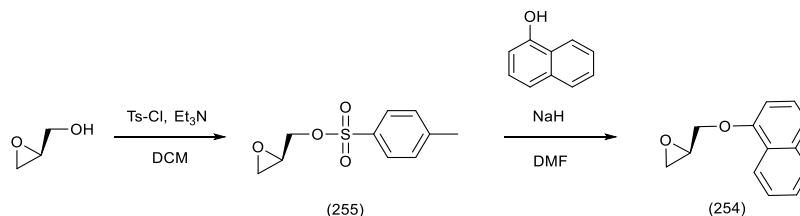


Figure 106 Targeted donors to combine hydrogen bonding and π - π interactions.

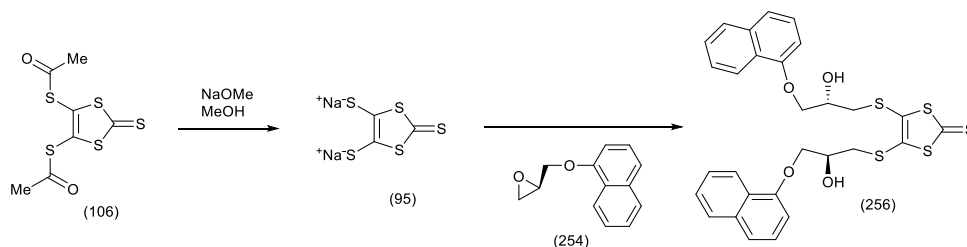
The simultaneous introduction of the naphthalene and the hydroxy groups on to the side chain of the TTF substituted electron donor is achieved using epoxide (**254**) whose synthesis was already reported in the literature³⁶. The substituted epoxide was prepared in two steps (Scheme 83). The commercially available starting material was (*S*)-glycidol which was reacted with tosyl chloride in pyridine to furnish (*S*)-(1'-tosyl-oxymethyl)oxirane (**255**) in 86% yield as a colourless oil. The next step was the reaction between the tosyl protected epoxide and sodium 1-naphthoate generated *in situ* by reacting 1-naphthol with sodium hydride in dry DMF. Isolation of the product furnished (*S*)-(1'-naphthoxymethyl-oxirane (**254**) in 76% yield as a light brown oil.



Scheme 79. Preparation of substituted epoxide (**254**).

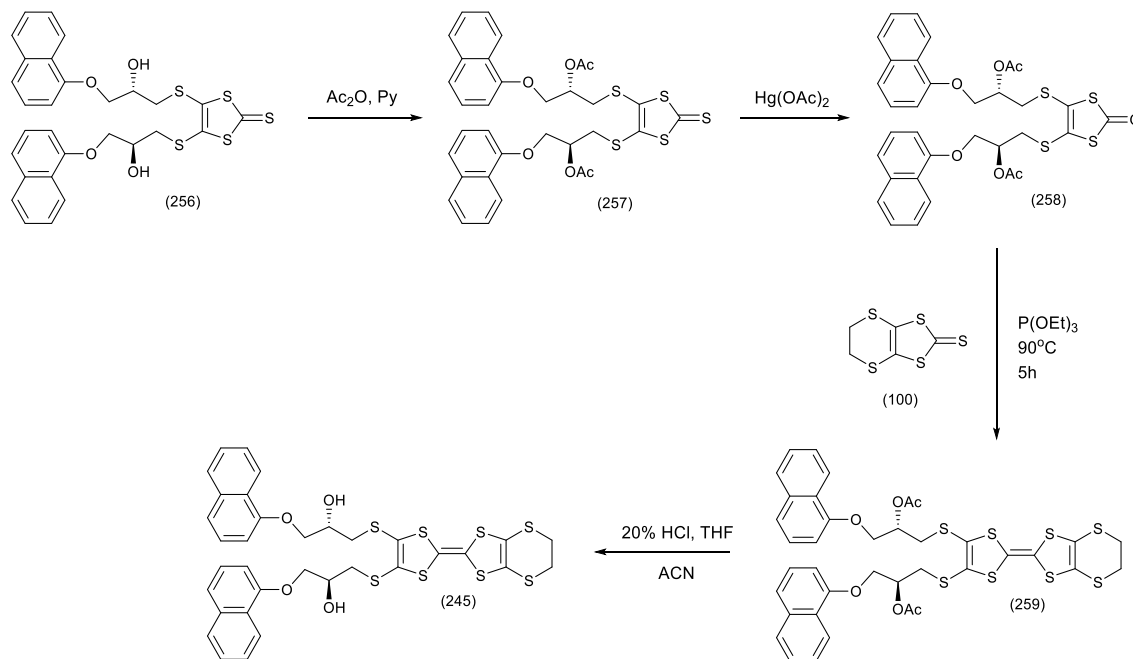
The next step is the nucleophilic attack on the substituted enantiopure epoxide from dithiolate (**95**), which is most likely to attack on the less hindered carbon of the epoxide ring. The acetyl protected thione (**106**) was treated at 0°C with the NaOMe/MeOH to generate dithiolate (**95**) to which then enantiopure oxirane (**254**) was added dropwise. The reaction mixture was allowed to warm up to r.t. and stirred over a period of 7.5 hours. The product was isolated and purified by flash chromatography to furnish desired thione (**256**) in 78% yield as a deep red oil. The characterisation by ¹H-NMR showed the presence of the peaks belonging to the naphthyl group together with peaks at 4.24 ppm for the $-CH(OH)$ protons, while the $-OH$'s protons resonate as a doublet at 2.91 ppm. The peak at 4.14 ppm was assigned to the protons of the $-CH_2$ group next to the ether oxygen

and the two doublets at 3.27 and 3.19 ppm for the $-\text{CH}_2$ protons next to the sulphur atom. The ^{13}C -NMR also shows the thiocarbonyl resonance at 210.5 ppm, together with the carbon next to the ether oxygen at 70.1 ppm, the carbon at 69.2 ppm which is from the $-\text{CH}(\text{OH})$ and the carbon next to the sulphur at 40.6 ppm. The compound was also characterised by IR where the $-\text{OH}$ group was clearly visible at 3380 cm^{-1} as a broad peak.



Scheme 80. Preparation of bis-substituted chiral thione (256).

After the successful preparation of *bis*-substituted thione (256) the rest of the synthetic route was performed following the standard procedure to achieve final cross-coupled donor (245) (Scheme 81).



Scheme 81. Preparation of desired donor (245).

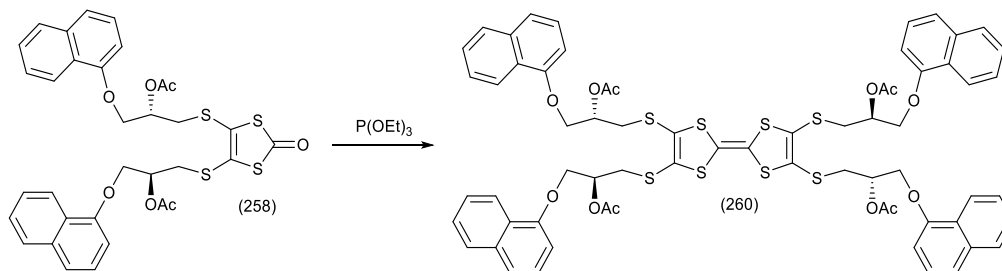
The preparation of the protected *bis* acetyl protected thione (257), in 93% yield, was successful as shown by NMR characterisation of the acetyl peaks at 2.03 ppm (^1H) and with peaks at 170.1 and 20.9 ppm (^{13}C). The exchange of sulphur for oxygen was carried out by using mercury (II) acetate and the ^{13}C -NMR showed the peak at 188.2 ppm for the carbonyl of the ring. The oxo-compound (258), obtained in 93% yield, and unsubstituted

thione (**100**) were reacted together in freshly distilled triethyl phosphite at 90°C for 5 h. The phosphite was distilled off by using a Kugelrohr oven and purification of the residue by flash chromatography afforded cross-coupled donor (**259**) in 44% yield as a red-orange oil. The characterisation by ^1H and ^{13}C -NMR showed a consistent pattern for the aromatic rings and the acetyl groups. The last step to obtain final diol (**245**) was the hydrolysis of the acetate groups which was performed in a variety of conditions to optimise the yield. The reaction was carried out in both acidic and basic conditions. In the former procedure to a solution of protected donor in THF was added HCl 20% and the solution had to be refluxed due to the lack of reactivity at r.t. and 50°C. Under these conditions the starting material was consumed but the ^1H -NMR suggested the presence of a mixture of compounds. The purification of the residue by column chromatography was found unsuccessful due to the fact that the by-product, formed by refluxing THF in the presence of acid, was 4-chlorobutanol which had the same R_f of the desired compound. A solution was found by washing the dark brown oil obtained with acetonitrile and by filtration of the black solid formed. The residue obtained from the filtrate was evaporated and analysed by ^1H and ^{13}C -NMR and was found to be pure. The desired diol was obtained as a brown solid in 80% yield.

In parallel to the procedure reported above the hydrolysis in basic conditions was performed by adding a solution of potassium carbonate in water to a solution of the donor in THF. After seven equivalents of potassium carbonate in refluxing THF the starting material was still present, so it was concluded that under these conditions a complete conversion of the acetates was not possible. The same transformation was also attempted by using LiAlH_4 as a reducing agent to convert the ester into the desired alcohol without success.

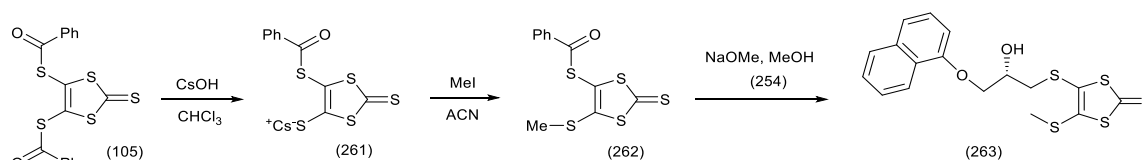
The chiral homo-coupled donor (**260**) has been obtained by treatment of the oxo-compound (**258**) with freshly distilled triethyl phosphite. The mixture was warmed up to 95°C and left stirring for 24 hours. The phosphite was distilled off by using a Kugelrohr oven and the residue was purified by column chromatography to furnish desired donor as an orange oil. In future a shorter reaction time will be explored since the yield is surprisingly low. The ^1H -NMR still showed some signs of phosphite, so the oil was vigorously stirred for 24 hours in hexane at r.t. The ^1H -NMR showed the consistent pattern for the aromatic rings and for the acetyl groups. The proton of the $-\text{CH}_2$ next to oxygen were found as a broad multiplet at 4.34-4.23 ppm and the other signal at 3.30 ppm was assigned to the $-\text{CH}_2$ next to the sulphur. In the ^{13}C -NMR spectrum the aromatic peaks were found to be

in accordance with the expected pattern and the peaks at 70.8 and 67.0 ppm were assigned to the $-\text{CH}_2\text{O}$ and the $-\text{CH}(\text{OAc})$ respectively. The peak at 36.4 ppm was assigned to the carbon next to the sulphur. It is worth mentioning that the peaks relative to the sp^2 carbons of the TTF unit were difficult to observe. The obtained compound was analysed only by NMR spectroscopy and no further characterisation was performed. The tetra-acetate donor was obtained in 14% yield.



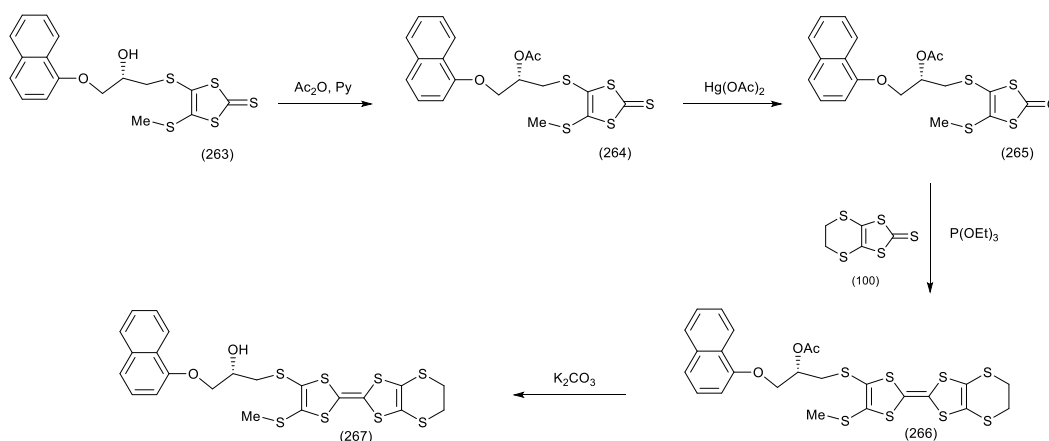
Scheme 82. Phosphite mediated coupling to generate protected homo-coupled compound (260).

Additional work has also been done to prepare the mono substituted donor as presented in Scheme 83 and 84.³⁷⁾ The first step was the preparation of the *mono*-benzoyl protected thione (261) by treating compound (105) with one equivalent of caesium hydroxide to deprotect the sulphur atom by forming a caesium salt which was then reacted with methyl iodide to furnish mono-benzoyl protected thione (262) in 85% yield. The latter compound was treated with NaOMe/MeOH and reacted with chiral oxirane (254) to furnish enantiopure thione (263) in 75% yield after purification by flash chromatography.



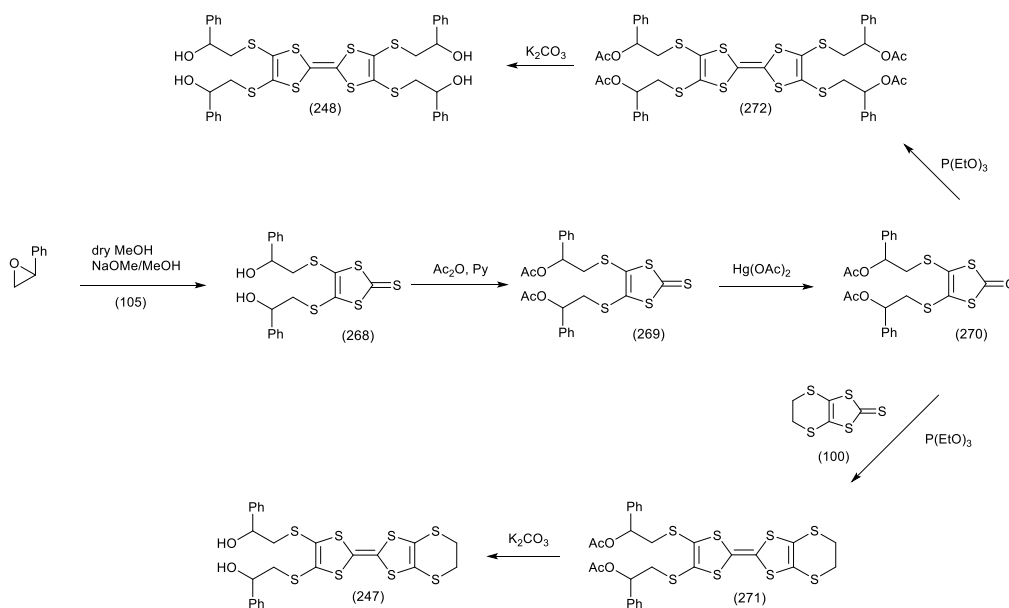
Scheme 83. Preparation of mono-substituted thione (263).

The rest of the synthetic route has been carried out by following standard procedures. Isolation of mono-acetyl protected thione (264) as a deep red oil was obtained in 75% yield. The oxo-compound (265) was prepared by reaction of (264) with mercury (II) acetate and the desired compound was recovered in 85% yield as a red oil. The phosphite mediated coupling of donor (265) with unsubstituted thione (100) was performed in freshly distilled triethyl phosphite for 16 h at 90°C and furnished chiral cross-coupled compound (266) in 45% yield after purification by column chromatography. The hydrolysis of the acetyl group to furnish the final enantiopure alcohol (267) in 90% yield was performed by treatment of donor (266) with potassium carbonate at r.t. for 18 hours (Scheme 84).

Scheme 84. Preparation of mono-substituted cross-coupled donor (**(267)**).

3.2.2.2 Attempt to prepare *tetrakis*(2-phenyl-1-hydroxyethylenethio) TTF donor from racemic 2-phenyloxirane.

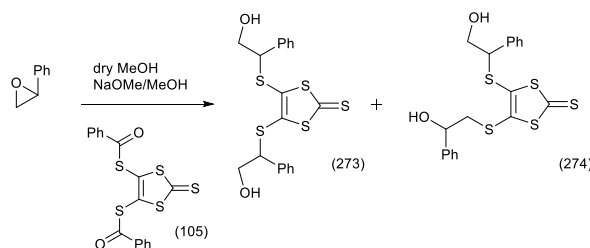
In the work described in this paragraph the π - π stacking interaction is due to the presence of the phenyl ring on each side chain. The strategy involved for preparing the targeted donors is shown (Scheme 85).



Scheme 85. Planned procedure for the preparation of targeted donors.

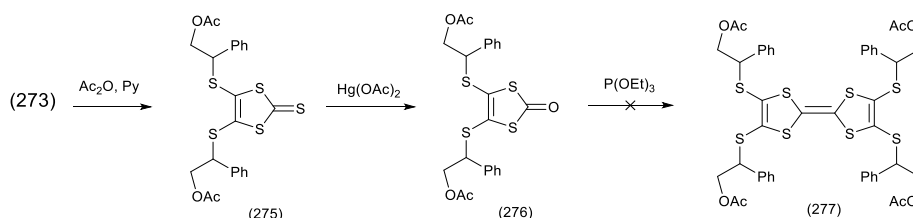
The main uncertainty was in the regioselectivity of the epoxide ring opening. The reaction was performed as usual by treatment of benzoyl protected thione (**(105)**) in dry methanol followed by addition of NaOMe/MeOH solution at 0°C to which was then added a solution of 2-phenyloxirane in dry MeOH. The resulting mixture was left to stir and warmed up to r.t. for several hours. After 6 hours monitoring of the reaction mixture by tlc confirmed the presence of a yellow spot. The reaction was quenched with acid and purification of

the product by flash chromatography afforded a mixture of thione (**273**) (major component) in 28% yield and (**274**) (minor component) in 25% yield, while no trace of the desired compound (**268**) was revealed. The dithiolate has first reacted exclusively at the phenyl substituted ring position, while the attack on a second oxirane is less selective.



Scheme 86. Mixture of thiones furnished by the reaction shown.

Even though the desired thione was not obtained the synthetic route was carried further using thione (**273**) but some reactivity problem may arise due to the presence of the phenyl ring next to the carbon. The following step was the conversion of the –OH groups to acetates. The thione (**273**) was reacted with acetic anhydride and pyridine overnight to give *bis*-acetyl protected compound (**275**) as a dark red oil in 85% yield. The product showed acetyl peaks with a singlet at 1.95 ppm on the $^1\text{H-NMR}$ and at 170.4 and 20.7 ppm in the $^{13}\text{C-NMR}$. The following step was the exchange of sulphur in thione (**275**) for oxygen by using mercury (II) acetate to furnish oxo-compound (**276**) in 90% yield. The oxo-compound was characterised only by proton NMR for this transformation but the change in colour of the isolated oil and the proton resonances are in accord with what was expected for the oxo-compound (**276**). The latter was then reacted with freshly distilled triethyl phosphite under a nitrogen atmosphere at 100°C overnight but no visible changes were seen on the tlc. The reaction was left on for an additional twelve hours but still without further changes on the tlc plate. The triethyl phosphite was distilled off and the residue isolated (yellow oil) was characterised by ^1H and $^{13}\text{C-NMR}$ but the identification of the desired compound (**277**) was not successful. It is possible that the triethyl phosphite has attached the side chain at the carbon bearing the sulphur and the phenyl groups.



Scheme 87. Standard procedure follow to achieve preparation of homo-coupled donor (**277**).

A new direction to prepare the desired donors in the future is to use the enantiopure 2-O-tosyl-phenylethanediol.

3.3.3 Preparation of donors from racemic and enantiopure 2-methoxymethyl-oxirane.

Chiral TTF substituted donors (**278**) and (**279**) have been prepared and reported in the literature³⁰ (Figure 104) to investigate even further how the hydrogen bonding functionalities can guide and influence the packing in the solid state. These non-covalent interactions can also be reflected in the conductive behaviour of the oxidised donors as previously explained.

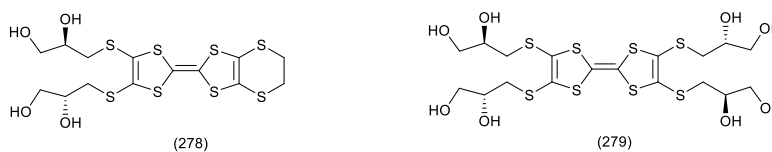


Figure 107. Examples of chiral donors bearing H bonding groups reported in the literature.

The preparation of new donors containing side chains able to modify the hydrogen bonding interactions was one of the targets of this work. The synthesis of new donors (**249**)-(**250**) has the purpose to compare the properties of all four donors where different numbers and types of hydrogen bonding functionalities are involved. By comparison with these two systems it would be possible to understand if by leaving unchanged the length of the chain the methoxy group can influence the packing and the properties of the corresponding radical salts.

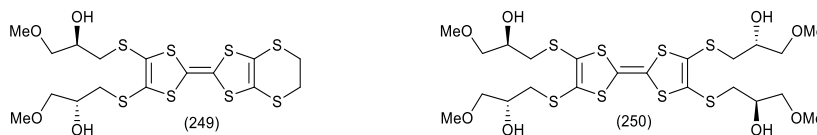
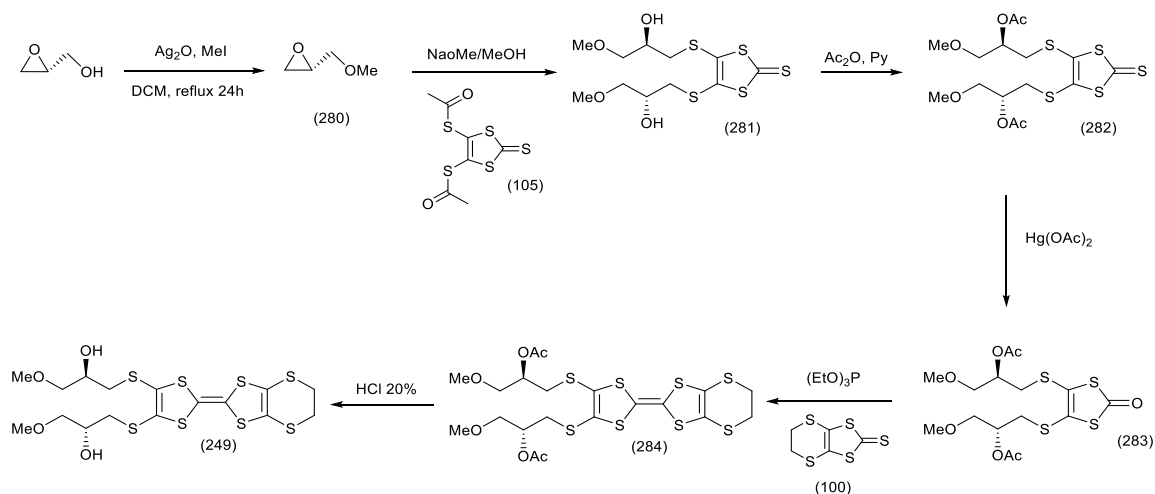


Figure 108. Targeted cross- and homo-coupled donors to be prepared.

The synthetic route for the preparation of enantiopure compound (**249**) is shown in Scheme 88. The procedure was tested first with the cheaper racemic starting material (\pm)-2-methoxymethyl-oxirane. For every transformation involving the racemic starting material the compounds have been analysed only by ^1H and ^{13}C -NMR. The synthetic route was tested up to the preparation of the acetate protected cross-coupled donor since the phosphite mediated coupling is, most of the time, the challenging step for the preparation of the donors. The synthesis of the protected donor was successful and the same procedure was transferred on to the enantiopure *R*-(+)-glycidol. All the intermediates prepared using the enantiopure starting material have been fully characterised.

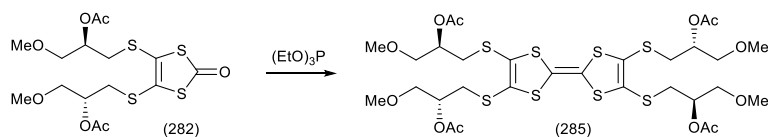
Scheme 88. Preparation of enantiopure cross-coupled compound (**249**).

The first step was the methylation of *R*-(+)-glycidol using silver oxide and methyl iodide in refluxing DCM for 24 hours following a procedure reported in the literature³⁸. Substituted epoxide (**280**) was obtained as a colourless oil in 67% yield. Characterisation by ¹H and ¹³C-NMR was in accordance with the data reported in the literature. The next step was the reaction between dithiolate (**95**), generated *in situ* by treating acetyl protected thione (**105**) with NaOMe/MeOH, and the (*S*)-2-methoxymethyloxirane (**280**). The reaction mixture was allowed to stir for 6 hours at room temperature after which a change in colour was observed. Monitoring by tlc showed the presence of a yellow spot and the reaction was quenched with acetic acid and left to stir for an additional hour before the product was isolated and purified by flash chromatography to afford enantiopure thione (**281**) as a red oil in 47% yield. Characterisation by ¹H-NMR showed the presence of a multiplet at 3.86 ppm for the $-CH(OH)$ and a second multiplet at 3.41 ppm for the protons $-CH_2O$. The two double doublets at 3.03 and 3.00 ppm for the $-CH_2$ next to the sulphur atom of the side chain and the presence of a singlet at 3.33 ppm, assigned to the $-CH_3$ of the methoxy group completed the identification of the proton spectrum. The ¹³C-NMR showed the thiocarbonyl group at 210.4 ppm and the peaks for $-CH_2-O-$ and $-CH(OH)$ at 74.7 and 69.0 ppm. The carbon resonance showed also a peak at 59.3 ppm for the methoxy group. The following step was the conversion of the alcohol to acetate by reaction between thione (**281**) and acetic anhydride in pyridine overnight. The protected thione (**282**) was isolated, in 95% yield, as a dark-red oil and characterised by NMR. The proton resonance showed a singlet at 2.02 ppm assigned to the acetate group. The ¹H-NMR also presented a signal for the $-CH(OAc)$ proton which moved downfield from 3.8 to 5.0 ppm. The ¹³C-NMR peaks at 170.1 and 20.9 ppm correspond to acetyl groups. The following step was the exchange of the sulphur for oxygen to afford oxo-compound (**282**).

The protected thione (**282**) was reacted with mercury (II) acetate in chloroform and the resulted suspension was left to stir for 3 h. Isolation of the product afforded an orange oil identified as oxo-compound (**283**) in 85% yield. In the ^{13}C -NMR the presence of the peak at 188.8 ppm is evidence of a successful transformation. The oxo-compound (**283**) was reacted with unsubstituted thione (**100**) in the presence of freshly distilled triethyl phosphite under nitrogen atmosphere at 90°C for 5 h. Filtration of the BEDT-TTF formed and distillation of the phosphite by Kugelrohr oven afforded a crude red oil which was purified by column chromatography to furnish cross-coupled compound (**284**) as an orange-red oil in 40% yield. The ^1H -NMR spectrum presented a multiplet at 5.01 ppm which was assigned to the $-\text{CH}(\text{OAc})$ proton. The two double doublets which overlap each other at 3.51 ppm evidence the presence of the $-\text{CH}_2$ next to oxygen which bears the methyl group that resonates as a singlet at 3.30 ppm. The successful coupling is confirmed by the presence of a singlet at 3.23 ppm for the ethylene bridge. The presence of two double doublets at 3.07 and 2.97 ppm which belong to the $-\text{CH}_2$ next to the sulphur completed the proton analysis. The ^{13}C -NMR spectrum showed the presence of peaks at 128.0, 113.7, 112.4 109.9 ppm for the sp^2 carbons together with the carbonyl peak at 170.2 ppm and the methyl at 20.9 ppm for the acetyl group. The ethylene bridge is evidenced by the presence of a peak at 30 ppm. The last step was the hydrolysis of the acetyl groups to generate the desired compound (**249**). The hydrolysis was performed in basic conditions by dissolving the donor in 50:50 mixture of MeOH and THF and treating with an excess of aqueous potassium carbonate. The reaction mixture was left to stir overnight at room temperature before the product was isolated and characterised by NMR spectroscopy. The proton resonance showed the presence of a broad singlet at 3.85 ppm which was assigned to the $-\text{OH}$ groups. Moving upfield on the spectrum are the two double doublets at 3.43 and 3.40 ppm which were assigned to the protons of the $-\text{CH}_2$ next to the oxygen. The singlets at 3.32 and 3.23 ppm were assigned respectively to the methoxy and ethylene bridge groups. The two double doublets at 2.96 and 2.84 ppm belong to the protons of the $-\text{CH}_2$ next to the sulphur. The ^{13}C -NMR presented peaks at 128.4, 113.9, 110.2 ppm for the sp^2 carbons. The peak at 74.9 ppm was assigned to the carbon connected to the $-\text{OH}$, while the carbon next to the methoxy and the methyl of the methoxy group were assigned at 69.1 and 59.3 ppm respectively. The carbons of the ethylene bridge resonate at 30.2 ppm. To the best of our knowledge the identification of the NMR spectra suggested the compound analysed is the desired one. Despite this, the CHN analysis result does not match perfectly with the theoretical values. The experimental composition found C at 37.20% and H at

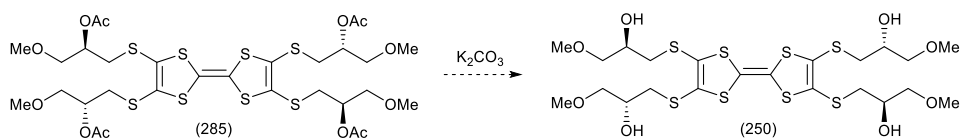
5.81%. The best match is found for $C_{16}H_{22}O_4S_8 \cdot 1.5(C_4H_8O_2) \cdot 2(H_2O)$ with C at 37.60% and H at 5.50%. The presence of ethyl acetate could be explained because it was the solvent used during the work-up procedure and the water was also used to dissolve the potassium carbonate used as a base for the hydrolysis.

After the identification of the final cross-coupled donor (**249**) the attention moved on to the preparation of the homo-coupled protected compound (**285**). The reaction involved the self-coupling of the oxo-compound in presence of freshly distilled triethyl phosphite. The reaction was carried out at 95°C for 24 hours under a nitrogen atmosphere (scheme 91). The crude compound was purified by flash chromatography after the phosphite was distilled off by using a Kugelrohr oven. The oil obtained was analysed only by 1H -NMR which evidenced the presence of a multiplet at 5.02 ppm for the proton $-CH(OAc)$. The presence of another multiplet at 3.51 ppm was assigned to the protons of the $-CH_2$ next to the oxygen, while the singlet at 3.30 ppm belongs to the $-CH_3$ of the methoxy group. At 3.05 and 2.98 ppm were the two double doublets for the protons of the $-CH_2-S$ resonance. The singlet at 2.03 ppm for the methyl group of the acetate complete the proton spectrum.



Scheme 89. Preparation of chiral homo-coupled protected donor (**285**).

The final step is the hydrolysis of the acetate groups which would have been performed in basic conditions following the same procedure explained for the cross-coupled compound. Unfortunately due to the lack of time this reaction was not performed and the final desired compound (**250**) was not obtained.

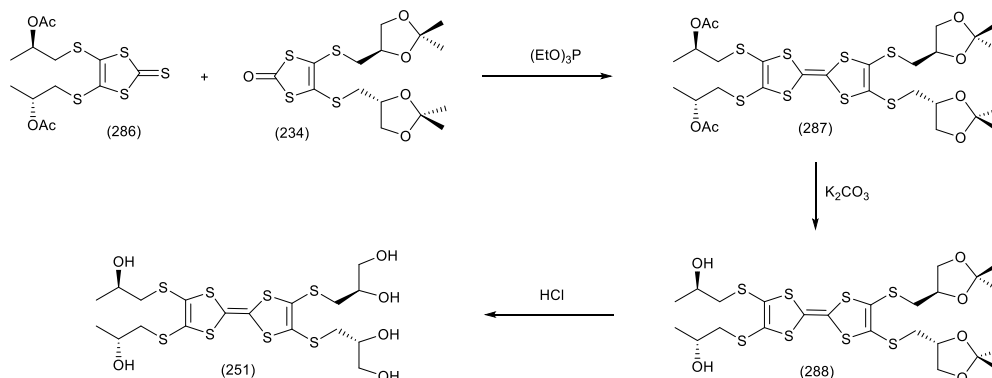


Scheme 90. Planned strategy to hydrolyse the acetyl group to furnish desired homo-coupled donor.

3.3.4 Preparation of an asymmetric chiral hexol donor (**251**).

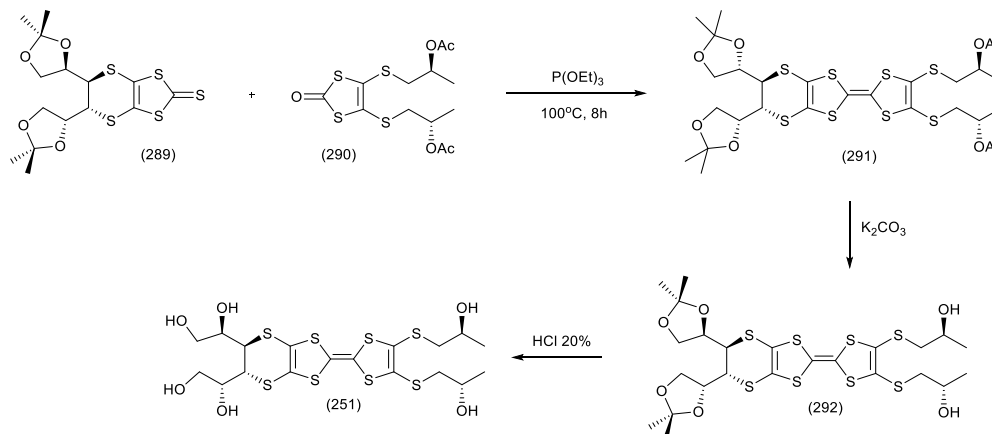
A versatile way to introduce multi-hydrogen bonding functionalities is to perform the coupling between different substituted thione and oxo compounds to introduce a different number of functionalities on each side. Previous mixed donors have been prepared in the Wallis laboratory and reported in the literature^{29,30}. The Scheme 91 below summarises

the preparation of a similar TTF based donor by showing only the later stages of the synthetic route.



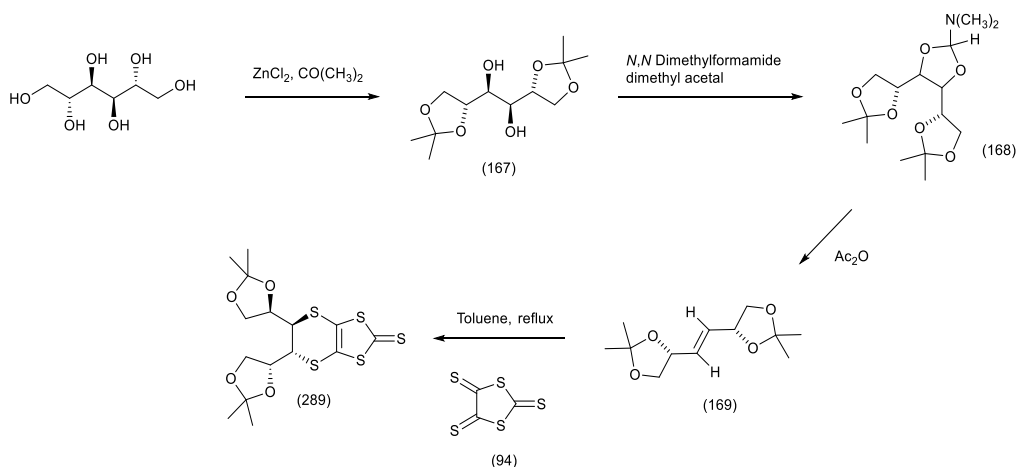
Scheme 91. Previous example of an asymmetric donor preparation.

A new mixed donor **(251)**, which is based on ethylenedithiotetrathiafulvalene, EDT-TTF has now been achieved by coupling together thione **(289)**^{30a)} and the oxo-compound **(290)**¹²⁾, prepared from (*S*)-propylene-oxide, in freshly distilled triethyl phosphite. Donor **(291)** was then converted into the final hexol **(251)** in two steps by selective hydrolysis of acetates first, to furnish **(292)** and then of the dimethyl-dioxolane groups to yield the final hexa-hydroxy donor **(251)** (Scheme 92).

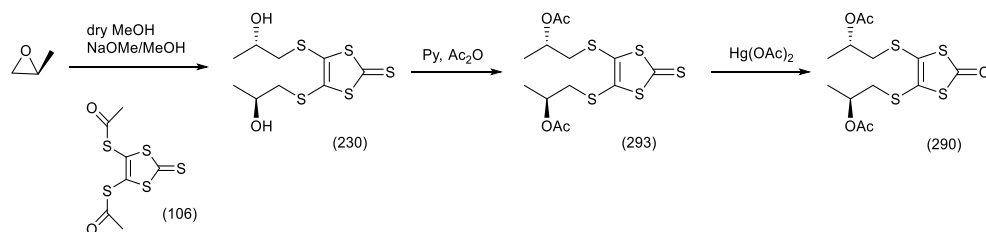


Scheme 92. Preparation of mixed donor **(251)**.

The preparation of the thione **(289)**¹²⁾ involved the transformation presented in the Scheme 93. In the first step *D*-mannitol was treated with zinc chloride and acetone (analytical grade) to afford protected diol **(167)** in 60% yield. The compound obtained was treated with DMF-dimethylacetal to convert the diol into a 2-dimethylamine-1,3-dioxolane **(168)**; which then underwent to an elimination reaction in refluxing acetic anhydride to furnish the *trans*-alkene **(169)** in 64% yield. The following and final step to generate the desired thione was achieved by reacting the alkene with trithione **(94)** in refluxing toluene overnight. The thione **(289)** was obtained in 20% yield after separation from a minor diastereoisomer.

Scheme 93. Preparation of thione (**289**) according to the literature procedure.

In Scheme 94 are outlined the steps performed to reach target oxo-compound (**290**)^{30a}. Acetyl protected thione (**106**) was used in place of the benzoyl protected thione (**105**) as starting material for a purely practical reason. The by-product of thione (**105**) is methyl benzoate which is a high boiling point liquid. Flash chromatography is usually not fully successful to separate this by-product from the desired thione formed. The solution is to distill off the methyl benzoate by using a Kugelkhor oven. The by-product of acetyl protected thione (**106**) is methyl acetate which is easily removed at the rotary evaporator. On the other hand the acetyl protected thione (**106**) is less soluble, and should not be stored for too long.

Scheme 94. Preparation of oxo-compound (**290**).

In the first step acetyl protected thione (**106**) was treated with sodium methoxide in methanol and then reacted with (*S*)-methyl oxirane to furnish diol (**230**) as a dark-red oil in 65% yield. The next step is the conversion of the hydroxy groups into acetates by reacting diol (**230**) with acetic anhydride in pyridine. This reaction furnished *bis*-acetyl protected thione (**293**) in 70% yield. The reaction was performed using an excess of acetic anhydride (5 eq) to avoid any mono-protected compound. Final exchange of oxygen for sulphur by treatment with mercury (II) acetate furnished oxo-compound (**290**) in 92% yield. After the desired thione (**289**) and oxo-compound (**290**) had been prepared the phosphite mediated coupling was performed by using freshly distilled triethyl phosphite. The reaction mixture was warmed up to 100°C for 8 h. Purification of the mixture by column

chromatography allowed the separation of fully protected donor (**291**) in 48% yield from the two homo-coupled by-products (Figure 109). Characterisation of compound (**291**) by $^1\text{H-NMR}$ confirmed its identity due to the presence of peaks at 1.98, 1.36, 1.28 and 1.27 ppm which were assigned to the acetate methyl group, the two dioxolane methyl groups and the terminal methyl groups of the side chains. The presence of a multiplet at 4.95 ppm for the $-\text{CH}$ next to the acetate and of two double doublets at 4.12 and 3.97 ppm for the $-\text{CH}_2-\text{O}$ were detected. The identification is completed by the presence of two doublets for the protons next to the sulphurs at 3.64 ppm for $-\text{CH-S}$ and 2.91 ppm for the $-\text{CH}_2-\text{S}$. Indeed the mass spectrometry analysis evidenced a peak at m/z 758.0315 for the composition $\text{C}_{28}\text{H}_{38}\text{O}_8\text{S}_8$ where a theoretical mass of m/z 758.0327 is required.

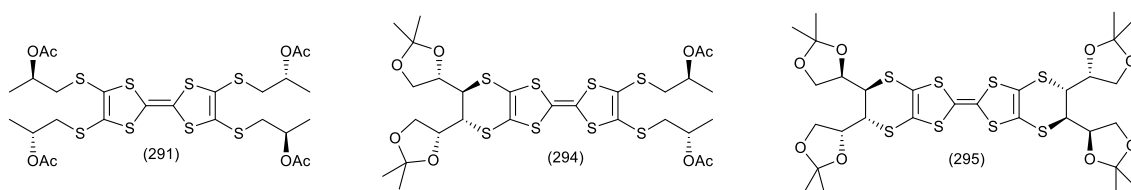
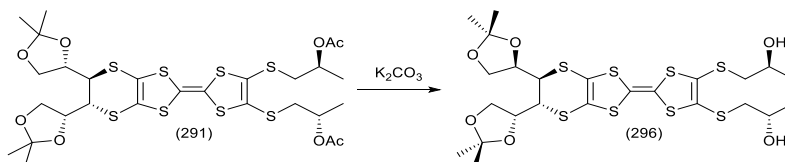


Figure 109. Desired cross-coupled donor (**291**) and the two homo-coupled donors formed in the coupling reaction.

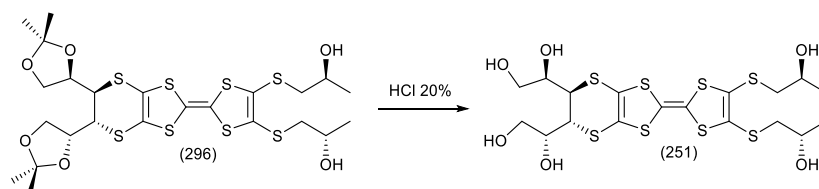
Donor (**291**) was then selectively deprotected in two different steps. The first involved hydrolysis of acetate groups in alkaline conditions, by using an excess of potassium carbonate, to furnish protected diol (**296**) in 83% yield. Characterisation by $^1\text{H-NMR}$ confirmed its identity by showing the expected pattern for the protected side of the donor and the presence of the multiplet at 3.80 ppm which has been assigned to the $-\text{CH}(\text{OH})$ group due to the shift from 4.95 ppm observed when next to the acetate. It is interesting to notice that the protons for the $-\text{CH}_2-\text{S}$ groups are now split into two double doublets at 2.97 and 2.62 ppm while in the fully protected donor (**291**) they resonated as a unique signal. No additional characterisation such as infrared, elemental or mass spectrometry analysis was performed for this compound.



Scheme 95. Selective hydrolysis of acetyl groups

The final donor was then achieved by hydrolysis of the two dioxolane groups by reacting the diol (**296**) with 20% HCl in THF. The final hexol (**251**) was obtained in 76% yield as a dark brown oil. Characterisation by $^1\text{H-NMR}$ evidenced the presence of a large multiplet at 3.66-3.86 ppm which in accordance with HMQC spectrum is related to the two –

CH-S, the *-CH(OH)*, the *-CH₂OH* and the *CH(OH)CH₃*. The double doublets at 2.83 and 2.75 ppm were assigned to the *-CH₂* next to the sulphur and the doublet at 1.65 ppm is the terminal *-CH₃* group for the side chains. In the carbon resonance are visible the peaks belonging to the six *sp²* carbons at 129.3, 113.8, 111.7 and 109.3 ppm. Along with these are the carbon atoms next to the three oxygen at 73.6 (*-CH-dioxolane*), 67.8 (*-CH(OH)*), and 65.0 ppm (*-CH₂-dioxolane*). The two carbons next to sulphurs resonate at 44.8 and 43.3 ppm, while the terminal *-CH₃* peak was found at 21.8 ppm.

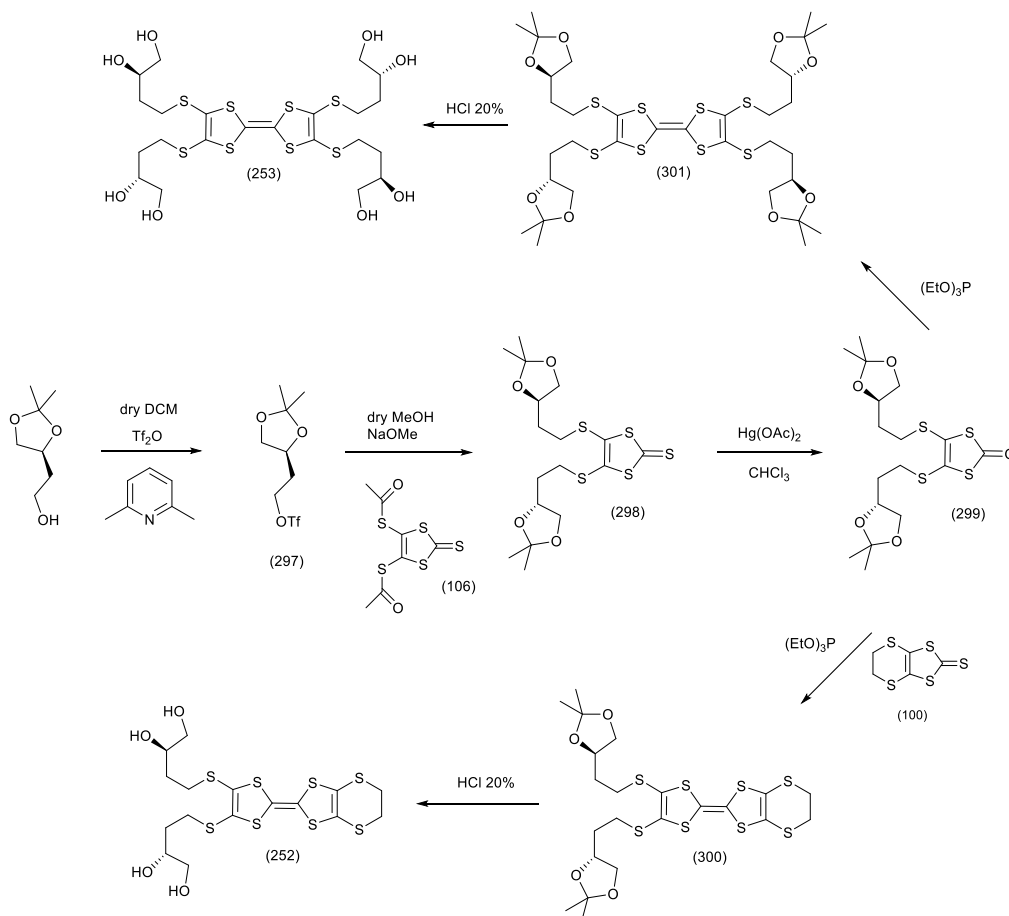


Scheme 96. Final hydrolysis in acidic conditions to furnish donor **(251)**.

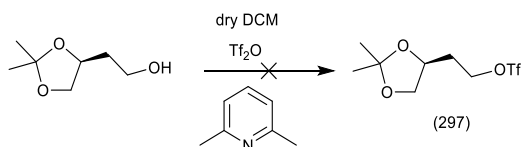
Despite the good characterisation by ¹H and ¹³C-NMR, it is worth mentioning that the identification of the final hexol **(251)** is not fully satisfactory. Elemental analysis was found to be a bit outside the usual range, with a “found” hydrogen percentage (3.65%) lower than the theoretical one (4.37%). The carbon percentage, although, was in accordance with the calculated one. The IR spectrum was recorded and the presence of a really broad and intense band at 3366 cm⁻¹ is evidence that the molecule contains the *-OH* functionality. Further investigation are currently in process to fully characterise and identify the obtained compound.

3.3.5 Attempted preparation of the new enantiopure tetrol donor **(252)**.

To continue the investigation of chiral enantiopure substituted TTF donors bearing hydrogen bonding functionalities a new target molecule was identified. The preparation of tetrol **(252)** was planned to guide the packing in the solid state by introducing hydrogen bonding functionalities, as in the case of the previously synthesised donor with one less methylene group per side chain whose preparation is reported in the literature.³⁰⁾ This will permit the investigation whether the length of the side chain may lead to different behaviour in the solid state and in the conducting properties. The designed synthetic route for novel enantiopure donor **(252)** and **(253)** is outlined in scheme 97.

Scheme 97. Strategy designed to reach preparation of tetra-ol (**252**) and octaol (**253**).

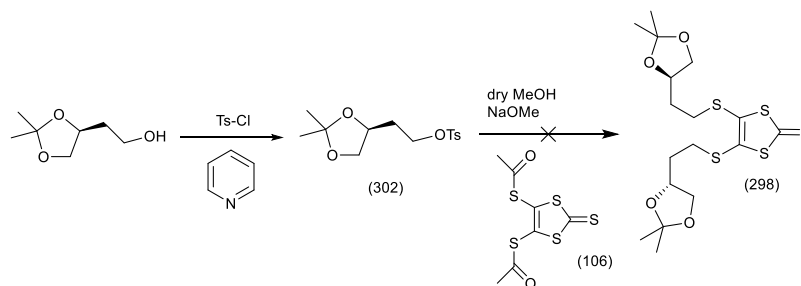
A suitable starting material was identified in the (4*S*)-(+)-4-(2-hydroxyethyl)-2,2-dimethyl-1,3-dioxolane. The first step is the conversion of the alcohol functionality to a better leaving group such as triflate to furnish compound (**297**), by reacting the starting material with triflic anhydride in the presence of lutidine in dry DCM under a nitrogen atmosphere. The synthesis of donor (**252**) turned out to be more difficult than expected due to the failure of the preparation of the triflate (**297**). The reaction was carefully carried out at low temperature and under inert conditions but a pink dense oil was isolated whose NMR was not consistent with (**297**).



Scheme 98. Attempted conversion of the alcohol to the triflate.

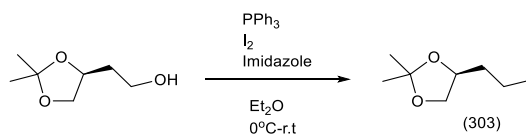
The alternative strategy was to convert the alcohol into a tosylate which is a better leaving group even if less reactive than the desired triflate. The reaction was carried out following a standard preparation using pyridine and acetic anhydride to furnish tosylate (**302**) in 60% yield³⁹. The tosylate (**302**) was then reacted with 0.5 equivalent of dithiolate (**95**)

generated from the *bis*-acetyl precursor (**106**) by treatment of the latter with NaOMe/MeOH at 0°C. However, after refluxing for twelve hours there was no visible change on the tlc. The reaction was then quenched with methyl iodide. The tosylate (**302**) is just not reactive enough to yield the desired product.



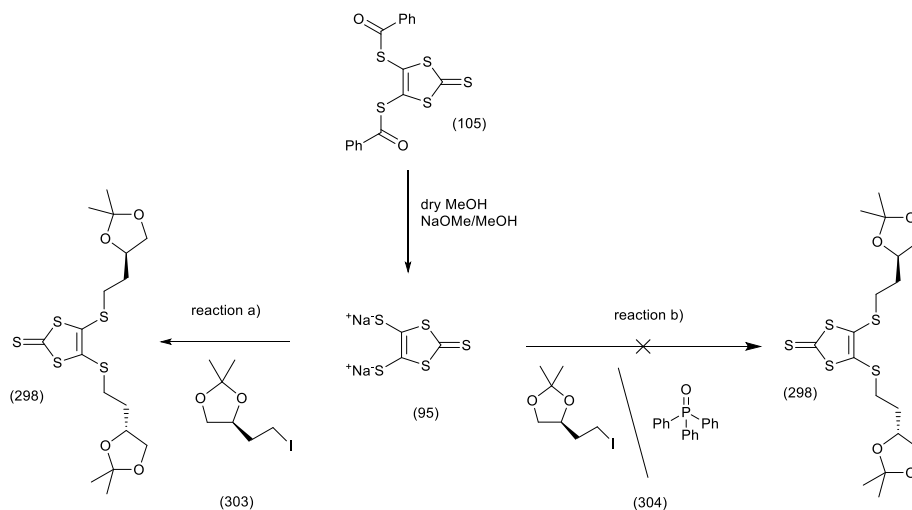
Scheme 99. Attempting preparation of the chiral bis-substituted thione (**297**).

A second alternative was the iodide (**303**). Its preparation seemed to be straightforward and in good yield according to the literature ⁴⁰). The methodology reported is illustrated in the Scheme 100 and it has been followed carefully in order to obtain the desired compound.



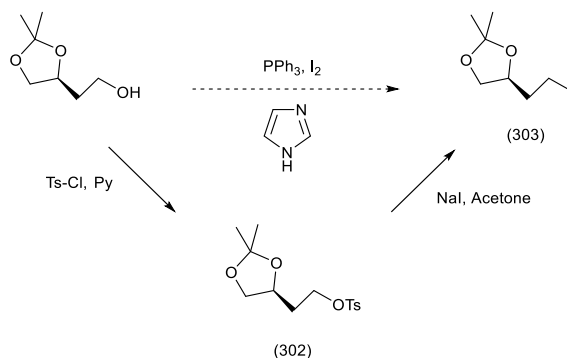
Scheme 100. Preparation of the iodo-derivate by using the Appel reaction.

This reaction was repeated a few times and unfortunately in every occasion the desired iodo-compound was found contaminated with triphenylphosphine oxide and purification of (**303**) was found really problematic. Only on one occasion a small portion (20%) of the desired compound (**303**) was obtained pure. It was decided to perform a parallel reaction using both pure iodo-compound (**303**) and the mixture (**304**) of iodo compound with triphenylphosphine oxide.



Scheme 101. Parallel reactions to generate bis substituted thione (**298**) from (**303**) and mixture (**304**).

Both reactions were carried out in the same way. The benzoyl-protected thione (**105**) in dry MeOH, under a nitrogen atmosphere at 0°C, was treated with NaOMe/MeOH (25% in weight) solution to furnish dithiolate (**95**) which was then reacted with compounds (**303**) and (**304**) in two different reaction vessels. The resulting mixtures were left to stir and warmed up to r.t. for several hours. In the case of reaction *a*) the mixture was allowed to stir and warmed up to r.t. for three hours until the solution turned to orange. Monitoring of the reaction vessel by tlc revealed the formation of a new yellow spot. The reaction was quenched and purification by column chromatography afforded a dark-red oil which was characterised by NMR and identified as desired thione (**298**) in 50% yield. The proton NMR for (**298**) showed a multiplet at 4.13 ppm for the –CHO proton together with two other multiplets at 4.00 and 3.50 ppm for the proton of the –CH₂O group in the dioxolane ring. The methyl groups resonate as two singlets at 1.34 and 1.28 ppm. The other peaks found were a multiplet at 2.83 ppm which belongs to the protons of the –CH₂S and another multiplet assigned to the adjacent –CH₂. The ¹³C-NMR shows peak at 210 ppm for the thiocarbonyl and peaks at 136.2, 129.8, 127.9 ppm for the sp² C. The quaternary carbon of the dioxolane resonate at 109.3 ppm, while the carbons next to the oxygen are at 74.0 and 68.9 ppm. The carbons of the alkyl chain were found at 33.9 and 33.1 ppm. In the case of reaction *b*), under the same conditions, no changes were seen even after 24 hours. Despite the success of the reaction with pure material it was decided not to continue the synthetic pathway due to the difficulty of obtaining iodide (**303**). A modified preparation of (**303**) in toluene⁴¹⁾ was attempted but resulted in the same purification problem. An alternative route to the preparation of compound (**303**) could be by following a two steps synthesis (Scheme 102) preparing the iodide (**303**) via the tosylate (**302**) even if the first step afforded the tosylate only in 60% yield.

Scheme 102. Transformation from alcohol to iodo-derivate by formation of tosylate (**302**).

The tosylate (**302**) was reacted with potassium iodide in Acetone AR and iodide (**303**) was recovered in 35% yield. The result achieved is better than the direct transformation from the alcohol and the yield could be improved by following a procedure reported in the literature ⁴². This may open the route to donor (**252**) and (**253**) in future work.

3.3.6 Cyclic voltammetry of the new donors prepared.

The cyclic voltammetry of some of the new donors prepared was measured using a three electrode set-up method (reference, working and counter electrodes). All the measurements are relative to Ag/AgCl at platinum electrode. A recorded amount of the desired donor was added to a 0.1 M solution of n-BuN₄PF₆ in dry dichloromethane which was used as charge carrier. All donors showed the typical two oxidation waves.

Table 3 Cyclic voltammetry potentials for the new substituted ET donors.

Donor	E ₁ (V)	E ₂ (V)
(103)	0.52	0.94
(245)	0.53	0.93
(249)	0.55	0.89
(251)	0.57	0.86
(267)	0.52	0.93

Electro-crystallisation and diffusion experiments are currently in progress to generate single crystals of oxidised materials and to measure their conductivities and investigate their crystal structures. Thus for the enantiopure donors, all with hydrogen bonding functionality have been prepared, and will now be used for preparing novel chiral conducting salts with chiral conducting pathway for electrons

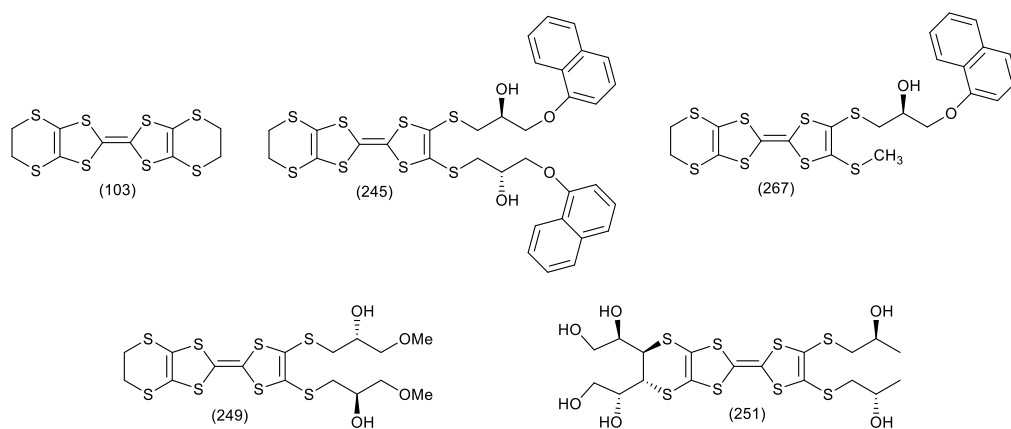


Figure 110. Donors characterised by C.V.

3.4 Conclusions and future work.

New enantiopure donors have been prepared such as donors **(245)**, **(249)** and **(251)** together with the protected homo-coupled donors **(79)** and **(104)**.

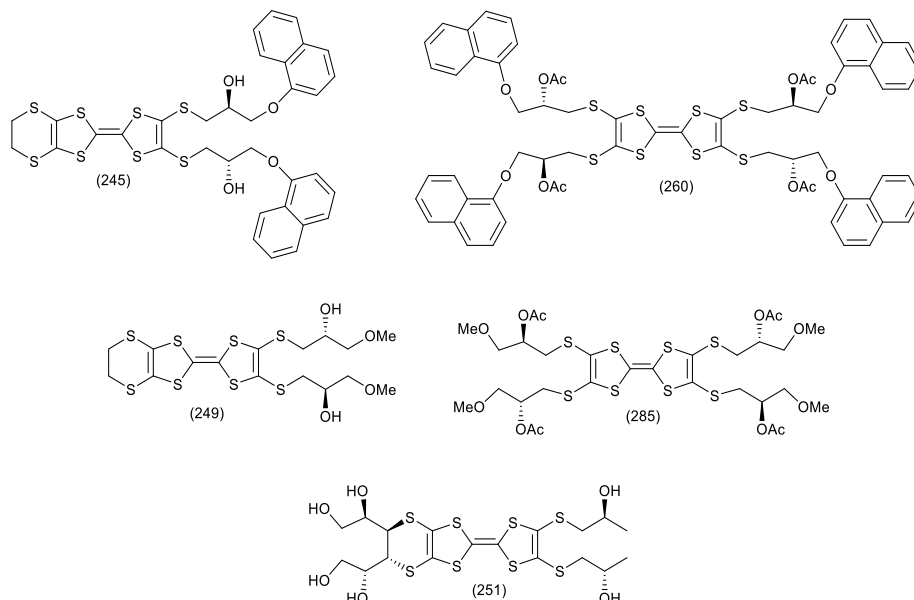
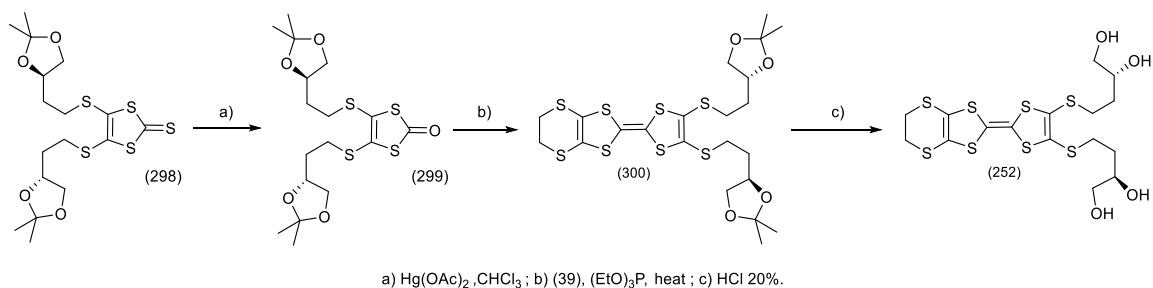


Figure 111. Novel enantiopure donors prepared.

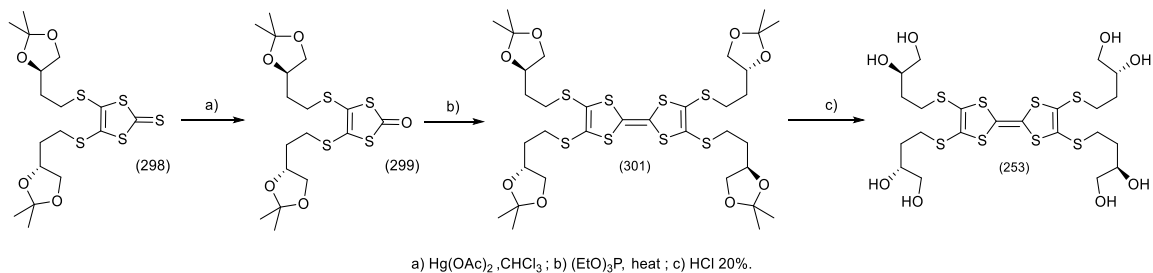
Donors **(245)** is currently under investigation to generate radical cation salts in order to obtain single crystals of oxidised material in the presence of different anions to measure the crystal structures and record the electrical conductivities. Donors **(249)** and **(251)** will be investigated further from future researcher due to some problem in a few of their characterisation such as elemental analysis and mass spectra. New batches of these donors will be prepared but the synthetic route has been established during this work.

For the tetra-acetate donors **(260)** and **(285)** the hydrolysis to generate the desired tetrol compounds is the only step remained unexplored. This reaction and the investigation of the electrical behaviour of the donors will be carried out by future researchers.

The future work will also be focused on the preparation of donor **(252)** (Scheme 103) and **(253)** (Scheme 104) whose synthesis had been stopped at the thione **(298)**. The future steps will follow the standard procedure applied for all the donors prepared in this work.



Scheme 103. Future steps to be performed for the preparation of tetrol (252).

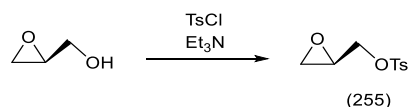


Scheme 104. Future steps to be performed to prepare the desired compound (253).

After the preparation and full characterisation of desired donors (252) and (253) their crystal structures and electrical properties will be investigated.

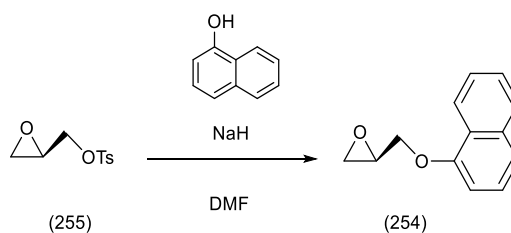
3.5 Experimental part.

3.5.1 Synthesis of (*R*)-tosyloxymethyl-oxirane (**255**)³⁶.



To a stirred solution of *S*-(-)-glycidol (2.83 g, 38.0 mmol) in DCM (50 ml) at -5°C triethylamine (5.9 ml, 42.0 mmol) and tosyl chloride (8.04 g, 42.0 mmol) were added and the colourless suspension was allowed to reach r.t. overnight under a nitrogen atmosphere. The reaction was monitored by tlc/PMA dip and after starting material was consumed the suspension was transferred into a separating funnel. The organic layer was washed with 10% tartaric acid (5 x 30 ml), water (30 ml) and brine (30 ml) and dried over MgSO₄. The solvent was evaporated and the mixture purified by flash chromatography (1:1=DCM : cyclohexane, 5% Et₃N) to yield compound (**255**) (7.45 g, 86%) as a colourless oil. δ_H (400 MHz, CDCl₃): 7.76 (2H, d, J= 8.2 Hz, Ar-*H*₂), 7.32 (2H, d, J= 8.0 Hz, Ar-*H*₂), 4.24 (1H, dd, J= 10.8, 3.3 Hz, -CH_αH-OTs), 3.88 (1H, dd, J= 10.8, 6.2 Hz, -CHH_β-OTs), 3.14 (1H, m, 2-*H*), 2.77 (1H, t, J= 4.6 Hz, 3-*H*_α), 2.55 (1H, t, J= 4.7 Hz, 3-*H*_β), 2.41 (3H, s, -CH₃); δ_C (100MHz, CDCl₃): 145.0, 132.4, 129.8, 127.8 (Ar-*C*₆), 70.4 (-CH₂-OTs), 48.7 (2-*C*), 44.4 (3-*C*), 21.5 (-CH₃).

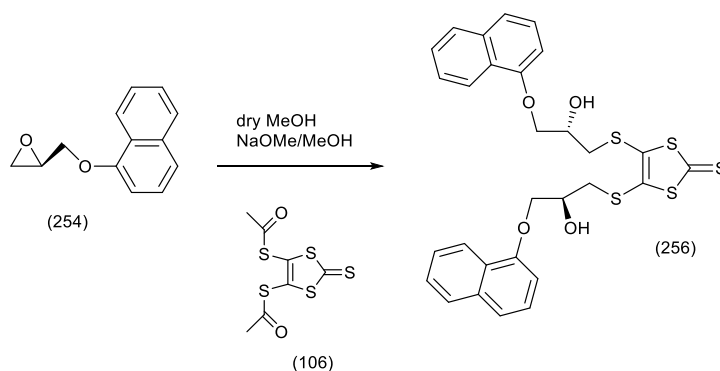
3.5.2 Synthesis of (*R*)-2-((naphth-1'-yloxy)methyl)oxirane (**254**)³⁶.



To a solution of 1-naphthol (3.22 g 22.4 mmol) in dry DMF (60 ml) under a nitrogen atmosphere was added oil-free sodium hydride (0.77 g, 31.9 mmol) and the suspension was left stirring until all solid dissolved. A solution of oxirane (**255**) (4.85 g, 21.3 mmol) in dry DMF (30 ml) was added dropwise. The resulting solution was stirred for 20 h and then quenched with saturated ammonium chloride solution. The suspension was washed with Et₂O (5 x 50 ml) and the organic layers were collected, washed with saturated NaHCO₃ solution (3 x 100 ml), 5% LiCl solution (5 x 50 ml), water (1 x 50 ml) and brine (50 ml) and dried over MgSO₄. Evaporation of the solvent yielded oxirane (**254**) as a brown oil (3.24g, 76%). The NMR characterisation showed that no further purification

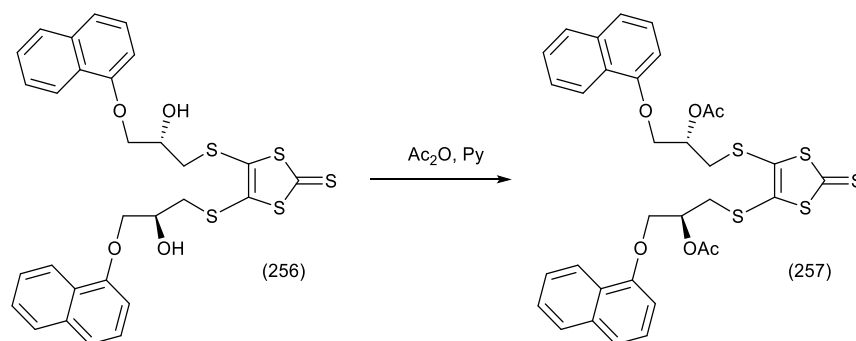
was necessary. δ_H (400 MHz, CDCl_3): 8.41 (1H, m, Ar- H_1), 7.85 (1H, m, Ar- H_1), 7.53 (3H, m, Ar- H_3), 7.40 (1H, t, $J = 8.0$ Hz, Ar- H_1), 6.76 (1H, d, $J = 7.7$ Hz, Ar- H_1), 4.32 (1H, dd, $J = 11.0, 2.7$ Hz, $-\text{CH}_\alpha\text{H}-\text{O}$ -naphthyl), 4.00 (1H, dd, $J = 11.0, 5.8$ Hz, $-\text{CHH}_\beta\text{O}$ -naphthyl), 3.43 (1H, m, 2- H), 2.90 (1H, t, $J = 4.8$ Hz, 3- H_α), 2.79 (1H, dd, $J = 4.8, 1.9$ Hz, 3- H_β), δ_C (100 MHz, CDCl_3): 153.8, 134.1, 127.1, 126.2, 125.5, 125.2, 125.0, 121.7, 120.4, 104.6 (Ar- C_{10}), 68.4 ($-\text{CH}_2\text{O}$ -naphthyl), 49.8 (2- C), 44.1 (3- C).

3.5.3 Synthesis of 4,5-bis(2'S-2'-hydroxy-3'-(naphth-1''-yloxy)propylthio)-[1,3]dithiol-2-thione (**256**).



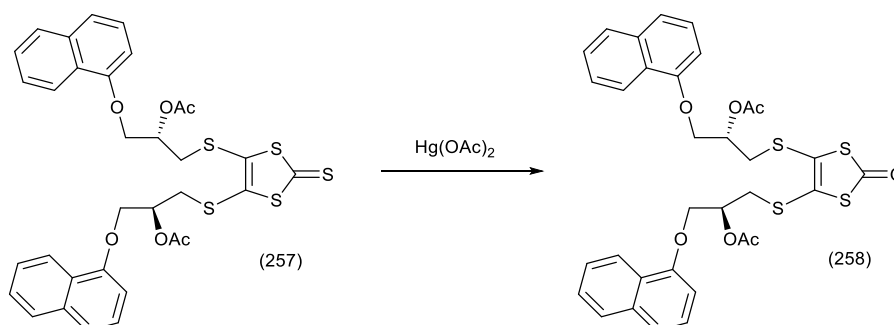
To a suspension of *bis* acetyl protected thione (**106**) (2.58 g, 9.12 mmol) in dry MeOH (50 ml) at 0°C under nitrogen atmosphere was added a methanol solution of sodium methoxide (4.17 ml, 18.25 mmol, 25% by weight) and the suspension was left stirring until the appearance of a deep red-purple solution. At this point a solution of enantiopure oxirane (**254**) (3.65 g, 28.25 mmol) in dry MeOH (5 ml) was added to the dithiolate solution. The reaction was kept at 0°C for 1 h. and then at r.t. for 8 h. The yellow-orange solution was quenched with acetic acid (3 ml) and the solvent was evaporated. DCM (50 ml) was added to the residue and the organic layer was collected and washed with saturated NaHCO_3 solution (3 x 50 ml), water (50 ml) and brine (50 ml) and dried over MgSO_4 . Evaporation of the solvent gave a dark red oil which was purified by flash chromatography (3:1=pet ether: ethyl acetate) to give the *bis*-substituted thione (**256**) as a red oil (4.24 g, 78%); δ_H (400 MHz, CDCl_3): 8.11 (2H, m, Ar- H_2), 7.72 (2H, m, Ar- H_2), 7.40 (6H, m, Ar- H_6), 7.28 (2H, t, $J = 8.2$ Hz, Ar- H_2), 6.70 (2H, d, $J = 7.8$ Hz, Ar- H_2), 4.24 (2H, m, 2 x 2'- H), 4.14 (4H, d, $J = 5.0$ Hz, 2 x 3'- H_2), 3.27 (2H, dd, $J = 14.0, 4.4$ Hz, 2 x 1'- H_α), 3.19 (2H, dd, $J = 13.9, 7.9$ Hz, 2 x 1'- H_β), 2.91 (2H, d, $J = 5.5$ Hz, 2 x $-\text{OH}$); δ_C (100 MHz, CDCl_3): 210.5 (C=S), 153.8, 136.7, 134.6, 127.8, 126.8, 125.9, 125.7, 125.4, 121.7 (Ar- C_{18}), 121.2 (4-, 5- C) 105.1 (Ar- C_2), 70.1 (2 x 3'- C), 69.2 (2 x 2'- C), 40.6 (2 x 1'- C); ν_{max} : 3380 ($-\text{OH}$), 1578, 1507, 1457, 1395, 1266, 1239, 1101, 1061 (C=S), 907; found C, 58.16; H, 4.20%, $\text{C}_{29}\text{H}_{26}\text{O}_4\text{S}_5$ requires C, 58.26, H, 4.34%; $^{297}[\alpha]_{\text{D}} = -90.0$ ($c = 1$, DCM).

3.5.4 Synthesis of 4,5-bis(2'S-2'-acetoxy-3'-(naphth-1''-yloxy)propylthio)- [1,3]dithiol-2-thione (257).



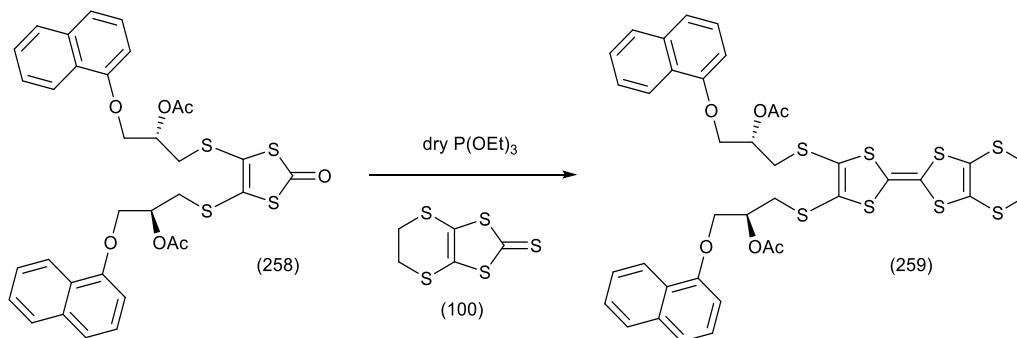
To a solution of thione (**256**) (2.42 g, 4.05 mmol) in pyridine (20 ml) at 0°C was added dropwise acetic anhydride (0.95 ml, 10.1 mmol) and the solution was left to stir and warm up to r.t. over 20 h. The solution was transferred into a separating funnel containing 50 g of ice and the obtained slurry was washed with DCM (5 x 30 ml). The organic washes were collected and washed with 2M HCl (5 x 50 ml), water (50 ml) and brine (50 ml) and dried over MgSO₄. Evaporation of DCM gave the desired protected thione (**257**) as a red oil (2.49 g, 93%); δ_H (300 MHz, CDCl₃): 8.09 (2H, m, Ar-*H*₂), 7.71 (2H, m, Ar-*H*₂), 7.41 (6H, m, Ar-*H*₆), 7.26 (2H, t, *J* = 7.6 Hz, Ar-*H*₂), 6.69 (2H, d, *J* = 7.6 Hz, Ar-*H*₂), 5.35 (2H, m, 2 x 2'-*H*), 4.23 (2H, m, 2 x 3'-*H*₂), 3.32 (2H, dd, *J* = 14.2, 5.5 Hz, 2 x 1'-*H*_α), 3.22 (2H, dd, *J* = 14.2, 6.5 Hz, 2 x 1'-*H*_β), 2.03 (6H, s, 2 x -CH₃); δ_C (100 MHz, CDCl₃): 210.5 (C=S), 170.1 (2 x -C=O), 153.6, 136.3, 134.5, 127.5, 126.6, 125.7, 125.6, 125.3, 121.6 (Ar-C₁₈), 121.1 (4-,5-C), 104.8 (Ar-C₂), 70.6 (2 x 2'-C), 66.9 (2 x 3'-C), 37.0 (2 x 1'-C), 20.9 (2 x -CH₃); ν_{max} : 3052, 2923, 1737 (C=O), 1578, 1393, 1369, 1218, 1102, 1059, 768; found C, 57.83; H, 4.54%, C₃₃H₃₀O₆S₅ requires C, 57.98, H, 4.40%; ²⁹⁷[α]_D = -44.4 (c = 0.99, DCM).

3.5.5 Synthesis of 4,5-bis(2'S-2'-acetoxy-3'-(naphth-1''-yloxy)propylthio)- [1,3]dithiol-2-one (258).



To a solution of *bis*-acetyl protected thione (**257**) (1.2 g, 1.77 mmol) in CHCl_3 (24 ml) was added mercury (II) acetate (1.41 g, 4.42 mmol) and the resulting suspension was left stirring for 2 h at r.t. under a nitrogen atmosphere. The solid formed was filtered off and washed with CHCl_3 until washings ran clear. The filtrate was washed with saturated NaHCO_3 solution (5 x 25 ml), water (25 ml), brine (25 ml) and dried over MgSO_4 . The chloroform was evaporated to give oxo-compound (**258**) as a pink oil (1.09 g, 93%); δ_H (400 MHz, CDCl_3): 8.09 (2H, m, Ar- H_2), 7.71 (2H, m, Ar- H_2), 7.38 (6H, m, Ar- H_6), 7.25 (2H, t, $J = 8.0$ Hz, Ar- H_2), 6.67 (2H, d, $J = 7.7$ Hz, Ar- H_2), 5.35 (2H, m, 2 x 2'- H), 4.26 (2H, dd, $J = 10.8, 4.6$ Hz, 3'- H_α), 4.22 (2H, dd, $J = 10.8, 4.7$ Hz, 3'- H_β), 3.29 (2H, dd, $J = 14.2, 5.7$ Hz, 2 x 1'- H_α), 3.19 (2H, dd, $J = 14.2, 6.5$ Hz, 2 x 1'- H_β), 2.01 (6H, s, 2 x - CH_3); δ_C (100 MHz, CDCl_3): 188.2 (2-C), 170.1 (2 x $\text{O}=\text{C}(\text{CH}_3)$), 153.6, 134.4, 127.6, 127.5, 126.5, 125.6, 125.4, 125.2, 121.6 (Ar- C_{18}), 121.0 (4-,5-C), 104.7 (Ar- C_2), 70.6 (2 x 2'-C), 66.9 (2 x 3'-C), 36.9 (2 x 1'-C), 20.9 (2 x - CH_3); ν_{max} : 3055, 2927, 1738 ($\text{C}=\text{O}(\text{CH}_3)$), 1665 ($\text{C}=\text{O}$), 1579, 1394, 1370, 1221, 1101, 769; HRMS: (ASAP) found: 666.0864 (100%) $\text{C}_{33}\text{H}_{30}\text{O}_7\text{S}_4 + \text{H}$: requires: 666.0869; $^{297}[\alpha]_{\text{D}} = -52.0$ ($c = 1.02$, DCM).

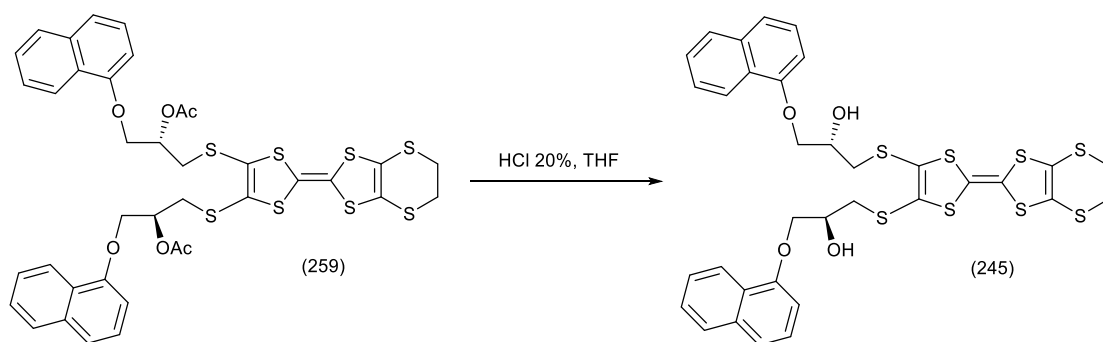
3.5.6 Synthesis of 4,5-bis(2''S-2''-acetoxy-3''-(naphth-1''-yloxy)propylthio)-(ethylenedithio)-TTF (259).



A mixture of oxo-compound (**258**) (1.50 g, 2.26 mmol) and unsubstituted thione (**100**) (1.02 g, 4.53 mmol) in freshly distilled triethyl phosphite (34 ml) was warmed up to 90°C and left stirring for 5 h under a nitrogen atmosphere. The reaction was left to cool down and the solid formed was filtered off and washed with CHCl_3 until washings ran clear. The filtrate was concentrated at the rotary evaporator and the triethyl phosphite was distilled off using a Kugelrohr oven. The residue was purified by flash chromatography (7:3 = hexane : ethyl acetate) to furnish the desired cross-coupled compound (**259**) as a red-orange oil (0.84 g, 44%); δ_H (400 MHz, CDCl_3): 8.13 (2H, m, Ar- H_2), 7.70 (2H, m, Ar- H_2), 7.38 (6H, m, Ar- H_6), 7.24 (2H, t, $J = 7.7$ Hz, Ar- H_2), 6.68 (2H, d, $J = 7.6$ Hz, Ar- H_2), 5.34 (2H, m, 2 x 2''- H), 4.26 (2H, dd, $J = 10.1, 4.7$ Hz, 2 x 3''- H_α), 4.22 (2H, dd, $J =$

10.1, 4.7 Hz, $-2 \times 3''\text{-}H_{\beta}$), 3.28 (2H, dd, $J = 14.2, 5.6$ Hz, $2 \times 1''\text{-}H_{\alpha}$), 3.22 (4H, s, $5''\text{-}, 6''\text{-}H_2$), 3.16 (2H, dd, $J = 14.2, 6.4$ Hz, $2 \times 1''\text{-}H_{\beta}$), 2.02 (6H, s, $2 \times \text{-CH}_3$); δ_C (100 MHz, CDCl_3): 170.2 ($2 \times \text{C=O}$), 153.7, 134.4, 128.0, 127.8, 126.4, 125.6, 125.4, 121.7, 120.9 (Ar- C_{18}), 113.8, 111.8 ($2\text{-}, 2''\text{-}, 4\text{-}, 3''\text{a-}, 5\text{-}, 7''\text{a-C}$), 104.6 (Ar- C_2), 70.9 ($2 \times 2''\text{-C}$), 66.9 ($2 \times 3''\text{-C}$), 36.4 ($2 \times 1''\text{-C}$), 30.1 ($5''\text{-}, 6''\text{-C}$), 21.0 ($2 \times \text{-CH}_3$); ν_{\max} : 3051, 2929, 1737 (C=O), 1578, 1508, 1394, 1369, 1219, 1101, 1043, 1020, 768; found C, 51.05; H, 4.15%, $\text{C}_{38}\text{H}_{34}\text{O}_6\text{S}_8$ requires C, 51.38, H, 4.28%; $^{296}[\alpha]_{\text{D}} = -35.0$ ($c = 0.6$, DCM).

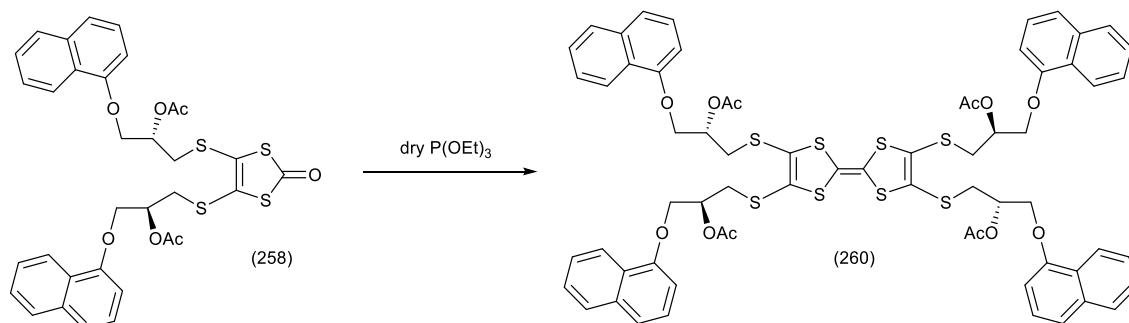
3.5.7 Synthesis of 4,5-bis(2''S-2''-hydroxy-3''-(naphth-1''-yloxy)propylthio)-(ethylenedithio)TTF (245).



To a solution of *bis*-acetyl protected donor (**259**) (0.19 g, 0.22 mmol) in THF (4 ml) was added 20% HCl (2 ml) and the suspension was left to stir under reflux overnight. The reaction was stopped and left to cool down to r.t. and the THF was evaporated. DCM (20 ml) was added and the organic layer was washed with saturated sodium hydrogen carbonate solution (5 x 20 ml), water (20 ml) and brine (20 ml) and dried over Na_2SO_4 . Evaporation of DCM afforded a red-brown oil which was purified by flash chromatography (3:1 = cyclohexane: ethyl acetate) to afford a dark brown solid but NMR showed presence of 4-chlorobutanol as a by-product. Acetonitrile was added to the residue until all the oil was in solution. A solid precipitated out from the solution and was filtered off. The filtrate was evaporated to furnish a brown solid identified by NMR as the desired donor (**245**) (0.14 g, 80%); m.p. 90.5-91.5°C δ_H (400 MHz, CDCl_3): 8.14 (2H, m, Ar- H_2), 7.68 (2H, m, Ar- H_2), 7.35 (6H, m, Ar- H_6), 7.23 (2H, t, $J = 7.8$ Hz, Ar- H_2), 6.64 (2H, d, $J = 7.8$ Hz, Ar- H_2), 4.15 (2H, m, $2 \times 2''\text{-}H$), 4.07 (4H, d, $J = 5.0$ Hz, $2 \times 3''\text{-}H_2$), 3.28 (6H, m, $2 \times 3''\text{-}H_{\alpha}$ and $5''\text{-}, 6''\text{-}H_2$), 3.04 (4H, m, $2 \times 3''\text{-}H_{\beta}$ and $2 \times \text{OH}$); δ_C (100 MHz, CDCl_3): 153.8, 134.4, 127.5, 126.5, 125.7, 125.5, 125.3, 121.7, 120.9 (Ar- C_{18}), 113.8, 111.8 ($2\text{-}, 2''\text{-}, 4\text{-}, 3''\text{a-}, 5\text{-}, 7''\text{a-C}$), 104.9 (Ar- C_2), 70.0 ($2 \times 2''\text{-C}$), 66.9 (br, $2 \times 3''\text{-C}$), 40.2 (br, $2 \times 1''\text{-C}$), 30.2 ($5''\text{-}, 6''\text{-C}$), ν_{\max} : 3380 (OH), 3051, 2922, 1578, 1395, 1266, 1238, 1100, 767;

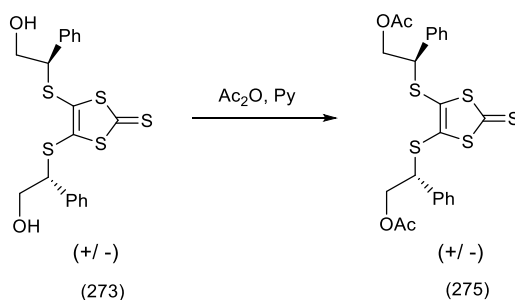
HRMS: (EI+) found: 757.9900 (33%) $C_{34}H_{30}O_4S_8^+$: requires: 757.9904; $^{297}[\alpha]_D = -542.8$ ($c = 0.14$, DCM).

3.5.8 Synthesis of *tetrakis*(2''*S*-2''-acetoxy-3''-(naphth-1''yloxy)propylthio)-TTF (260).



A solution of oxo-compound (**258**) (1.09 g, 1.64 mmol) in freshly distilled triethyl phosphite (15 ml) was stirred under a nitrogen atmosphere for 24 h at 95°C. The reaction was left to cool to r.t. and the triethyl phosphite was distilled off using the Kugelrohr oven. The residue was purified by flash chromatography using 3:1 = cyclohexane: ethyl acetate as eluent. The homocoupled compound (**260**) was obtained as an orange oil (0.30 g, 14%); δ_H (400 MHz, $CDCl_3$): 8.18 (4H, m, Ar- H_4), 7.74 (4H, m, Ar- H_4), 7.45 (12H, m, Ar- H_{12}), 7.24 (4H, m, Ar- H_4), 6.71 (4H, m, Ar- H_4), 5.39 (4H, m, 4 x 2''- H), 4.34-4.23 (8H, m, 4 x 3''- H_2), 3.32 (4H, dd, $J = 14.1, 5.4$ Hz, 4 x 1''- H_α), 3.21 (4H, dd, $J = 14.2, 6.8$ Hz, 4 x 1''- H_β), 2.07 (12H, s, 4 x - CH_3); δ_C (100 MHz, $CDCl_3$): 170.1 (4 x - $C=O$), 153.8, 134.4, 128.0, 127.4, 126.5, 125.7, 125.4, 121.8, 120.9 (Ar- C_{36}), 110.9 (2-, 2'', 4-, 4'', 5-, 5''- C), 104.7 (Ar- C_4), 70.8 (4 x 2''- C), 67.0 (4 x 3''- C), 36.4 (4 x 1''- C), 20.9 (4 x - CH_3);

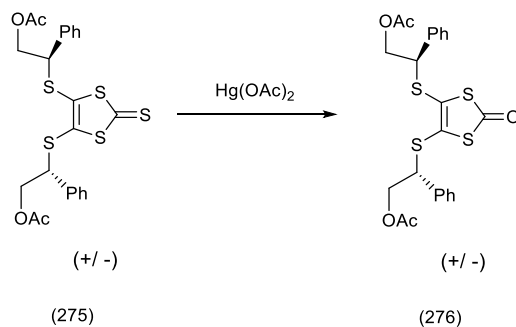
3.5.9 Synthesis of 4,5-bis(2'-acetoxy-1'-phenylethylthio)-1,3-dithiol-2-thione (275).



A solution of thione (**273**) (0.13 g, 0.30 mmol) in pyridine (15 ml) was cooled down to -5°C and acetic anhydride (0.054 ml, 0.57 mmol) was added dropwise. The resulting solution was left to stir and warmed up to r.t. overnight. TLC evidenced the presence of a single bright yellow spot so the reaction was stopped and iced water was added (50 ml). The mixture was extracted with DCM (3 x 25 ml) and the organic layer collected and

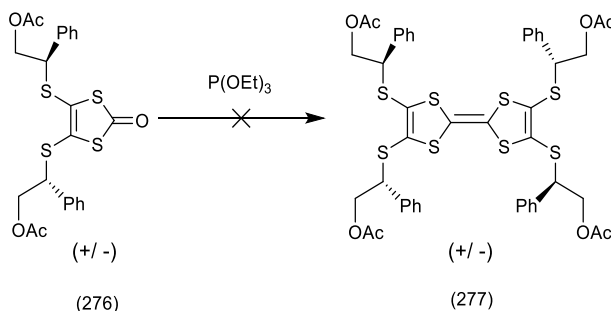
combined, and washed with 2M HCl (5 x 25 ml), water (1 x 25 ml) and brine (1 x 25 ml) and dried over MgSO₄. The solvent was evaporated under reduced pressure to furnish protected thione (**275**) as a deep red oil (0.12 g, 90%); δ_H (400 MHz, CDCl₃): 7.19-7.30 (10H, m, Ar-*H*₁₀), 4.43-4.32 (6H, m, 2 x 1'-*H*, 2 x 2'-*H*₂), 1.95 (6H, s, 2 x -CH₃); δ_C (100 MHz, CDCl₃): 210.9 (C=S), 170.4 (2 x -C=O), 137.5, 136.3, 129.0, 128.8 (Ar-*C*₁₂), 128.1 (4-,5-*C*), 66.1 (2 x 2'-*C*), 53.6 (2 x 1'-*C*), 20.7 (2 x -CH₃).

3.5.10 Synthesis of 4,5-bis(2'-acetoxy-1'-phenylethylthio)-1,3-dithiol-2-one (**276**).



To a solution of *bis*-acetyl protected thione (**275**) (0.14 g, 0.27 mmol) in chloroform (10 ml) under nitrogen atmosphere was added mercury (II) acetate (0.22 g, 0.69 mmol) and the mixture was left to stir for 2 h. The suspension was filtered and the filtrate was washed with saturated sodium hydrogen carbonate solution (5 x 10 ml), water (10 ml) and brine (10 ml) and dried over MgSO₄. The residue was purified by chromatography to furnish oxo-compound (**276**) (0.12 g, 88%) as a brown oil; δ_H (400 MHz, CDCl₃): 7.19-7.28 (10H, m, Ar-*H*₁₀), 4.37 (6H, m, 2 x 1'-*H*, 2 x 2'-*H*₂), 1.95 (6H, s, 2 x -CH₃).

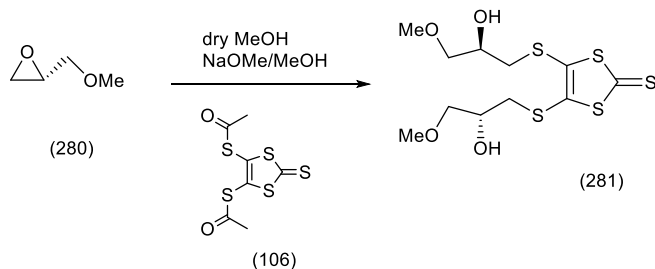
3.5.11 Attempted synthesis of tetrakis [(2''-acetoxy-1''-phenylethylthio)-TTF (**277**).



Oxo-compound (**276**) (0.031 g, 0.061 mmol) and freshly distilled triethyl phosphite (10 ml) were warmed up to 100°C under nitrogen atmosphere and left to stir for 24 h. Triethyl phosphite was distilled off using a Kugelrohr oven to give a crude yellow oil. Homocoupled donor (**277**) was not identified in the residue analysed by NMR spectroscopy.

3.5.12 Synthesis of (*S*)-2-(methoxymethyl)oxirane (**280**).³⁸

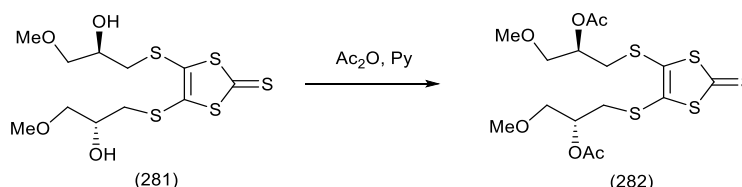
To a solution of *R*-(+)-glycidol (5.0 g, 67.6 mmol) in DCM (50 ml) were added silver oxide (15.7 g, 67.6 mmol) and methyl iodide (676.0 mmol, 42.1 ml) and the resulting suspension was left stirring under reflux for 24 h. The reaction was allowed to cool down to r.t. and the silver oxide was filtered off. The solid was washed with DCM (5 x 20 ml). The filtrate was concentrated *in vacuo* to afford oxirane (**280**) as a pale yellow oil (3.98 g, 67%); δ_H (400 MHz, $CDCl_3$): 3.57 (1H, d, $J = 11.2$ Hz, 2- CH_α), 3.23 (3H, s, - OCH_3), 3.14 (1H, m, 2- CH_β), 2.97 (1H, m, 2- H), 2.62 (1H, m, 3- H_α), 2.43 (1H, m, 3- H_β); δ_C (100 MHz, $CDCl_3$): 72.5 (2- CH_2), 58.2 (O- CH_3), 49.9 (2- C), 43.1 (3- C).

3.5.13 Synthesis of 4,5-bis(2'*R*-2'-hydroxy-3'-methoxypropyl)thio)-1,3-dithiole-2-thione (**281**).

A solution of *bis* acetyl protected thione (**106**) (7.37 g, 26.1 mmol) in dry MeOH (140 ml) under a nitrogen atmosphere was treated with a NaOMe/MeOH (25% by weight) solution (11.95 ml, 52.3 mmol) at $-25^\circ C$. After the change in colour was observed (from yellow to dark red/purple) the suspension was left to stir for a further 30 min. A solution of (*S*)-O-methyl-glycidol (**280**) (4.60 g, 52.3 mmol) in dry THF (5 ml) was added. The resulting suspension was left to stir and warm up to r.t. for 7 h. The suspension was quenched with acetic acid (10 ml) and left stirring for additional 30 min. The solution was concentrated *in vacuo* and ethyl acetate was added to the residue. The organic layer was washed with saturated sodium hydrogen carbonate solution (3 x 100 ml), water (100 ml) and brine (100 ml) and dried over $MgSO_4$. The evaporation of solvent afforded a dark red oil which was purified by flash chromatography (1:1 = cyclohexane: ethyl acetate) to yield thione (**281**) as a red oil (4.6 g, 47%); δ_H (400 MHz, $CDCl_3$): 4.12 (2H, br s, 2 x ($-OH$)), 3.86 (2H, br d, $J = 3.5$ Hz, 2 x 2'- H), 3.41 (4H, m, 2 x 3'- H_2), 3.33 (6H, br s, 2 x $-CH_3$), 3.02 (2H, dd, $J = 13.8, 4.4$ Hz, 2 x 1'- H_α), 2.89 (2H, dd, $J = 13.9, 4.1$ Hz, 2 x 1'-

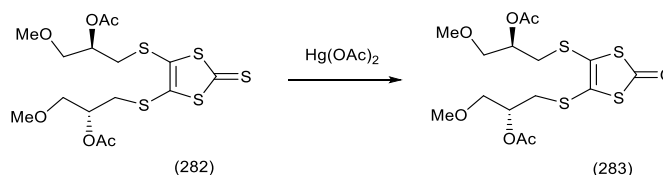
H_{β}); δ_C (100 MHz, $CDCl_3$): 210.7 (C=S), 136.6 (4-,5-C), 74.7 (2 x 2'-C), 69.0 (2 x 3'-C), 59.3 (2 x -OCH₃), 40.2 (2 x 1'-C); ν_{max} : 3398 (-OH), 2886, 1665, 1449, 1404, 1195, 1116, 1056, 959, 883; found C, 35.04; H, 4.68%, C₁₁H₁₈O₄S₅ requires C, 35.29, H, 4.81%; $^{298}[\alpha]_D = -49$ (c = 1, MeOH).

3.5.14 Synthesis of 4,5-bis(2'R-2'-acetoxy-3'-methoxypropylthio)-1,3-dithiole-2-thione (282).



To a solution of thione (**281**) (1.10 g, 2.97 mmol) in pyridine (20 ml) at 0°C was added acetic anhydride (1.9 ml, 20.1 mmol) dropwise and the reaction mixture was left to stir and allowed to warm to r.t. over 20 h. The solution was poured into a separating funnel containing iced water (50 ml) and DCM was added (20 ml). The organic layer was collected and washed with 2M HCl (5 x 40 ml), water (40 ml) and brine (40 ml) and dried over MgSO₄. The dichloromethane was evaporated to yield the desired protected thione (**282**) as a red oil (1.30 g, 95%); δ_H (400 MHz, $CDCl_3$): 5.03 (2H, m, 2 x 2'-H), 3.54 (2H, dd, J = 10.2, 4.6 Hz, 2 x 3'-CH_α), 3.49 (2H, dd, J = 10.2, 4.7 Hz, 2 x 3'-CH_β), 3.31 (6H, s, 2 x -OCH₃), 3.14 (2H, dd, J = 14.1, 7.0 Hz, 1'-H_α), 3.05 (2H, dd, J = 14.1, 5.4 Hz, 1'-H_β), 2.03 (6H, s, 2 x -CH₃); δ_C (100 MHz, $CDCl_3$): 210.4 (C=S), 170.1 (2 x C=O), 136.3 (4,5-C), 71.5, 70.0 (2 x 2'-C, 2 x 3'-C), 59.3 (2 x -OCH₃), 36.8 (2 x 1'-C), 20.9 (2 x -CH₃); ν_{max} 3052, 2923, 1737 (-C=O), 1578, 1508, 1458, 1393, 1369, 1218, 1102, 1059, 768; found C, 39.15; H, 4.87%, C₁₅H₂₂O₆S₅ requires C, 39.30, H, 4.80%; $^{298}[\alpha]_D = -30.3$ (c = 0.99, DCM).

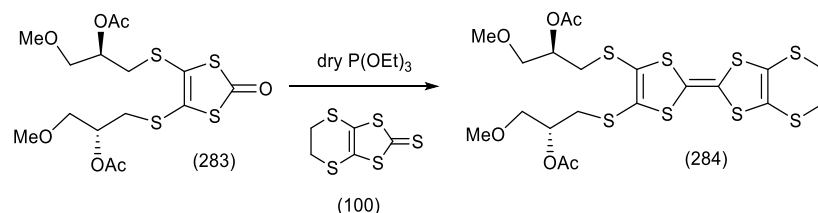
3.5.15 Synthesis of 4,5-bis(2'R-2'-acetoxy-3'-methoxypropylthio)-1,3-dithiole-2-one (283).



To a solution of bis-acetyl protected thione (**282**) (1.30 g, 2.84 mmol) in $CHCl_3$ (30 ml) was added mercury (II) acetate (2.27 g, 7.10 mmol) and the resulting suspension was left stirring for 2 h. at r.t. The solid formed was filtered off and washed with $CHCl_3$ until

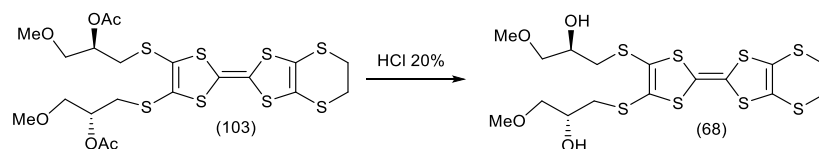
washes ran clear. The filtrate was washed with saturated sodium hydrogen carbonate solution (5 x 15 ml), water (15 ml) and brine (15 ml) and dried over MgSO₄. Evaporation of chloroform afforded oxo-compound (**283**) as a pink oil (1.05 g, 84%); δ_H (400 MHz, CDCl₃): 5.02 (2H, m, 2 x 2'-H), 3.55 (2H, dd, J = 10.5, 4.6 Hz, 2 x 3'-H_α), 3.49 (2H, dd, J = 10.5, 4.4 Hz, 2 x 3'-H_β), 3.30 (6H, s, 2 x -OCH₃), 3.10 (2H, dd, J = 14.0, 5.6 Hz, 2 x 1'-H_α), 3.00 (2H, dd, J = 14.0, 6.6 Hz, 2 x 1'-H_β), 2.02 (6H, s, 2 x -(C(O)CH₃)); δ_C (100 MHz, CDCl₃): 188.8 (2-C), 170.0 (2 x -C=O), 127.5 (4-,5-C), 71.5, 71.0 (2 x 2'-C, 2 x 3'-C), 59.1 (2 x -OCH₃), 36.6 (2 x 1'-C), 20.9 (2 x -CH₃); ν_{\max} 3055, 2927, 1738 (-C=O(CH₃)), 1665 (C=O), 1579, 1508, 1458, 1394, 1370, 1221, 1101, 769; found C, 40.53; H, 5.13%, C₁₅H₂₂O₇S₄ requires C, 40.72, H, 4.97%; ²⁹⁸[α]_D = -72 (c = 1, DCM).

3.5.16 Synthesis of bis(2''R-2''-acetoxy-3''-methoxypropylthio)-(ethylenedithio)-TTF (**284**).



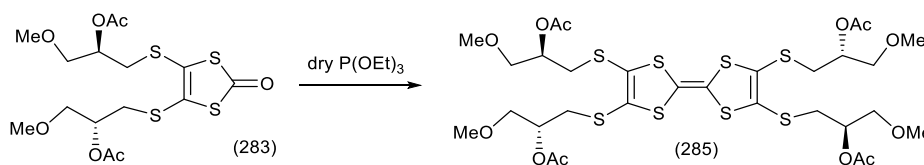
A mixture of oxo-compound (**283**) (1.00 g, 2.26 mmol), unsubstituted thione (**100**) (1.04 g, 4.64 mmol) and freshly distilled triethyl phosphite (10 ml) was warmed up to 80°C under a nitrogen atmosphere and left stirring for 5 h. The reaction was left to cool to r.t. and the solid formed was filtered off and washed with CHCl₃. The filtrate was concentrated at the rotary evaporator and the triethyl phosphite was distilled off using a Kugelrohr oven. The residue was purified by flash chromatography (7:3 = hexane: ethyl acetate) to furnish the desired cross-coupled compound (**284**) as a red-orange oil (0.45g, 38%); δ_H (400 MHz, CDCl₃): 5.01 (2H, m, 2 x 2''-H), 3.53 (2H, dd, J = 10.6, 4.7 Hz, 2 x 3''-H_α), 3.49 (2H, dd, J = 10.5, 4.4 Hz, 2 x 3''-H_β), 3.30 (6H, s, 2 x -OCH₃), 3.23 (4H, s, S-CH₂-CH₂-S), 3.07 (2H, dd, J = 14.2, 5.6 Hz, 2 x 1''-H_α), 2.97 (2H, dd, J = 14.2, 6.6 Hz, 2 x 1''-H_β), 2.03 (6H, s, 2 x -(C(O)CH₃)); δ_C (100 MHz, CDCl₃): 170.2 (2 x -C(O)CH₃), 128.0, 113.7, 112.4 109.9 (2-, 2'', 4-, 5-, 3'a-, 7'a-C), 71.6, 71.2 (2 x 2''-C, 2 x 3''-C), 59.2 (2 x -OCH₃), 36.2 (2 x 1''-C), 30.0 (S-CH₂-CH₂-S), 20.9 (2 x -CH₃); ν_{\max} 3051, 2929, 1737 (-C=O), 1578, 1507, 1394, 1369, 1219, 1101, 768; found C, 39.11; H, 4.31%, C₂₀H₂₆O₆S₈ requires C, 38.83, H, 4.20%; ²⁹⁸[α]_D = -85.29 (c = 1.02, DCM).

3.5.17 Synthesis of *bis*(2''*R*-2''-hydroxy-3''-methoxypropylthio)-(ethylenedithio)-TTF (**249**).



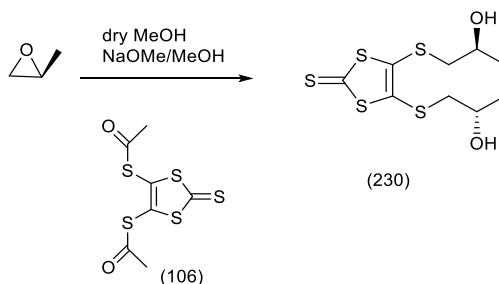
To a solution of *bis*-acetyl protected EDT-TTF derivative (**284**) (0.35 g, 0.67 mmol) in MeOH : THF = 1:1 (20 ml) was added a solution of potassium carbonate (0.37 g, 2.7 mmol) in water (8 ml) and the resulting suspension was left stirring at r.t. for 10 h. The reaction was stopped and the solvent evaporated. The aqueous residue was extracted with ethyl acetate (3 x 15 ml). The organic layers were combined and washed with water (15 ml) and brine (15 ml) and dried over NaSO₄. Evaporation of the solvent afforded the desired *bis*-hydroxy-compound (**249**) as a red-orange oil (0.30 g, 84%); δ_H (400 MHz, CDCl₃): 3.85 (2H, br s, 2 x 2'-*H*), 3.43 (1H, dd, *J* = 9.8, 4.0 Hz, 2 x 3''-*H*_α), 3.40 (1H, dd, *J* = 9.8, 5.5 Hz, 2 x 3''-*H*_β), 3.32 (6H, s, 2 x O-CH₃), 3.23 (4H, s, S-CH₂-CH₂-S), 2.98 (2H, br, 2 x -OH), 2.96 (2H, dd, *J* = 13.9, 4.1 Hz, 2 x 1''-*H*_α), 2.84 (2H, dd, *J* = 13.9, 8.2 Hz, 2 x 1''-*H*_β); δ_C (100 MHz, CDCl₃): 128.4, 113.9, 110.2 (2-, 2'-, 4-, 5-, 3'a-, 7'a-C), 74.9 (2 x 2''-C), 69.1 (2 x 3''-C), 59.3 (2 x -OCH₃), 39.9 (2 x 1''-C), 30.2 (S-CH₂-CH₂-S); ν_{\max} 3380 (-OH), 3051, 2922, 1700, 1578, 1507, 1395, 1266, 1238, 1100, 767; found C, 37.20; H, 5.81%, C₁₆H₂₀O₄S₈·1.5·(C₄H₈O₂)·2(H₂O) requires C, 37.60, H, 5.50%; ²⁹⁶[α]_D = -173.5 (c = 0.34, DCM).

3.5.18 Synthesis of *tetrakis*(2''*R*-2''-acetoxy-3''-methoxypropylthio)-(ethylenedithio)-TTF (**285**).



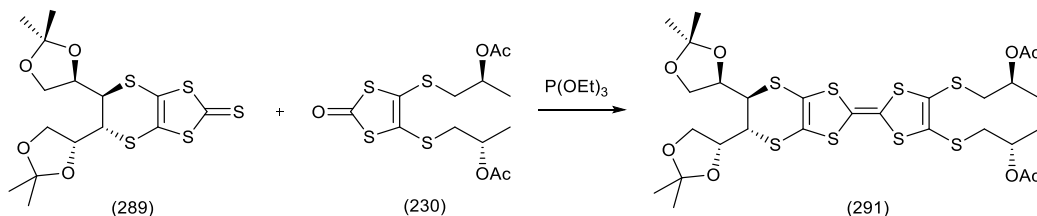
A solution of oxo-compound (**283**) (1.09 g, 1.64 mmol) in freshly distilled triethyl phosphite (15 ml) was stirred under a nitrogen atmosphere for 24 h at 95 °C. The reaction was left to cool to r.t. and the triethyl phosphite was distilled off using a Kugelrohr oven. The residue was purified by chromatography using 3:1 = cyclohexane: ethyl acetate as eluent. The desired homo-coupled compound (**285**) was obtained as an orange solid (0.42 g, 30%); δ_H (400 MHz, CDCl₃): 5.02 (4H, m, 4 x 2''-*H*), 3.51 (8H, m, 4 x 3''-*H*₂), 3.30 (12H, s, 4 x -OCH₃), 3.05 (4H, dd, *J* = 14.0, 5.8 Hz, 4 x 1''-*H*_α), 2.98 (4H, dd, *J* = 14.6, 6.6 Hz, 4 x 1''-*H*_β), 2.03 (12H, s, 4 x -C(O)CH₃); ²⁹⁸[α]_D = -41.24 (c = 0.97, DCM).

3.5.19 Synthesis of 4,5-bis(2'-S-2'-hydroxypropylthio)-1,3-dithiole-2-thione (230).



To a solution of acetyl protected thione (**106**) (10.92 g, 38.7 mmol) in dry MeOH (240 ml) and dry THF (60 ml) cooled down to 0°C and under a nitrogen atmosphere was added NaOMe/MeOH (25% by weight) (4.20 g, 77.0 mmol). The resulting suspension was left to stir until no solid could be seen. To the resulting dark red-purple solution was added (*S*)-propylene oxide (5.5 ml, 77.0 mmol) and the reaction mixture was left to warm up to r.t. and stirred for 5 h. It was quenched with AcOH (10 ml) and left stirring for a further 30 min. The MeOH and THF were evaporated. To the residue was added DCM (50 ml) which was washed with water (3 x 50 ml) and brine (50 ml) and dried over MgSO₄. The residue was purified by column chromatography to furnish diol (**230**) (7.25 g, 67%) as a deep red oil; δ_H (400 MHz, CDCl₃): 3.91 (2H, m, 2 x 2'-*H*), 3.57 (2H, br s, 2 x OH), 2.99 (2H, dd, *J* = 13.7, 3.9 Hz, 2 x 1'-*H_a*), 2.81 (2H, dd, *J* = 13.7, 8.2 Hz, 2 x 1'-*H_β*), 1.24 (6H, d, *J* = 6.3 Hz, 2 x -CH₃); δ_C (100 MHz, CDCl₃): 210.5 (C=S), 136.5 (2 x 4-, 5-C), 66.1 (2 x 2'-C), 45.2 (2 x 1'-C), 21.9 (2 x -CH₃). Previously³⁰⁾ this compound was from made from the benzoyl protected thione (**105**).

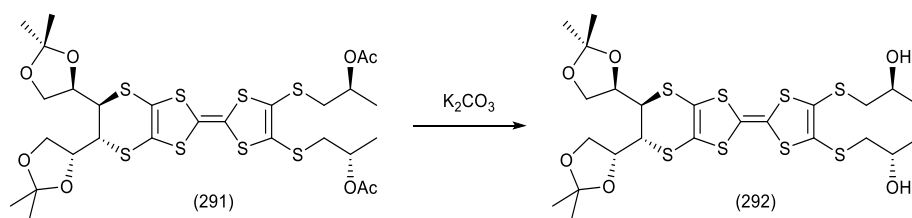
3.5.20 Synthesis of 4,5-bis(2''-S-2''-acetoxy-propylthio)-5'R, 6'R-5',6'-bis-(4''''R-2''''-dimethyl-1,3-dioxolan-4''''-yl)-ethylenedithio-TTF (291).



A mixture of the oxo-compound (**230**)^{30a)} (1.04 g, 2.92 mmol) and thione (**289**)¹²⁾ (2.48 g, 5.83 mmol) was heated at 100°C in freshly distilled triethyl phosphite (125 ml) under a nitrogen atmosphere and left stirring overnight. Monitoring of the reaction by tlc showed the presence of three distinct spots. The reaction mixture was allowed to cool down to r.t., and the triethyl phosphite was distilled off using a Kugelrohr oven. The residue was then purified by flash chromatography (4:1 = pet ether : ethyl acetate) to furnish

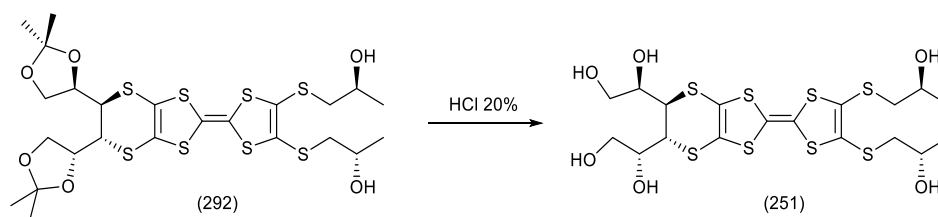
the cross-coupled donor (**291**) as a dark orange oil (1.07 g, 48%). δ_H (400 MHz, $CDCl_3$): 4.95 (2H, m, 2 x 2''-H), 4.33 (2H, m, 2 x 4'''-H), 4.12 (2H, dd, J = 9.6, 5.7 Hz, 2 x 5'''- H_α), 3.97 (2H, dd, J = 9.6, 4.8 Hz, 2 x 5'''- H_β), 3.64 (2H, d, J = 9.6 Hz, 2 x 5', 6'-H), 2.91 (4H, d, J = 5.9 Hz, 2 x 1''- H_2), 1.98 (6H, s, 2 x (-C=O(CH_3))), 1.36, 1.28 (12H, 2 x s, 2 x 2'''-(CH_3)₂), 1.27 (6H, d, J = 6.7 Hz, 2 x 3''- H_3); δ_C (100 MHz, $CDCl_3$): 170.2 (2 x -C=O), 128.1, 110.3, 109.7 (2-, 2'-, 4-, 5-, 3'a-, 7'a-C, 2'''-C), 76.0 (2 x 4'''-C), 69.4 (2 x 2''-C), 67.9 (2 x 5'''-C), 44.8 (5', 6'-C), 41.0 (2 x 1''-C), 27.0, 25.3 (2 x 2'''-(CH_3)₂), 21.1 (2 x CO(CH_3)), 19.0 (2 x -3'' H_3); HRMS: (ASAP) found: 758.0315 $C_{28}H_{38}O_8S_8^+$: requires: 758.0327.

3.5.21 Synthesis of 4,5-bis(2''S-2''-hydroxy-propylthio)- 5', 6'-R-5',6'-bis-(4'''R-2''',2'''-dimethyl-1,3-dioxolan-4'''-yl)-(ethylenedithio)-TTF (**292**).



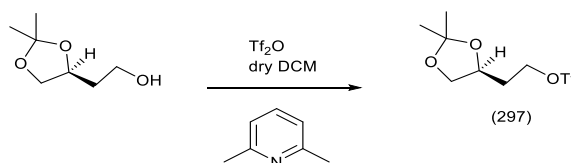
To a solution of protected donor (**291**) (1.07 g, 1.39 mmol) in a mixture of MeOH: THF (20 ml: 50 ml) was added a solution of potassium carbonate (1.27 g, 9.20 mmol) in water (25 ml). The mixture was left to stir at r.t. overnight. The reaction was stopped and the MeOH and THF were evaporated to furnish a suspension of a dark red oil in water. To the residue was added DCM (50 ml). The organic layer was collected and washed with water (3 x 30 ml) and brine (30 ml) and dried over $MgSO_4$. Evaporation of DCM afforded the diol (**292**) as a red oil (0.53 g, 83%). δ_H (400 MHz, $CDCl_3$): 4.31 (2H, m, 2 x 4'''-H), 4.12 (2H, dd, J = 12.0, 8.0 Hz, 2 x 5'''- H_α), 3.97 (2H, dd, J = 12.0, 5.8 Hz, 2 x 5'''- H_β), 3.80 (2H, m, 2 x 2''-H), 3.64 (2H, d, J = 9.6 Hz, 2 x 5', 6'-H), 2.97 (2H, dd, J = 13.8, 3.2 Hz, 2 x 1''- H_α), 2.62 (2H, dd, J = 13.8, 9.0 Hz, 2 x 1''- H_β), 1.36, 1.28 (12H, 2 x s, 2 x 2'''-(CH_3)), 1.20 (6H, d, J = 6.2 Hz, 2 x 3''- H_3); δ_C (100 MHz, $CDCl_3$): 128.3, 110.4, 109.7 (2-, 2'-, 4-, 5-, 3'a-, 7'a-C, 2'''-C), 76.0 (4'''-C), 67.9 (2 x 2''-C), 65.9 (2 x 5'''-C), 44.8, 43.3 (5', 6'-C, 2 x 1''-C), 27.1, 25.4 (2 x 2'''-(CH_3)), 21.8 (2 x 3''-C).

3.5.22 Synthesis of 4,5-bis(2''S-2''-hydroxy-propylthio)- 5', 6'-R 5',6'-bis-(1'''R-1'''-(1''',2'''-dihydroxyethyl)-ethylenedithio)-TTF (**251**).



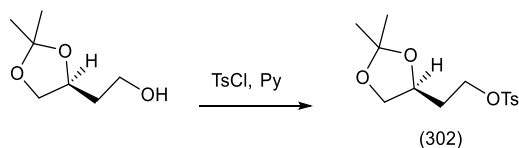
To a solution of protected diol (**292**) (0.53 g, 0.78 mmol) in THF (50 ml) was added 20% HCl (20 ml) and the solution was left to stir at r.t. overnight. The THF was evaporated and the residue washed with ethyl acetate (3 x 10 ml). The organic layers were combined and washed with saturated sodium hydrogen carbonate solution (3 x 30 ml), water (30 ml) and brine (30 ml) and dried over MgSO₄. The solvent was evaporated to furnish a brown oil identified as desired hexol donor (**251**) (0.35 g, 76%). δ_H (400 MHz, CD₃OD): 3.66-3.86 (10H, m, 2 x 5'-, 6'-H, 1''''-H₃, 2''''-H₂, 2 x 2''-H), 2.84 (2H, dd, J = 14.1, 6.4 Hz, 2 x 2''-H_a), 2.76 (2H, dd, J = 13.5, 6.0 Hz, 2 x 2''-H_b), 1.27 (6H, d, J = 6.0 Hz, 2 x 3''-H₃); δ_C (100 MHz, CDCl₃): 128.3, 110.4, 109.7 (6 x *sp*² C), 76.0 (2 x 1''''-C), 67.9 (2 x 2''-C), 65.9 (2 x 2''''-C), 44.8, 43.3 (5'-, 6'-C, 2 x 1''-C), 21.8 (2 x 3''-C); ν_{\max} 3366 (br, OH), 2970, 2925, 1372, 1234, 1101, 1036, 932, 879, 825; found C, 36.73; H, 3.65%, C₁₈H₂₆O₆S₈ requires C, 36.36, H, 4.37%; ²⁹⁷[α]_D = -1600 (c = 0.07, MeOH).

3.5.23 Attempted synthesis of (S)-4-(2,2-dimethyl-1,3-dioxolan-4-yl)ethyl trifluoromethanesulfonate (**297**).



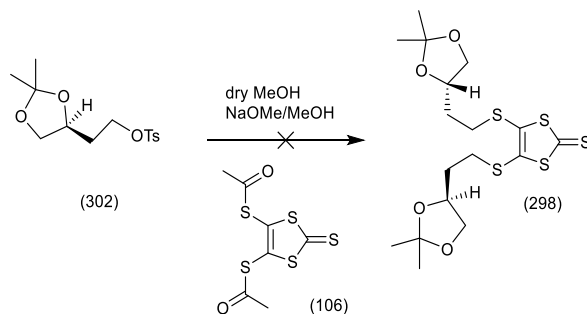
A solution of (4S)-(+)-4-(2-hydroxyethyl)-2,2-dimethyl-1,3-dioxolane (1.0 ml, 7.03 mmol) in dry DCM (10 ml) under a nitrogen atmosphere was cooled down to -40 °C. Lutidine (1.0 ml, 7.73 mmol) was added followed by a dropwise addition of trifluoromethanesulfonate anhydride (1.3 ml, 7.73 mmol). The resulting mixture was left to stir and slowly warmed up to r.t. for 2 h. Following monitoring by tlc, a further 0.3 eq of lutidine (0.3 ml) and triflic anhydride (0.4 ml) were added to allow the reaction to go to completion. The reaction mixture was left to stir for a further 2.5 h, diluted with DCM (50 ml) and washed with NaOH/ citric acid buffer solution (pH 4) (5 x 30 ml). The combined organic layer was washed with water (1 x 30 ml) and brine (1 x 30 ml) and dried over Na₂SO₄. The DCM was evaporated under reduced pressure to furnish a dense pink oil which could not be identified by NMR.

3.5.24 Synthesis of (*S*)-4-(2,2-dimethyl-1,3-dioxolane-4-yl)ethyl *p*-methylbenzenesulfonate (**302**).



A stirred solution of (*S*)-(+)-4-(2-hydroxyethyl)-2,2-dimethyl-1,3-dioxolane (0.4 ml, 2.81 mmol) in pyridine (0.5 ml) under a nitrogen atmosphere was cooled down to -5°C and tosyl chloride (0.63 g, 3.30 mmol) was added. The mixture was left to stir and warm up to r.t. for 2.5 h and then Et_2O (3 ml) was added. The organic layer was washed with 1M HCl (5 x 3 ml), saturated sodium hydrogen carbonate solution (3 x 3 ml), water (3 ml) and brine (3 ml) and dried over MgSO_4 to furnish (**302**) as a colourless oil (0.45 g, 60%); δ_{H} (400 MHz, CDCl_3): 7.71 (2H, d, $J = 6.2$ Hz, Ar- H_2), 7.27 (2H, d, $J = 8.6$ Hz, Ar- H_2), 4.05 (2H, m, 5- H_2), 3.93 (2H, m, - CH_2 -OTs), 3.43 (1H, m, 4- H), 2.37 (3H, s, Ar- CH_3), 1.83 (2H, m, 4- CH_2), 1.23 (6H, dd, 2 x 2- CH_3); δ_{C} (100 MHz, CDCl_3): 144.7, 132.9, 129.7, 127.7 (Ar- C_6), 108.9 (2- C), 72.2 (4- C), 68.9 (- CH_2 -OTs), 67.3 (5- C), 33.0 (4- CH_2), 26.7, 25.4 (2 x 2- CH_3) 21.5 (Ar- CH_3).

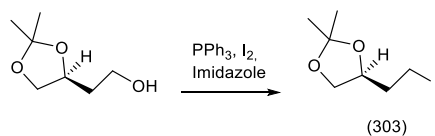
3.5.25 Attempted synthesis of 4,5-bis(*S*-4'-(2',2'-dimethyl-1',3'-dioxolan-4-yl)ethylthio)-1,3-dithiol-2-thione (**298**).



To *bis*-acetyl protected dithiolate (**106**) (62 mg, 0.21 mmol) under a nitrogen atmosphere was added a mixture of dry MeOH/dry THF (4 ml/ 2 ml). The flask was cooled to 0°C and solid sodium methoxide added (26 mg, 0.48 mmol). The usual change in colour was observed (from yellow/light brown to deep red/purple) and the resulting mixture was left to stir for further 30 min after the change in colour was detected. A solution of tosylate (**302**) (0.126 g, 0.42 mmol) in dry THF (4 ml) was added dropwise and the mixture was left to stir and warm up to r.t. for 3 h. No changes were detected after monitoring the reaction by tlc so the temperature was increased to 45°C for 2 h and then up to 60°C for further 7 h without any visible change on the tlc plate. The reaction was quenched with

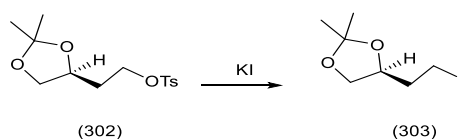
methyl iodide and stopped. The desired product was not identified after purification by flash chromatography.

3.5.26 Attempted synthesis of (*S*)-4-(2'-iodoethyl)-2,2-dimethyl-1,3-dioxolane (**303**)



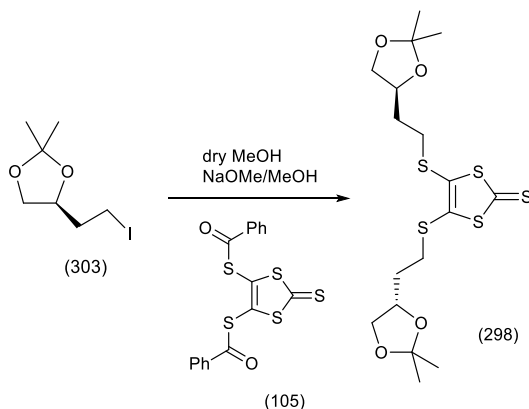
A mixture of triphenyl phosphine (1.35 g, 5.14 mmol), iodine (1.31 g, 5.14 mmol) and imidazole (0.37 g, 5.44 mmol) in diethyl ether (15 ml) was cooled down to 0°C under a nitrogen atmosphere. A solution of (*S*)-(+)-4-(2-hydroxyethyl)-2,2-dimethyl-1,3-dioxolane (0.5 g, 3.42 mmol) in diethyl ether (5 ml) was added and the suspension was left to stir and warm up to r.t. for 3 h. The reaction mixture was quenched with sodium thiosulphate (30 ml) and ammonium chloride (30 ml). Ether (10 ml) was added and the organic layer collected and washed with water (30 ml) and brine (30 ml) and dried over MgSO₄. After the ether was evaporated a white solid and a colourless oil were visible in the flask. Characterisation by NMR evidenced the presence of triphenyl phosphine oxide (20%) together with the desired iodo compound (**303**). Attempted purification by flash chromatography and removal of the triphenyl phosphine oxide by recrystallization at low temperature was not completely successful.

3.5.27 Synthesis of (*S*)-4-(2'-iodoethyl)-2,2-dimethyl-1,3-dioxolane (**303**).



The tosylate (**302**) (0.43 g, 1.45 mmol) and potassium iodide (0.80 g, 4.82 mmol) were dissolved in acetone AR (15 ml) and the solution was left to stir at 50°C overnight. Diethyl ether (10 ml) was added and the organic layer was washed with water (20 ml) and brine (20 ml) and dried over Na₂SO₄. The desired iodo compound (**303**) (0.13 g 35%) was recovered as a colourless oil; δ_H (400 MHz, CDCl₃): 4.10 (1H, m, 4-*H*), 4.00 (1H, dd, *J* = 16.0, 8.1 Hz, 5-*H_α*), 3.49 (1H, dd, *J* = 16.0, 10.5 Hz, 5-*H_β*), 3.17 (2H, m, 2'-*H₂*), 2.0 (2H, m, 1'-*CH₂*), 1.32 (3H, s, 2-*CH₃*), 1.27 (3H, s, 2-*CH₃*); δ_C (100 MHz, CDCl₃): 107.8 (2-*C*), 74.3 (4-*C*), 67.4 (5-*C*), 36.6 (1'-*CH₂*), 25.7, 24.3 (2 x 2-*CH₃*), 0.0 (2'-*C*).

3.5.28 Synthesis of 4,5-bis(4''-S-2''-(2'',2''-dimethyl-1'',3''-dioxolan-4''-yl)ethylthio)-1,3-dithiol-2-thione (298).



A mixture of the *bis*-benzoyl protected thione (**105**) (99 mg, 0.24 mmol) in dry MeOH (5 ml) under a nitrogen atmosphere was cooled down to 0 °C and treated with NaOMe/MeOH (25% by weight) solution to furnish dithiolate (**95**). The usual dark red-purple solution appeared. After 30 min. a solution of iodo-compound (**303**) (0.13 g, 0.49 mmol) in dry MeOH (4 ml) was added dropwise. The mixture was left stirring and allowed to warm up to r.t. for 4 h. during which time an orange solution appeared. The methanol was evaporated under reduced pressure and DCM was added to the mixture. The organic layer was washed with water (30 ml) and brine (30 ml) and dried over MgSO₄. DCM was evaporated and the methyl benzoate was distilled off using a Kugelrohr oven. The crude product was purified by column chromatography (9:1 = cyclohexane: ethyl acetate) to furnish (**298**) (55 mg, 50%) as a red oil; δ_H (300 MHz, CDCl₃): 4.13 (2H, m, 2 x 4''-H), 4.00 (2H, m, 2 x 5''-H_w), 3.50 (2H, m, 2 x 5''-H_β), 2.83 (4H, m, 2 x 1'-H₂), 1.81 (4H, m, 2 x 2'-H₂), 1.34 (6H, s, 2 x 2''-CH₃), 1.28 (6H, s, 2 x 2''-CH₃); δ_C (100 MHz, CDCl₃): 210.0 (C=S), 136.2 (4-, 5-C), 109.3 (2 x 2''-C), 74.0 (2 x 4''-C), 68.9 (2 x 5''-C), 33.9, 33.1 (2 x 1'-, 2'-C), 26.9, 25.5 (4 x 2''-CH₃).

In the reaction performed involving the mixture (**303**)/O=P(Ph₃) no new product was observed under the same conditions reported above.

3.6 Bibliography.

1. F. Wudl, G. Smith and E. Hufnagel, *J. Chem. Soc. D: Chem. Comm.*, 1970, **21**, 1453; F. Wudl, D. Wobschall and E. J. Hufnagel, *J. Am. Chem. Soc.*, 1972, **94**, 670; J. Ferraris, D. Cowan, V. T. Walatka and J. Perlstein, *J. Am. Chem. Soc.*, 1973, **95**, 948.
2. a) E. Coronado, A. Forment-Aliaga, J. Galán-Mascarós, C. Giménez-Saiz, C. Gómez-García, E. Martínez-Ferrero, A. Nuez and F. Romero, *Solid State Sci.*, 2003, **5**, 917; b) E. Coronado and J. R. Galán-Mascarós, *J. Mater. Chem.*, 2005, **15**, 66; c) E. Coronado and P. Day, *Chem. Rev.*, 2004, **104**, 5419.
3. N. Avarvari and J. D. Wallis, *J. Mater. Chem.*, 2009, **19**, 4061;
4. G. Rikken and E. Raupach, *Nature*, 1997, **390**, 493; b) G. Rikken, J. Fölling and P. Wyder, *Phys. Rev. Lett.*, 2001, **87**, 236602; c) V. Krstić, S. Roth, M. Burghard, K. Kern and G. Rikken, *J. Chem. Phys.*, 2002, **117**, 11315.
5. J. D. Wallis, A. Karrer and J. D. Dunitz, *Helv. Chim. Acta*, 1986, **69**, 69.
6. F. Pop, P. Auban-Senzier, E. Canadell, G. L. Rikken and N. Avarvari, *Nature Comm.*, 2014, **5**, 3757.
7. B. Bleaney and B. Bleaney, *Electricity and Magnetism*, Volume 1, Oxford University Press, 2013.
8. a) J. Chalker and S. Sondhi, *Phys. Rev. B*, 1999, **59**, 4999; b) A. Kleiner, *Phys. Rev. B*, 2003, **67**, 155311; c) R. Roy and C. Kallin, *Phys. Rev. B*, 2008, **77**, 174513.
9. G. Grüner, *Rev. Mod. Phys.*, 1988, **60**, 1129; b) D. Jérôme and H. Schulz, *Adv. Phys.*, 1982, **31**, 299; c) D. Jerome, *Science*, 1991, **252**, 1509; d) L. P. Gor'kov and G. Grüner, *Charge Density Waves in Solids*, Elsevier, 2012.
10. a) G. Saito and S. Kagoshima, *The Physics and Chemistry of Organic Superconductors: Proceedings of the ISSP International Symposium*, Tokyo, Japan, August 28-30, 1989, Springer Verlag, 1990; b) J. M. Williams, J. R. Ferraro and R. J. Thorn, *Organic Superconductors*, 1992; c) K. Yamaji and G. Saitō, *Organic Superconductors*, Springer Verlag, 1998.
11. a) F. Pop, S. Laroussi, T. Cauchy, C. J. Gomez-Garcia, J. D. Wallis and N. Avarvari, *Chirality*, 2013, **25**, 466; b) F. Pop, M. Allain, P. Auban-Senzier, J. Martínez-Lillo, F. Lloret, M. Julve, E. Canadell and N. Avarvari, *Eur. J. Inorg. Chem.*, 2014, **24**, 3855; c) S. Yang, F. Pop, C. Melan, A. C. Brooks, L. Martin, P.

- Horton, P. Auban-Senzier, G. L. Rikken, N. Avarvari and J. D. Wallis, *CrystEngComm*, 2014, **16**, 3906.
12. R. J. Brown, A. C. Brooks, J. Griffiths, B. Vital, P. Day and J. D. Wallis, *Org. Biomol. Chem.*, 2007, **5**, 3172.
13. J. Griffiths, H. Nie, R. J. Brown, P. Day and J. D. Wallis, *Org. Biomol. Chem.*, 2005, **3**, 2155.
14. C. Réthoré, M. Fourmigué and N. Avarvari, *Chem. Comm.*, 2004, **12**, 1384; C. Réthoré, N. Avarvari, E. Canadell, P. Auban-Senzier and M. Fourmigué, *J. Am. Chem. Soc.*, 2005, **127**, 5748.
15. M. Chas, M. Lemarié, M. Gulea and N. Avarvari, *Chem. Comm.*, 2008, **2**, 220.
16. M. Lakshmikantham, A. F. Garito and M. P. Cava, *J. Org. Chem.*, 1978, **43**, 4394.
17. L. Martin, P. Day, S. Nakatsuji, J. Yamada, H. Akutsu and P. Horton, *CrystEngComm*, 2010, **12**, 1369.
18. a) P. Day and M. Kurmoo, *J. Mater. Chem.*, 1997, **7**, 1291; b) L. Martin, P. Day, H. Akutsu, J. Yamada, S. Nakatsuji, W. Clegg, R. W. Harrington, P. N. Horton, M. B. Hursthouse and P. McMillan, *CrystEngComm*, 2007, **9**, 865.
19. A. M. Madalan, E. Canadell, P. Auban-Senzier, D. Brânzea, N. Avarvari and M. Andruh, *New J. Chem.*, 2008, **32**, 333.
20. C. J. Gómez-García, E. Coronado, S. Curreli, C. Giménez-Saiz, P. Deplano, M. L. Mercuri, L. Pilia, A. Serpe, C. Faulmann and E. Canadell, *Chem. Comm.*, 2006, **47**, 4931; b) E. Coronado, S. Curreli, C. Giménez-Saiz, C. J. Gómez-García, P. Deplano, M. L. Mercuri, A. Serpe, L. Pilia, C. Faulmann and E. Canadell, *Inorg. Chem.*, 2007, **46**, 4446.
21. E. Coronado, J. R. Galán-Mascarós, C. J. Gómez-García, A. Murcia-Martínez and E. Canadell, *Inorg. Chem.*, 2004, **43**, 8072.
22. M. Brezgunova, K. Shin, P. Auban-Senzier, O. Jeannin and M. Fourmigué, *Chem. Comm.*, 2010, **46**, 3926.
23. J. Lieffrig, R. Le Pennec, O. Jeannin, P. Auban-Senzier and M. Fourmigué, *CrystEngComm*, 2013, **15**, 4408.
24. S. Yang, A. C. Brooks, L. Martin, P. Day, M. Pilkington, W. Clegg, R. W. Harrington, L. Russo and J. D. Wallis, *Tetrahedron*, 2010, **66**, 6977.
25. a) C. Piguet, G. Bernardinelli and G. Hopfgartner, *Chem. Rev.*, 1997, **97**, 2005; b) H. Miyake and H. Tsukube, *Chem. Soc. Rev.*, 2012, **41**, 6977.

26. F. Riobé, F. Piron, C. Réthoré, A. M. Madalan, C. J. Gómez-García, J. Lacour, J. D. Wallis and N. Avarvari, *New J. Chem.*, 2011, **35**, 2279.
27. P. Metrangolo, H. Neukirch, T. Pilati and G. Resnati, *Acc. Chem. Res.*, 2005, **38**, 386.
28. G. R. Desiraju and G. W. Parshall, *Mater. Sci. Monographs*, 1989, **54**, 326.
29. J. D. Wallis and J. Griffiths, *J. Mater. Chem.*, 2005, **15**, 347.
30. a) I. Awgheda, S. J. Krivickas, S. Yang, L. Martin, M. A. Guziak, A. C. Brooks, F. Pelletier, M. Le Kerneau, P. Day and P. N. Horton, *Tetrahedron*, 2013, **69**, 8738; b) L. Martin, J. D. Wallis, M. A. Guziak, J. Oxspring, J. R. Lopez, S. Nakatsuji, J. Yamada and H. Akutsu, *CrystEngComm*, 2014, **16**, 5424.
31. S. Yang, A. C. Brooks, L. Martin, P. Day, H. Li, P. Horton, L. Male and J. D. Wallis, *CrystEngComm*, 2009, **11**, 993.
32. J. O. Jeppesen, K. Takimiya, F. Jensen, T. Brimert, K. Nielsen, N. Thorup and J. Becher, *J. Org. Chem.*, 2000, **65**, 5794.
33. I. Danila, F. Riobé, F. Piron, J. Puigmartí-Luis, J. D. Wallis, M. Linares, H. Ågren, D. Beljonne, D. B. Amabilino and N. Avarvari, *J. Am. Chem. Soc.*, 2011, **133**, 8344.
34. a) K. Heuzé, M. Fourmigué, P. Batail, E. Canadell and P. Auban-Senzier, *Chem. Eur. J.*, 1999, **5**, 2971; b) A. N. Sokolov, T. Frišcic and L. R. MacGillivray, *J. Am. Chem. Soc.*, 2006, **128**, 2806; c) M. Mas-Torrent and C. Rovira, *J. Mater. Chem.*, 2006, **16**, 433.
35. a) R. Gómez, J. L. Segura and N. Martín, *Org. Lett.*, 2000, **2**, 1585; b) A. Saad, O. Jeannin and M. Fourmigué, *CrystEngComm*, 2010, **12**, 3866.
36. J. M. Klunder, S. Y. Ko and K. B. Sharpless, *J. Org. Chem.*, 1986, **51**, 3710; J. M. Klunder, T. Onami and K. B. Sharpless, *J. Org. Chem.*, 1989, **54**, 1295.
37. B. A. Baatz, M. Chem. Project: "Development of New Chiral Organic Donors for Use in Conductors and Superconductors", 2013, unpublished results
38. W. Felzmann, D. Castagnolo, D. Rosenbeiger and J. Mulzer, *J. Org. Chem.*, 2007, **72**, 2182.
39. S. P. Tanis and J. W. Raggon, *J. Org. Chem.*, 1987, **52**, 819.
40. K. Nicolaou, W. Qian, F. Bernal, N. Uesaka, P. M. Pihko and J. Hinrichs, *Angew. Chem. Int. Ed.*, 2001, **40**, 4068.
41. M. Yadav, R. Raghupathy, V. Saikam, S. Dara, P. P. Singh, S. D. Sawant, S. Mayor and R. A. Vishwakarma, *Org. Biomolec. Chem.*, 2014, **12**, 1163.

42. D. F. Taber, M. Xu and J. C. Hartnett, *J. Am. Chem. Soc.*, 2002, **124**, 13121

Chapter 4

**Synthesis of new metal binding
BEDT-TTF donors and their mag-
netic properties.**

4.1 Introduction.

The work presented in this chapter found its origin in the really exciting possibility of generating dual or multifunctional compounds which is one of the major goals in the field of material chemistry ¹⁾. The concept is to couple the conductivity of the organic electron donor (TTF, BEDT-TTF or derivatives) with a second species which exhibit a different property such as magnetism or optical activity (chapter 3). In the specific example of a material where electrical and magnetic properties are together different strategies have been applied over the years by many research groups ²⁾. The common factor is the presence of the TTF building block to ensure conductivity and they differ in the way the magnetic counterpart is introduced in the system ³⁾. The strategies are:

- a) by electrocrystallisation with an inorganic anion containing a paramagnetic centre ⁴⁻⁶⁾;
- b) by introduction of an organic radical on to the TTF or BEDT-TTF skeleton ⁷⁻¹⁰⁾;
- c) by forming a coordination complex with a paramagnetic centre via a ligand attached to the donor ¹¹⁻¹⁸⁾;

The situation *a)* has been investigated considerably and some examples of the inorganic anion containing a paramagnetic transition metal centre used are $[MX_4]^-$, $[M(CN)_6]^-$ or $[M^{III}(ox)_3]^{3-}$ and polyoxometallates such as Keggin $[M(H_2O)-(PW_{11}O_{39})]^{5-}$ and Dawson-Wells $[M(H_2O)-(P_2W_{17}O_{61})]^{8-}$ anions. The situation *a)* found its success with the preparation in 1995 of the first family of paramagnetic superconductors which contained layers of BEDT-TTF which were separated by $[M(ox)_3]^{3-}$ anions and solvent molecules. These compounds showed superconductivity between 4.0-8.3 K which showed a strong dependence on the solvent molecule in the lattice. It is worth mentioning that the experimental data showed the independence of the two networks from each other. Shortly afterwards a second family of superconductors was prepared from $[MX_4]^-$ anions (where X = Cl and Br) and BETS (*bis*-(ethylenedithio-tetraselenafulvalene) donor where the donor network and the anions were close to each other, enough for π -d and d-d interactions to have an effect on the resulting properties. The examples described above used discrete paramagnetic anions to afford magnetic ordering, whereas to achieve ferromagnetism a different strategy was followed. By using a polymeric anionic network such as a bimetallic oxalate-based layered complex successful results were achieved. To achieve ferromagnetism it is necessary that the polymeric anionic system, consisting of a mixed metal oxalate network and the cationic network of BEDT-TTF, assemble together in alternating layers. This was

obtained in the case of $(\text{BEDT-TTF})_3[\text{MnCr}(\text{ox})_3]$ which was found to be ferromagnetic below 5.5 K and metallic down to 0.2 K where the sublattices were found quasi-independent and the material to be anisotropic ²⁾. A similar material was formed with BETS ¹⁹⁾. These papers opened the route to the preparation of the first chiral ferromagnetic metal based on the enantiopure (S,S,S,S) -tetramethyl-ET (TM-ET) with the same inorganic polymeric anion used in the cases cited above ²⁰⁾. A common factor in these three examples is the disorder of the electron density between the organic layers and this can be explained by the compound being an incommensurate phase.

In the situation *b*) the introduction of magnetism by linking an organic radical to an organosulphur electron donor by a covalent bond can be found in the case of a TTF or EDT-TTF core as in **(305)** and **(306)** or in the case of a tetra-radical **(307)**, which have been prepared, characterised and studied by Sugawara *et al.* ^{7,10)} (Figure 112).

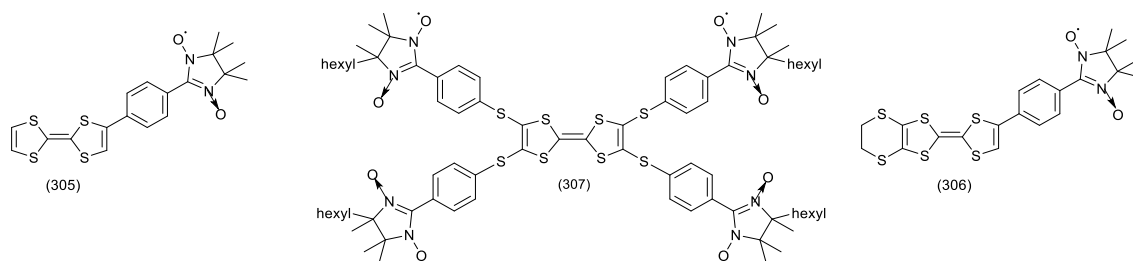


Figure 112. Examples of TTF derivatives bearing organic radicals by Suguwara *et al.*

Recently new TTF derivatives have been realised with a pyridyl-verzadyl **(308)** and ethenyl-verzadyl **(309)** radical by Pilkington *et al.* ^{8,9)} where the two units are connected by a conjugated spacer as shown below (Figure 113).

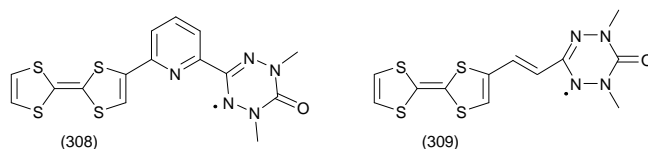
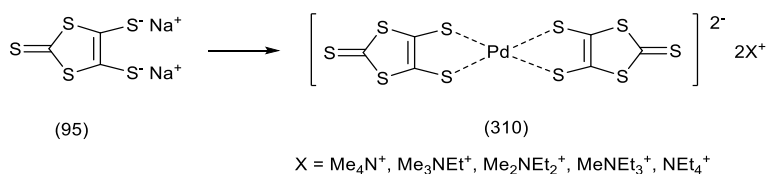


Figure 113. TTF donors substituted with organic radicals by Pilkington *et al.*

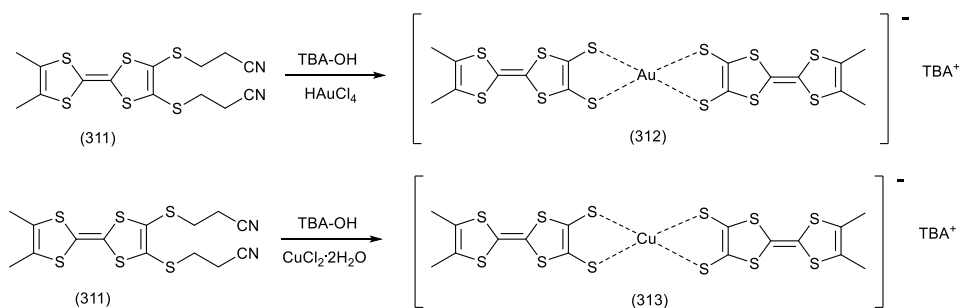
The situation *c*) is the type of hybrid organic-inorganic molecules whose preparation was attempted and is discussed in this chapter. The formation of a metallorganic discrete unit where the metal centre is directly connected with the organic donors has been studied and investigating deeply. In the literature there are many examples of TTF based ligands and their magnetic complexes ^{16,17)}, but very few examples of BEDT-TTF based ligands. ^{21,22)} For the situation *c*) the most widely used ligand involved in the preparation of organometallic species containing TTF is dithiolate (dmit) **(310)** (where $(\text{dmit})^{2-}$ is 2-thioxo-1,3-dithiol-4,5-dithiolato) and its analogues which form square planar complexes. The first superconductor containing a transition metal complex, $(\text{TTF})[\text{Ni}(\text{dmit})_2]_2$, was prepared

by Brossard *et al.*²³⁾. Below is shown, a palladium *bis*-(dmit) prepared by Qi *et al.*¹³⁾ where changing the size of the cation changed the conducting properties of the compound itself.



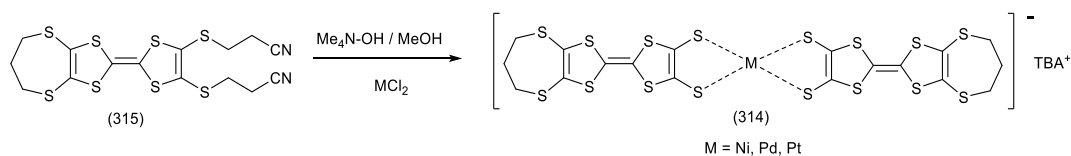
Scheme 105. A series of Pd(dmit)₂ complexes by Qi *et al.*

Another example of how metal centre and ligand based donors have been prepared as a dimeric species is presented below. For example Kobayashi *et al.*¹²⁾ deprotected a *bis*-(cyanoethyl) precursor (311) to give a TTF dithiolate from which a gold complex (312) and a copper complex (313) have been prepared.



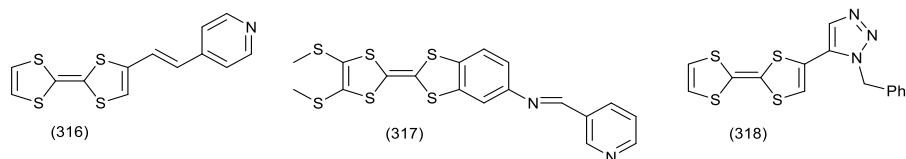
Scheme 106. Examples of dmit complexes prepared by Kobayashi *et al.*

By using the same strategy a series of *bis* complexes of palladium, nickel and copper (314) were prepared from donor (315)²¹⁾ as showed in the Scheme 112.



Scheme 107. Other examples of dmit complexes prepared.

More recently the TTF based ligands with pyridine or other nitrogen containing heterocycles as the binding site such as the TTF-CHCH-py (316) and its complexes have been prepared by Ouahab *et al.*¹⁷⁾. The Schiff base ligand (317) and related complexes were reported very recently by Zuo *et al.*¹⁵⁾. Another example is the work from Avarvari *et al.* on TTF-1,2,3-triazoles (318) and its complexes¹⁸⁾.

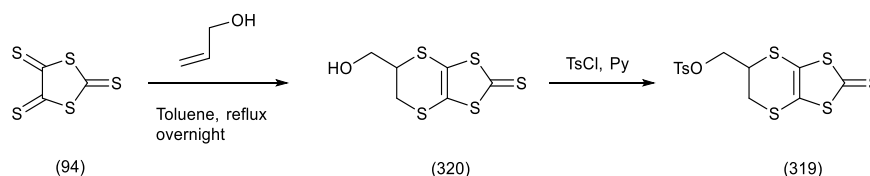


Scheme 108. TTF-ligands substituted with heterocycle as binding groups.

4.2 Background.

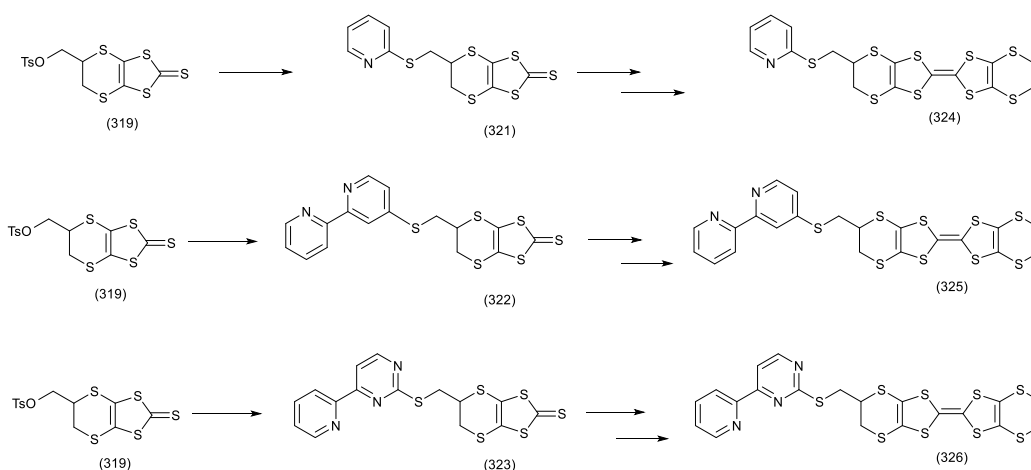
Over the past decade a range of BEDT-TTF functionalised donors have been prepared with the aim of coordinating a metal centre to achieve the preparation of multifunctional materials where electrical conductivity and magnetism could co-exist. In this section a few example of the molecules synthesised in the Wallis group are reported. The donors are under continuous investigation due to the large variety of metal salts available. The first batch of compounds prepared involved as binding site *a)* pyridine, *b)* 2, 2'-bipyridine and *c)* a 2,4'-pyridylpyrimidine and the synthetic strategy applied was to introduce the binding site before the completion of the sulphur network (Scheme 110).

In the Scheme 109 is reported the preparation of the tosyl-oxo-methyl-thione (**319**)²¹ and in the Scheme 110 is reported how this was a useful building block for the introduction of different types of metal binding group.



Scheme 109. Preparation of thione (**319**).

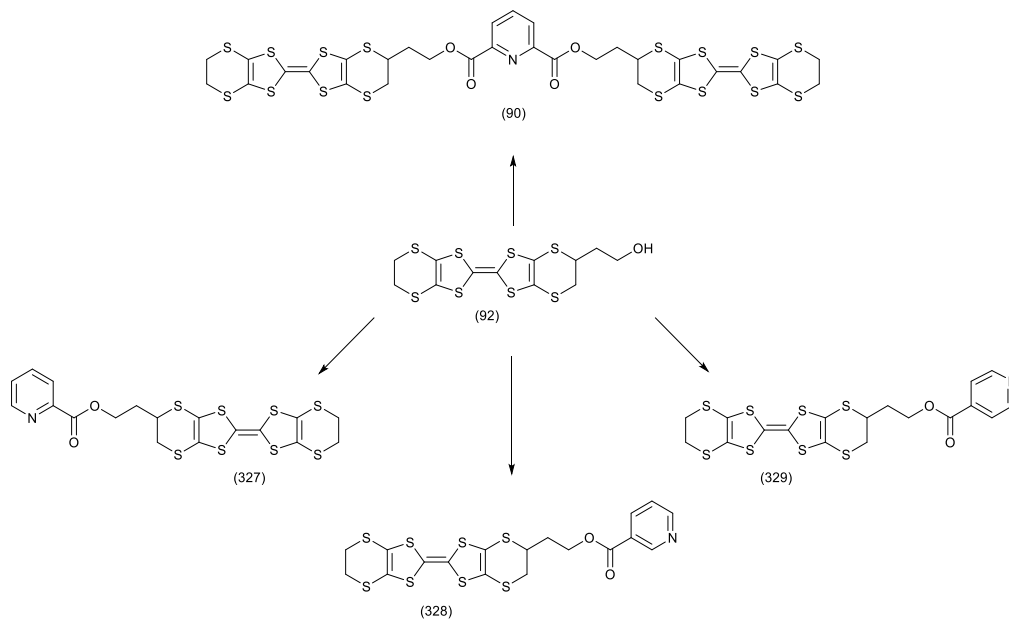
The preparation of thione (**321**), (**322**) and (**323**) has been achieved by reacting thione (**319**) with pyridyl-2-thiolate, 2,2'-bipyridyl-4-thiolate and 2,4'-pyridylpyrimidine-2'-thiolate respectively²¹ in order to prepare final donors (**324**), (**325**) and (**326**) by following standard procedures.



Scheme 110. Preparation of thiones (**321**), (**322**) and (**323**) and final donors bearing metal binding sites.

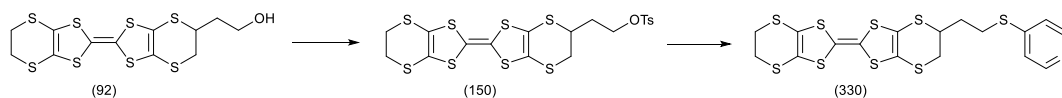
The synthesis of further metal binding BEDT-TTF type ligands followed a different strategy which involved the introduction of the binding site at the end of the synthetic

route shown below in Scheme 111. The suitable starting material for these new donors was the HEET donor **(92)** previously synthesised and reported in the literature ²¹).



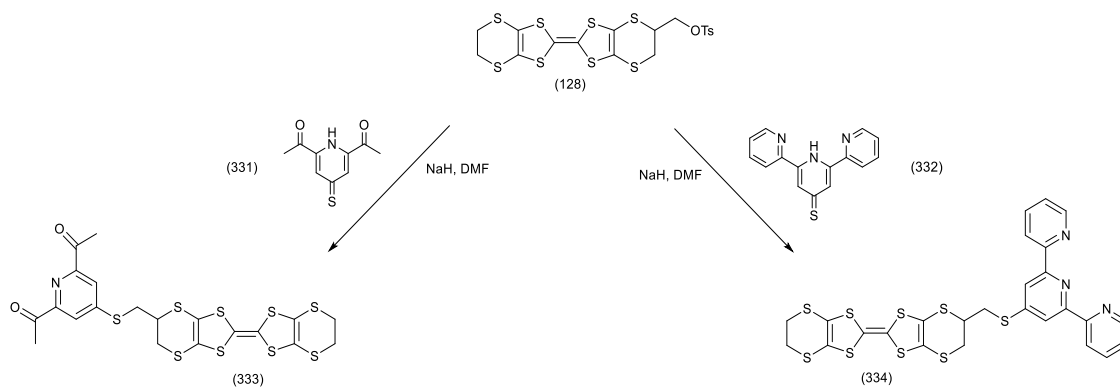
Scheme 111. Preparation of a second batch of metal binding ET donors.

The same strategy has been used to generate another metal ligating donor, such as **(330)** which is similar to donors **(324)**-**(326)** previously reported. The starting material was in this occasion the tosyl-oxo-ethyl-BEDT-TTF **(150)** whose preparation is reported in the literature.



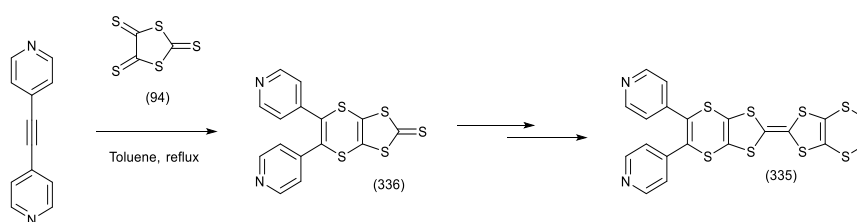
Scheme 112. Preparation of donor **(330)**.

Some more metal binding BEDT-TTF type donors were prepared by reacting the tosylate of HMET donor **(128)** with a thiolate such as **(331)** or **(332)** to give the methyl-thio pyridyl and terpyridyl substituted donors **(333)** and **(334)**.



Scheme 113. Preparation of donors (333) and (334).

The last example we report is interesting due to the π -connection between the donor and the binding site as shown in the scheme below ²¹).



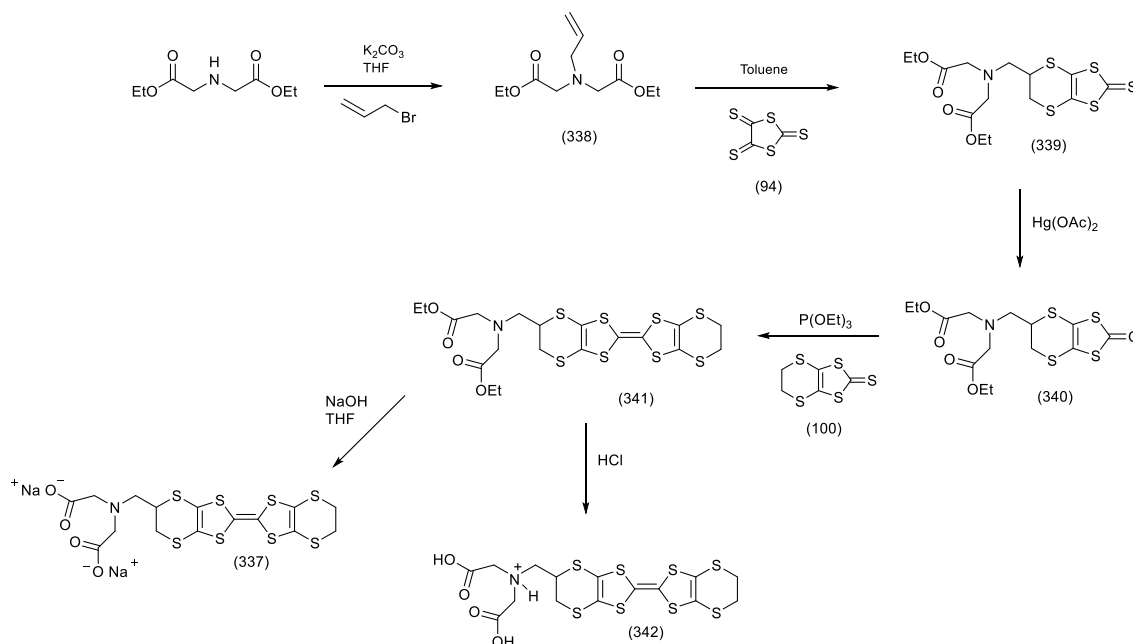
Scheme 114. Preparation of donor (335) by dipyritylacetylene.

These are just a few examples of the metal-binding-substituted-ET prepared in the Wallis laboratory and currently under investigation. This chapter is focused on the work undertaken during this PhD to prepare new BEDT-TTF substituted ligands with side chain suitable for metal coordination.

4.3. Results and Discussion.

4.3.1 Synthesis of the new BEDT-TTF donors containing the imino-diacetate ligand.

To explore the field of multi-property material where a paramagnetic metallic centre is linked to one or more BEDT-TTF units, the synthesis of novel donor (**337**) was designed. This donor contains a tridentate ligand binding site thanks to the presence of a nitrogen and two carboxylate functions in the iminodiacetate group. The synthesis was planned as described below (Scheme 115).



Scheme 115. Synthetic route to novel ligands (**337**).

The preparation of donor (**337**) involved as first step the reaction between allyl bromide and diethyl iminodiacetate to furnish alkene (**338**) in 86% yield as a yellow oil. Characterisation by NMR spectroscopy evidenced the presence of the terminal double bond thanks to the multiplet at 5.88 ppm and the two double doublets at 5.22 and 5.17 ppm with a coupling constant of 18.8 and 10.1 Hz for the *trans* and *cis* protons respectively. The same evidence is outlined in the carbon resonance where the two sp^2 carbons fall at 134.9 and 118.3 ppm. The 1H -NMR spectrum showed also the presence of the ethyl chains with peaks at 4.17 ppm at 1.27 ppm. It is worth to mention that in these two signals some extra peaks are present even if no solvent such diethyl ether or ethanol was used ²⁴).

The extra peaks may belong to the starting material, the diethyl iminodiacetate, but according to the literature ²⁵, the $-\text{CH}_2$ falls at 3.35 ppm and this signal is not visible in the recorded spectrum of (**338**).

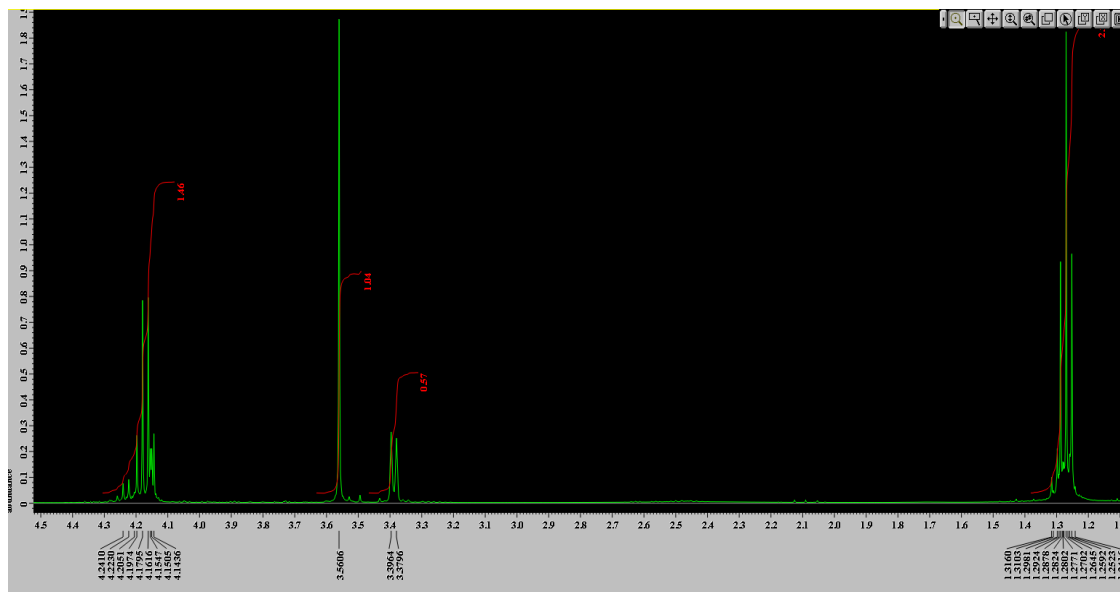


Figure 114. Proton NMR for alkene (**338**).

An enlargement is also presented (Figure 115) to visualise better the extra peaks in the ethyl and methyl regions. An enlargement is also shown for the range where the $\text{NH}(\text{CH}_2)$ signal of the starting material should fall if present.

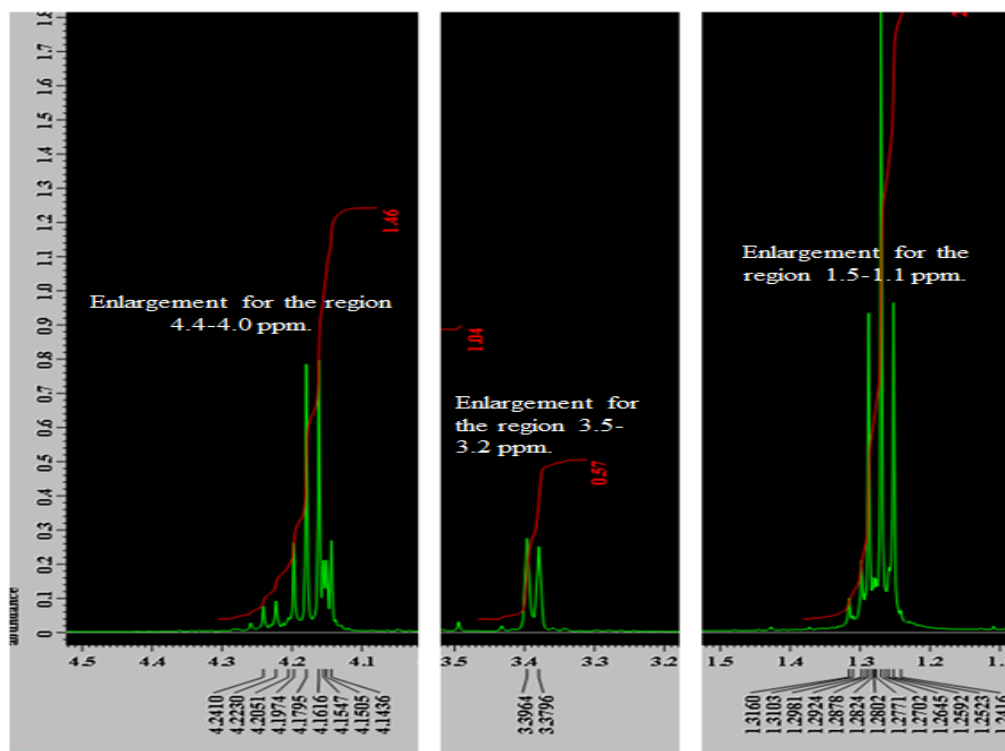


Figure 115. Enlargement for the zones where extra peaks are seen and where $\text{NH}-\text{CH}_2$ in the starting material should fall if present.

The ^1H -NMR is completed by the presence of a singlet at 3.57 ppm for the two $-\text{CH}_2$ groups in between the nitrogen and the ester groups and of a doublet at 3.39 ppm for the allylic $-\text{CH}_2$ group. The ^{13}C -NMR pattern evidenced the presence of the two ester functionalities by showing peaks at 170.6 ppm for the carbonyl and at 60.0 ppm for $-\text{CH}_2$ and 13.8 ppm for the methyl group. Characterisation was completed by the elemental and the MS analysis where a peak at m/z 230.1383 was revealed for $[\text{M}-\text{H}]^+$ against the theoretical m/z at 230.1387. The next step is the Diels-Alder type cyclo-addition by reacting **(338)** with trithione **(94)** in refluxing toluene overnight. Thione **(339)** was isolated after column chromatography as a dark-red solid in 90% yield. It is worth to mention that a small amount of crude thione **(339)** was also analysed by NMR spectroscopy, before purification of the compound itself, and it was found pure enough to proceed with the next step. Due to this comparison thione **(339)** was obtained simply by filtration of the solid formed during the cyclo-addition reaction and was used as it was after evaporation of solvent without further purification. By following this procedure the thione **(339)** has been obtained in quantitative yield. Proton and carbon resonances showed clean NMR spectra but nevertheless the tlc showed few spots, of weak intensities, above desired compound (yellow spot) so the isolated thione is still a mixture. ^1H and ^{13}C -NMR spectra evidenced the formation of the six-membered ring due to the presence of a multiplet at 3.72 ppm which was assigned to the 5-H and the two double doublets at 3.14 and 3.04 ppm for the protons of the ring $-\text{CH}_2$ next to the sulphur. The presence of a second set of two double doublets at 3.44 and 3.29 ppm was assigned to the 5- CH_2 -N protons. It is interesting to note that the corresponding hydrogen atoms gave a double doublet in the spectrum of dienophile **(338)** while in the thione **(339)** is splitted into two double doublets. This change is likely to be caused by the stereogenic centre at the ring 5-position. Characterisation by elemental analysis and mass spectrometry supported the structure.

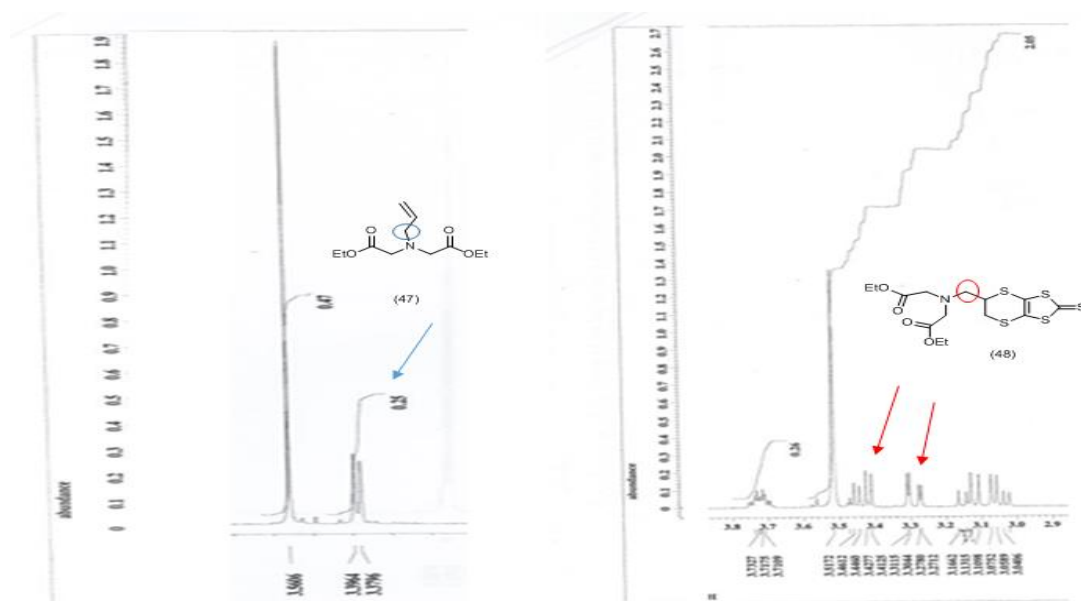


Figure 116. Proton signals split after cyclisation reaction (red arrows).

Exchange of the thione sulphur for oxygen was carried out using the standard procedure to give oxo compound (**340**) in 91% yield. Characterisation by ^{13}C - NMR showed the peak at 188.2 ppm which confirmed the desired transformation occurred. The mass spectrum showed a peak at m/z 410.0208 for $[\text{M}-\text{H}]^+$ against a theoretical value at m/z 410.0219. The final step for the completion of the sulphur network is the coupling between oxo species (**340**) with unsubstituted thione (**100**) using freshly distilled triethyl phosphite to give donor (**341**) in 34% yield after purification by chromatography. The orange solid obtained was characterised by NMR spectroscopy where the proton resonance showed the presence of a singlet at 3.03 ppm which was assigned to the 5', 6'- CH_2 of the ethylenedithio bridge of the unsubstituted side of the donor. The presence of this signal among all the other peaks belonging to the methyl-amino-diacetate chain suggested the coupling was successful. The ^{13}C -NMR showed the peak of the unsubstituted ethylene bridge at 30.1 ppm together with multiple peaks for the sp^2 carbons at 113.8, 113.7, 112.6, 112.2 and 111.3 ppm. Elemental analysis completed the identification of the donor. The identity of the cross-coupled donor (**341**) has also been confirmed by X-ray crystallography. A single crystal suitable for XRD analysis of the donor was obtained by slow evaporation of a DCM solution. In Figure 117 the structure of donor is presented in the picture *a*), while its packing in the unit cell is presented in *b*).

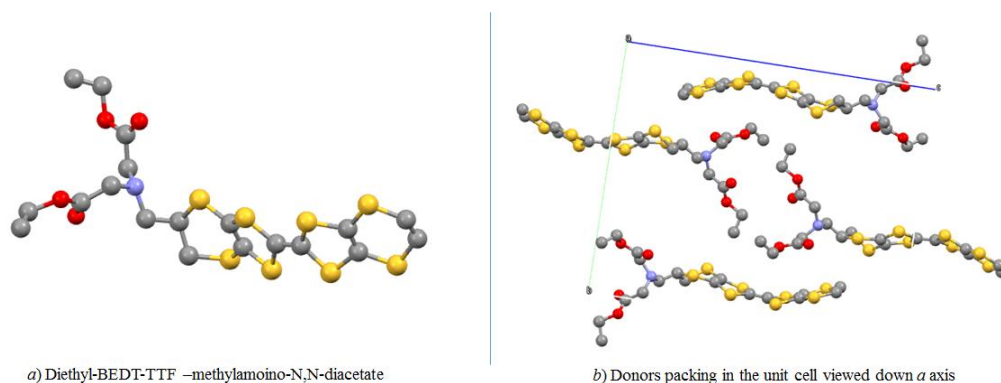


Figure 117. Crystal structure of *a*) donor (**341**) and *b*) its packing in the unit cell viewed from *a* axis.

It is interesting to see how in this case the donors do not form the usual dimer motif due to the π - π stacking and S---S non-covalent interaction on account of the steric hindrance of the lateral chain, but they are arranged one next to the other in long lines. This is even more visible in Figure 117 *b*) where the chains face each other and the donors are pushed in the opposite direction to each other. In Figure 118 *b*) this concept is outlined by developing the short contacts S---S between donors (3.378(5) and 3.418(3) Å) and indeed is very clearly how the two chains, by facing each other, form some sort of cavity in between them and here could be the metal once the ethyl chain would be removed.

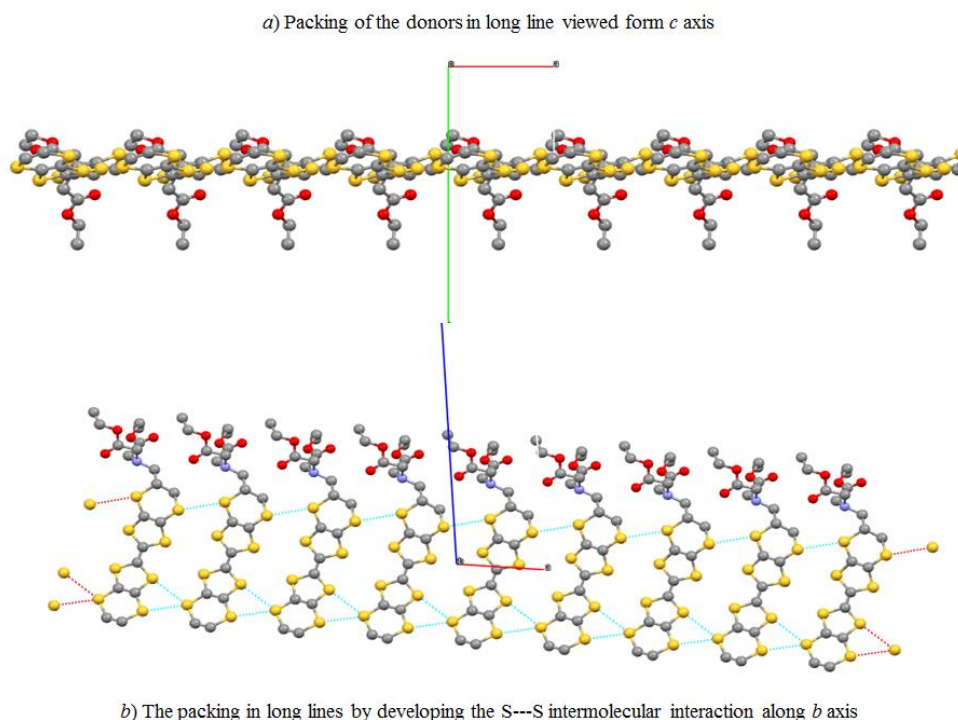


Figure 118. Infinite line of donors connected through S---S intermolecular interactions viewed along *a*) *c* and *b*) *b* axis.

In Figure 119 is also recognisable the “Y” shaped formed by the donor itself and the motif formed by the two lines of donors approaching each other.

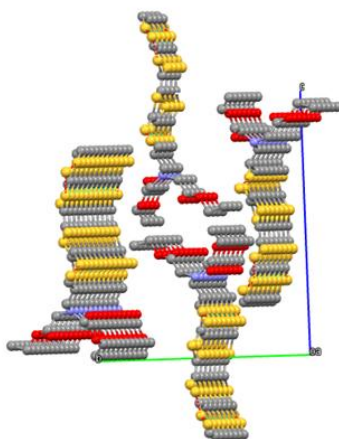
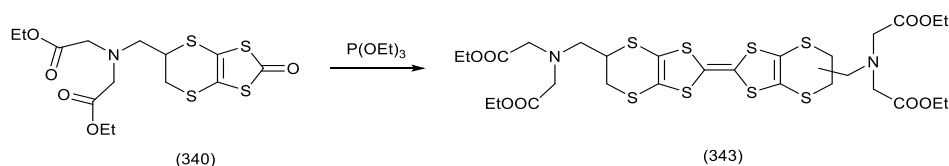


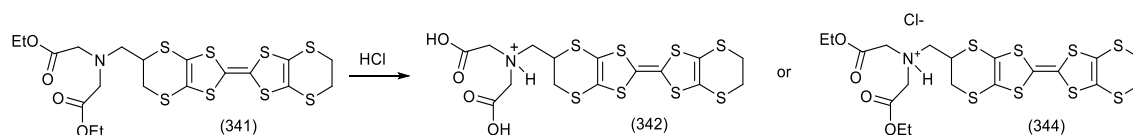
Figure 119. Characteristic “Y” shaped formed by donors packing one next to each other.

After preparation of the cross-coupled donor (**341**), the homo-coupled donor (**343**) was also prepared by performing a separate reaction. This tetra-ester compound (**343**) is one of the by-products of the phosphite mediated coupling reaction between unsubstituted thione (**100**) and oxo-compound (**340**) but it is usually isolated in very small yield. The self-coupling reaction of the oxo-compound (**340**) in freshly distilled triethyl phosphite was carried out at 90°C overnight under a nitrogen atmosphere. The phosphite was distilled off by Kugelrohr oven and the residue purified by flash chromatography (3:1=cyclohexane: ethyl acetate) to yield homo-coupled compound (**343**), as a mixture of two diastereoisomers, as a dark-red oil in 14% yield. The 5,5' and 5, 6'-substituted diastereoisomers are present and the only difference in ¹H-NMR is showed for signals at 3.40 and 3.25 ppm. In more details the ¹H-NMR showed the presence of the 5-H proton as a multiplet at 3.87 ppm, then at 3.52 ppm is the singlet for the –CH₂ group in between the esters and the nitrogen. Then a series of multiplet 3.42-3.38, 3.28-3.22 and 3.05-3.01 ppm are the protons for the 6-H₂ and 5-CH₂ which for the homo-coupled compound are difficult to interpret due to the presence of two diastereoisomers. The ¹³C-NMR shows the peaks for the ester functionalities at 171.6 ppm, carbonyl, 60.8 and 14.5 ppm for the –CH₂ and CH₃. The *sp*² carbons resonate at 115.7, 113.8, 114.6 and 114.1 ppm. The –CH₂ next to the nitrogen is visible at 58.8 ppm and the carbon 5-CH₂ resonate at 56.3 ppm. Then the carbon of the six-membered ring are visible at 44.5 and 33.2 ppm.



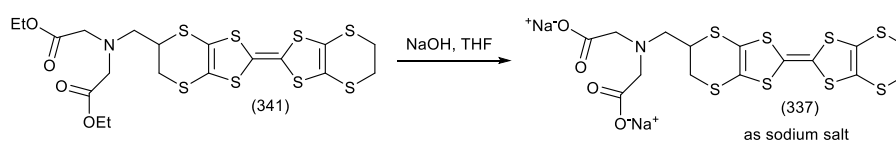
Scheme 116. Preparation of homo-coupled donor (**343**).

At this stage the donor synthesis is not complete because the two ester functionalities have no metal ion binding properties in the neutral form. Hydrolysis of the two ester groups was necessary and as shown in the Scheme 117 two options were available. The first option could be the hydrolysis in acidic conditions to try to generate the acid (**342**) which could be a very interesting metal binding donor even in the neutral form. Unfortunately the hydrolysis can also lead to the formation of the ammonium salt (**344**) and for this reason the hydrolysis in acidic condition has not been performed.



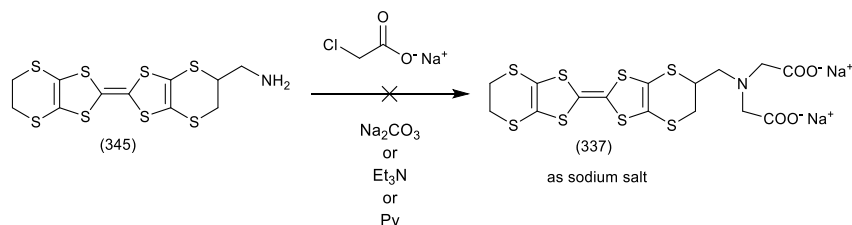
Scheme 117. Possible products formed after an acidic hydrolysis on donor (**341**).

The second option would be to use a base, such a sodium hydroxide in order to liberate the oxygens and make them free to coordinate the metallic centre. The downside of this hydrolysis is that the donor obtained would be a salt and would probably be more difficult to handle as experience demonstrated. In the end it was decided to carry out the hydrolysis in basic conditions in order to generate a donor with binding properties. The reaction was carried out using two equivalents of sodium hydroxide in THF at 50°C and the mixture was left to stir overnight. The THF was evaporated and the residue was washed with dichloromethane to dissolve any unreacted starting material. The residue was also washed with small portions of water to eliminate the sodium hydroxide followed by washing with diethyl ether to dry the filtered solid. The residue obtained was a red-pink solid identified as disodium salt (**337**). It was completely insoluble in the common organic solvents and in water and characterisation by NMR was not possible. The only solvents where the solution was slightly coloured were carbon disulphide, DMF and DMSO but even with long experiments no NMR peaks were visible other than solvent. Indeed no crystals of the disodium salt itself could be obtained for X-ray crystallography. Characterisation by IR spectroscopy helped outline the difference between the neutral donor and the disodium salt and the elemental analysis result was in accordance with a tetra-hydrate of the disodium salt donor. This evidence does not complete the identification of the final salt obtained, but is reasonably supportive.



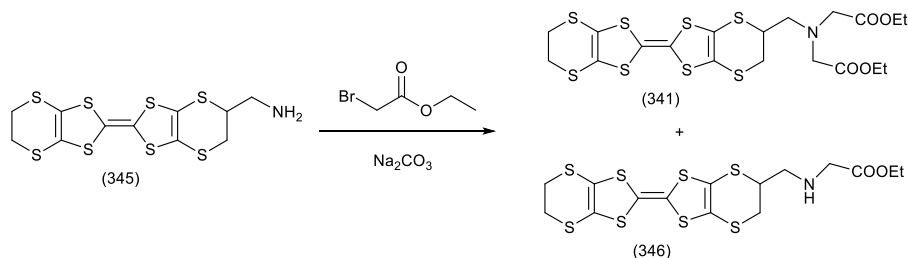
Scheme 118. Preparation of sodium salt of donor (**337**) by basic hydrolysis.

The procedure outlined in the Scheme 115 to generate donor (**337**) is the result of various previous attempts²⁶⁾ which are worth mentioning. The first strategy was to prepare the ligand (**337**) by reacting the AMET donor (**345**) with sodium chloroacetate in presence of a base, such as *a*) sodium carbonate, *b*) triethylamine or *c*) pyridine. Unfortunately in all the cases the compound isolated and characterised by NMR spectroscopy was not the desired one.



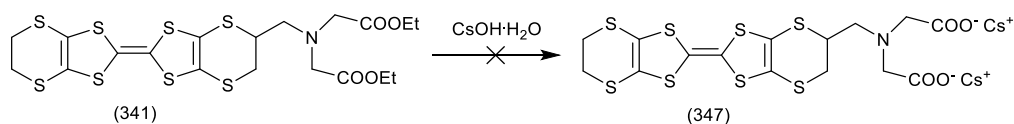
Scheme 119. First attempted reaction to achieve preparation of donor (**337**).

A more successful strategy was to react the AMET donor (**345**)²⁷⁾ with ethyl bromoacetate which yielded after purification by flash chromatography the desired diester (**341**) in 16% yield and the monoester (**346**).



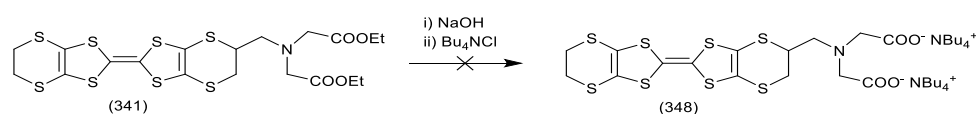
Scheme 120. Mixture of product obtained by reacting AMET donor (**345**) and bromoethylacetate.

A more soluble salt would be preferable for preparing coordination compounds. The strategy adopted was to attempt to increase the solubility by replacing the sodium with *a*) caesium or with *b*) a tetrabutylammonium cation which may be more soluble in organic solvents. To attempt to make the caesium salt (**347**), the diester donor (**341**) was reacted with caesium hydroxide first at room temperature and then in refluxing THF due to lack of reaction. The TLC plate still showed presence of starting material after 24 hours under reflux. The aqueous soluble product was isolated as an oil, but characterisation by NMR was impossible due to an instantly jelling of the sample in DMSO- d_6 and no spectrum was observed.



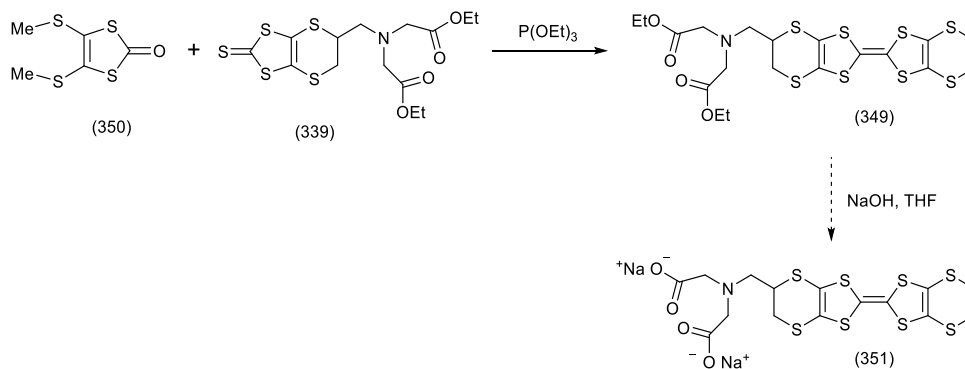
Scheme 121. Attempting preparation of a caesium salt of donor (347).

The second attempt involved the reaction between the diester (341) and two equivalents of sodium hydroxide in THF followed by addition of 2 equivalents of tetrabutylammonium chloride. The reaction was conducted at room temperature, followed by evaporation of the THF and addition of DCM. Isolation of the organic compound furnished a brown oil which characterised by ¹H-NMR evidenced the presence of tetrabutylammonium protons only, no other peaks were visible.



Scheme 122. Attempting preparation of the TBA salt of donor (348).

The second strategy designed to improve the solubility of the sodium salt of (337) was to replace the unsubstituted dithiin ring with two methylthio groups. The preparation of the new donor (349) is outline in Scheme 128 and it was generated by reacting thione (339) and oxo-compound (350)²⁸⁾ in freshly distilled triethyl phosphite at 95°C. The mixture was purified by column chromatography and desired donor (349) was obtained as a brown oil in 22% yield. The two methyl groups can help to increase the solubility and reduce the stacking interaction between the donors in the solid state. Characterisation by ¹H-NMR showed the presence of a singlet at 2.34 ppm which belongs to the two methylthio groups together with the peaks for the diethyl iminoacetate group. The required hydrolysis to generate final donor (351) will be performed in the next future by other researchers.



Scheme 123. Preparation of new donor (349) and final hydrolysed donor (351).

4.3.2 Preparation, characterisation and investigation of the magnetic properties of metal complexes formed using donor (337).

Despite the solubility of the sodium salt of donor (337) being an issue from the first moment it was decided to develop some coordination chemistry by reacting the novel donor with various metallic salts containing paramagnetic and diamagnetic transition metal centres. This work was done in order to establish if it was possible to introduce magnetism and conductivity in the same metallorganic compound eventually formed where the two units, metallic centre and donor, were connected by a covalent bond. The purpose was also to gain more knowledge of the coordination chemistry of BEDT-TTF based donors which has not been explored in depth by the academic community.

The first batch of experiments carried out with the sodium salt of donor (337) involved the use of distilled water as a solvent and metal salts such as iron (III) chloride, ruthenium (III) chloride hydrate, manganese (II) chloride tetrahydrate and manganese (II) (hexafluoroacetylacetonate) trihydrate. The selected metal centres $\text{Ru}^{\text{(III)}} (d^3)$, $\text{Mn}^{\text{(II)}} (d^3)$, $\text{Fe}^{\text{(III)}} (d^5)$ are all paramagnetic and this could lead to magnetic behaviour of the final compound. Water has been chosen, initially, because the metal salts used were soluble in it while the donor was not, so any precipitate eventually formed from the reaction of different colour or composition would be an evidence of the formation of a new coordination complex between donor and metal salt. After the first few reactions performed in water the solvent was changed to MeOH. Addition of the metal salt to a stirred suspension of the sodium salt of donor (337) in water or MeOH led to an immediate precipitate in every reaction performed. The mixture stirred for few hours to ensure complete reaction and the solid formed was isolated by filtration and washed with diethyl ether and dried. The compounds have been analysed by elemental analysis and infra-red spectroscopy to gain information on composition and functional groups present. No suitable crystals have been obtained due to the high insolubility of the solids recovered from the reactions. The solid obtained were shipped to the Pilkington group at Brock University for magnetic measurements using a SQUID to detect their magnetic properties.

For all the reactions performed the data available were limited and difficult to interpret to give an unambiguous solution. The results reported in this paragraph represent simple proposals for the structures based on the data available and no complete conclusion nor confirmation of the identity has been yet achieved. It is also worth mentioning that the

tridentate ligand may present either a carboxylate binding site or a neutral carboxylic acid function. Investigation has been carried out in the Cambridge Structural Database and examples were found to support this ²⁹).

4.3.2.1 FeCl₃+ligand (337): Complex (1);

Iron ^(III) chloride was reacted with an excess of the sodium salt of ligand (337) and immediately a dark solid precipitated out from the suspension. The solid was filtered and analysed by CHN. The dark colour is due to the oxidation of the donor in the presence of Fe^(III), so in the complex formed the metal is in its reduced form Fe^(II) and the donor is a radical cation. As a result of this oxidation process the organic radicals are likely to be dimerised in the solid state, where two donors are probably facing each other (π - π stacking and S---S interactions) and their magnetic influences would cancel out one. So in this case the magnetism is purely due to the metal centre. The CHN data showed such a composition C 27.45; H 2.20; N 2.32% which would be in accordance with the formula C₁₅H₁₃S₈O₄NFeCl·2H₂O that requires C 27.46, H 2.18, N 2.33%. If this is the situation the Fe^(II) would be surrounded by one ligand (337), one chloride and two molecules of water as outlined in Figure 120.

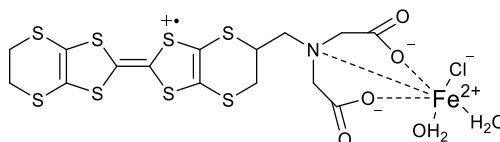


Figure 120 Proposed structure for Fe (II) complex with ligand (337).

The magnetic measurement gave, for the MW suggested, a high temperature value $\chi(T) = \sim 1.4 \text{ cm}^3 \cdot \text{K} \cdot \text{mol}^{-1}$. The expected value for the Fe (III) oxidation state is $\chi(T) = \sim 4.38 \text{ cm}^3 \cdot \text{K} \cdot \text{mol}^{-1}$ for a high spin state ($S=5/2$), or $\chi(T) = \sim 0.38 \text{ cm}^3 \cdot \text{K} \cdot \text{mol}^{-1}$ for a low spin state ($S=1/2$). Due to the fact that the iron is now in its reduced state, Fe(II), the recorded magnetic susceptibility value could be the result of a mixture of high spin and low spin Fe (II) centres. This is not unreasonable because the Fe(II) high spin should give a value of $\chi(T) = \sim 3.00 \text{ cm}^3 \cdot \text{K} \cdot \text{mol}^{-1}$ while the Fe (II) low spin should give $\chi(T) = \sim 0 \text{ cm}^3 \cdot \text{K} \cdot \text{mol}^{-1}$ because of its d electrons all paired. The average value of this two configurations would give $\chi(T) = \sim 1.5 \text{ cm}^3 \cdot \text{K} \cdot \text{mol}^{-1}$ which is very close to the experimental one. Indeed from the plot $\chi(T)$ vs T , reported in Figure 121, there is a visible gradual downward slope which is consistent with a slow and incomplete spin crossover transition to more low spin centres as the temperature decreases. On Figure 121 at 300 K the $\chi(T)$ value of 1.43 suggests a ratio 1:1 of high spin and low spin centres, while at 2 K the $\chi(T)$ value is 0.85

closer to a 1:2 or 1:3 ratio. In conclusion at this preliminary stage the situation is consistent with a mixture of Fe (II) high spin and low spin, but a more complex structure with more spin centres cannot be excluded. The next steps to gain more information on this solid would be a chlorine analysis to establish without doubt the presence or not of chlorine and the use of Mossbauer spectroscopy to determine the exact ratio between high spin to low spin centres as temperature changes.

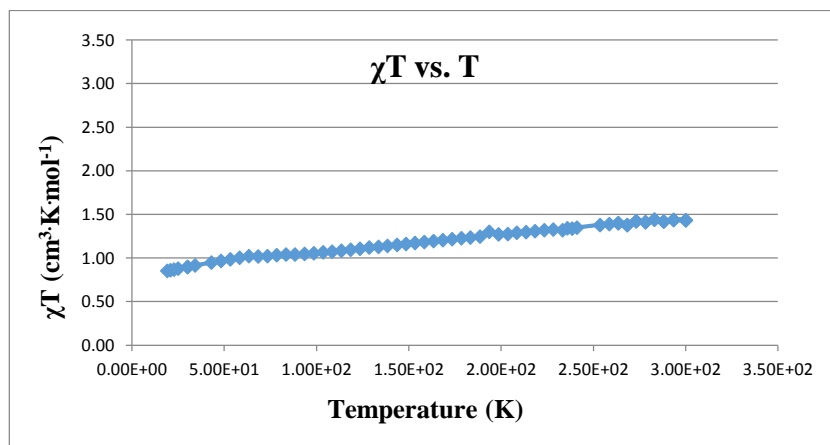


Figure 121. $\chi(T)$ vs T data for Fe (II) complex with (337).

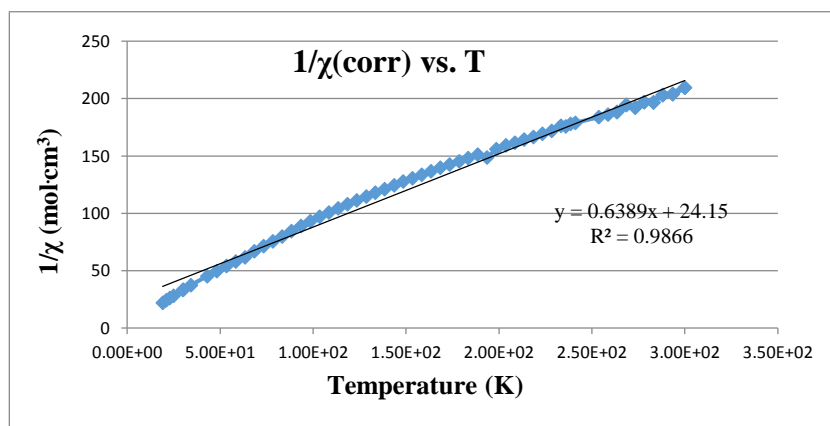


Figure 122. $1/\chi$ vs T data for Fe (II) complex with (337).

The $1/\chi$ vs T graph shows that the compound display a classical Curie-Weiss behaviour, with a Curie constant $C = 1.64 \text{ cm}^3 \cdot \text{K} \cdot \text{mol}^{-1}$ and a Weiss constant $\theta = -41.4 \text{ K}$. The negative value of this constant means the compound is showing an antiferromagnetic character.

4.3.2.2 $\text{RuCl}_3 \cdot \text{X} \cdot \text{H}_2\text{O}$ +ligand (337): Complex (2);

Ruthenium (III) chloride was added to a stirred suspension of the sodium salt of ligand (337) in water and immediately a dark precipitate formed which was isolated by filtration. CHN analysis gave the composition as C 26.45, H 2.11, N 2.17%. This is consistent with

a 1:1 salt of the dianion of (**337**) with ruthenium, with a chloride and a water. The calculated CHN is in agreement with a composition such as $C_{15}H_{13}S_8O_4NRuCl \cdot H_2O$ which gives C 26.41, H 2.22, N 2.05%. $Ru^{(III)}$ can be low spin or high spin and the expected values for each spin state is: low spin $S=1/2$, $\chi(T) = \sim 0.38 \text{ cm}^3 \cdot K \cdot \text{mol}^{-1}$ or high spin $S=5/2$, $\chi(T) = \sim 4.38 \text{ cm}^3 \cdot K \cdot \text{mol}^{-1}$. The magnetic measurement for the structure and MW proposed gave a high temperature value of $\chi(T) = \sim 4.9 \text{ cm}^3 \cdot K \cdot \text{mol}^{-1}$ which is in fairly close agreement with the expected value reported above for the presence of one high spin Ru^{3+} centre. With all the evidence in accordance the proposed structure is shown below (Figure 123). A chlorine analysis is likely to be the next step to investigate this structure.

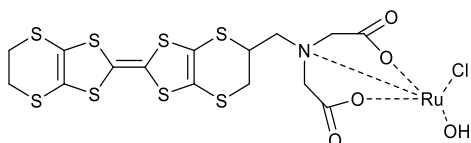


Figure 123. Proposed structure for Ru (III) complex with ligand (**337**).

For the proposed structure the plots $1/\chi$ vs T (Figure 124) and $\chi(T)$ vs T (Figure 125) are presented below.

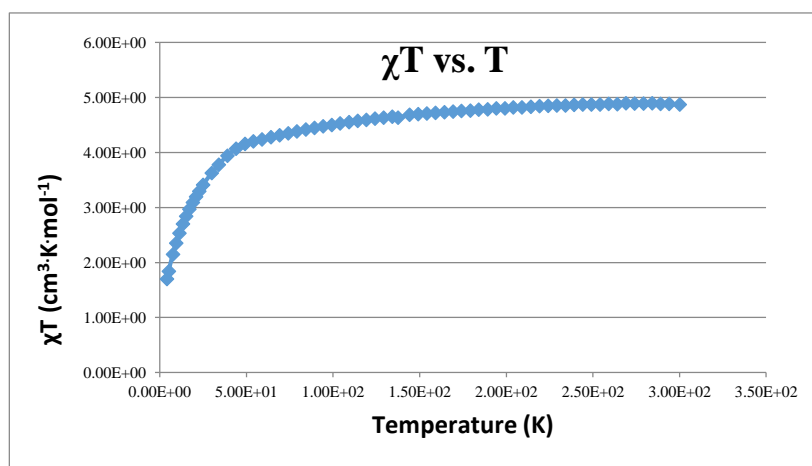


Figure 124. $\chi(T)$ vs T data for Ru (III) complex with (**337**).

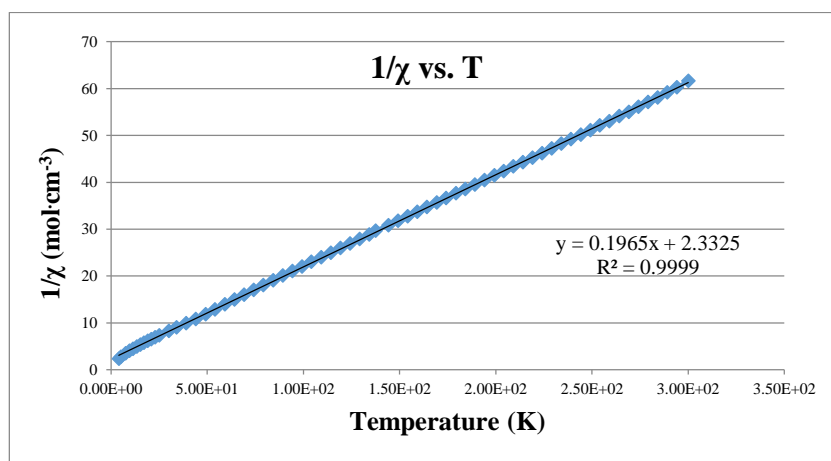


Figure 125. $1/\chi$ vs T data for Ru (III) complex with (337).

The $1/\chi$ vs T graph shows that the compound displays a classical Curie-Weiss behaviour, with a Curie constant $C = 5.09 \text{ cm}^3 \cdot \text{K} \cdot \text{mol}^{-1}$ and a Weiss constant $\theta = -11.9 \text{ K}$. The negative value of this constant means the compound is showing an antiferromagnetic character.

4.3.2.3 $\text{MnCl}_2 \cdot 4\text{H}_2\text{O}$ +ligand (39): Complex (3);

Manganese (II) chloride was added to a stirring suspension of the sodium salt of ligand (337) in water and immediately formed a red precipitate which was filtered and left to dry. CHN analysis found the composition to be C 29.28, H 2.57, N 2.58%. The proposed structure for this complex would have a MW of 1221 g mol^{-1} and sees two ligands, as their of bis carboxylic acids, two chlorides and two molecules of water around the manganese ion. It is likely that the chloride anions and the water molecules are not coordinated to the manganese as either of these would result in eight coordinated $\text{Mn}^{(\text{II})}$ which is not very common for this metal centre. The calculated CHN values for the proposed structure $\text{C}_{30}\text{H}_{30}\text{S}_{16}\text{O}_8\text{N}_2\text{MnCl}_2 \cdot 2\text{H}_2\text{O}$ are C 29.50, H 2.81, N, 2.29%. The $\text{Mn}^{(\text{II})}$ could only be high spin, so the expected value is $S=5/2$, $\chi(T) = \sim 4.38 \text{ cm}^3 \cdot \text{K} \cdot \text{mol}^{-1}$. The experimental measurement of the sample gave a high temperature value of $\chi(T) = \sim 4.40 \text{ cm}^3 \cdot \text{K} \cdot \text{mol}^{-1}$ which is well within the expected value for high spin Mn (II). The next step would be, even in this case, to submit the sample to a chlorine analysis.

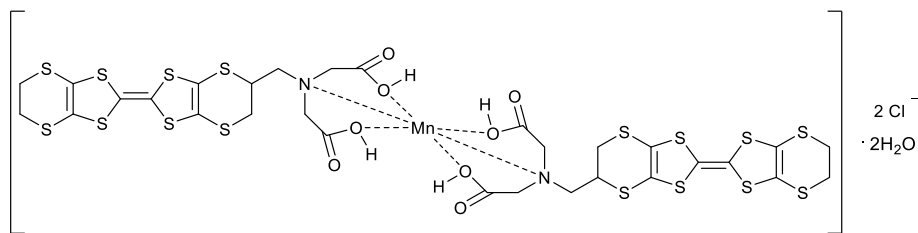
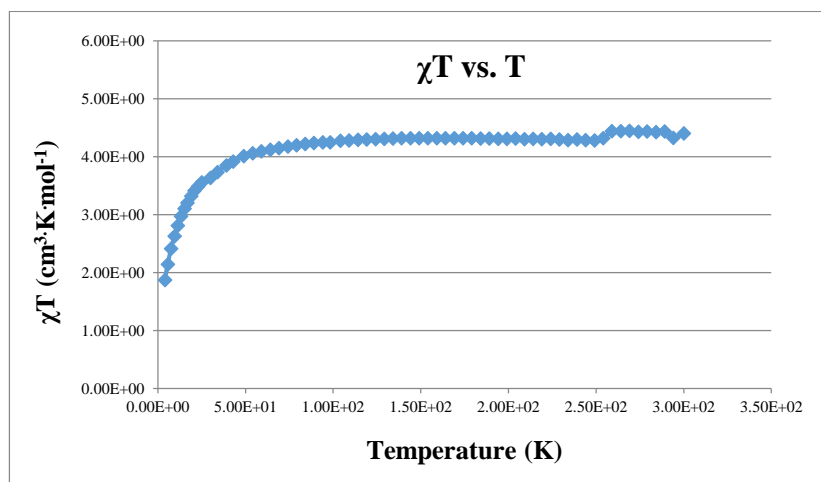
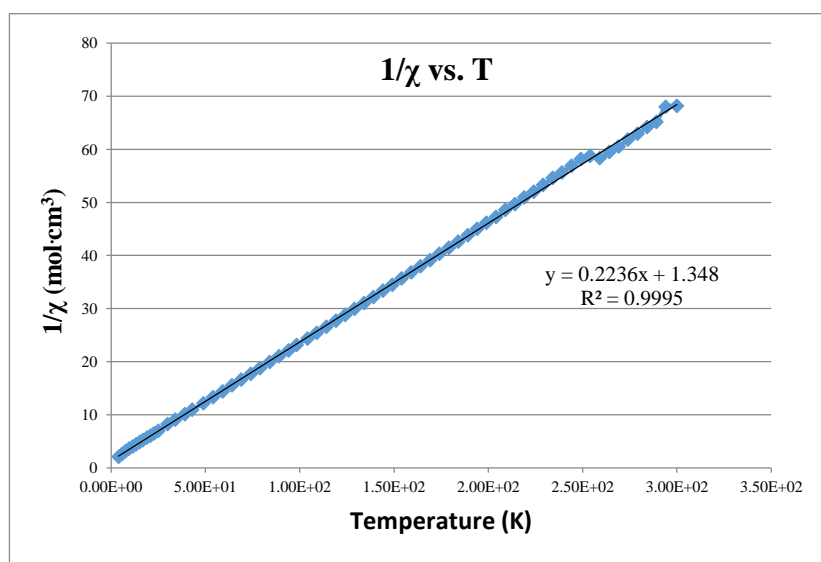


Figure 126. Proposed structures for Mn (II) complex of (337).

For the proposed structure the plots $1/\chi$ vs T (Figure 127) and $\chi(T)$ vs T (Figure 128) are presented below.

Figure 127. $\chi(T)$ vs T data for Mn (II) chloride complex with (337).Figure 128. $1/\chi$ vs T data for Mn (II) chloride complex with (337).

The $1/\chi$ vs T graph shows that the compound displays a classical Curie-Weiss behaviour, with a Curie constant $C = 4.47 \text{ cm}^3 \cdot \text{K} \cdot \text{mol}^{-1}$ and a Weiss constant $\theta = -6.07 \text{ K}$. The negative value of this constant means the compound is showing an antiferromagnetic character.

4.3.2.4 Mn^(II)(hfac)₂·3H₂O+ligand (337): Complex (4);

Mn(II) (bis-hexafluoroacetylacetonate), known as Mn (II) (hfac)₂, was added to a stirred suspension of the sodium salt of donor (337) in dry MeOH at r.t. under a nitrogen atmosphere. Immediately after the addition a brown precipitate precipitated out from the suspension and was isolated by filtration. Analysed by elemental analysis the composition was found to be C, 29.58; H, 1.88; N, 1.48%. This is consistent with the ligand (337) in its deprotonated form complexed to Mn^(II)(hfac)₂ with one molecule of water. The magnetic data for this compound are expected to give a value of $\chi(T) = \sim 4.38 \text{ cm}^3 \cdot \text{K} \cdot \text{mol}^{-1}$ which is the value for a manganese high spin state nucleus, as encountered for the Mn^(II)Cl₂ salt above. The magnetic measurement for a suggested structure with MW of 1019 g / mol furnished $\chi(T) = \sim 4.5 \text{ cm}^3 \cdot \text{K} \cdot \text{mol}^{-1}$ which is fairly close to the expected value for a manganese (II) high spin centre. The possible structure for a MW of 1019 g / mol which would fit with the found CHN is shown below.

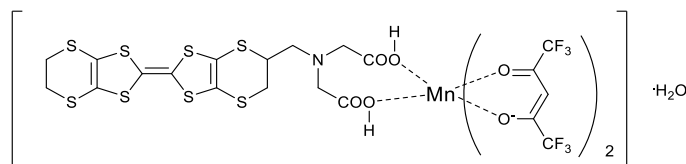


Figure 129. Proposed structures for Mn^(II)(hfac)₂ complex with ligand (337).

For the proposed structure the plots $1/\chi$ vs T (Figure 130) and $\chi(T)$ vs T (Figure 131) are presented below.

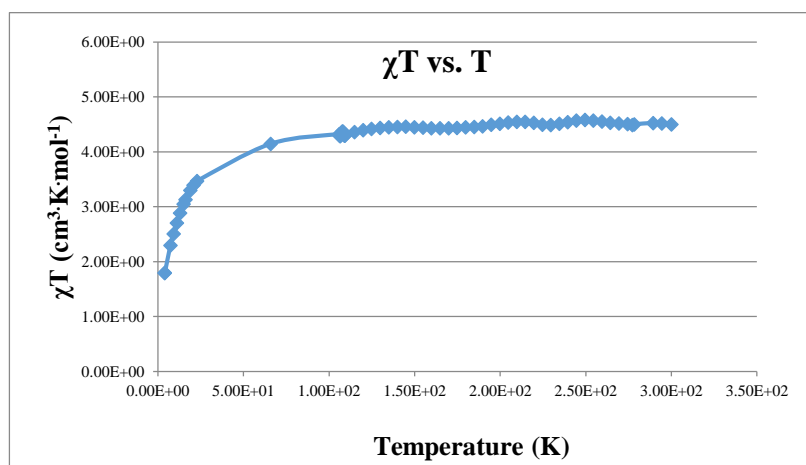


Figure 130. $\chi(T)$ vs T data for Mn^(II)(hfac)₂ complex with (337).

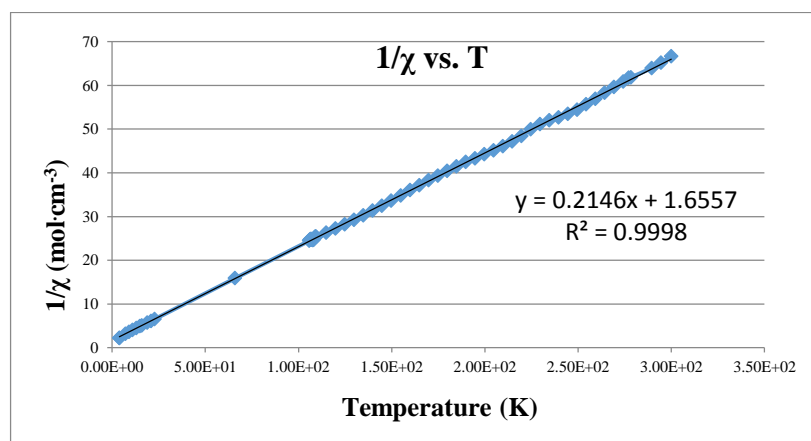


Figure 131. $1/\chi$ vs T data for $\text{Mn}^{\text{II}}(\text{hfac})_2$ complex with (337).

The $1/\chi$ vs T graph shows the compound displays a classic Curie-Weiss behaviour, with a Curie constant $C = 4.47 \text{ cm}^3 \cdot \text{K} \cdot \text{mol}^{-1}$ and a Weiss constant $\theta = -6.07 \text{ g mol}^{-1}$ which revealed the antiferromagnetic character of the solid analysed. The few points missing below 100 K are due to problems with MPMS overnight but this had no effect on the shape of the plot or the values of C and θ .

The presence of hfac ligands in the solid obtained was investigated by IR spectroscopy. In the Figure 132 is presented the comparison between two infrared spectra (starting material Mn salt-blue line and complex formed-green line) and some differences are clear. With regards to the IR spectrum of the complex the major intensity of the carbonyl stretching is visible, the absence of two stretching frequencies at 1566 and 1540 cm^{-1} and the presence of two bending frequencies at 994 and 901 cm^{-1} .

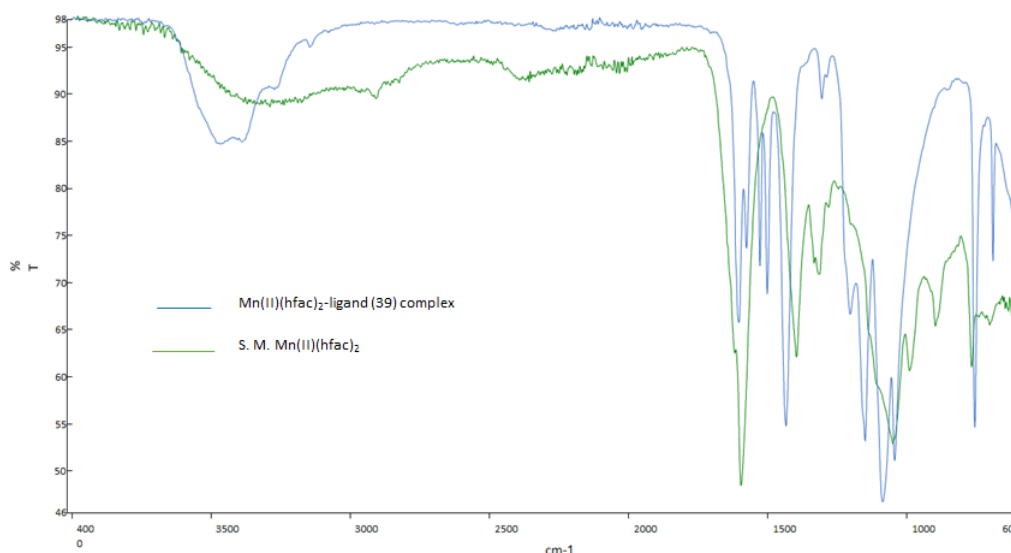


Figure 132. IR spectra of starting material and solid obtained-Mn (II) (hfac)₂-complex.

In the Figure 133 the zone $1500\text{-}1000 \text{ cm}^{-1}$ is presented in more detail because this is the window where the vibrational frequencies of the $-\text{CF}_3$ group should be visible for both

spectra. This area had great importance in order to establish the presence of the hfac ligand in the complex to support the proposed structure. The $-\text{CF}_3$ stretching mode in the starting material spectra (blue spectra) is far more defined than in the spectra of the complex where only one broad peak is detected at 1054 cm^{-1} . A final conclusion has not been reached but the presence of the hfac ligand in the complex formed is not clear. More investigation needs to be done to find an agreement for the magnetic measurement data, CHN and IR.

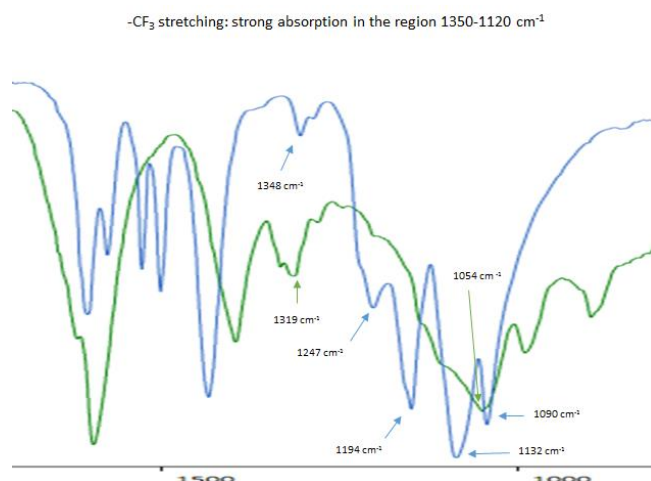


Figure 133. Enlargement for the $-\text{CF}_3$ zone for manganese salt (blue line) and for the complex formed (green line).

Complexes of ligand (337) with triflate salts.

A series of triflate salts was then involved in the realisation of more complexes of donor (337) with transition metal centres, including lanthanides. The salts used were: praseodymium(III)triflate, $\text{Pr(III)(CF}_3\text{SO}_3)_3$ and dysprosium(III)triflate, $\text{Dy(III)(CF}_3\text{SO}_3)_3$ as lanthanides in addition to iron(II) and iron(III)triflate, manganese(II)triflate, copper(II)triflate and zinc(II)triflate. The procedure followed was the same for all the triflate salts and involved the addition of the specific metal salt to a stirred suspension of donor (337) in dry MeOH at r.t under a nitrogen atmosphere. In all cases the reaction evolved by immediate formation of a precipitate with various colours which was filtered and analysed by elemental analysis and infrared spectroscopy. All the samples were sent for magnetic measurement to the Pilkington group at Brock University and are currently under investigations. The only sample which was not sent was the zinc (II) complex formed due to the diamagnetic character of the transition metal centre involved. Also in the case of these triflate salts the data available were limited and difficult to interpret to give an unambiguous solution. The results reported represent simple proposals for the structures based on

the data available and no complete conclusion nor confirmation of the identity has been yet achieved.

4.3.2.5 Zn(CF₃SO₃)₂+ligand (337): Complex (5);

Zinc(II)triflate was added to a stirred suspension of the sodium salt of donor (337) in dry MeOH at r.t. under nitrogen atmosphere. Immediately a red-orange solid was formed and isolated by filtration. Elemental analysis revealed a composition fully in accordance with the suggested structure where the transition metal ion is surrounded by two ligands where the tridentate site contains one carboxylate, one carboxylic acid group and one nitrogen involved in the coordination of the metallic species. Elemental analysis found C, 31.95; H, 2.41; N, 2.64% where C₃₀H₂₈S₁₆O₈N₂Zn requires C, 32.09; 2.51; N, 2.49%.

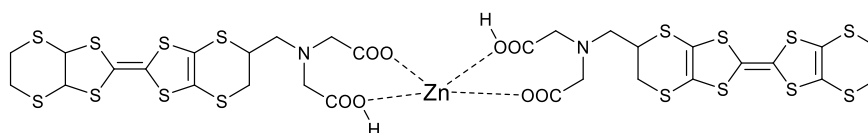


Figure 134. Proposed structures for Zn(II) triflate complex with ligand (337).

A confirmation of the absence of the triflate group was obtained from the infra-red spectra where the complex obtained with ligand (337) does not show the characteristic peaks at 1229, 1189 and 1033 cm⁻¹ for the -CF₃ and SO₃ groups which appear in the spectrum of the zinc triflate.

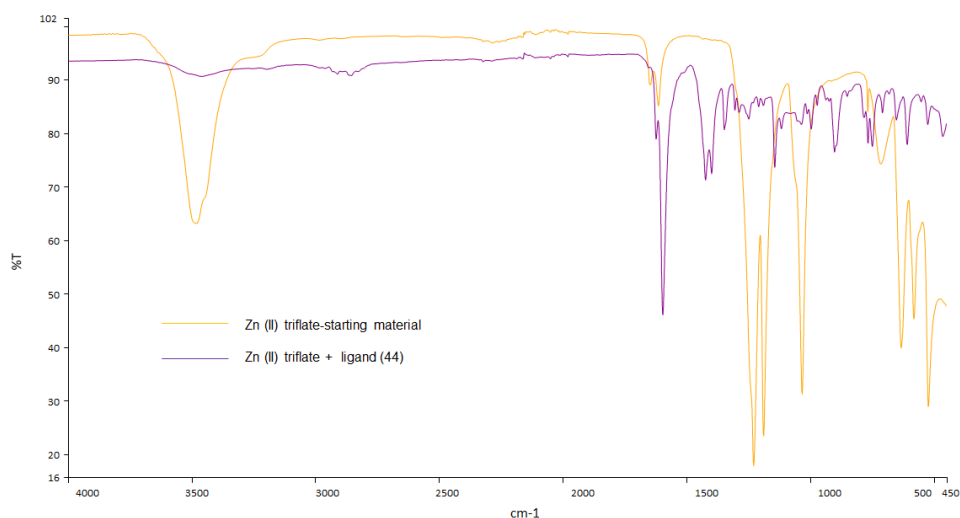


Figure 135. IR spectra for the complex of (337) with zinc triflate.

4.3.2.6 Mn(CF₃SO₃)₂+ligand (337): Complex (6);

Manganese (II) triflate was added to a stirred suspension of the sodium salt of donor (337) in dry MeOH at r.t. under a nitrogen atmosphere. Immediately the suspension became

coloured pink and the solid formed was isolated by filtration. CHN analysis of the product gave C, 22.15; H, 2.17, N 1.76%. The proposed structure for this complex involves the presence of one ligand in its di-acid form, two triflate groups and a molecule of water around one manganese (II). The molecular formula is $C_{17}H_{19}S_{10}O_{12}F_6NMn$ which requires C, 22.22; H, 2.08; N, 1.52% which is in good accordance with the experimental result. The IR spectra for the product and the manganese (II) triflate recorded are compared in Figure 129 and some sort of match was found between the two spectra in the region where the triflate shows its characteristic vibration modes. The bands are not really intense in the complex's spectrum but they are at the expected frequencies.

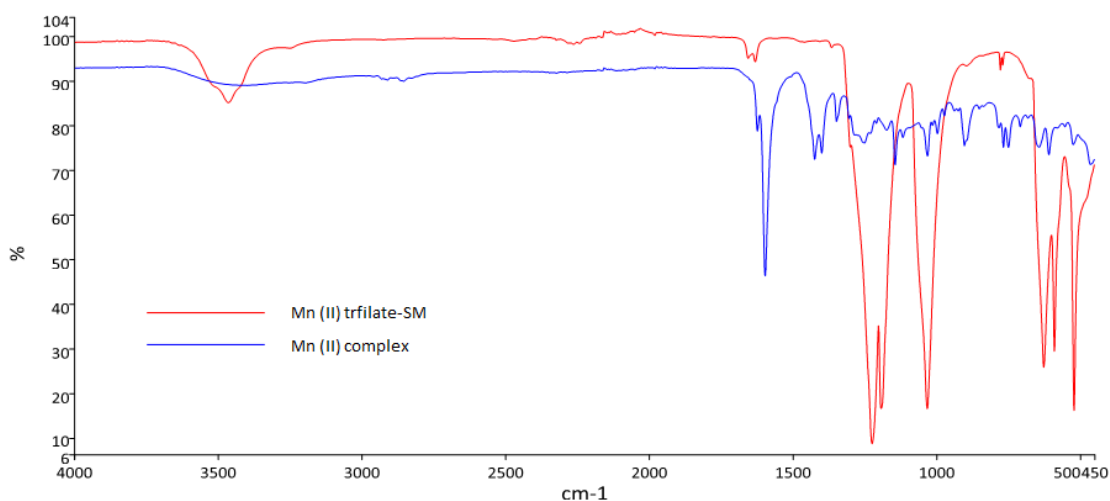


Figure 136. IR spectra for the manganese (II) triflate and the complex with ligand (**337**).

In the spectra below the region of interest is shown in more details and the peaks can be seen more clearly.

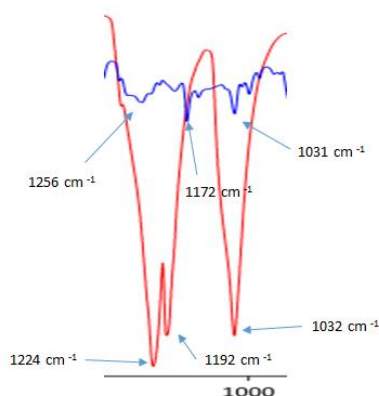


Figure 137. Enlargement in the characteristic triflate zone.

4.3.2.7/8 Dy $(CF_3SO_3)_2$ +ligand (**337**): Complex (**7**) and Complex (**8**);

Dysprosium (III) triflate was involved in two different reactions with the sodium salt of ligand (**337**) in different solvents, dry MeOH and dry ACN, to furnish a red and a brown

solid respectively. The procedure followed is the usual reported for the salts above. The solids were both analysed by CHN and the results are showed in Table 4.

Table 4. CHN results for the two reactions involving Dy (III) triflate.

Dy(III)-ACN	found		Dy(III)-MeOH	found
	C 22.08%			C 26.58%
	H 1.42%			H 1.85%
	N 2.25%			N 1.88%.

In the case of the reaction performed in dry ACN the proposed structure involves the presence of one ligand, in its mono-anion form and two triflate groups around the lanthanide and one molecule of solvent. The molecular formula for the suggested structure is $C_{19}H_{17}S_{10}O_{10}N_2F_6Dy$ which requires C, 22.15; H, 1.65; N, 2.72% which is a bit out on nitrogen but gives an idea of the composition. A better fit was found by decreasing the solvent to 0.8 molecules.

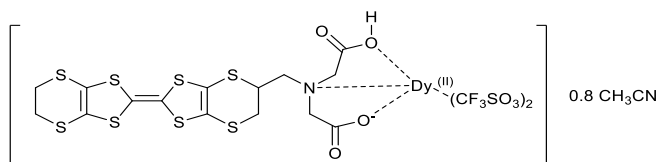
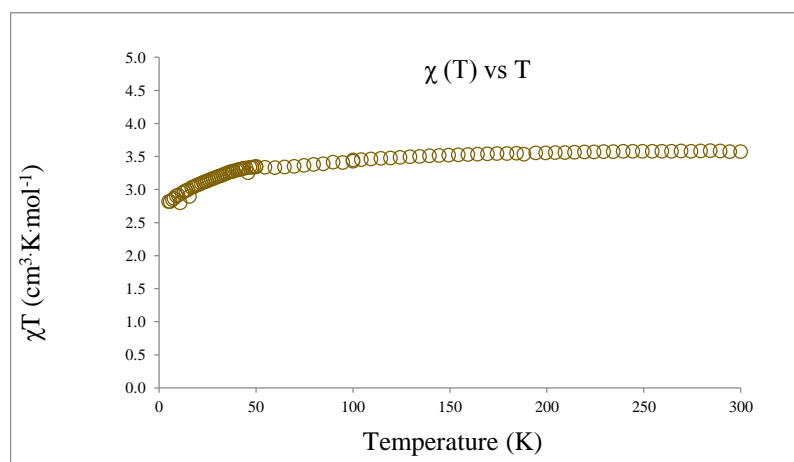


Figure 138. Proposed structures for Dy (III) complex with ligand (337). Reaction in ACN.

The magnetic measurement for a suggested structure with MW of 1022 g / mol would require $\chi(T) = \sim 14.2 \text{ cm}^3 \cdot \text{K} \cdot \text{mol}^{-1}$ which is far from the experimental value obtained, $\chi(T) = \sim 3.6 \text{ cm}^3 \cdot \text{K} \cdot \text{mol}^{-1}$. For the solid obtained the magnetic data have been recorded and the plots $\chi(T)$ vs T (Figure 139) and $1/\chi$ vs T (Figure 140) are presented below.

Figure 139. $\chi(T)$ vs T data for Dy (III) (triflate)₃ complex with (337). Reaction in ACN.

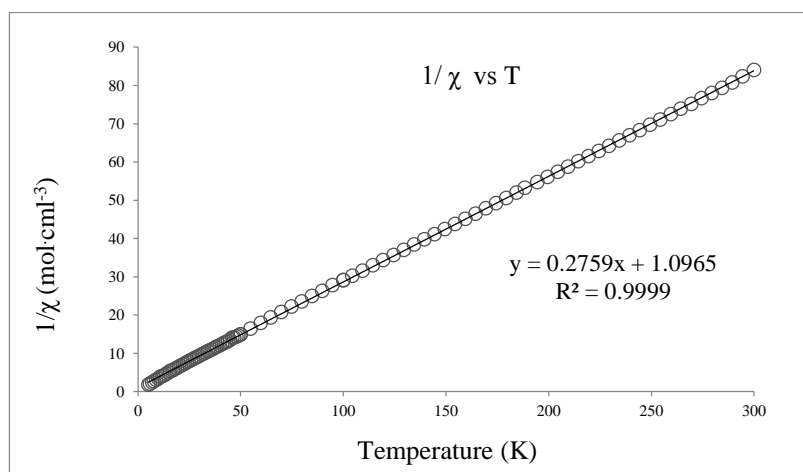


Figure 140. $1/\chi$ vs T data for Dy (III) (triflate)₃ complex with (337). Reaction in ACN.

The $1/\chi$ vs T graph shows the compound displays a classic Curie-Weiss behaviour, with a Curie constant $C = 3.62 \text{ cm}^3 \cdot \text{K} \cdot \text{mol}^{-1}$ and a Weiss constant $\theta = -3.97 \text{ g mol}^{-1}$ which revealed the antiferromagnetic character of the solid analysed.

In the case of the reaction performed in dry MeOH the proposed structure involved the presence of one ligand, in its di-anion form and a methoxy group to balance the charges. The molecular formula for the suggested structure is $\text{C}_{16}\text{H}_{17}\text{S}_8\text{O}_5\text{N}_1\text{Dy}$ which requires C, 26.63; H, 2.36; N, 1.94% which is a bit out on hydrogen.

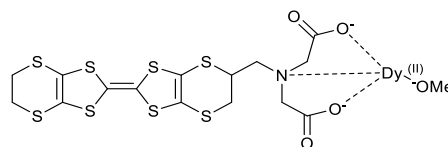


Figure 141. Proposed structures for Dy (III) complex with ligand (337). Reaction in MeOH.

The theoretical value expected is again $\chi(T) = \sim 14.2 \text{ cm}^3 \cdot \text{K} \cdot \text{mol}^{-1}$ which is, even for this complex, far from the experimental value obtained, $\chi(T) = \sim 7.0 \text{ cm}^3 \cdot \text{K} \cdot \text{mol}^{-1}$. The magnetic data have been collected also for this solid and the plots $\chi(T)$ vs T (Figure 142) and $1/\chi$ vs T (Figure 143) are outlined below.

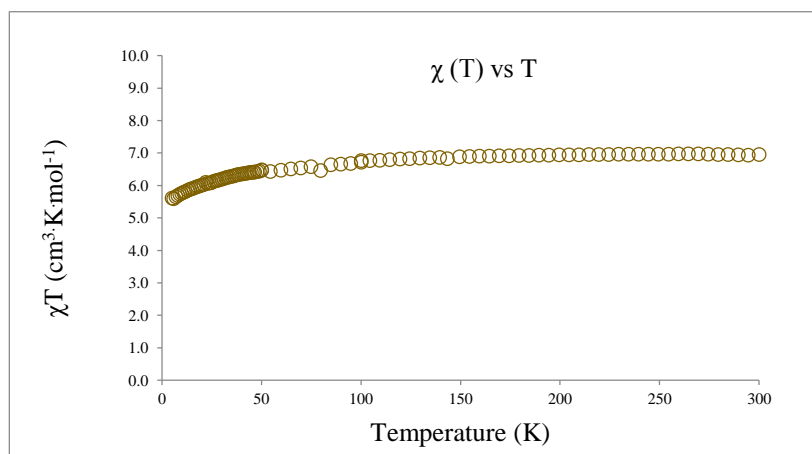


Figure 142. $\chi(T)$ vs T data for Dy (III) (triflate)₃ complex with (337). Reaction in MeOH.

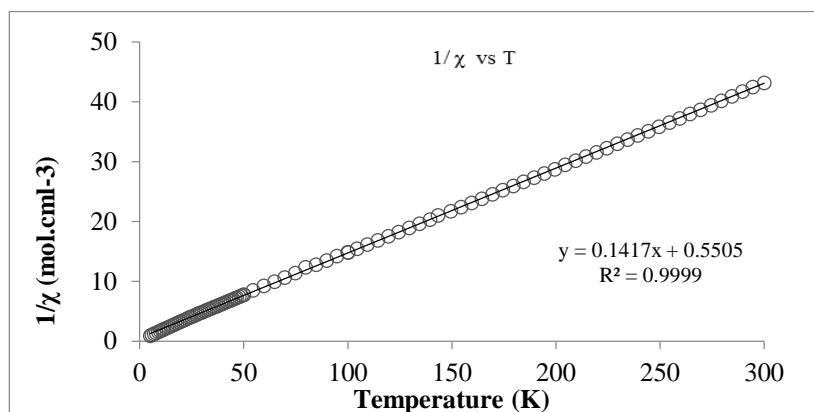


Figure 143. $1/\chi$ vs T data for Dy (III) (triflate)₃ complex with (337). Reaction in MeOH.

The $1/\chi$ vs T graph shows the compound displays a classic Curie-Weiss behaviour, with a Curie constant $C = 7.06 \text{ cm}^3 \cdot \text{K} \cdot \text{mol}^{-1}$ and a Weiss constant $\theta = -0.51 \text{ g mol}^{-1}$ which revealed the antiferromagnetic character of the solid analysed.

It has to be said that no confirmation of the proposed structures have been given by the magnetic measurements for both the solids. In the two cases the χ (T) registered at high temperature for the proposed structures is not in agreement with the expected value. The magnetic data looked nice and in agreement with the Curie-Weiss law but the composition need to be investigated in depth before reaching any conclusions.

To outlined and enforce the proposed structures and their differences the IR spectra have been recorded. In the Figure 144 the IR spectra of the dysprosium triflate and the two complexes formed are compared.

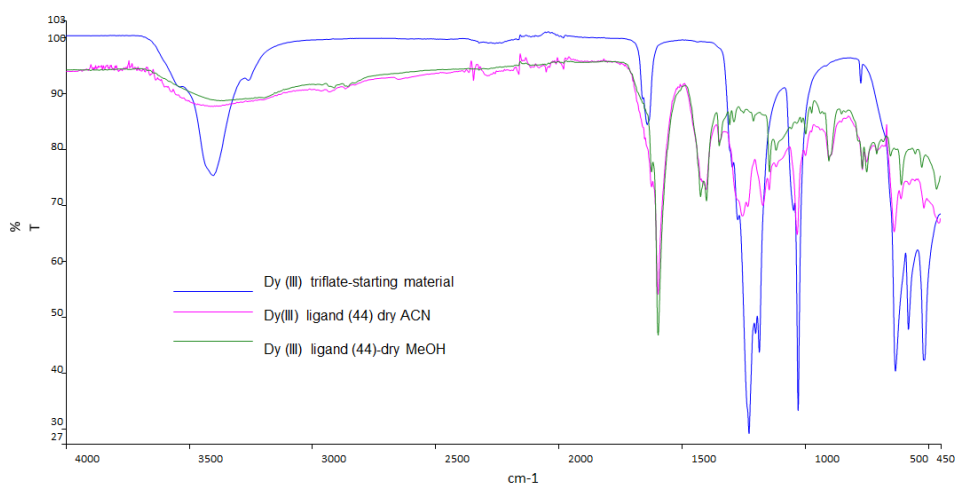


Figure 144. IR spectra for the Dy(III) (triflate)₃ and the two complexes formed with ligand (337).

The starting material has been used as a reference to locate the characteristic peaks of the -CF_3 and SO_2 groups which were found at 1224 , 1182 and 1026 cm^{-1} .

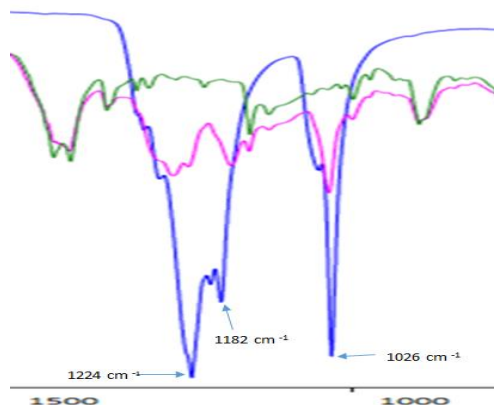


Figure 145. Enlargement of the critical zone for triflate bands.

In the IR spectra of the Dy (III)-ACN (pink line) (reaction of the triflate in acetonitrile) these peaks are present even if less intense than in the starting material. On the other spectra Dy(III)-MeOH (green line) (reaction of the triflate in methanol) the peaks are absent and this is an evidence which confirm that the complex obtained from the reaction in ACN still contains triflate while the solid yielded by the reaction in methanol does not. This is a confirmation of the proposed structures reported above.

4.3.2.9 Pr (CF_3SO_3)₂+ligand (337): Complex (9);

Praseodimium (II) triflate was added to a stirred suspension of the sodium salt of donor (337) in dry MeOH at r.t. under a nitrogen atmosphere. Immediately an orange solid was formed and isolated by filtration. The solid gave a CHN analysis: C, 29.85; H, 2.17; N, 2.38%. The suggested structure for this complex sees the lanthanide ion surrounded by two ligands one in its di-anion form and the second one in the mono-anion form. The proposed structure $\text{C}_{30}\text{H}_{28}\text{S}_{16}\text{O}_8\text{N}_2\text{Pr}$ requires C, 30.10; 2.26; N, 2.34% which shows a good fit with the experimental composition. A confirmation of the absence of the triflate group in the complex with (337) was obtained by the infra-red spectrum which did not show the characteristic peaks at 1229 , 1192 and 1031 cm^{-1} , which are present in the spectrum obtained from the commercially available praseodymium(III) triflate starting material. The sample has been sent for magnetic measurement and is currently under investigation.

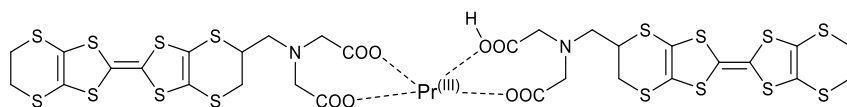


Figure 146. Proposed structures for Pr(III) triflate complex with ligand (337).

As reported before for the dysprosium complexes, the IR spectra of the Pr (III) triflate and of the complex obtained by reacting the salt with ligand (**337**) are reported in Figure 147 in full scale.

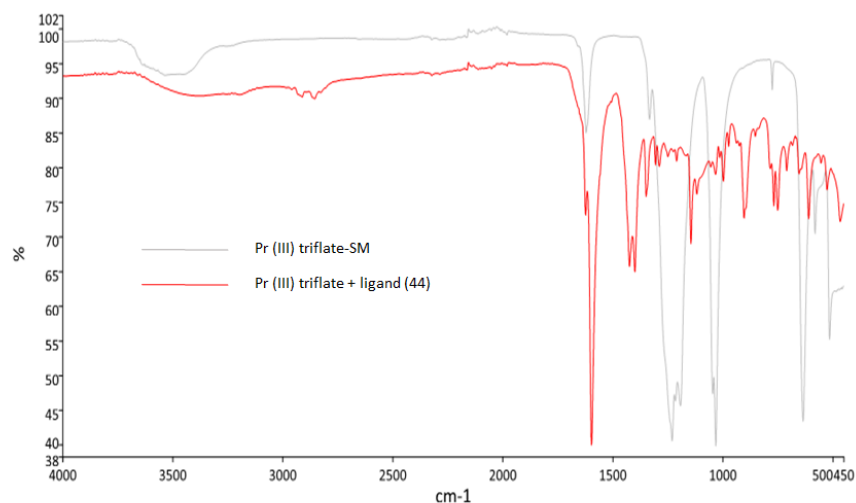


Figure 147. IR spectra for praseodimium (III) triflate and its complex with ligand (**337**).

In the Figure 148 it is possible to see in better details how the triflate characteristic bands are not present in the complex formed (red-line).

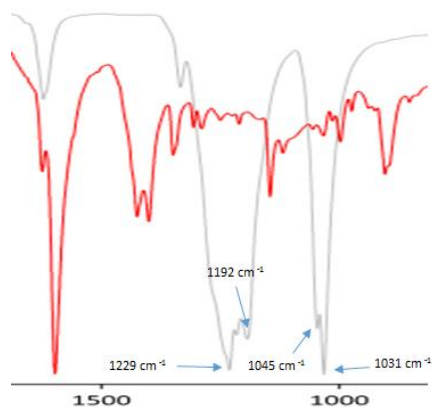
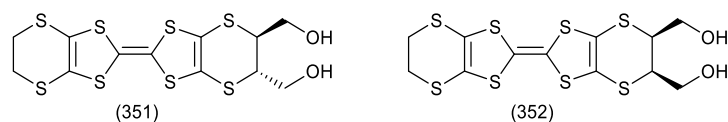


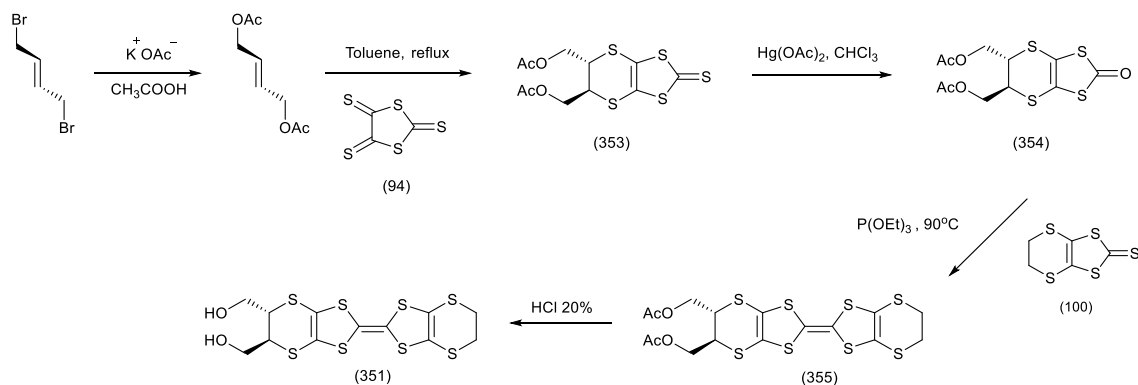
Figure 148. Enlargement for the characteristic triflate zone.

4.3.3 Preparation and characterisation of metal complexes formed using donor (**351**).

The coordination chemistry of transition metal salts and BEDT-TTF derivatives has been investigated also by using neutral donor (**351**) whose preparation and characterisation have been already reported in the literature³⁰. It is worth mentioning that this donor has been prepared in both its isomers *trans* (**351**) and *cis* (**352**).

Figure 149. Diol donors in their *trans* and *cis* conformation.

The preparation of the desired compound has been achieved by following the established procedure outlined in the Scheme 124.

Scheme 124. Preparation of *trans*-donor (**351**).

The first step from dibromo-but-2-ene to the *bis* acetoxy but-2-ene has been performed according to the procedure found in the literature³¹⁾ by reacting the dibromo compound with potassium acetate in refluxing acetic acid for 24 hours. The second step is the reaction between trithione (**94**) and *trans*-1,4-*bis* acetoxy-2-butene in refluxing toluene overnight to obtain, after purification by column chromatography, thione (**353**). Exchange of sulphur for oxygen by standard methodology afforded oxo-compound (**354**). The next step was the coupling reaction of the former with unsubstituted thione (**100**) in freshly distilled triethyl phosphite which yielded *trans*-*bis*-acetate-donor (**355**) after purification by flash chromatography. The final step was the hydrolysis in acidic condition to furnish the diol (**351**).

Donor (**351**) is a really interesting ligand for coordinating transition metal centres due to its bidentate character and its neutral form. The investigation of its coordination chemistry have been explored by reacting it with metal salts such as manganese(II)hexafluoroacetylacetonate, Mn(II)(hfac)₂, manganese(II)acetylacetonate, Mn(II)(acac)₂ and titanium(IV) tetra(isopropoxide).

4.3.3.1 Ti (OCH(CH₃)₂)₄+ligand (**351**): Complex (**10**);

Titanium(IV)tetra(isopropoxide) was slowly added into a stirred solution of donor (**351**) in THF at r.t. under a nitrogen atmosphere. The addition immediately developed smoke and formed a dark coloured suspension. The solid was filtered and analysed by CHN

analysis and IR spectroscopy. The elemental analysis gave composition C, 27.20; H, 2.57%. The aim of the reaction was to form a neutral complex where two ligands (both -2) coordinate the titanium centre (+4). The titanium (isopropoxide)₄ can act as a base so no additional base was used to deprotonate the diol. The suggestion is that the titanium isopropoxide reacted with water (present in the solvent, or in the flask or old reagent) to form titanium dioxide³²⁾ which is the form in which titanium is in the complex formed. The proposed structure is that one ligand, in its dianion form, is coordinated around the titanium which has two -OH groups as additional ligands. Such a structure would give a molecular formula of C₁₂H₁₂O₂S₈Ti(OH)₂ that requires C, 27.47; H, 2.31%. It is also possible that the complex is formed by multiples of this unit where the units would be connected to one another by the oxygen atoms of the hydroxyl groups.

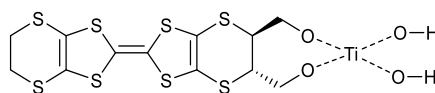
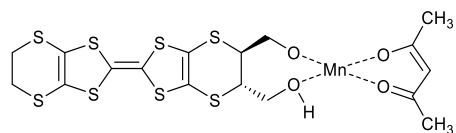


Figure 150. Suggested structure for the **complex (10)**.

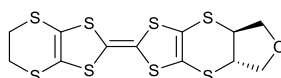
4.3.3.2 Mn (acac)₂+ligand (351): Complex (11);

Manganese(II)acetylacetonate cannot act as a base, so the reaction was performing in a different way. Sodium hydride was slowly added into a stirred solution of donor (**351**) in dry THF at r.t. under a nitrogen atmosphere. The addition immediately developed turbidity and the suspension was left stirring for ten minutes before the manganese salt was added. The suspension turned to a dark brown colour and the solid was filtered and collected. This reaction has been performed using a M:L=1:1 ratio in the attempt to form a neutral complex where one donor and one acetylacetonate ligand coordinate the metal. Elemental analysis found a composition of C, 34.27; H, 2.38%. Unfortunately no IR spectrum has been recorded for the complex obtained, so there is no additional information to evidence the presence or not of the acetyl-acetonate group in the complex formed.

The proposed structure, based only on the CHN composition sees the presence of one ligand, where only one alcohol is deprotonated, and one acac ligand around the metal. The molecular formula for the suggested structure C, 34.16; H, 3.04% which is not far from the experimental values ($\Delta = 0.66$ for H). No sample has been sent for magnetic measurement due to the small quantity obtained.

Figure 151. A possible structure for **complex (11)**.

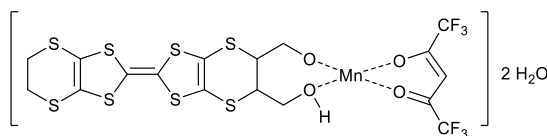
An alternative structure would also fit the experimental composition. Here the manganese acted as a catalyst to make the $-OH$ a better leaving group to lead to the formation of a five membered cyclic ether ring. If this is the case the molecular formula $C_{12}H_{10}OS_8$ would give a composition such as C, 3378; H, 2.36% which is in close agreement with the experimental one.

Figure 152. An alternative structure for **complex (11)**.

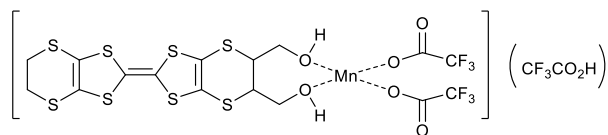
4.3.3.3 Mn (hfac) $_2$ ·3H $_2$ O+ligand (351): Complex (12);

As in the case of Mn(II)(acac) $_2$, even the manganese(II)hexafluoroacetylacetonate cannot act as a base, so the reaction was performing in the same way as described before. Sodium hydride was added into a solution of donor (351) at r.t. and under a nitrogen atmosphere. Then the manganese salt was added and immediately the suspension became coloured brown. The solid was filtered and collected. This reaction has been performed using the same M:L=1:1 ratio in order to generate a neutral complex. Elemental analysis found a composition of C, 25.53; H, 1.65%. The IR spectrum of the solid could not be recorded to evidence the presence of the original hfac ligand due to the lack of sample.

The proposed structure involves one donor (351), in its mono-anion form, one hfac ligand and two molecules of water around the manganese (II) centre. The molecular formula for the suggested structure would be $C_{12}H_{11}O_2S_8Mn_2 C_5HF_6O_2 \cdot 2H_2O$, which requires C, 25.64; H, 1.91%. Experimental and found composition are in fairly close agreement but no additional information have been collected, so no conclusion has been reached yet.

Figure 153. Proposed structure for **complex (12)**.

A second suggestion is that in the alkaline environment the Mn (II) (hfac) $_2$ has been hydrolysed to furnish a complex where one ligand, in its neutral form, and two trifluoroacetate units are coordinated to the metal where a molecule of trifluoroacetic acid is present maybe as a crystallisation solvent.

Figure 154. An alternative structure for **complex (12)** following hydrolysis of the metal salt.

Such a complex would have a molecular formula of $C_{12}H_{12}O_2S_8MnC_2F_6O_4CF_3COOH$ which would require C, 25.75; H, 1.56% a composition which would fit with the experimental one. This suggestion is based on a recent example found in the literature³³). No sample was sent for magnetic measurement due to the small amount in which the solid was isolated.

4.3.4 Cyclic voltammetry of the new donor synthesised.

The cyclic voltammeteries of some of the new donor prepared were measured using a three electrode set-up method (reference, working and counter electrodes). All the measurements are relative to Ag/AgCl at platinum electrode. A recorded amount of the desired donor was added into a 0.1 M solution of $n\text{-BuN}_4\text{PF}_6$ in dichloromethane which was used a carrier charge.

Table 5. Cyclic voltammetry potentials for the new substituted ET donors.

Donor	E_1 (V)	E_2 (V)
(103)	0.52	0.94
(337)	0.51	0.91
(341)	0.53	0.94
(349)	0.54	0.91

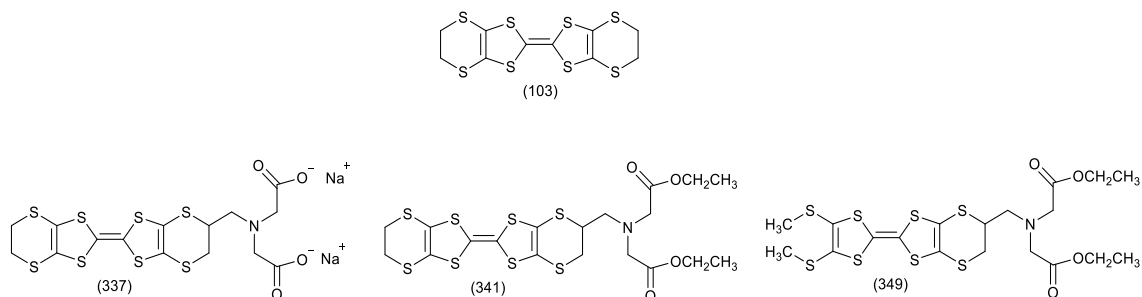


Figure 155. Donors characterised by CV measurement.

Electro-crystallisation and diffusion experiments are currently in progress to generate single crystals of the oxidised material in order to measure the conductivity and investigate

the crystal structure. Up to date the complete insolubility of the donor (**337**) in the all of the solvent tried has been the real limitation in every aspects of its characterisation.

4.4 Conclusions and future work.

To conclude the work presented in this chapter the preparation of new donors have been achieved such as donor (341) and (349) The hydrolysis in alkaline conditions of donor (341) led to the preparation of sodium salt of donor (337) whose capability of forming metal complexes was investigated together with the magnetic properties of the solid isolated. In the early stage of this investigation the solubility of donor (337) and its complexes limited the understanding of the structures products obtained and their characterisation. The magnetic measurements are still ongoing for a few of the compounds prepared to provide more information.

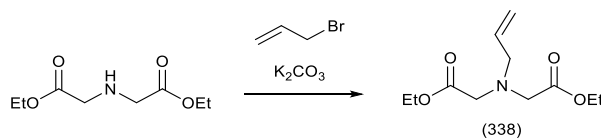
The future work for this chapter would involve the hydrolysis of donor (349) to provide a new donor which is thought to be more soluble than the sodium salt of donor (337). Preparation of complexes with various metal centres and investigation of their magnetic behaviour is one of the next steps. Alternative new metal complexes could be prepared involving thione (339) after hydrolysis of the two ester groups. This compound could present a better solubility than the sodium salt of donor (337) due to its lower ability to make stacking interactions.

The future work would focus also on the preparation of new donors bearing different substituents in order to achieve better solubility and so that single crystal could be obtained and characterised. The neutral donor (351) and its complexes are worth investigating further since only a few examples were made here.

Alternative other metal salts such as acetates or oxalates could be used in the hope that these ligands would increase the solubility of the complexes prepared. It is also worth mentioning that new synthetic methods such as hydrothermal synthesis could be taken into consideration to test if single crystals could be obtained directly.

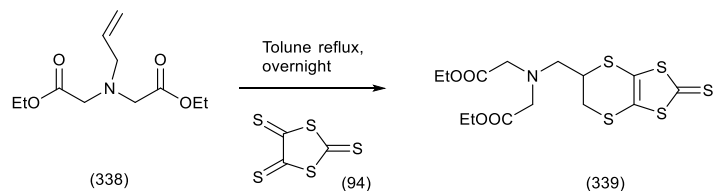
4.5 Experimental part.

4.5.1 Synthesis of diethyl allyl-amino-N,N-diacetate (**338**);



To a stirred solution of diethyl amino-N,N-diacetate (3.04 g, 16.1 mmol) in THF (50 ml) allyl bromide (2.20 ml, 25.3 mmol) was slowly added followed by addition of K_2CO_3 (3.42 g, 24.7 mmol) and the resulting suspension was warmed up to reflux and left to stir for 20 h. Monitoring of the reaction by tlc showed starting materials were consumed and a single spot was present. The reaction mixture was allowed to cool down to r.t. and THF was evaporated under reduced pressure. DCM was added to the residue (100 ml) and the organic layer was washed with water (100 ml) and brine (100 ml) and dried over Na_2SO_4 . Evaporation of DCM afforded diethyl allyl-amino-N,N-diacetate (**338**) (3.16 g, 86%) as a pale yellow oil; δ_H (400 MHz, $CDCl_3$): 5.88 (1H, m, $-CH=CH_2$), 5.22 (1H, dd, $J = 18.8, 1.7$ Hz, $-CH=CH_{trans}H$), 5.17 (1H, dd, $J = 10.1, 1.8$ Hz, $-CH=CH_{cis}H$), 4.17 (4H, q, $J = 7.2$ Hz, $-O-CH_2-CH_3$), 3.57 (4H, s, $2 \times -N(CH_2COOEt)_2$), 3.38 (2H, d, $J = 6.7$ Hz, $-CH_2-CH=$), 1.27 (6H, t, $J = 7.0$ Hz, $2 \times -CH_3$); δ_C : (100 MHz, $CDCl_3$): 170.6 ($2 \times -C=O$), 134.9 ($=CH$), 118.0 ($=CH_2$), 60.0 ($2 \times -O-CH_2-CH_3$), 57.0 ($=CH-CH_2-N-$), 53.8 ($2 \times -N-CH_2CO$), 13.8 ($2 \times -CH_3$); ν_{max} 2981, 1737, 1674, 1399, 1333, 1190, 714; HRMS: (ASAP) found: 230.1383 (100%), $C_{11}H_{20}NO_4 + H$: requires: 230.1387; found C, 57.69; H, 8.36; N, 6.19%; $C_{11}H_{20}NO_4$ requires C, 57.64; H, 8.29; N, 6.11%.

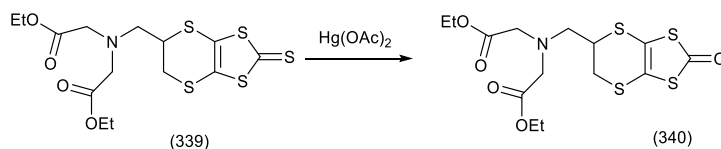
4.5.2 Synthesis of diethyl 5,6-dihydro-2-thioxo-[1,3]dithiol [4,5-b]-[1,4]-dithiin-5-methylamine-N,N-diacetate (**339**).



To a suspension of trithione (**94**) (3.25 g, 17.0 mmol) in toluene (100 ml) was added diethyl allyl-amino-N,N-diacetate (**338**) (1.17 g, 5.0 mmol) and the resulted suspension was warmed up to reflux and left to stir overnight under a nitrogen atmosphere. The solid formed during the reaction was filtered off, and washed with $CHCl_3$ until washes ran clear. The combined filtrates were evaporated under reduced pressure to give the desired

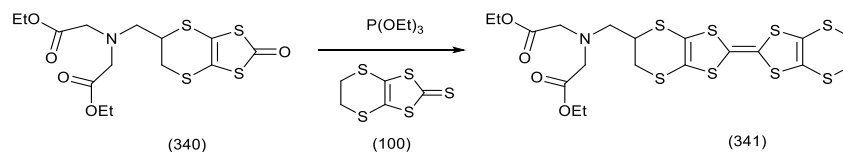
thione (**339**) as a dark red oil (2.29 g, quantitative). It is worth to mention that by NMR thione (**339**) looks reasonably pure and it was used for the next step without any further purification. Nevertheless, minor impurities appeared on the tlc, but not in the NMR spectra. δ_H (400 MHz, $CDCl_3$): 4.10 (4H, q, $J = 7.0$ Hz, $-O-CH_2-CH_3$), 3.72 (1H, m, 5-*H*), 3.51 (4H, s, 2 x $(-N-CH_2-C=O)$), 3.43 (1H, dd, $J = 13.4, 6.1$ Hz, 5- $(CH_\alpha H)-N$), 3.29 (1H, dd, $J = 13.3, 2.8$ Hz, 5- $(CHH_\beta)-N$), 3.13 (1H, dd, $J = 13.8, 8.7$ Hz, 6- $H_\alpha H$), 3.05 (1H, dd, $J = 13.8, 6.5$ Hz, 6- HH_β), 1.20 (6H, t, $J = 7.2$ Hz, 2 x $-CH_3$); δ_C : (100 MHz, $CDCl_3$): 208.0 ($C=S$), 170.9 (2 x $C=O$), 123.6, 122.2 (3a-, 7a- C), 60.8 (2 x $-O-CH_2$), 58.7 (5- CH_2-N), 56.2 (2 x $-N-CH_2-C=O$), 42.6 (5- C), 31.9 (6- C), 14.2 (2 x $-CH_3$); ν_{max} 2975, 1729 ($C=O$), 1483, 1368, 1259, 1180, 1140, 1054 ($C=S$), 883, 799, 512; *HRMS*: (ASAP) found: 425.9995 (100%), $C_{14}H_{19}NO_4S_5+H$: requires: 425.9990; found C, 39.55; H, 4.51; N, 3.35%, $C_{14}H_{19}NO_4S_5$ requires C, 39.53; H, 4.47; N, 3.29%.

4.5.3 Synthesis of diethyl 5,6-dihydro-2-oxo-[1,3]dithiole[4,5-b]-[1,4]-dithiin-5-methylamine-N,N-diacetate (**340**).



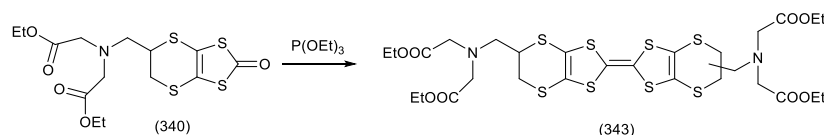
To a solution of thione (**339**) (1.88 g, 4.40 mmol) in $CHCl_3$ (100 ml) was added mercury (II) acetate (3.54 g, 11.0 mmol) and the suspension was left stirring for 3h at r.t. under a nitrogen atmosphere. The solid formed during the reaction was filtered off and washed with $CHCl_3$ until washes ran clear. The combined filtrates were washed with saturated sodium hydrogen carbonate solution (5 x 50 ml). The organic layer was then washed with water (50 ml) and brine (50 ml) and dried over $MgSO_4$. Evaporation of the chloroform yielded the desired oxo-compound (**340**) as a brown oil (1.71 g, 91%); δ_H (400 MHz, $CDCl_3$): 4.17 (4H, q, $J = 7.12$ Hz, $-O-CH_2CH_3$), 3.82 (1H, m, 5-*H*), 3.59 (4H, s, 2 x $-N-CH_2-C=O$), 3.49 (1H, dd, $J = 13.3, 6.2$ Hz, 5- $(CH_\alpha H)N-$), 3.39 (1H, dd, $J = 13.3, 3.1$ Hz, 5- $(CHH_\beta)N-$), 3.23 (1H, dd, $J = 13.8, 8.7$ Hz, 6- $H_\alpha H$), 3.13 (1H, dd, $J = 13.8, 6.4$ Hz, 6- HH_β), 1.28 (6H, t, 2 x $-CH_3$); δ_C (100 MHz, $CDCl_3$): 188.8 ($C=O$), 171.0 (2 x $-C=O(OEt)$), 113.7, 111.8 (3a-, 7a- C), 60.8 (2 x $-O-CH_2-CH_3$), 58.8 ($-CH_2-N-$), 56.2 (2 x $-N-CH_2-C=O$), 44.1 (5- C), 32.9 (6- C), 14.2 (2 x $-CH_3$); ν_{max} : 2978, 1731(CO_2Et), 1670 ($C=O$), 1443, 1411, 1368, 1186, 1139, 1024, 762, 463; *HRMS*: (ASAP) found: 410.0208, $C_{14}H_{19}NO_5S_4+H$: requires: 410.0219; found for C, 40.94; H, 4.72; N, 3.50%, $C_{14}H_{19}NO_5S_4$ requires C, 41.07; H, 4.64; N, 3.42%.

4.5.4 Synthesis of diethyl BEDT-TTF-methylamino-N,N-diacetate (**341**).



To a solution of oxo compound (**340**) (2.01 g, 5.0 mmol) in freshly distilled triethyl phosphite (50 ml) was added unsubstituted thione (**100**) (1.79 g, 8.0 mmol) and the resulting suspension was left stirring at 90°C for 6.5 h under a nitrogen atmosphere. The solid formed was filtered, washed with CHCl₃ and the combined filtrates were concentrated under reduced pressure. The triethyl phosphite was distilled off by using a Kugelrohr apparatus. The residue was purified by flash chromatography (6:1= cyclohexane: ethyl acetate) to give the desired product as an orange solid (0.99 g, 34%), m.p. 107-108°C; δ_H (400 MHz, CDCl₃): 4.09 (4H, q, J = 7.1 Hz, 2 x -O-CH₂-CH₃), 3.64 (1H, m, 5-H), 3.50, 3.51 (2 x 2H, 2 x s, 2 x (-N-CH₂-C(O))), 3.33 (1H, dd, J = 13.1, 6.0 Hz, 5-(CH_αH)-N), 3.21 (4H, s, (5', 6'-CH₂)), 3.20 (1H, dd, J = 12.9, 3.1 Hz, 5-(CH_βH)-N), 3.03 (2H, m, 6-H₂), 1.20 (6H, t, J = 7.2 Hz, 2 x -CH₃); δ_C (100 MHz, CDCl₃): 171.0 (2 x C=O), 113.8, 113.7, 112.5, 111.5, 109.8 (2-, 2'-, 3a-, 7a-, 3'a-, 7'a-C), 60.6 (2 x -O-CH₂-CH₃), 58.7 (5-CH₂-N-), 56.1 (2 x -N-CH₂-C=O), 42.6 (5-C), 32.5 (6-C), 30.1 (5', 6'-C) 14.1 (2 x -CH₃); ν_{max} : 2921, 1733 (C=O), 1449, 1412, 1372, 1190, 1022, 770; found C, 39.16; H, 4.00; N, 2.29%; C₁₉H₂₃NO₄S₈ requires C, 38.97; H, 3.93; N, 2.39%; *Crystal data for (341)*: C₁₉H₂₃NO₄S₈, M_r = 585.8, monoclinic, $a = 6.5916(2)$, $b = 17.9519(9)$, $c = 22.2783(8)$ Å, $\beta = 97.261(3)^\circ$, $V = 2615.09(18)$ Å³, $Z = 4$, $P2_1/c$, $D_c = 1.49$ g cm⁻³, $\mu = 0.709$ mm⁻¹, $T = 150(2)$ K, 5831 unique reflections ($R_{int} = 0.090$), 4196 with $F^2 > 2\sigma$, $R(F, F^2 > 2\sigma) = 0.087$, $R_w(F^2, \text{all data}) = 0.23$.

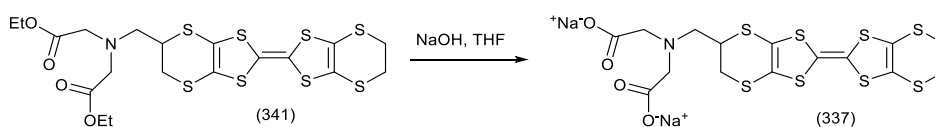
4.5.5 Synthesis of tetraethyl BEDT-TTF-5, 5' and 5, 6'-bis-methylamino-N,N,N',N'-tetraacetate (**343**).



A suspension of oxo-compound (**340**) (0.74 g, 1.81 mmol) and triethyl phosphite (6 ml) was warmed up to 90°C and left stirring overnight under a nitrogen atmosphere. The reaction was allowed to cool down, the phosphite was distilled off using a Kugelrohr apparatus and the residue was purified by column chromatography (3:1= cyclohexane:

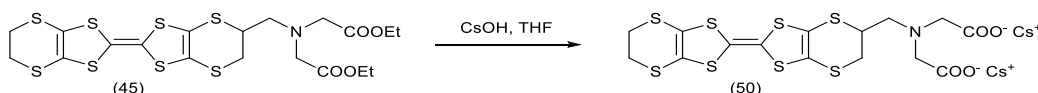
ethyl acetate) to furnish homo-coupled compound (**343**) (0.20 g, 14%) as a dark-red oil. δ_H (400 MHz, $CDCl_3$): 4.00 (4H, q, $J=7.1$ Hz, 2 x $-O-CH_2-CH_3$), 3.87 (1H, m, 5-, 5'/6'-H), 3.53, 3.52 (2 x 4H, 2 x s, 2 x $(-N-CH_2-C(O))$), 3.40 (2H, m, 5, 5'/6'-($CH_\alpha H$)N), 3.25 (2H, m, 5, 5'/6'-($CH_\beta H$)N), 3.03 (4H, m, 6, 5'/6'- H_2), 1.20 (6H, t, $J=7.2$ Hz, 2 x $-CH_3$); δ_C (100 MHz, $CDCl_3$): 171.6 (2 x $C=O$), 115.7, 113.8, (2-, 2'-, 3a-, 7a-, 3'a-, 7'a-C), 60.6 (2 x $-O-CH_2$), 58.7 (5,5'/6'- CH_2-N -), 56.3 (4 x $-N-CH_2-C=O$), 42.6 (5, 5'/6'-C), 33.2 (6, 5'/6'-C), 14.5 (2 x $-CH_3$); ν_{max} : 2975, 1729 ($C=O$), 1451, 1409, 1369, 1186, 1135, 1023, 951, 770;

4.5.6 Synthesis of disodium BEDT-TTF-methylamino-N,N-dicarboxylate (**337**).



The di-ester donor (**341**) (0.37 g, 6.40 mmol) was dissolved in THF (10 ml) and an aqueous solution of NaOH (5 ml, 0.256 M, 12.8 mmol) was added. The suspension was warmed up to 50°C and left stirring overnight. Monitoring of the reaction by tlc showed all starting material was consumed. The THF was evaporated and the residue washed with DCM (3 x 5 ml) to dissolve any remaining starting material. The residue was washed with water (3 x 5 ml) to remove any NaOH left and finally with ether (3 x 10 ml) to dry the residue which was then isolated by filtration to yield (**337**) as a red solid. (0.41 g, quantitative); m.p. 240°C (dec). The compound (**337**) was insoluble in every deuterated solvent used, so characterisation by NMR was not possible. ν_{max} : 2917, 1582, 1400, 1326, 1122, 995, 904, 771, 669; found C, 28.16; H, 3.03; N, 2.38%, $C_{14}H_{19}NO_4S_5 \cdot 4H_2O$ required C, 27.91; H, 3.25; N, 2.17%.

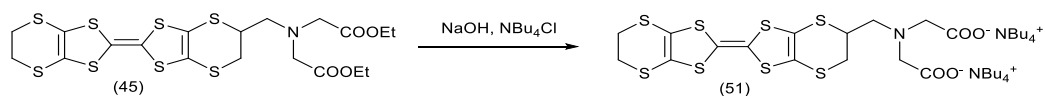
4.5.7 Attempted synthesis of dicaesium BEDT-TTF-methylamino-N,N-dicarboxylate (**50**).



To a solution of diester (**45**) (0.12 g, 0.21 mmol) in THF (4 ml) was added $CsOH \cdot H_2O$ (0.054 g, 0.36 mmol) and the solution was left stirring under reflux for 24 h. The reaction was stopped, left to cool down and the THF was evaporated. Ethyl acetate (10 ml) was added to the residue and the organic layer was washed with water (3 x 10 ml) and then the aqueous phase was collected and the water evaporated to give an orange jelly oil. No

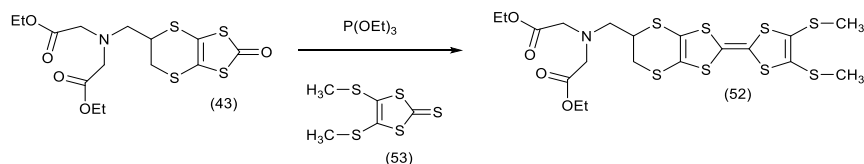
NMR spectra were observed due to the instant jellification of the sample in the NMR tube.

4.5.8 Attempted synthesis of di(tetrabutylammonium) BEDT-TTF-methylamino-N,N-dicarboxylate (**51**).



To a solution of diester (**45**) (0.13 g, 0.24 mmol) in THF (10 ml) was added a solution of NaOH (4 ml, 0.205 M, 0.82 mmol) and the solution was left stirring for 24h at r.t. until the tlc showed all starting material had disappeared. Bu₄NCl (0.239 g, 0.86 mmol) was added to the solution and after 5 min the THF was evaporated and DCM was added. The organic phase was washed with water and dried over MgSO₄ to give a red oil which was analysed by NMR. Unfortunately the spectra showed only the protons belonged to the NBu₄ cation and no other peaks were recorded.

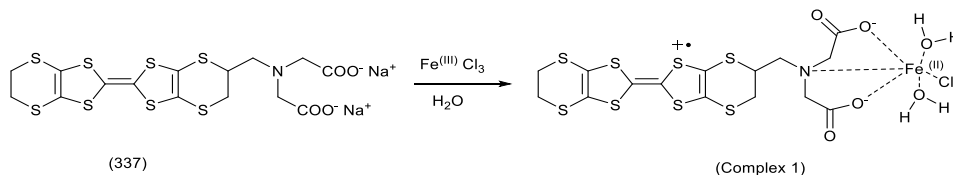
4.5.9 Synthesis of 3,4-bis(methylthio)-5'-methylamino- EDT-TTF-N,N-diacetate (**52**);



To a solution of thione (**43**) (1.11 g, 2.71 mmol) in freshly distilled triethyl phosphite (20 ml) was added oxo-compound (**53**) (0.6 g, 26.5 mmol) and the resulting suspension was warmed up to 95°C and left to stir overnight under a nitrogen atmosphere. Monitoring by tlc showed the formation of three major spots as expected. The reaction vessel was allowed to cool down to r.t. and triethyl phosphite was distilled off using a Kugelrohr oven. The residue was purified by flash chromatography (4:1=cyclohexane:EtOAc) to yield unsymmetric donor (**52**) as a brown oil (0.33 g, 21%). δ_H (400 MHz, CDCl₃): 4.09 (4H, q, $J = 7.1$ Hz, -O-CH₂-CH₃), 3.65 (1H, m, 5'-H), 3.52, 3.51 (2 x 2H, 2 x s, 2 x (-N-CH₂-C(O))), 3.34 (1H, dd, $J = 13.4, 5.6$ Hz, 5'-(CH_αH)N), 3.19 (1H, dd, $J = 13.6, 3.0$ Hz, 5'-(CH_βH)N), 3.04 (2H, m, 6'-CH₂), 2.34 (6H, s, 2 x (S-CH₃)), 1.20 (6H, t, $J = 3.4$ Hz, 2 x -CH₃); δ_C (100 MHz, CDCl₃): 170.8 (2 x C=O), 127.1, 113.6, 113.2, 112.4, 109.3 (2, 2', 3a-, 7a-, 4'-, 5'-C), 60.5 (2 x -O-CH₂-CH₃), 58.6 (5'-CH₂-N), 55.9 (2 x -N-CH₂-C=O), 42.5 (5'-C), 32.3 (6'-C), 19.1 (2 x S-CH₃), 14.0 (2 x -CH₃); ν_{max} : 2978, 2919, 1733 (C=O),

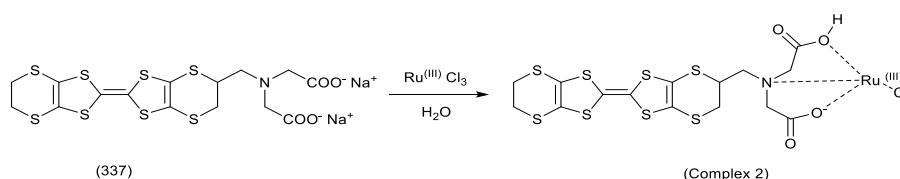
1415, 1369, 1186, 1138, 1024, 985, 968, 887, 753; found C, 38.84; H, 4.26; N, 2.38%; $C_{19}H_{25}NO_4S_8$ requires C, 38.97; H, 4.17; N, 2.47%.

4.5.10 Fe(III)Cl₃ + ligand (337) [Complex (1)].



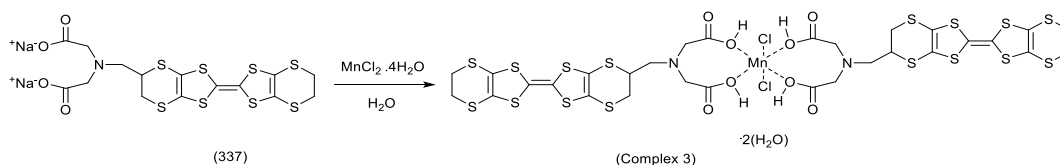
To a suspension of sodium salt of donor (337) (0.21 g, 0.37 mmol) in distilled water (15 ml) was added an excess of FeCl₃ (35 mg, 0.21 mmol) and immediately after the addition the suspension become coloured brown. Reaction was stopped immediately and the solid obtained was filtered, washed with diethyl-ether and left to dry in air (150 mg, 61%); m.p. slowly decomposing on heating, ν_{max} : 3451, 1622 (C=O), 1392, 1109, 1024, 886, 769; found C, 27.46; H, 2.18; N, 2.33%; $C_{15}H_{13}S_8O_4NFe \cdot 2H_2O$ requires C, 27.50; H 2.61; N, 2.14%;

4.5.11 Ru(III)Cl₃ + ligand (337) [Complex (2)].



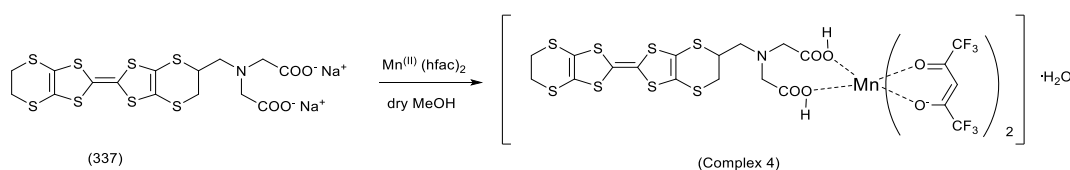
To a suspension of sodium salt of donor (337) (170 mg, 0.30 mmol) in distilled water (5 ml) at r.t. was added an excess of RuCl₃·xH₂O (29 mg, 0.14 mmol) and immediately after the addition the suspension became dark. The reaction was stopped after 1 h, the solid was isolated by filtration and washed with diethyl-ether and left to dry in air. (66 mg, 71%); m.p. slowly decomposing on heating, ν_{max} : 3366, 2958, 2917, 1579 (C=O), 1399, 1259, 1020, 882, 769; found C, 26.45; H, 2.11; N, 2.17%; $C_{15}H_{13}O_4S_8NCl_1Ru$ requires C, 27.11; H, 1.97; N, 2.11%;

4.5.12 Mn(II)Cl₂·4H₂O + ligand (337) Complex (3)].



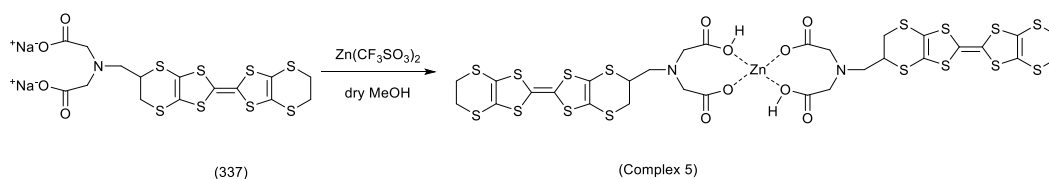
To a suspension of sodium salt of donor **(337)** (0.212 g, 0.37 mmol) in distilled water (5 ml) at r.t. was added $\text{MnCl}_2 \cdot 4\text{H}_2\text{O}$ (0.035 g, 0.18 mmol) and immediately after the addition a red precipitate was formed. The obtained solid was filtered and washed with diethyl-ether and left to dry in air (147 mg, 66%) m.p. 206-207°C (dec). ν_{max} : 3321, 2914, 2166, 1595 (C=O), 1399, 1364, 1194, 1143, 996, 892; found C, 29.28; H, 2.57; N, 2.58%; $\text{C}_{30}\text{H}_{30}\text{O}_8\text{S}_{16}\text{N}_2\text{Cl}_2\text{Mn} \cdot 2\text{H}_2\text{O}$ required C, 29.50; H, 2.81; H, 2.29%.

4.5.13 Mn(II)(hfac)₂ + ligand **(337)** [Complex **(4)**].



To a suspension of sodium salt of donor **(337)** (26.0 mg, 0.052 mmol) in dry MeOH (6 ml) at r.t. under a nitrogen atmosphere was added $\text{Mn}(\text{hfac})_2$ (24 mg, 0.046 mmol). Immediately after the addition a brown solid precipitated out from the mixture. The reaction was left to stir for 1h and then the solid was filtered. The brown precipitate was collected, washed with diethyl-ether and left to dry in air (22 mg, 48%); ν_{max} : 3296, 1601, 1401, 1319, 1054, 994, 902, 771; found C, 29.61; H, 1.76; N, 1.81%; $\text{C}_{25}\text{H}_{19}\text{NO}_9\text{F}_{12}\text{S}_8\text{Mn}$ requires C, 29.53; H, 1.88; N, 1.38%.

4.5.14 Zn(II)triflate + ligand **(337)** [Complex **(5)**].

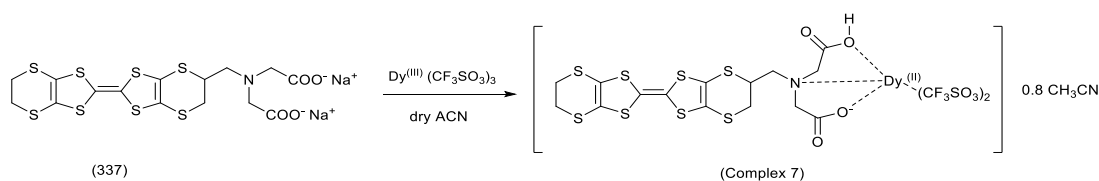


To a suspension of disodium salt of donor **(337)** (77 mg, 0.13 mmol) in dry MeOH (8 ml) at r.t. under a nitrogen atmosphere was added zinc triflate (25 mg, 0.07 mol) and immediately after the addition a brown suspension was formed. The reaction mixture was left to stir for 1 h, then the solid was filtered off, washed with diethyl-ether and left to dry in air (45 mg, 58%); m.p. 243-244°C (dec.), ν_{max} : 2950, 2854, 1596, 1422, 1398, 1342, 1143, 996, 893, 766, 748; found C, 31.94; H, 2.41; N, 2.64%; $\text{C}_{30}\text{H}_{28}\text{N}_2\text{O}_8\text{S}_{16}\text{Zn}$ requires C, 32.09; H, 2.51; N, 2.49%.

4.5.15 Mn(II)triflate + ligand **(337)** [Complex **(6)**].

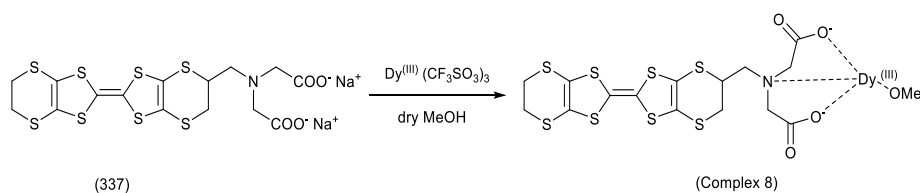
To a suspension of disodium salt of donor **(337)** (78 mg, 0.14 mmol) in dry MeOH (8 ml) at r.t. under a nitrogen atmosphere was added manganese triflate (25 mg, 0.07 mol) and immediately after the addition a brown solid precipitated out. The reaction mixture was left to stir for 1 h and then the solid was filtered, washed with diethyl-ether and left to dry in the air (47 mg, 65%); m.p. 223-224°C (dec). ν_{max} : 3417, 2912, 2856, 1596, 1422, 1398, 1347, 1256, 1143, 1031, 901, 766, 748; found C, 22.15; H, 2.17; N, 1.76%; $C_{17}H_{19}NO_{12}S_{10}F_6Mn$ requires C, 22.22; H, 2.08; N, 1.52%;

4.5.16 Dy(III)triflate + ligand **(337)**-in dry ACN [Complex **(7)**].



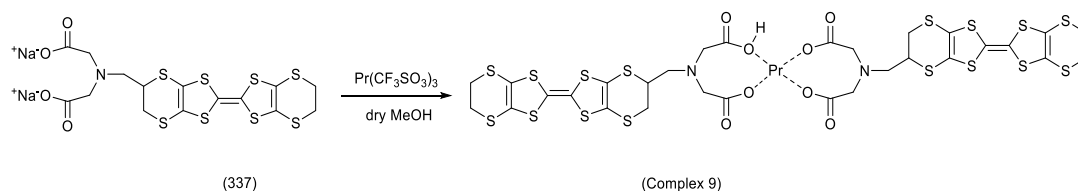
To a suspension of disodium salt of donor **(337)** (61 mg, 0.11 mmol) in dry ACN (10 ml) at r.t. under a nitrogen atmosphere was added dysprosium triflate (33 mg, 0.054 mol) and immediately after the addition a pink-red solid precipitated out. The reaction was left to stir for 1h and then the solid was filtered, washed with diethyl-ether and left to dry in air (42 mg, 76%); m.p. 216-217°C (dec.). ν_{max} : 3368, 2923, 1597, 1399, 1256, 1132, 1169, 1031, 901, 766, 634; found C, 22.09; H, 1.42; N, 2.25%; $C_{15}H_{14}N_1O_4S_8Dy \cdot C_2F_6S_2O_6 \cdot 0.8CH_3CN$ requires C, 21.85; H, 1.62; N, 2.47%.

4.5.17 Dy(III)triflate + ligand **(337)**-in dry MeOH [Complex **(8)**].



To a suspension of disodium salt of donor **(337)** (86 mg, 0.13 mmol) in dry MeOH (5 ml) at r.t. under a nitrogen atmosphere was added dysprosium triflate (40 mg, 0.07 mol) and immediately after the addition a pink-red solid precipitated out. The reaction was left to stir for 1h and then the solid was filtered, washed with diethyl-ether and left to dry in air (28 mg, 59%); m.p. 222-223°C (dec.). ν_{max} 3368, 2923, 1596, 1423, 1399, 1143, 901, 766, 748; found C, 26.57; H, 1.85; N, 1.88%; $C_{15}H_{14}N_1O_4S_8Dy \cdot OCH_3$ requires C, 26.24; H, 2.24; N, 1.94%.

4.5.18 Pr(III) triflate + ligand **(337)** [Complex **(9)**].

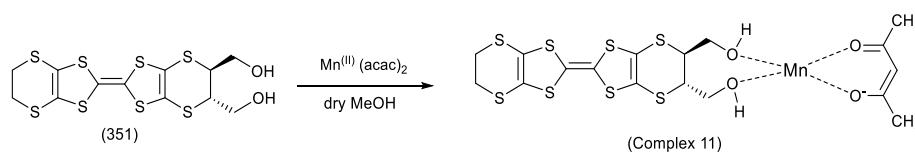


To a suspension of disodium salt of donor (**337**) (72 mg, 0.12 mmol) in dry MeOH (10 ml) at r.t. under nitrogen atmosphere was added praseodymium triflate (39 mg, 0.07 mol) and immediately after the addition a bright pink solid precipitated out. The reaction was left to stir for 1h and then the solid was filtered, washed with diethyl-ether and left to dry in the air (48 mg, 61%); m.p. 223-224°C (dec.). ν_{max} : 3383, 2913, 2855, 1595, 1421, 1397, 1342, 1346, 1143, 995, 766, 747; CHN found C, 29.85; H, 2.17; N, 2.38%; $C_{30}H_{28}N_2O_8S_{16}Pr$ requires C, 30.00; H, 2.27; N, 2.34%.

4.5.19 Ti (IV) ($OCH(CH_3)_2$)₄ + ligand (**351**) [Complex (10)].

To a solution of diol (**351**) (85 mg, 0.19 mmol) in dry THF (10 ml) at r.t. under a nitrogen atmosphere was added titanium (IV) isopropoxide (28 μ l, 0.01 mol) and immediately after the addition an orange-brown solid precipitated out. The reaction was left to stir for 1h and then the solid was filtered, washed with diethyl-ether and left to dry in air. m.p. 190-191°C (dec.). ν_{max} : 3298, 2930, 1678, 1461, 1404, 1283, 1115, 1027; found C, 27.20; H, 2.57%; $C_{12}H_{12}O_2S_8TiO_2 \cdot 4H_2O$ requires C, 27.32; H, 2.71%;

4.5.20 Mn (II) (acetyl-acetonate)₂ + diol (**351**) [Complex (11)].



To a solution of diol (**351**) (65 mg, 0.15 mmol) in dry THF (10 ml) at r.t. under a nitrogen atmosphere was added sodium hydride (7.3 mg, 0.30 mmol) and the resulting turbid suspension was left stirring for 10 min before manganese (acac)₂ (38 mg, 0.15 mmol) was added. Immediately after the addition the suspension became a brown colour and after 1h the solid formed was filtered, washed with diethyl-ether and left to dry in air (27 mg, 30%); found C, 34.27; H, 2.38%; $C_{17}H_{18}O_4S_8Mn$ requires C, 34.16; H, 3.04%.

4.5.21 Mn (II) (hfac)₂ + ligand (**351**) [Complex (12)].

To a solution of diol (**351**) (62 mg, 0.14 mmol) in dry THF (10 ml) at r.t. under nitrogen atmosphere was added an excess of sodium hydroxide (7.5 mg, 0.31 mmol) and the resulting turbid suspension was left stirring for 10 min before manganese (hfac)₂ trihydrate (66 mg, 0.13 mmol) was added. After few minutes the suspension became a darker colour and the solid formed was filtered, washed with diethyl-ether and left to dry in air (5 mg, 44%); found C, 25.53; H, 1.65%; C₁₂H₁₁O₂S₈Mn₂ C₅HF₆O₂·5H₂O; requires C, 25.64; H, 1.91%.

4.6 Bibliography

1. P. Batail, *Chem. Rev.*, 2004, **104**, 4887-4890, L. Ouahab and T. Enoki, *Eur. J. Inorg. Chem.*, 2004, **2004**, 933.
2. a) E. Coronado, J. R. Galán-Mascarós, C. J. Gómez-García and V. Laukhin, *Nature*, 2000, **408**, 447, b) E. Coronado and P. Day, *Chem. Rev.*, 2004, **104**, 5419, c) E. Coronado and J. R. Galán-Mascarós, *J. Mater. Chem.*, 2005, **15**, 66.
3. L. Kaboub, A. Gouasmia, J. Legros, E. Harte, C. Coulon and J. Fabre, *Synth. Met.*, 2009, **159**, 2075.
4. L. Martin, S. S. Turner, P. Day, P. Guionneau, J. A. Howard, D. E. Hibbs, M. E. Light, M. B. Hursthouse, M. Uruichi and K. Yakushi, *Inorg. Chem.*, 2001, **40**, 1363.
5. B. Zhang, Y. Zhang and D. Zhu, *Chem. Comm.*, 2012, **48**, 197.
6. F. Pop, M. Allain, P. Auban-Senzier, J. Martínez-Lillo, F. Lloret, M. Julve, E. Canadell and N. Avarvari, *European J. Inorg. Chem.*, 2014, **24**, 3855.
7. G. Harada, T. Jin, A. Izuoka, M. M. Matsushita and T. Sugawara, *Tetrahedron Lett.*, 2003, **44**, 4415.
8. M. Chahma, X. Wang, A. van der Est and M. Pilkington, *J. Org. Chem.*, 2006, **71**, 2750.
9. M. Chahma, K. Macnamara, A. Van der Est, A. Alberola, V. Polo and M. Pilkington, *New J. Chem.*, 2007, **31**, 1973.
10. H. Komatsu, M. M. Matsushita, S. Yamamura, Y. Sugawara, K. Suzuki and T. Sugawara, *J. Am. Chem. Soc.*, 2010, **132**, 4528.
11. D. Lorcy, N. Bellec, M. Fourmigué and N. Avarvari, *Coord. Chem. Rev.*, 2009, **253**, 1398.
12. H. Tanaka, H. Kobayashi and A. Kobayashi, *J. Am. Chem. Soc.*, 2002, **124**, 10002.
13. F. Qi, T. C. Mak, Z. Zhong-Yuan, Y. Qing-Chuan, L. Zhi, Y. Wen-Tao, Z. Dao-Ben and J. Min-Hua, *J. Chem. Soc., Dalton Trans.*, 2002, , 1377.
14. F. Setifi, L. Ouahab, S. Golhen, Y. Yoshida and G. Saito, *Inorg. Chem.*, 2003, **42**, 1791.
15. J. Qin, C. Qian, N. Zhou, R. Zhu, Y. Li, J. Zuo and X. You, *Eur. J. Inorg. Chem.*, 2012, **2012**, 234.
16. F. Iwahori, S. Golhen, L. Ouahab, R. Carlier and J. Sutter, *Inorg. Chem.*, 2001, **40**, 6541.

17. L. Ouahab, F. Iwahori, S. Golhen, R. Carlier and J. Sutter, *Synth. Met.*, 2003, **133**, 505.
18. T. Biet, T. Cauchy and N. Avarvari, *Chem. Eur. J.*, 2012, **18**, 16097.
19. A. Alberola, E. Coronado, J. R. Galán-Mascarós, C. Giménez-Saiz and C. J. Gómez-García, *J. Am. Chem. Soc.*, 2003, **125**, 10774.
20. J. R. Galán-Mascarós, E. Coronado, P. A. Goddard, J. Singleton, A. I. Coldea, J. D. Wallis, S. J. Coles and A. Alberola, *J. Am. Chem. Soc.*, 2010, **132**, 9271.
21. J. Griffiths, R. J. Brown, P. Day, C. J. Matthews, B. Vital and J. D. Wallis, *Tetrahedron Lett.*, 2003, **44**, 3127, A. C. Brooks, P. Day, S. I. Dias, S. Rabaça, I. C. Santos, R. T. Henriques, J. D. Wallis and M. Almeida, *Eur. J. Inorg. Chem.*, 2009, **2009**, 3084.
22. Q. Wang, P. Day, J. Griffiths, H. Nie and J. D. Wallis, *New J. Chem.*, 2006, **30**, 1790.
23. M. Bousseau, L. Valade, J. P. Legros, P. Cassoux, M. Garbaskas and L. V. Interrante, *J. Am. Chem. Soc.*, 1986, **108**, 1908.
24. G. R. Fulmer, A. J. Miller, N. H. Sherden, H. E. Gottlieb, A. Nudelman, B. M. Stoltz, J. E. Bercaw and K. I. Goldberg, *Organometallics*, 2010, **29**, 2176.
25. I. Matos, E. Pérez-Mayoral, E. Soriano, A. Zukal, R. M. Martín-Aranda, A. J. López-Peinado, I. Fonseca and J. Čejka, *Chem. Eng. J.*, 2010, **161**, 377.
26. A. Matuszek, MChem Project-“Synthesis of Materials with Conducting and Magnetic Properties, 2008, unpublished results.
27. J. Griffiths, A. A. Arola, G. Appleby and J. D. Wallis, *Tetrahedron Lett.*, 2004, **45**, 2813.
28. a) P. Wu, G. Saito, K. Imaeda, Z. Shi, T. Mori, T. Enoki and H. Inokuchi, *Chem. Lett.*, 1986, , 441-444, b) Y. Zhu, Y. Kan, Y. Lin, W. Pan, Z. Su and H. Cui, *Acta Chim. Sin.Chin. Ed.*, 2003, **61**, 1916.
29. G. S. Smith and J. Hoard, *J. Am. Chem. Soc.*, 1959, **81**, 556; C. Wang, C. Yang, C. Lee and G. Lee, *Inorg. Chem.*, 2002, **41**, 429; S. Bandyopadhyay, A. Das, G. Mukherjee, A. Cantoni, G. Bocelli, S. Chaudhuri and J. Ribas, *Polyhedron*, 2004, **23**, 1081; S. Laborda, R. Clérac, C. E. Anson and A. K. Powell, *Inorg. Chem.*, 2004, **43**, 5931; P. Siega, J. Wuerges, F. Arena, E. Gianolio, S. N. Fedosov, R. Dreos, S. Geremia, S. Aime and L. Randaccio, *Chemistry-A European Journal*, 2009, **15**, 7980; J. Gao, D. Li, J. Wang, X. Jin, P. Kang, T. Wu, K. Li and X. Zhang, *Journal*

- of Coordination Chemistry*, 2011, **64**, 2284; N. Kumari, B. D. Ward, S. Kar and L. Mishra, *Polyhedron*, 2012, **33**, 425.
30. R. J. Brown, A. C. Brooks, J. Griffiths, B. Vital, P. Day and J. D. Wallis, *Org. & Biomol. Chem.*, 2007, **5**, 3172.
31. S. Bouquillon and J. Muzart, *Eur. J. Orga. Chem.*, 2001, **2001**, 3301.
32. S. Mahshid, M. Askari and M. S. Ghamsari, *J. Mater. Process. Technol.*, 2007, **189**, 296.
33. J. Wang, J. J. Hayward, R. Gumbau-Brisa, J. D. Wallis, H. Stoeckli-Evans and M. Pilkington, *CrystEngComm*, 2015, *in press*.